UNIVERSITÉ DU QUÉBEC À MONTRÉAL

# PALEOHYDROGRAPHY OF BAFFIN BAY, DAVIS STRAIT, AND THE NORTHWEST LABRADOR SEA DURING THE LAST CLIMATIC CYCLE

DISSERTATION
PRESENTED
AS PARTIAL REQUIREMENT
OF THE DOCTORATE OF EARTH AND ATMOSPHERIC SCIENCES

BY

OLIVIA GIBB

JUNE 2015

UNIVERSITÉ DU QUÉBEC À MONTRÉAL

# PALEOHYDROGRAPHIE DE LA BAIE DE BAFFIN, DU DÉTROIT DE DAVIS, ET DU NORD-OUEST DE LA MER DU LABRADOR AU COURS DU DERNIER CYCLE CLIMATIQUE

THÈSE
PRÉSENTÉE
COMME EXIGENCE PARTIELLE
DU DOCTORAT EN SCIENCES DE LA TERRE ET DE L'ATMOSPHÈRE

PAR

OLIVIA GIBB

JUIN 2015

ACKNOWLEDGEMENTS

My doctoral journey began in August 2008 aboard the CCSG Hudson. I volunteered to assist Chief Scientist Anne de Vernal, and the scientific crew in sampling marine sediment cores from Labrador Sea to Baffin Bay. Through that mission I learned the importance and necessity of working within a group of motivated people who shared a vast range of knowledge and expertise. This valuable experience further developed my interests in paleoceanographic research, and with Anne's unyielding enthusiasm, I started a PhD at GEOTOP. I would like to express my sincere gratitude to Anne for her invitation on this journey, and to her and my co-supervisor Claude Hillaire-Marcel for their valuable guidance and support during my PhD. Cohabitation between Montreal and Halifax/St. John's proved to be a great challenge, and I am very grateful for their patience and cooperation.

I would also like to express my gratitude towards those who have helped fund this project. The research chapters have been a contribution to the Past4Future project of the 7th Framework Program of the European Commission. Support from the following foundations is also acknowledged: *Ministère du Développement Économique, Innovation et Exportation* (MDEIE) and *Fonds Québécois de Recherche sur la Nature et les Technologies* (FQRNT), the Canadian Foundation for Climate and Atmospheric Sciences (CFCAS), Natural Resources Canada (NRCan), and the Natural Sciences and Engineering Research Council of Canada (NSERC) for their financial support of the HU2008029 expedition in the Labrador Sea. I personally thank FARE-UQAM and GEOTOP for bursaries toward my tuition and stipend, and to IODP-Canada and the Geological Society of America for granting me student research awards which contributed to supporting my radiocarbon and isotopic analyses.

A special thanks to Maryse Henry for introducing me to the world of dinocysts. Her help and expertise in the Micropaleontology and Marine Palynology Laboratory (UQAM) were exceptional. Thank you to Jean-François Hélie and Agnieszka Adamowicz for your support in the Stable Isotope Geochemistry Laboratory (UQAM). Their confidence and patience allowed me to analyse my samples on my crazy schedules. I would also like to thank the following researchers and technicians for their in kind support of laboratory equipment that enabled me to work from home: Kate Jarrett, Owen Brown, Rob Fensome, Peta Mudie, and Graham Williams at NRCan (Bedford Institute of Oceanography), Elliott Burden, Helen Gillespie, Danny Boyce, and Susan Fudge at Memorial University. I would like to thank Anne Jennings (INSTARR) and André Rochon (UQAR) for their evaluation of my thesis proposal.

I would also like to thank all of my peers at GEOTOP-UQAM. Working with such a knowledgeable and talented group of students off of whom I could bounce ideas was a blessing. Firstly, I would like to thank my office mate Jenny Maccali, for her friendship and great playlists. Many, many thanks to Laurence Nuttin and Dimitri Bouvry for their hospitality and kindness. You had always made Montreal feel like home. Thank you Laurence for helping be submit my thesis. Thanks to Quentin for his continued support with the Baffin Bay project, and for always keeping things, interesting. Thanks to Audrey Limoges and Nicolas Van Nieuwenhove for their expertise and companionship in the microscope room. I would also like to thank Sandrine Solignac, for her friendship, support, and for good times at *la Québécoise*.

Thank you to Isa Lemire-Claudé, for her friendship, hospitality and support.

A special thank you to my family for their love and encouragement. It was great to have company in Montreal, but also to be occasionally closer to home.

And last but not least, I thank my husband Jon. Thank you for your love and patience throughout the difficult times apart. Thank you for your support and encouragement

when times were tough. Thank you for your insight, suggestions, and last minute corrections. Thank you for this chapter and for the one that is to come with Wesley.

I love you.

TABLE OF CONTENTS

LIST OF FIGURES

LIST OF TABLES



APPENDIX B

# RÉSUMÉ

La baie de Baffin est une voie importante d'exportation d'eau douce de l'Arctique vers l'Atlantique Nord. Les exercices de modélisation climatiques suggèrent que le réchauffement climatique s'accompagnera d'une augmentation de l'exportation d'eau douce l'Arctique ce qui affecterait le taux de formation de la masse d'eau de la mer du Labrador (LSW) et la circulation océanique globale. L'étude paléocéanographique de la baie de Baffin est donc pertinente afin de prévoir l'impact des changements climatiques à des échelles régionale et globale. Dans ce contexte, l'objectif de la thèse est de reconstituer les conditions océanographiques et climatiques de cette région pendant le dernier cycle glaciaire-interglaciaire (~ 115-0 ka). Plus précisément, il s'agit de documenter la variabilité spatio-temporelle de la circulation océanique, notamment les apports d'eau de fonte des glaciers pendant les épisodes de réchauffement.

Les chapitres présentés dans la thèse tentent de répondre à ces questions à partir de l'analyse de carottes sédimentaires. Le premier chapitre porte sur une séquence sédimentaire du nord-ouest de la mer du Labrador couvrant les derniers 36 000 ans. Le deuxième chapitre concerne une séquence du centre de la baie de Baffin enregistrant les derniers 115 000 ans. Enfin, le troisième chapitre porte sur la déglaciation et postglaciaire, soit les derniers ~ 15 000 ans dans le nord-ouest de la mer du Labrador, le détroit de Davis, et les régions est et centrale de la baie de Baffin. Les objectifs principaux poursuivis sont les suivants : (1) reconstituer les conditions de surface de l'océan, y compris les températures estivales et hivernales, la salinité, la productivité primaire et la couverture de glace de mer; (2) caractériser la variabilité temporelle de la température, de la salinité et du carbone inorganique dissous de la masse d'eau intermédiaire afin de retracer la stratification et la ventilation dans la colonne d'eau; (3) établir des relations entre les changements paléocéanographiques de la baie de Baffin et la circulation dans l'Atlantique Nord et le climat. Ces objectifs de recherche ont été atteints et nous avons pu retracer la chronologie des changements paléocéanographiques de la baie de Baffin au cours des derniers ~115 000 ans.

Pendant la majeure partie du dernier intervalle glaciaire, la baie de Baffin a été occupée par une couverture de glace continue. Cependant, une advection d'eau Atlantique par le détroit de Davis semble caractériser certains intervalles froids (stadiaires) et chauds (interstadiaires). Des valeurs élevées du $\delta^{18}O$ des foraminifères planctoniques (*Neogloboquadrina pachyderma* senestres; Npl) et des foraminifères benthiques (> +4‰) suggèrent qu'une seule masse d'eau froide et salée d'origine

Atlantique était présente sous la couche de mélange lors des stades isotopiques 5d et une partie des stades 3 et de la transition 2/1. Une couverture de glace de mer pérenne a été déduite de la faible productivité de foraminifères et de l'absence de dinokystes. De faibles valeurs du $\delta^{18}$O-Npl (+2,6 à +3,6‰) lors d'épisodes des stades 5c, 5a, 3 et lors de la transition 2/1 sont enregistrées à des niveaux également marqués par des abondances relativement élevées de dinokystes, ce qui laisse supposer la pénétration épisodique d'une masse d'eau Atlantique un peu plus chaude ou une ouverture occasionnelle du couvert de glace de mer. Pendant le dernier dernier maximum glaciaire et lors de la transition vers l'Holocène, le nord-ouest de la mer du Labrador était couvert de glace de mer tel qu'illustré par la faible abondance des dinokystes et des valeurs élevées du $\delta^{18}$O-Npl. Les événements de Heinrich 1 et 2 ont y ont été marqués par des des faibles teneurs en $\delta^{18}$O qui indiqueraient une production élevée de glace de mer. En raison de conditions froides et de la proximité de la calotte Laurentidienne, le Bølling-Allerød et le Dryas récent ne se sont pas accompagnés d'enregistrement particulier à une échelle régionale.

La déglaciation, caractérisée par une diminution du couvert de glace de mer de pérenne à saisonnière, s'est établie progressivement du sud vers le nord, soit de la mer de Labrador vers la baie de Baffin. La séquence d'événements a été la suivante. De ~ 12 à 7,5 cal ka BP, le nord-ouest de la mer du Labrador a connu un changement très important des conditions de surface, avec des températures d'été élevées (~ 11°C) mais froides en hiver (~ 0°C), une couverture de glace de mer de près de 3 mois par an et une faible salinité (~28) Les forts gradients thermiques saisonniers auraient été une conséquence de la forte stratification due aux apports d'eau de fonte de la calotte glaciaire laurentidienne. Dans le secteur est de la baie de Baffin, à environ 9,5 cal ka BP, une augmentation de salinité de surface de 28 à > 32 et une diminution du couvert de glace de mer sont enregistrés, sans doute en relation avec le retrait des marges de la calotte glaciaire du Groenland, notamment dans Disko Bugt. Par la suite, plusieurs changements sont survenus à environ 7,5 cal ka BP. Dans le nord-ouest de la mer du Labrador, les conditions interglaciaires actuelles se sont établies suite à l'augmentation de la salinité qui a atteint environ 34, s'accompagnant d'une augmentation des températures hivernales en dépit d'étés plus frais. Cette transition est associée à de moindres apports d'eau de fonte, une stratification réduite et une augmentation de la pénétration des masses d'eau de l'Atlantique Nord en surface. De telles conditions sont favorable à la convection hivernale et à la formation de la masse d'eau de la mer du Labrador (LSW), dont témoignent par ailleurs des valeurs élevées du $\delta^{13}$C-Npl. Dans l'est de la baie de Baffin, le réchauffement de surface en hiver et des salinités plus élevée ont conduit à une forte réduction de la durée de la couverture de glace de mer et de la productivité primaire. Les enregistrements du centre de baie de Baffin indiquent également une advection accrue des eaux de l'Atlantique Nord en surface pendant le postglaciaire, mais avec une réponse fortement atténuée par rapport au secteur est. Ces résultats suggèrent de grandes fluctuations des conditions de surface marines à l'Holocène, différentes dans

les secteurs hauturiers et côtiers, mais étroitement contrôlées par le courant chaud de l'ouest du Groenland et froid de la Terre de Baffin.

Mots clés : paléocéanographie, paléoclimatologie, baie de Baffin, mer du Labrador, glaciaire, Holocène, dinokystes, foraminifères, isotopes de l'oxygène et du carbone

# ABSTRACT

Baffin Bay is currently an important pathway for Arctic freshwater export to the North Atlantic. Modeling forecasts of an increase in freshwater export driven by a warming Arctic may affect the rate of Labrador Sea Water (LSW) formation and global oceanic circulation. Investigating the paleoceanographic history of the Baffin Bay corridor is therefore relevant for forecasting potential climate impacts both regionally and globally. The focus of this thesis is to reconstruct the oceanographic conditions in this region through the last glacial cycle (~115 ka), with emphasis on the spatio-temporal variability of ocean circulation through large scale climate oscillations, including meltwater outflow and warming temperatures during the deglacial.

Three research chapters address these issues using marine core sediment samples. The first analyses a record spanning the last ~36 ka from the northwest Labrador Sea, the second records the last ~115 ka from central Baffin Bay, and the third correlates higher resolution records from a multiple-core transect from the northwest Labrador Sea, Davis Strait, and eastern and central Baffin Bay focusing on the last deglacial and the Holocene (last ~15 ka). Three main objectives were followed for each research chapter: (1) reconstruct sea surface conditions including summer and winter temperatures (SST), summer salinity (SSS), productivity, and sea ice cover as they respond to changes in climate, the subsurface water mass, and meltwater input; (2) characterize temporal variability in relative temperature, salinity, and dissolved inorganic carbon of the subsurface water mass due to the advection of other water masses, changes in sea ice cover, and stratification and/or ventilation throughout the water column, and; (3) spatially and temporally correlate changes in paleoceanographic conditions among sites throughout the Baffin Bay corridor and with other records from the North Atlantic to identify associations with oceanic circulation and climate.

Results show that Baffin Bay remained completely ice covered during most of the last glacial interval. However advection of saline Atlantic water entered Baffin Bay through Davis Strait during both cooler (stadial) and warmer (interstadial) intervals. High $\delta^{18}O$ values of both planktic *Neogloboquadrina pachyderma* left-coiled (Npl) and benthic foraminifera (>+4‰) suggest a single cold, saline Atlantic water mass was present during Marine Isotope Stages (MIS) 5d, 3, and the MIS 2/1 transition. Continued perennial sea ice cover was inferred from low productivity and the absence of dinocysts. Low $\delta^{18}O$-Npl values (+2.6 to +3.6 ‰) were present during MIS 5c, 5a, 3 and the MIS 2/1 transition. The low values, coupled with occurrences of dinocysts, suggest the Atlantic water mass was slightly warmer, or affected by the addition of

isotopically light brines through heavy sea ice production during occasional seasonally open water. The northwest Labrador Sea was also cold and perennially ice covered during MIS 2 and the MIS 2/1 transition, as documented by low dinocyst abundance and high $\delta^{18}$O-Npl values. The termination of Heinrich Events 1 and 2 were recorded with light-$\delta^{18}$O excursions indicating heavy ice production. The Bølling-Allerød and Younger Dryas were not recorded or weakly recorded, likely due to close proximity to Laurentide Ice Sheet (LIS).

The deglaciation, characterised by the shift from perennial to seasonal sea ice cover, occurred diachronously northward through the Baffin Bay corridor. From ~12 to 7.5 cal ka BP, the northwest Labrador Sea experienced a dramatic shift to warm summer (~11°C) but cold winter (~0°C) sea surface temperatures (SST), sea ice cover during about 3 months per year, and low sea surface salinity (SSS) (~28), likely due to enhanced subsurface inflow of North East Atlantic Deep Water. The large seasonal gradients in temperature were due to a strongly stratified upper water layer in relation to meltwater supply from the LIS. At around 9.5 cal ka BP in eastern Baffin Bay, SSS increased significantly (28 to > 32) and the breakup of perennial sea ice began as the Greenland Ice Sheet retreated into Disko Bugt. Several changes occured throughout the corridor at about 7.5 cal ka BP. In the northwest Labrador Sea, postglacial conditions were established after SSS had progressively increased to about 34, and winter SSTs became warmer and summers cooler. This was facilitated by the reduced water mass stratification by the retreat of the LIS and enhanced penetration of North Atlantic water, all contributing to winter convection and Labrador Sea Water formation which is reflected in increased $\delta^{13}$C-Npl values (i.e., enhanced ventilation). In eastern Baffin Bay, warming and more importantly, higher salinity conditions, led to a strong reduction in the duration of the sea ice cover and to significant primary productivity. Central Baffin Bay likely evolved with the eastern sector of the Bay as it responded to the advection of North Atlantic waters, but with a strongly attenuated response. This diachronous evolution toward modern sea surface conditions in the Baffin Bay corridor was likely due to limited North Atlantic advection through the Davis Strait sill. These postglacial records demonstrate large fluctuations in sea surface conditions independent to the variability of surrounding coastal records, but are likely controlled by the relative strengths and shifts of the warmer West Greenland Current and colder Baffin Island Current.

Key words: paleoceanography, paleoclimatology, Baffin Bay, Labrador Sea, glacial, Holocene, dinocysts, foraminifera, stable isotopes of oxygen and carbon

# INTRODUCTION

## 0.1 The context of the study

Contemporary decline in Arctic sea ice extent is related to Arctic warming within recent decades, as the result of thermodynamic and sea ice-albedo feedback (cf. Stroeve et al., 2012). The increased sea-ice melting, along with increases in freshwater inputs from land, the Pacific Ocean, and precipitation have greatly increased the amount of freshwater to the Arctic Ocean (Serreze et al., 2006). This has lead to enhanced overall freshwater export, as demonstrated by a decreasing salinity of the North Atlantic, which may affect the Atlantic Meridional Overturning Circulation (AMOC) (Curry and Mauritzen, 2005; Peterson et al., 2006; Dickson et al., 2007; Sutherland et al., 2009). Within the AMOC, deep water masses such as North Atlantic Deep Water (NADW) are created when relatively warm, but saline surface waters of the North Atlantic Current (NAC) enter the Greenland, Iceland and Norwegian (GIN) Seas and also the Labrador Sea and loose buoyancy (Fig. 0.1). Deep convection in the water column is caused by the sinking of a dense upper water mass. The densification is caused by warm surface waters losing heat to the atmosphere, or when brines are released during sea ice formation (Curry and Mauritzen, 2005).

Increasing greenhouse gas concentrations may affect the AMOC in two dominant processes. Increasing air temperatures will reduce the cooling (densification) of the sea surface. Also, an increase in freshwater will decrease the sea surface salinity, thereby reducing the density. Debates on the effects of climate change on the AMOC focus on the magnitude of these triggers and the reaction time of these systems (Curry

and Mauritzen, 2005). Coupled atmosphere-ocean General Circulation Models (GCMs) are used to forecast the effects of climate change on the AMOC (Jahn and Holland, 2013). In some modeling scenarios, cessation of the AMOC is projected under conditions of large freshwater influx due to the melting of Arctic ice (Greenland Ice Sheet, permanent sea ice) (Driesschaert et al., 2007), while others suggest non linearity (Swingedouw et al., 2009). GCMs have also been used to understand changes in past climate and oceanic circulation, specifically illustrating their large-scale fluctuations during the last glacial cycle and the roles of freshwater and climate in changing the AMOC (Manabe and Stouffer, 1995; Clark et al., 2007).

Currently, the amount of freshwater exiting the Arctic is increasing, and a significant proportion is exiting through the Canadian Arctic Archipelago (CAA) via Lancaster Sound, Jones Sound, and Nares Strait (Serreze et al., 2006; Dickson et al., 2007; Curry et al., 2011), which collect in Baffin Bay and pass through Davis Strait into the Labrador Sea (Fig. 0.1). Models suggest that Arctic freshwater output through the western route (i.e., west of Greenland) is colder and fresher than the eastern output (Fram Strait; Aksenov et al., 2010). Freshwater forcing through the Baffin Bay corridor is required in models to reconstruct decreases in sea surface salinity resulting in decreased convection in the Labrador Sea (Goosse et al., 1997; Wadley and Bigg, 2002; Cheng and Rhines, 2004; Wekerle et al., 2013). Labrador Sea Water (LSW) is an important component of the modern AMOC. It is an intermediate water mass which contributes to NADW (Yashayaev and Loder, 2009 and references therein). LSW is formed when cold winter surface air temperatures over the Labrador Sea cool a western branch of the warm, saline North Atlantic Drift (West Greenland Current - WGC), which then sinks due to increased density (Lazier, 1973). The rate of LSW formation is variable and responds to both changes in salinity and atmospheric circulation, which affect stratification and therefore convective mixing. Thus, changes in Arctic freshwater outflow through the CAA, Baffin Bay, Davis Strait to

the Labrador Sea (hereafter described as the Baffin Bay corridor) and warmer climate may modify the LSW production rates. Such changes were observed during the Great Salinity Anomaly in the late 1960s, early 1970s, and 1990s (e.g., Dickson et al., 1988; Gelderloos et al., 2012). In the context of extreme climate shifts, it is relevant to investigate the past history of the sea surface conditions, the subsurface water mass, and sea ice formation in relation to freshwater fluxes and climate from Baffin Bay to the Labrador Sea. These results, based on past conditions, contribute baselines to forecasting the potential impacts of future freshwater fluxes and increasing sea surface temperature on the formation of LSW and variability of the AMOC.

### 0.1.1 The northwest Labrador Sea

Throughout the last glacial interval (the last ~115 ka), the Labrador Sea has evolved from being cold and mainly ice covered to warm and mainly ice free (de Vernal and Hillaire-Marcel, 2000; de Vernal et al., 2000; de Vernal et al., 2005). A few paleoceanographic records (black circles Fig. 0.1) have been reconstructed from various proxies including foraminiferal species assemblages (e.g. Bilodeau et al., 1994; Seidenkrantz et al., 2013), the oxygen and carbon stable isotopes of foraminiferal tests (e.g. Hillaire-Marcel et al., 1994; Hillaire-Marcel and Bilodeau, 2000; Rasmussen et al., 2003; Seidenkrantz et al., 2013), and sea surface reconstructions based on dinoflagellate cyst assemblages (e.g. de Vernal et al., 1994, 2000, 2001; Rochon and de Vernal, 1994; Levac and de Vernal, 1997; de Vernal and Hillaire-Marcel, 2000; Solignac et al., 2004; Hillaire-Marcel et al., 2007). Those studies have illustrated that the Labrador Sea has been greatly influenced by advances and retreats of the northeastern margin of the Laurentide Ice Sheet (LIS) and by the advection of North Atlantic waters. For example, increased sea ice cover occurred during the last glacial maximum, Heinrich Events (HE), and the Younger Dryas,

while the 8.3 cal ka BP-drainage layer event is not easily recognizable in sea surface reconstructions.

The northern Labrador Sea is however particularly interesting because the Hudson Strait was one of the main sources for sediment, ice and meltwater supply during the glacial period and deglaciation of the LIS (Andrews and Tedesco, 1992; Andrews et al., 1994). However, areas north and east of the outlet of Hudson Strait do not always receive such deliveries as in the case of HE 3 (Stoner et al., 1996; Rashid et al., 2003) and possibly the 8.3 cal ka BP-drainage layer event (Hillaire-Marcel et al., 2007). Few reconstructions have been undertaken in the northwest Labrador Sea, near the outlet of Hudson Strait. Previous reconstructions include bottom water conditions during periods of LIS flux from foraminiferal abundances (Jennings, 1993; Jennings et al., 1996, 1998) and changes to the intermediate water layer during Heinrich Events from planktic foraminiferal oxygen isotopes ($\delta^{18}O$; Rashid and Boyle, 2007). However reconstructions of sea surface conditions have yet to be investigated.

### 0.1.2 Baffin Bay

Paleoceanographic reconstructions from sediment cores in Baffin Bay (black circles Fig. 0.1) can be divided into two groups. The first consists of records collected from shallow (< 1000 m) shelf areas surrounding Baffin Bay where high sedimentation rates (e.g. 100 cm $ka^{-1}$) are linked to coastal and glacial erosion. This creates records with high temporal resolution of deglacial and Holocene sediments that mainly reflect local variability in atmospheric and oceanic circulation and meltwater discharge (Seidenkrantz et al., 2008; Erbs-Hansen et al., 2013). Most of these paleoceanographic studies used foraminiferal abundances as proxies of subsurface-bottom water mass properties, that are in turn associated with the relative strength of Atlantic vs. Arctic water in Baffin Bay (e.g. Osterman and Nelson, 1989; Levac et al.,

2001; Seidenkrantz et al., 2007, 2008, 2012; Knudsen et al., 2008; Ledu et al., 2008; Lloyd et al., 2005, 2007; Mudie et al., 2006; Møller et al., 2006; Moros et al., 2006; Andresen et al., 2011; Perner et al., 2013; Erbs-Hansen et al., 2013; Jennings et al., 2013). However, some records used dinoflagellates cysts as proxies to reconstruct sea surface conditions since the deglaciation (e.g. Levac et al., 2001; Hamel et al., 2002; Ledu et al., 2008; Seidenkrantz et al., 2008; Andresen et al., 2011; Ouellet-Bernier et al., 2014). Other used diatoms as proxies for sea surface conditions (e.g. Williams, 1990; Moros et al., 2006; Knudsen et al., 2008; Ren et al., 2009). Some of these records document the large meltwater inputs from the deglaciation of the LIS and Innuitian Ice Sheet (IIS), or the ice margin retreat and continued discharge from the Greenland Ice Sheet (GIS). Most of these coastal sites record local to regional ocean variations during the Holocene.

The second group of paleoceanographic records previously analysed were collected from the deepest, central areas of Baffin Bay. Ocean Drilling Project (ODP) Site 645 (Leg 105; Baldauf et al., 1989) extends back to the early Miocene. There are also piston cores spanning the last glacial cycle (Fig. 0.1; Aksu and Piper, 1979; Aksu, 1981, 1983; de Vernal et al., 1987), including site survey core 85-027-016 for ODP Site 645 (Fig. 0.1; Hillaire-Marcel et al., 1989; Scott et al., 1989). The primary challenge in analysing marine sediments from Baffin Bay is the difficulty in establishing a chronostratigraphy. This is caused by two factors. Sediment delivery from surrounding ice sheets active during glacial periods cause variable sedimentation rates in this region (Simon et al., 2012 and references therein). Additionally, the lack of calcareous foraminifera precludes radiocarbon analyses or the establishment of a $\delta^{18}O$ stratigraphy. However, Simon et al. (2012) recently proposed a chronostratigraphy spanning the last 115 ka based on detailed paleomagnetic data that overcomes some of these challenges.

Paleoceanographic reconstructions based on the $\delta^{18}O$ of planktic foraminifera and dinoflagellate cyst assemblages over the last glacial interval have been attempted on several deep Baffin Bay cores despite the chronological uncertainty and interpretation challenges (Aksu, 1981, 1983; Mudie and Aksu, 1984; de Vernal et al., 1987; Hillaire-Marcel et al., 1989; Scott et al., 1989). Intervals containing little to no microfossils prevent continuous records that are difficult to interpret. Low concentrations of microfossils have been explained by dilution due to high sedimentation rates (Scott et al., 1989), low productivity due to harsh, ice covered conditions and low salinities (Hillaire-Marcel et al., 1989), carbonate dissolution (Aksu, 1983), or a combination of these factors (Hillaire-Marcel et al., 1989).

Carbonate dissolution in Baffin Bay characterizes Holocene sediments collected from depths > 900 m (Aksu 1983; Osterman and Nelson, 1989; de Vernal et al., 1992; Schröeder-Adams and Van Rooyen, 2011; Steinhauer, 2012). This greatly hindered the study of circulation in Baffin Bay throughout the glacial stage. There were also other limitations that have since been discovered and/or improved since the 1980s. In those days, isotopic analyses required a sample size >50 foraminiferal tests. Smaller sample sizes could have introduced analytical bias, while large samples could have been drawn from several planktic populations due to the low sedimentation rates and due to the presence of reworked foraminifera (Hillaire-Marcel et al., 1989). More importantly, any detrital carbonate material, which is found in abundance within Baffin Bay sediments (Hiscott et al., 1989), remaining within foraminiferal tests could bias their isotopic composition and result in misleading values (Hodell and Curtis, 2008). Lastly, interpretations of a planktic-$\delta^{18}O$ signal from this polar to subpolar environment can not be directly correlated with the global marine isotope stratigraphy, notably because of the isotopic imprint of sea ice formation (Hillaire-Marcel and de Vernal, 2008). The early planktic-$\delta^{18}O$ records from Baffin Bay revealed large range in values, initially interpreted as glacial-interglacial oscillations (Aksu, 1983; Aksu and Mudie, 1985). The low planktic-$\delta^{18}O$ values have since been

interpreted as the result of episodic depletions due to meltwater inputs (de Vernal et al., 1987). Most recently, this pattern is thought to reflect the sinking of isotopically depleted brines during sea ice production along the pycnocline to Npl habitat depth (Hillaire-Marcel and de Vernal, 2008). Therefore, an established chronostratigraphy along with the recognition of these limitations will allow for the adaptation of different techniques and interpretations in order to further pursue paleoceanographic reconstructions of Baffin Bay.

## 0.2 Statement of problem and objectives of this study

The Baffin Bay corridor is currently an important pathway for Arctic freshwater export and global oceanic circulation. These processes are expected to change in the near future. Information on responses to changes in the past glacial-to-interglacial periods provides insight on future dynamics. The focus is set here on deeper, more central sites as a means to generate records of large-scale changes in oceanographic conditions that predominantly vary in response to the regional ocean dynamics rather than to coastal processes. Also, my assessment of the limitations of paleoceanographic research in a harsh, Arctic environment such as Baffin Bay and analysing the data with new methods and a wider suite of potential mechanisms, provide a precedent for other areas.

The focus of this thesis is thus to reconstruct the oceanographic history of the Baffin Bay corridor (Baffin Bay, Davis Strait, northwest Labrador Sea) through the last glacial cycle (~115 ka). More specifically, my goal is to document variability in oceanographic conditions including temperature, salinity, sea ice cover, freshwater fluxes and the occurrence of multiple water masses due to the effects of large scale climate oscillations and ocean circulation. Various climate intervals and transitions

throughout the last glacial cycle will be addressed. These include the last five marine isotope stages, the Greenland stadials and interstadials, Heinrich Events, intense meltwater incursions, increasing insolation, climate events of the recent deglacial interval (e.g. Bølling-Allerød, Younger Dryas, drainage of glacial lake Agassiz), and the millennial scale climate oscillations of the Holocene (e.g. Mid-Holocene optimum, Medieval Warm Period, Little Ice Age). The following three main objectives will be applied to various sites within the Baffin Bay corridor and form the basis of three research chapters organized by location and chronology:

Objective 1: Reconstruct sea surface conditions including summer and winter temperatures, salinity, productivity, and sea ice cover as they respond to changes in climate, the subsurface water mass, and meltwater input.

Objective 2: Characterize temporal variability in relative temperature, salinity, and dissolved inorganic carbon of the subsurface water mass due to the advection of other water masses, changes in sea ice cover, and stratification and/or ventilation throughout the water column.

Objective 3: Spatially and temporally correlate changes in paleoceanographic conditions among sites throughout the Baffin Bay corridor and with other records from the North Atlantic to identify associations with oceanic circulation and climate.

The specific goals required to achieve these objectives are to: (1) use dinoflagellate cyst species assemblages to reconstruct past sea ice cover, sea surface temperature and salinity, (2) set oxygen isotope records in planktic and benthic foraminifera to recreate relative changes in temperature and salinity of the mesopelagic and bottom water masses and relative amounts of sea ice formation, (3) set carbon isotope records

in planktic and benthic foraminifera to identify sources of the mesopelagic and bottom water masses as well as productivity, nutrient supply, and ventilation of water masses, (4) establish chronologies or temporally constrain oceanographic changes using the results from goals 1 through 3, as well as $^{14}C$ dating, ice-rafted detritus and detrital carbonate contents.

## 0.3 Geographic and hydrographic setting

Baffin Bay is a semi-enclosed, oblong basin approximately 1450 km long and between 110 and 650 km wide (690,000 $km^2$ surface area; Fig. 0.1). It is bordered by Greenland to the east with a wide shelf extending ~150 km, Baffin Island to the west with a narrower shelf extending ~35 km, and the CAA to the north, all with relatively steep slopes to the sea floor. Baffin Bay reaches a maximum water depth of 2136 m, and connects to both the Arctic and Atlantic oceans across sills. Although they restrict deep water flow, the sills permit cold Arctic surface waters to enter Baffin Bay from the north via Lancaster Sound (55 km wide, 125 m deep), Jones Sound (30 km wide, 190 m deep), and Nares Strait (~40 km wide, ~220 m deep) in the north. They also permit warmer intermediate waters from the Atlantic to enter from the south via Davis Strait (640 m depth). During the last glacial maximum, Baffin Bay was surrounded by the Innuitian, Laurentide and Greenland Ice Sheets which extended onto the shelves (Briner et al., 2003, 2006; Dyke 2004; Ó Cofaigh et al., 2013; Funder et al., 2011). This may have greatly impeded flow into or through Baffin Bay during this time. Davis Strait connects Baffin Bay to the Labrador Sea, which expands along the Northwest Atlantic mid-ocean channel reaching ~3500 m water depth. It is bordered to the west by Labrador with a wide shelf extending 150

km on average, and to the northeast by Greenland with a narrow shelf extending ~50 km.

Northward flowing warm high-salinity Atlantic waters and southward flowing cold low-salinity Arctic waters form a counter clockwise gyre throughout the Baffin Bay corridor (Fig. 0.1) (see Bourke et al., 1989; Buch, 2000, 2008; Cuny et al., 2002, 2005; Tang et al., 2004; Ribergaard, 2008; Münchow et al., 2014 for details listed below). Along the West Greenland shelf, the West Greenland Current (WGC) carries cool, less saline Arctic water from the East Greenland Current (temperature, T, ~ -1.8°C, salinity, $S \leq 34.5$) that has been slightly warmed by Atlantic water ($T \sim 4.5$°C, $S \leq 34.95$) which is a western branch of the Irminger Current (IC) that flows within 30 km of the West Greenland slope. Therefore the WGC consists of an upper 100 m of cooler, less saline water ($T \sim 2.3$°C, $32 \leq S \leq 33$) above a warmer more saline water layer ($T \sim 1.6$°C, $S \sim 34.4$), which both flow north along eastern Davis Strait). Once the WGC reaches northern Baffin Bay and turns west, it (upper 300 m, T ~ -1.5°C, $S \leq 34$) mixes with cold, less saline Arctic water that enters via the Canadian Arctic Archipelago (Nares Strait, Lancaster Sound, and Jones Sound) and becomes the Baffin Island Current (BIC). Baffin Bay Intermediate Water consists of the Irminger component of the WGC that has recirculated in Baffin Bay and some warmer Arctic Intermediate water of Atlantic origin that passes over the sills of Nares Strait. Baffin Bay Deep and Bottom waters cool with depth. The BIC flow south along the Baffin Island coast on the continental shelf and slope through Davis Strait into the northwest Labrador Sea. Finally, the BIC mixes with Arctic water exiting Hudson Strait to form the Labrador Current (LC) ($T \sim -1.5$°C, $S \leq 34$) which flows along the eastern Canadian shelf and upper slope. The colder, less saline surface layer of the LC overlies a branch of the WGC that has extended westward near Davis Strait and circulated through the gyre. Below the LC lies the Labrador Sea Water (LSW; $T \sim 3.0$°C, $S \sim 34.9$) which is formed by vertical convection due to the sinking of dense waters cooled in winter (Lazier, 1973). LSW extends to 2500 m water depth and lies

above the North East Atlantic Deep Water and the Denmark Strait Overflow Water (Yashayaev, 2007). Sea ice cover across the 30° latitudinal range along the Baffin Bay corridor is quite variable, ranging from 0 to > 10 months per year or concentration ranging from 0 to about 90% from fall through spring. Sea ice formation begins in September in northwest Baffin Bay and extends southward reaching nearly complete cover by March (Wang et al., 1994; Tang et al., 2004), occasionally reaching the northwest Labrador Sea. The warm WGC prevents sea ice formation along the southwestern Greenland coast and reduces the extent in eastern Baffin Bay. The cold and stratified LC fosters sea ice growth along the Newfoundland and Labrador shelf. Sea ice begins to melt in April in northern Baffin Bay's North Water Polynya and the Greenland coast moving westward until ice free conditions occur during August or September. The strong seasonality in air temperatures and wind patterns produce the large interannual variability in sea ice cover (Tang et al., 2004).

## 0.4 Materials

The cores used to address the research objectives are from the HU2008-029 cruise aboard the *CCGS Hudson* in 2008 (Fig. 0.1; Campbell et al., 2009). Piston and associated trigger core HU2008-029-004 (PC04 and TWC04) were collected off the Southern Baffin Island shelf in the northwestern Labrador Sea (61.46 °N, 58.04 °W) at a water depth of 2163 m. Core PC04 and TWC04 are 896 and 56 cm in length, respectively. Piston and trigger core HU2008-029-016 (PC16 and TWC16) were collected from deep Baffin Bay (70.77 °N, 64.66 °W) at a water depth of 2063 m. The coring site is in close proximity to cores ODP Site 645 and 85-029-16, which is useful for correlating with previous records. Cores PC16 and TWC16 are 741 and 155 cm in length, respectively. Core PC16 was previously described by Simon et al. (2012), and core TWC16 by Steinhauer (2012). Piston and trigger core HU2008-029-

070 (PC70 and TWC70) were collected off western Greenland (68.23 °N, 57.62°W) at a water depth of 444 m. Cores PC70 and TWC70 are 245 and 208 cm long, respectively. PC70 was previously described by Jennings et al. (2013). Piston and trigger cores HU2008-029-008 (PC08 and TWC08) were collected south of Davis Strait (64.39 °N, 58.13 °W) at a water depth of 858 m. Cores PC08 and TWC08 are 964 and 156 cm in length, respectively. Core PC08 was previously described by Andrews et al. (2014). Due to difficulties in establishing a chronology, PC08 was not used in this study.

## 0.5 Methodology

### 0.5.1 Chronology

Establishing the chronostratigraphy should be the first step in paleoceanographic studies from sediment cores. Radiocarbon ($^{14}C$) dating of calcareous foraminifera is the most common method in the northwest Atlantic. The most appropriate sample to use is a single species of planktic foraminifera from within a narrow size fraction to best represent a single foraminiferal population. Other methods of temporal correlation including paleomagnetic data and $\delta^{18}O$ stratigraphies will also be used.

The presence of calcareous foraminifera within northwest Labrador Sea sediments (Jennings et al., 1996) will allow for a chronostratigraphy based on $^{14}C$ dating. However, the presence of Heinrich Events, as determined by an abundance of coarse grained sediments with detrital carbonate content, will also be considered since they have been extensively dated in the area (Andrews and Tedesco, 1992; Andrews et al., 1994; Hillaire-Marcel et al., 1994; Stoner et al., 1995, 1996; Rashid et al., 2003).

Recently, the establishment of a high resolution chronostratigraphic framework of

PC16 based on magnetic, mineralogical, and physical properties of the sediment has provided an age model spanning the last 115 ka (Simon et al., 2012). Previous attempts were based on the correlation of $\delta^{18}O$ records which were discontinuous due to the lack of calcareous foraminifera in some intervals (Aksu and Piper, 1979; Aksu, 1981, 1983; Mudie and Aksu, 1984; de Vernal et al., 1987; Hillaire-Marcel et al., 1989; Scott et al., 1989). Calcium carbonate dissolution due to low carbonate saturation states (Azetsu-Scott et al., 2010) and oxidation of organic matter produced in the North Water Polynya eliminates calcareous foraminifera for radiocarbon dating as a postglacial stratigraphic tool in Baffin Bay and Davis Strait (Aksu 1983; Osterman and Nelson, 1989; de Vernal et al., 1992; Schröeder-Adams and Van Rooyen, 2011). The paleomagnetic properties of this interval also problematic and not used in the age model (Simon et al., 2012). I will therefore use the palynological analyses to tentatively correlate Holocene records.

### 0.5.2 Paleoceanographic proxies

Several proxies are used for the paleoceanographic reconstructions of the Baffin Bay corridor in order to recreate conditions throughout the water column. Palynological analyses and the carbon and oxygen stable isotope analyses of planktic and benthic foraminifera will be combined to identify three (or potentially more) water masses when possible. Reworked palynomorphs and ice rafted debris and detrital carbonate content will complement interpretations on sedimentation and oceanographic processes. These proxies are described below, along with the method of analysis.

### 0.5.3 Foraminiferal stable isotopes ($\delta^{18}O$ and $\delta^{13}C$)

Foraminifera are single-celled organisms whose tests are preserved within ocean sediments given the proper conditions. There are several forms of foraminifera: epibenthic (living on sea floor sediments), endobenthic (living within sea floor sediments), other species of benthic foraminifera living on substrate or other organisms, and planktonic species living in the water column. Changes in the oxygen stable isotope values ($\delta^{18}O$) of calcareous epibenthic and planktic foraminifera reflect changes in temperature, salinity and the $\delta^{18}O$ of the water in which the test was precipitated. Therefore oceanographic changes due to climate variability, large isotopically depleted meltwater supply, increase in isotopically depleted brines during sea ice formation, or an inflow of different water masses may be observed.

Changes in the carbon stable isotope values ($\delta^{13}C$) of benthic and planktic calcareous foraminifera reflect the values of the dissolved inorganic carbon (DIC) in the water where they precipitate their carbonate test, and affected by vital (biological) effects and kinetic isotope fractionation. Increased photosynthesis within surface waters sequesters isotopically depleted $CO_2$, which increases DIC and planktic foraminiferal $\delta^{13}C$ and can therefore reflect increased primary productivity during a shift to seasonally ice covered conditions within a paleorecord. Increases in freshwater influx during periods of warmer climate boost the influx of depleted, terrestrially-derived DIC (Ravelo and Hillaire-Marcel, 2007). Increased respiration due to an influx of organic matter to the sediment surface negatively fractionates $CO_2$ (DIC) producing decrease in benthic $\delta^{13}C$. Bottom water circulation is also traced with changes in the $\delta^{13}C$ of benthic foraminifera which increases due to increased ventilation and decreases with the influx of a nutrient-rich water mass.

To determine variation in water temperature, salinity, primary productivity, and therefore changes in water mass characteristics and origin, the $\delta^{18}O$ and $\delta^{13}C$ are analysed on the most abundant and common planktic and epibenthic species through each core, when possible. The planktonic foraminifer *Neogloboquadrina pachyderma* left-coiled (Npl) is polar species found in Arcitc waters (e.g., cf. Kucera, 2007) and within the Baffin Bay corridor (e.g. Hillaire-Marcel et al., 1989; Hillaire-Marcel et al., 1994). Npl most commonly lives in cold saline (~34) waters in 50-250 m water depth along the pycnocline (Bé and Tolderlund, 1971; Hilbrecht, 1996; Carstens et al., 1997; Volkmann and Menshc, 2001; Simstich et al., 2003; Pados and Spielhagen, 2014). They are also influenced by food availability living in the chlorophyll maximum (upper 50 m) under permanent ice cover (Volkmann and Mensch, 2001; Pados and Spielhagen, 2014; Xiao et al., 2014). Npl stratify with size (shell density) and calcify at different depths within the water column (Bauch et al., 1997; Volkmann, 2000; Volkmann and Mensch, 2001; Hillaire-Marcel et al., 2004; Xiao et al., 2014). Samples can be analysed from different size fractions of Npl (e.g. 106-150 μm, 150-250 μm, and >250 μm) to identify temperature-salinity (i.e., density) gradients within the intermediate (mesopelagic) water (Hillaire-Marcel et al., 2004). However caution during interpretation is required due to changes in metabolic activity in older stages (Volkmann and Mensch, 2001) and depth of habitat (Xiao et al., 2014).

The most common species of benthic species throughout a core are analysed where possible. If low numbers persist, all size fractions will be used although some effect on the isotopic composition cannot be totally discarded (Barras et al., 2010). No correction for global ice volume or vital effects are made on the benthic $\delta^{18}O$ and $\delta^{13}C$ since the results are used to document relative changes in a water mass within the same records.

### 0.5.4 Palynology

Four groups of palynomorphs are utilised as paleoceanographic proxies. The first and foremost are dinoflagellate cysts, or dinocysts, which are composed of resistant organic compound protecting the dinoflagellate cell during the course of their reproductive cycle. Dinoflagellates can be either phototrophic (photosynthetic) or heterotrophic (preying mainly on diatoms and ciliates), blooming in well lit, productive surface waters (upper 50 m). Unlike dissolvable calcareous microfossils (foraminifera), these cysts can be well preserved in marine sediments from all environments. Instances of poor preservation can occur with certain heterotrophic species susceptible to degradation due to oxidation (Zonneveld et al., 1997, 2001, 2007). Although potentially comprised of samples spanning many years (1 to 1000) of dinocyst flux, the dinocyst assemblage of the marine surface sediments corresponds to the cyst-forming dinoflagellate assemblage in the overlying surface waters (de Vernal and Rochon, 2011). The dinocyst species assemblage is therefore related to sea surface temperature, sea surface salinity, sea ice conditions, and primary productivity. The distribution pattern and abundance of dinocysts in marine sediments relative to various sea surface conditions is well known, and a database (http://www.geotop.ca) of these relationships is continuously increasing, especially in remote locations of the Arctic (de Vernal et al., 2001, 2005, 2013; Radi and de Vernal, 2008). This database is then applied in transfer functions using the modern analogue technique (MAT) to each sample through the core, to produce a record of the sea surface conditions through time. Therefore the reconstructed sea surface conditions include sea surface temperatures (SST) in both summer and winter, summer sea surface salinity (SSS), months per year of sea ice cover with a concentration > 50 %, and productivity in gC $m^{-2}$. The data are initially manipulated to provide a format for R (http://cran.r-project.org/), the statistical software used for

MAT using the scripts prepared by Joel Guiot (CEREGE, France) and the procedure described by de Vernal et al. (2005).

### 0.5.5 Pollen and spores

The presence of fresh terrestrial palynomorphs, which include pollen and spores, indicate material has been transported to marine sediments by ice rafting, ice meltwater, runoff, wind, and currents. Since the cores used in this project are relatively far from the coast, the presence of modern (fresh) pollen and spores is an indication of vegetation on adjacent land and subsequent hydrodynamic or atmospheric transport.

### 0.5.6 Reworked (fossil) palynomorph

The presence of reworked (fossil) palynomorphs, including dinocysts, pollen, spores, and acritarchs in mid-high latitude marine sediments is due to glacial erosion, transport, and meltwater. An abundance of reworked palynomorphs in Baffin Bay and the northwest Labrador Sea during the last glacial period is therefore an indication of glacial activity of surrounding Ice Sheets (Laurentide, Innuitian, and Greenland). The reworked palynomorphs within Heinrich Events are likely eroded from the Paleozoic-Mesozoic sedimentary formations of the Canadian Arctic and West Greenland (e.g., Hiscott et al., 2001) and deposited with ice rafted debris or meltwater flow within the nepheloid layer (Rashid et al., 2003).

### 0.5.7 Foraminiferal organic linings

The organic linings of benthic foraminifera are often found among the palynomorphs. They remain preserved in sediments after the carbonate test has dissolved (de Vernal et al., 1992). Dissolution occurs due to increased dissolved $CO_2$ in surface waters from increased $CO_2$ in the atmosphere, high DIC ($HCO_3^-$, $CO_3^{-3}$) through respiration of organic matter causing an increase in pH, and to low calcium carbonate ($CaCO_3$) saturation states (Azetsu-Scott et al., 2010) which are a function of temperature, salinity and pressure. Therefore carbonate dissolution is ubiquitous to cold, deep Arctic environments due to ice melt, reduction in sea ice cover which increases $CO_2$ sequestration and primary productivity. Concentrations of benthic foraminiferal organic linings are thus a measure of the amount of carbon flux to the sea floor by proxy of benthic production (Rochon and de Vernal, 1994), sea ice cover and primary productivity in surface waters (de Vernal et al., 1992), and possibly the inflow of Pacific derived Arctic water (Azetsu-Scott et al., 2010).

### 0.5.8 Ancillary parameters

There are other sedimentological parameters used in conjunction with micropaleontological proxies to provide additional inforamation on the hydrography and sedimentary influx. These ancillary parameters include weight percent of ice rafted debris (% IRD) as estimated by the weight percent fraction >106 μm, and weight percent carbonate which is calculated from the weight percent inorganic carbon (% $C_{inorg}$). IRD is produced by ice sheets or ice streams that have ground up sediments at the base, and calved off icebergs along the ice margin. The icebergs then travel along surface currents and eventually melt and deposit the sediments trapped

within. The presence of IRD is not only an indicator of cooler times with ice sheet advance and iceberg calving, but also the presence of surface waters conducive to the movement of icebergs (no permanent ice pack). In this thesis, the >106 μm fraction mostly contains detrital material and possibly a low abundance of light biological remains (microfossils) making this coarse fraction a representative proxy for IRD. High amounts of IRD and carbonate can be used to identify the rapidly deposited Heinrich layers in the North Atlantic (Heinrich, 1988; Andrews and Tedesco, 1992; Bond et al., 1992; Broecker et al., 1992) and detrital carbonate events of Baffin Bay (Andrews et al., 1998) and are therefore used as a parameter for chronology.

## 0.6 Thesis structure

This thesis is divided into three chapters that focus on a different location within the Baffin Bay corridor, and/or time interval within the last glacial cycle. Chapter 1 consists of an article published in Quaternary Science Reviews entitled: *Oceanographic regimes in the northwest Labrador Sea since Marine Isotope Stage 3 based on dinocyst and stable isotope proxy records*. It focuses on the timing and variability of sea surface conditions and intermediate water properties of the northwest Labrador Sea. It characterizes their responses to the glacial and deglacial regimes influenced by the LIS and relative advection of Atlantic waters, and to the establishment of postglacial conditions.

Chapter 2 reveals the challenges and opportunities in conducting paleoceanographic research in the harsh Arctic environment of Baffin Bay using proxies from the last glacial cycle. Specifically, this examines the robustness of the data in terms of isotopic offsets due to large foraminiferal populations and detrital carbonate contamination, and re-evaluates the foraminiferal isotope records based on new

hypotheses of potential mechanisms and improved analytical methods. The advection of Atlantic water, sea ice formation, detrital carbonate contamination, and carbonate dissolution are identified and discussed as important contributors. This chapter is entitled: *Paleohydrography of Baffin Bay during the last climatic cycle from planktic vs benthic foraminiferal records*. This chapter will be submitted for publication in *Paleoceanography*.

Chapter 3 is entitled: *Diachronous evolution of sea surface conditions from the Labrador Sea to Baffin Bay since the last deglaciation* and is submitted for publication in the *Holocene*. This chapter attempts to spatially and temporally correlate a transect of cores through the Baffin Bay corridor since the last glacial interval using sea surface reconstructions of dinocyst assemblages. A progressive shift in sea surface conditions from cold and ice covered to warmer and seasonally ice free is revealed through the deglaciation. Also discussed are the effects of relative contributions of the warmer Atlantic vs colder Arctic waters and of meltwater inputs from the surrounding ice sheets on sea surface conditions and dinocyst assemblages, and of the establishment of modern circulation.

Figures

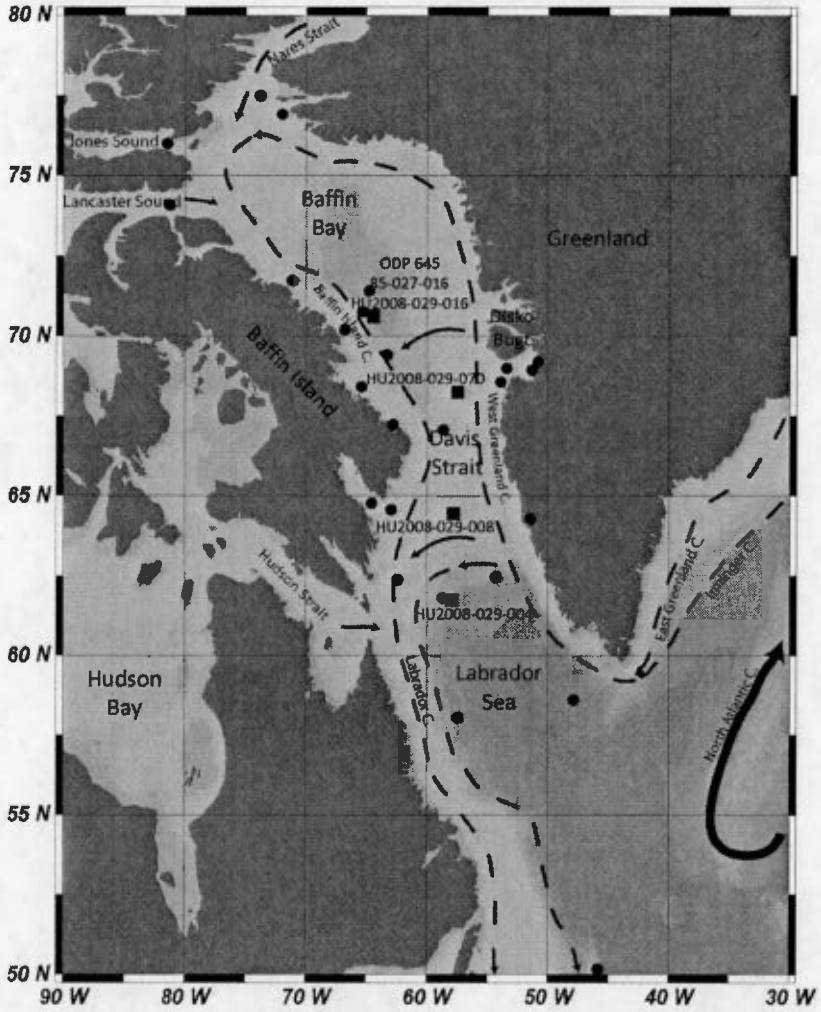


Figure 0.1. Map indicating the locations of cores used in my thesis, including HU2008-029-004, -008, -016, -070 identified by black squares. Cores ODP Site 645 and 85-027-016 were collected at the same location as HU2008-029-016. Black circles mark the location of other paleoceanographic records in the region. Surface currents (North Atlantic Current (NAC), Irminger Current (IC), East Greenland Current (EGC), West Greenland Current (WGC), Baffin Island Current (BIC), and Labrador Current (LC)) are also displayed.

# CHAPTER I

## Oceanographic regimes in the northwest Labrador Sea since Marine Isotope stage 3 based on dinocyst and stable isotope proxy records

Olivia T. Gibb[1], Claude Hillaire-Marcel[1], and Anne de Vernal[1]

[1]GEOTOP Research Center, CP. 8888 Succ Centre Ville, Montréal, QC H3C 3P8, Canada

This chapter was published in *Quaternary Science Reviews, 2014*

Abstract

Sea surface temperature (SST), salinity and density gradients in the upper water column of the northwest Labrador Sea have been reconstructed based on high resolution analysis of a core (HU2008-029-004PC) spanning the last ~36 ka, raised off Hudson Strait. The modern analogue technique was applied to dinocyst assemblages and combined with stable isotope data from *Neogloboquadrina pachyderma* left-coiled (Npl) for this purpose. Three oceanographic regimes were identified, broadly corresponding to the "glacial", "deglacial" and "post-glacial" intervals. The site remained under the direct influence of the Laurentide Ice Sheet (LIS) margin until the postglacial and did not record the Bølling-Allerød warming and weakly recorded the Younger Dryas event. The "glacial" regime lasted until ~12.2 cal ka BP. It was characterized by generally low concentrations of dinocysts within an assemblage indicative of quasi-perennial sea ice. The "deglacial" regime (ca. 12.2-8.3 cal ka BP) was marked by increased biogenic fluxes and more diversified dinocyst assemblages and possibly an enhanced subsurface inflow of North East Atlantic Deep Water. Warm summer (~11°C) but low winter (~0°C) sea surface temperatures, sea ice cover during about 3 months per year, and low summer salinity (~28) suggest strong stratification in the upper water layer in relation to meltwater supply from the LIS. Following the final drainage of glacial Lake Agassiz through Hudson Strait, which is dated here at ~8.3 cal ka BP, and the subsequent LIS collapse, increased summer salinity (up to ~35) was accompanied by a reduced seasonal gradient of sea surface temperature from winter (~3.8°C) to summer (~8.6°C) suggesting enhanced penetration of North Atlantic Water. Weakened stratification of the surface water layer then allowed for winter convection and Labrador Sea Water formation, which is consistent with increased Npl-$\delta^{13}C$ values in response to higher ventilation of the subsurface water layer.

## 1.1 Introduction

Labrador Sea Water (LSW) is an important component of the modern Atlantic Meridional Overturning Circulation (AMOC). The cold winter surface air temperatures above the Labrador Sea cool a western branch of the saline North Atlantic Drift, which sinks due to increased density and forms the intermediate LSW (Lazier, 1973) and contributes to North Atlantic Deep Water (NADW) (Yashayaev and Loder, 2009 and references therein). The rate of LSW formation is variable and responds to both changes in atmospheric circulation and salinity, which affect stratification and therefore convective mixing. As such, periods of warmer climate with increased freshwater flux can inhibit LSW formation. Over one third of Arctic freshwater export presently flows via the Canadian Arctic Archipelago and Nares Strait into the Labrador Sea (Serreze et al., 2006), making Hudson Strait and Davis Strait very important Arctic freshwater pathways (Curry et al., 2011). Therefore any change in temperature and freshwater outflow from the Arctic may modify the LSW production rates as during the Great Salinity Anomaly (e.g., Gelderloos et al., 2012). It may also modify the strength of the AMOC as suggested from modeling experiments (Goosse et al., 1997; Cheng and Rhines, 2004; Wadley and Bigg, 2002). In this context, it is relevant to investigate the past history of water masses and sea ice formation, in relation to freshwater fluxes through the northern Labrador Sea to quantify the potential impacts of future freshwater fluxes and increasing sea surface temperature on the formation of LSW.

Throughout the last glacial cycle, the Labrador Sea has been marked by meltwater supplies from the northeastern margin of the Laurentide Ice Sheet (LIS). Sedimentological and paleoceanographic studies of marine cores from the shelf and slope off Labrador and eastern Baffin Island have permitted to identify phases of LIS margin advance, waning, retreat, and Heinrich Events (Andrews et al., 1994b, 1998,

2012; Hillaire-Marcel et al., 1994; Hillaire-Marcel and Bilodeau, 2000; Jennings et al., 1998; Rashid and Piper, 2007; Rashid et al., 2003). However, the impact of changing climate and meltwater pulses on the oceanic conditions (temperature, salinity, sea ice cover, upper water mass stratification) has yet to be determined on a regional scale, especially in the northwest Labrador Sea and at the outlet of Davis Strait and Hudson Strait.

For this study, we had access to a new core (HU-2008-029-004) ideally located in the northern Labrador Sea. The core was recovered from mid-slope, about 200 nautical miles east of Hudson Strait and south of Davis Strait. It spans over 36 ka and provides detailed information on the impacts of meltwater pulses from the northeastern margin of the LIS on the regional ocean conditions and northwest North Atlantic circulation. Sea surface temperature (SST), sea surface salinity (SSS), seasonal cover of sea ice, and productivity (gC $m^{-2}$) were reconstructed from dinocyst assemblages (de Vernal et al., 2001, 2005, 2008, 2013; Radi and de Vernal, 2008). Subsurface dwelling planktonic foraminifera were analyzed for oxygen and carbon stable isotopes to provide complementary information about subsurface temperature and salinity, ventilation, variations in convective mixing and intermediate water formation (e.g., Ravelo and Hillaire-Marcel, 2007), and also information on major meltwater pulses and their impact on sea ice production rates (Hillaire-Marcel and de Vernal, 2008).

## 1.2 Modern hydrographic setting and location of core collection

The hydrography of the Labrador Sea is influenced by both relatively warm and saline waters flowing from the south and cold low-salinity waters flowing from the north (Fig. 1.1). Along the western Greenland margins, the West Greenland Current (WGC), which flows to the north, consists of a mix of the cool and low saline waters

(temperature ~ -1.8°C, salinity ≤ 34.5) carried through the East Greenland Current (EGC) along the shelf. The warm, saline North Atlantic waters (core at 200-700 m, temperature ~ 4.5°C, salinity ≤ 34.95) that are transported via a western branch of the Irminger Current (IC) flow above the slope (Cuny et al., 2002). Along the Labrador Shelf, the Labrador Current (LC) flows southward. It is formed from the Baffin Island Current (BIC) (temperature ~ -1.5°C, salinity ≤ 34) and outflow from the Hudson Strait, which both consist of cold and low saline Arctic waters. Along the upper slope, the LC overlies Irminger water that has circulated around Baffin Bay. Below the surface layer, the Labrador Sea Water (LSW; temperature ~ 3.0 °C, salinity ~ 34.9) is formed by vertical convection due to the sinking of dense waters cooled in winter (Lazier, 1973). LSW has depths reaching down to 2500 m above the North East Atlantic Deep Water (NEADW) and the Denmark Strait Overflow Water (DSOW) (Yashayaev, 2007).

Piston core HU-2008-029-004 (henceforth PC04) was collected in 2008 off the Southern Baffin Island shelf in the northern Labrador Sea (61.46 °N, 58.04 °W; Campbell et al., 2009) at a water depth of 2163 m (Fig. 1.1). At the coring site, summer surface waters are predominantly those carried by the WGC (Wu and Tang, 2011). The present mean winter and summer SSTs are 3.7 ± 0.5°C and 7.3 ± 1.2°C, respectively, and summer SSS averages 34.2 ± 0.3 (NODC 2001). Sea ice is occasional and occurs only once every 3 years on average. The 1953 to 2003 sea ice compilation using data provided by the National Snow and Ice Data Center (NSIDC) indicates that the core site has a mean of 0.7 ± 1.3 months per year with more than 50% of sea ice, calculated with observations for 1 to 5 months per year for 15 years.

## 1.3 Methods

The core PC04 is 896 cm in length. Onboard measurements included magnetic

susceptibility, spectrophotometry, and sedimentary descriptions, which can be found in the HU2008029 cruise report (Campbell et al., 2009) together with core photographs. The core was not showing any handling disturbance. The working half was sampled onboard at 1-cm intervals. For this study, subsamples were taken at every 4 cm throughout the core, for a total of 220 samples.

The chronostratigraphy of PC04 was established from radiocarbon dates of planktonic foraminiferal populations that consist of > 95 % *Neogloboquadrina pachyderma* left-coiled (Npl). Accelerator mass spectrometry (AMS) radiocarbon measurements were made at Lawrence Livermore National Laboratory and at the National Ocean Sciences AMS Facility of Woods Hole. Radiocarbon ages were calculated using the Libby half-life of 5568 years and normalized to a $\delta^{13}C$ of -25 ‰. The ages were converted to calibrated years and modeled using the Marine09 calibration curve (Reimer et al., 2009) with a marine reservoir correction of 400 years in OxCal 4.2 (Ramsey, 2008). No additional correction ($\Delta R$) was made as it was the case for other $^{14}C$-based chronologies from planktonic foraminifers in the area (see a discussion in Hillaire-Marcel et al., 2007; supplementary material). We have chosen to use the *p_sequence* model in OxCal, which relies on a Bayesian approach using information that includes the $^{14}C$ dates, the depths, and the changes in deposition rate for modeling the probability of each age (Ramsey, 2008). This approach was regarded as adequate considering the changes in sedimentary processes related to the dynamics of the LIS margin during glaciation and deglaciation, including Heinrich Events. The resulting age model assumes constant $^{14}C$-carrier flux settling through the water column to the bottom, constant habitat (water depth) within and among Npl samples, and homogeneous mixed layer at the sediment-water interface (Berger and Johnson, 1978; Bard, 2001). The calibrated ages are reported as the modeled median cal. years BP (see Table 1.1).

For palynological preparations, 5 $cm^3$ subsamples were rinsed and sieved through 106 μm and 10 μm sieves. The dried > 106 μm size fraction, which mostly contains detrital material, was weighed as a proxy for ice rafting deposition. It was also used to hand pick foraminifera for stable isotope analyses. The 10-106 μm size fraction was processed following the detailed methods described by de Vernal et al. (1999). The residual organic matter was mounted onto a slide with Kaiser's glycerol gelatin. Palynological analyses were conducted by identifying and counting all palynomorphs, which include cysts of dinoflagellates (dinocysts), pollen and spores, organic linings of benthic foraminifera and reworked pre-Quaternary palynomorphs. The marker-grain method (Matthews, 1969) was used to calculate the number of total palynomorphs providing an accuracy of approximately ±10 % for a 95% confidence interval (de Vernal et al., 1987). A minimum of 300 dinocysts were identified when possible at species or genera level and counted for the application of the modern analogue technique (MAT) to reconstruct sea surface conditions including temperature, salinity, sea ice cover, and productivity (e.g., de Vernal et al., 2008). Dinocyst species were identified following the nomenclature provided by Rochon et al. (1999), de Vernal et al. (2001), and Head et al. (2001). The pollen and spores were identified with reference to McAndrews et al. (1973) and Moore et al. (1991) and counted to evaluate the inputs from the terrestrial vegetation. Reworked palynomorphs include pollen, spores, dinocysts and acritarchs of pre-Quaternary age, which were differentiated from recent palynomorphs based on their taxonomic identity and preservation state. They are used as indicator of erosion of Phanerozoic rocks and subsequent outwash deposition. In the Labrador Sea, they have been used to identify detrital events (cf. Hiscott et al., 2001). Foraminifer organic linings are related to benthic productivity and can help determine the degree of calcium carbonate dissolution (de Vernal et al., 1992). The total numbers of dinocysts, pollen and spores, foraminifer linings, and total reworked palynomorphs are expressed as individuals per $cm^3$ of sediment. Relative abundances of dinocysts used for paleoceanographical reconstructions were calculated from the sum of dinocysts

counted. A concentration threshold of 100 cysts $cm^{-3}$ was used as minimum reliability requirement (Forcino, 2012).

The modern analogue technique (MAT) was used to reconstruct sea surface temperature (SST) in summer and winter, sea surface salinity (SSS) in summer, sea ice cover as expressed as the number of months per year with a concentration > 50 %, and productivity ($gC \cdot m^{-2}$). MAT was applied on the updated "modern" dinocyst database of the Northern Hemisphere that includes 1492 sites and 66 taxa (see database at http://www.geotop.ca; de Vernal et al., 2013), using the scripts prepared by Guiot (CEREGE, France) for the software R (http://cran.r-project.org/) and the procedure described by de Vernal et al. (2005). We applied a logarithmic transformation to emphasize the weight of accompanying taxa. We calculated the most probable conditions from the average of the 5 best analogues weighted inversely to their distance, and the variance provided the upper and lower limits. Validation tests were performed by dividing the database in 5, with 1193 samples in the reference data set and 299 samples in the verification data set to evaluate the error or root mean square error of prediction (RMSEP), which also corresponds to the standard deviation of the difference between observation and reconstruction. The RMSEP established at ± 1.4 months/year for the sea ice cover, ±1.2°C and ±1.6°C for winter and summer SSTs and ± 2.6 for SSS.

The stable isotope compositions of oxygen ($\delta^{18}O$) and carbon ($\delta^{13}C$) were measured for the planktonic foraminifer *N. pachyderma* left-coiled (Npl), which is a mesopelagic species that lives in cold saline waters along the pycnocline and commonly found in Arctic waters (e.g., Bé and Tolderlund, 1971; Carstens et al., 1997; Simstich et al., 2003). Npl was chosen because it is the species that is by far the most abundant among planktonic foraminifera throughout the core. Actually, Npl constitutes an almost monospecific assemblage, which is expected given the location of the core in the Arctic province of the modern planktonic foraminifer distribution

(cf. Kucera, 2007). Npl specimens were picked from the 150-250 μm size fraction of the > 106 μm residue from the palynological preparations. Stable isotopic analyses were conducted at GEOTOP by acidification with 102 % orthophosphoric acid (Wendeberg et al., 2011) in a Multicarb™ preparation device coupled to an IsoPrime™ isotope ratio mass spectrometer. The isotopic composition for each sample was measured relative to the international reference, the Vienna Pee Dee Belemnite (VPDB), using the conventional "δ-per mil" notation. Reference (NBS 19, IAEA) and working (UQ6 carbonate, GEOTOP, Hillaire-Marcel et al., 2004) standards were used for each analytical run. The reproducibility of measurements as estimated from daily measurements of the UQ6 standard material is better than ±0.05 ‰ at ±1σ level for both isotopes (Hillaire-Marcel et al., 2004).

Some sedimentological parameters were used in conjunction with the micropaleontological proxies to provide better constraints on the sedimentary influx when creating the age model. These parameters included magnetic susceptibility, weight percent coarse fraction, and weight percent carbonate. The magnetic susceptibility data was collected shipboard with a Multi-Sensor Core Logger (MSCL; cf. Campbell et al., 2009). The coarse fraction percentage was calculated using the dry weight of the >106 μm fraction relative to the initial dry weight of the sample, as indicated above. The low abundance of light biological remains in this fraction makes this measurement essentially representative of ice-rafted deposition. The weight percent carbonate was calculated from the inorganic carbon fraction (% $C_{inorg}$) as the difference between the total carbon (% $C_{tot}$) and organic carbon (% $C_{org}$) as measured with a combustion furnace coupled to an elemental analyser (Carlo-Erba™). The $C_{org}$ percentage was determined after acidification by fumigation for 24 h with 12M HCl to remove the inorganic carbon and corrected for weight loss (Hélie, 2009). The $C_{org}$ and $C_{inorg}$ are estimates of the total organic and total inorganic contents respectively. However, potential biases may occur with detrital dolomite and/or HCl-leachable mineral and compounds present in the sediment (e.g., Maccali et al., 2013). XRD

analyses indicate the presence of dolomite in the carbonate rich layers, resulting in minor differences of estimates for $C_{inorg}$ contents (Laurence Nuttin, unpublished data).

## 1.4 Results

### 1.4.1 Chronostratigraphy

Lithology, magnetic susceptibility, weight % coarse fraction and weight % carbonate were used to gather prior information for constructing the age-depth model in OxCal, in addition to the 15 radiocarbon dates (Table 1.1). Sediment core PC04 consists of hemipelagic dark gray silty clay interbedded with two to three layers of graded mud intervals with laminae and sand and gravels (Fig. 1.2; cf. Campbell et al., 2009). These layers have low magnetic susceptibility values, and high weight % carbonate and coarse fraction content (Fig. 1.2). They correspond to Labrador Sea detrital carbonate events as described previously by Andrews and Tedesco (1992), Andrews et al. (1994b, 1995) and Stoner et al. (1995, 1996). The sediment structure and coarse particles visible by CAT-scan images further suggest that these layers correspond to nepheloid-flow deposits as described by Hesse and Khodabakhshm (1998) and Rashid et al. (2003) from the Hudson Strait ice margin. The upper two layers are bracketed by $^{14}C$ dates (Table 1.1), which are within error of Heinrich Event (HE) intervals H1 and H2 in cores from the Labrador Sea (cf. Andrews and Tedesco, 1992; Andrews et al., 1994b; Hillaire-Marcel et al., 1994; Rashid et al., 2003; Stoner et al., 1995, 1996). Another detrital carbonate event probably corresponds to H3 (Stoner et al., 1996; Rashid et al., 2003), but it will not be considered further in this study due to poor age constraints. Since these layers are rapidly deposited (1-2 ka), the upper and lower stratigraphic boundaries of H1 and H2, as identified as the increase in carbonate content, have been used as stratigraphic boundaries in the model.

The $^{14}C$ samples at 36.5, 68.5, and 84.5 cm yielded almost identical dates. They indicate very rapid sediment accumulation rates at about 7852 ± 55 $^{14}C$ yrs BP as one may calculate from the average of the three dates. Since the 85-36 cm interval represents a short lived sedimentary phase, the three AMS dates were combined and two age-depth curves were made with OxCal, one for the lower part of the core below 85 cm and one for the upper part of the core above 36 cm (Table 1.1; Fig. 1.2). The modeled results provide an age range of 8441-8179 cal ka BP for the 85-36 cm interval, with an average value of 8327 cal ka BP. Such an age coincides with the final drainage of Lake Agassiz through Hudson Strait, as recorded in many cores from the Labrador margins (Barber et al., 1999; Hillaire-Marcel et al., 2007; Lewis et al., 2012). The age-depth model also bracketed Heinrich Events 1 and 2 with calibrated ages of 17.9 and 15.7 cal ka BP, and 25.4 and 24.4 cal ka BP, respectively.

Linear interpolation between each modeled date and boundary was used to calculate the sedimentation rates and the age-depth relationship, which were used to plot proxy data against age.

### 1.4.2 Dinocysts and other palynomorphs

The dinocyst concentrations are relatively low, of the order of 10 to $10^4$ cysts $cm^{-3}$. The minimum values are recorded during the glacial interval and until ~15.7 cal ka BP (< 100 cysts $cm^{-3}$; Fig. 1.3). There are a few intervals with slightly higher concentrations (from 100 to 1000 cysts $cm^{-3}$) centered at ~32, 29, 24 cal ka BP. From ~15.7 cal ka BP, dinocyst concentrations increased with maximums of up to 6000 cysts $cm^{-3}$. Pollen and spore concentrations are low (Fig. 1.3), which is expected due to distance from the coast (Rochon and de Vernal, 1994) and the then reduced vegetational cover inland. Samples are mostly barren until ~15.7 cal ka BP, and

increase to a maximum of 180 $cm^{-3}$ grains and spores during the Holocene. Concentrations of foraminifer linings are highly variable within a 0-$10^4$ $cm^{-3}$ range (Fig. 1.3). Moderate concentrations are present until after H2, decrease to < 10 $cm^{-3}$ until after H1, then increase to maximum values through the Holocene. These three groups of microfossils follow similar trends, with lower concentrations during the glacial interval and higher throughout the post-glacial. The deglacial interval depicts moderate concentrations of these palynomorphs, possibly due to higher sedimentation rates.

Reworked palynomorphs include pollen, spores and dinocysts, in addition to acritarchs. They reflect erosion from the Paleozoic-Mesozoic sedimentary formations of the Canadian Arctic and West Greenland (e.g., Hiscott et al., 2001). They are present until ~8.3 cal ka BP (Fig. 1.3) with concentrations reaching as much as 1200 $cm^{-3}$. The reworked palynomorph peaks are correlated with H3(?), 2, and 1. They likely correspond to sedimentary reworking during triggered ice-surging events.

The dinocyst assemblages are dominated by *Brigantedinium* spp., *Operculodinium centrocarpum*, *Nematosphaeropsis labyrinthus*, cysts of *Pentapharsodinium dalei* and *Islandinium minutum* (Fig. 1.4). They are accompanied by *Spiniferites elongatus*, *Spiniferites ramosus*, *Impagidinium sphaericum*, *Impagidinium pallidum*, and *Selenopemphix quanta*. The complete dataset is available at http://www.geotop.ca.

The interval from ca. 36 to 15.7 cal ka BP consists of nearly 100% *Brigantedinium* spp. From ca. 15.7 to 12.2 cal ka BP the dinocyst assemblage (Fig. 1.4) consists of > 80% *Brigantedinium* spp., and up to 12% *I. minutum* and 9% *S. quanta*.

After ~12.2 cal ka BP, the dinocyst assemblages are characterized by important changes. Several species emerge including *O. centrocarpum*, *N. labyrinthus*, the cysts of *P. dalei*, *S. elongatus*, *S. ramosus* and *I. sphaericum* (Fig. 1.4). *Brigantedinium*

spp. decreases to less than 25% and *I. minutum* increases to a maximum of 30%. The relative abundance of taxa depicts important changes from ca. 12.2 to 8.3 cal ka BP. In particular, there is an increasing trend of the cyst of *P. dalei*, which reached maximum values of 44% at ~8.3 ka cal BP.

The samples included in the ~8.3 cal ka BP-drainage layer may consist of a mixture of sediments from different environments (upper slope/shelf) and/or earlier deposits. Nonetheless, the dinocyst samples within this layer were analyzed assuming that they would mostly relate to productivity in the overlying water column, contemporaneous of the drainage event. The species assemblages of these samples are very similar to one another and comparable to underlying samples. However some contain ~1% of *Spiniferites mirabilis-hyperacanthus*, which is a temperate taxon (cf. Rochon et al., 1999).

From ca. 8.3 to 2.0 cal ka BP, the occurrence of *I. minutum* decreases significantly and the assemblages are dominated by *O. centrocarpum* (>60%). A near disappearance of *P. dalei*, a decrease in *Spiniferites* species, and the inception of *I. pallidum* are also observed. After ~2.0 cal ka BP, the relative abundance of *O. centrocarpum* decreases from > 60 to 40% and *N. labyrinthus*, which is a species currently found in the subarctic waters of the Labrador Sea (Rochon and de Vernal, 1994; Rochon et al., 1999), increases from 20 to 60%.

### 1.4.3 Reconstruction of sea surface conditions

The reconstruction of sea surface conditions using MAT shows the succession of three very different types of environment (Fig. 1.5a). The northwest Labrador Sea was perennially to quasi-perennially ice covered throughout the glacial interval and until ~12.2 cal ka BP. Most samples from ca. 36.6 to 15.7 cal ka BP contain

extremely low dinocyst concentrations. The cyst counts are low and are therefore statistically weak for quantitative reconstruction. Nevertheless, the few intervals that yielded reliable assemblages (at ~32, 29, 24 cal ka BP) led to reconstruct an almost perennial sea ice cover (> 9 months per year), with low summer SSTs (< 2.5 °C), low SSS (30-32.5) and extremely low productivity (< 100 gC $m^{-2}$). We are thus confident that the intervals almost barren in dinocysts correspond to even harsher conditions, close to nil productivity and perennial sea ice cover. The intervals of increased concentration and higher species diversity recorded between ca. 15.7-12.2 cal ka BP correspond to slightly milder conditions with sea ice for about 9 months per year and summer SST and SSS of about 1.7°C and 31.4, respectively.

A dramatic shift occurred at ~12.2 cal ka BP with increased summer SSTs up to 11°C (Fig. 1.5a, b). From ~12.2 to 8.3 cal ka BP, winter temperatures remained cold (0°C), which resulted in large seasonal gradients of temperature. This interval is also characterized by particularly low salinity, which reached minimum values of 28, and by seasonal sea ice cover to an average of 3 months per year and by an increase in productivity to > 300 gC $m^{-2}$. Whereas these conditions characterized the area until ~8.3 cal ka BP, some variability was recorded. For example, between ca. 10.2 and 10.6 cal ka BP, winter and summer SSTs were at their highest (2.4 and 11.4°C respectively), and SSS and sea ice cover were at their lowest (29.2 and 1.6 months per year respectively).

After ~8.3 cal ka BP until present, the sea surface conditions fluctuate around modern values. Winter SSTs ranged from 1.4 to 3.8°C, summer from 4.5 to 8.6°C, salinity from 33.3 to 34.9, sea ice cover between 0 and 2.9 months per year, and productivity between 133 and 210 gC $m^{-2}$. Unfortunately the low temporal resolution of the Holocene prevents any assessment of variations in sea surface conditions that could correlate to climate/ocean trends depicted elsewhere in the Labrador Sea (e.g., de Vernal and Hillaire-Marcel, 2006).

### 1.4.4 Foraminiferal $\delta^{18}O$ and $\delta^{13}C$

The stable oxygen and carbon isotopic analyses of 150-250 μm Npl were performed on 115 of the 220 intervals sampled (Fig. 1.5a). Many samples produced few Npl which made it impossible to perform representative isotopic analyses. $\delta^{18}O$ values increase from 4.0 ‰ to 4.8 ‰, from core-bottom to the LGM. Light excursions are recorded at the beginning and/or termination of Heinrich Events H2 (3.4 ‰) and H1 (3.3 and 2.3 ‰). Following H1, $\delta^{18}O$ values jump to ~ 4 ‰ then decrease gradually to < 3 ‰ following the 8.3 cal ka BP event, and remain within a 2.6-3 ‰ range throughout the remaining part of the Holocene.

Large fluctuations are also observed in the $\delta^{13}C$ Npl record (Fig. 1.5a). The $\delta^{13}C$ values varied between 0.4 ‰ and -0.2 ‰, with a minimum value bracketing H1. A lesser pronounced $\delta^{13}C$ minimum also occurs between ca 11 and 12 cal ka BP (Figs. 1.5a, b). Then $\delta^{13}C$ values increased through the Holocene to a maximum of 1.0 ‰ by ~3 ka, followed by a decrease towards ~0.5 ‰ in near surface samples.

## 1.5 Discussion

Aside short events and high frequency fluctuations in sea surface conditions, the palynomorph concentrations, dinocyst assemblages, sea surface reconstructions and stable isotopes of Npl highlight two major oceanographic changes over the last ~36 ka (Fig. 1.5a). They define three ecostratigraphic units that indicate the succession of different hydrographic environments in the area: (1) a glacial phase spanning from the base of the core to ca. 12.2 cal ka BP, (2) a regional deglacial phase from ca 12.2 to 8.3 cal ka BP, and (3) a fully "postglacial" interval from ~8.3 cal ka BP to present.

These ecostratigraphic units are discussed below with reference to large-scale oceanic circulation in the Labrador Sea and the glacial paleogeography of eastern Canada.

### 1.5.1 The glacial phase (ca 36.6-12.2 cal ka BP)

The glacial phase is characterized by extremely low concentrations of modern palynomorphs and foraminifera, indicating low productivity likely due to perennial or quasi-perennial sea ice cover (Fig. 1.3). Slightly higher dinocyst concentrations are observed, notably between ca 15.7 and 12.2 cal ka BP, with assemblages almost exclusively dominated by heterotrophic species such as *Brigantedinium* and *Islandinium* (Fig. 1.4) that tolerate harsh conditions with dense ice cover (de Vernal et al., 1997, 2001, 2013; Rochon et al., 1999). Reconstructions based on MAT confirm that modern analogues are from the Canadian Arctic where very cold conditions and quasi-perennial sea ice cover prevail (Fig. 1.5a). Therefore the northwest Labrador Sea was mainly perennially ice covered until 15.7 cal ka BP when conditions improved slightly allowing for some seasonal breakup and primary productivity. Sea surface reconstructions in sites located further south along the Labrador slope (P021; Fig. 1.1), also suggested harsh conditions during this interval (de Vernal et al., 2001). However, in the southern Labrador Sea (P094; Fig. 1.1), several high amplitude fluctuations of sea surface conditions with episodes of slightly warmer conditions and lesser extent of seasonal ice cover were reported (de Vernal et al., 2000, 2005). Such episodes marked by milder conditions were thus likely restricted to the southern Labrador Sea and did not extend to the northwest.

The high Npl-$\delta^{18}O$ values of the glacial interval are interrupted by light-$\delta^{18}O$ excursions at the end of H1 and H2 (Fig. 1.5a). Low concentrations of foraminifera, likely due to low productivity and dilution in sediment because of high depositional rates during HEs (Fig. 1.2), prevented analyses to be made within the detrital layers

related to the events. In any case, the light excursions associated with HEs have been recorded in other cores of the Labrador Sea and interpreted as reflecting dilution by meltwater pulses (e.g., Andrews et al., 1994a; Hillaire-Marcel and Bilodeau, 2000; Hillaire-Marcel et al., 1994; Rashid et al., 2011). Hillaire-Marcel and de Vernal (2008) suggested that they do not exclusively relate to meltwater, but reflect the transfer of the low sea surface salinity signal to subsurface waters through the production of isotopically-light brines which sank to Npl-habitat depth, i.e., on the pycnocline between the surface and intermediate water layers. Since Npl requires growth in waters with salinity above ~34 and can tolerate much higher salinities (Hilbrecht, 1996; Bergami et al., 2009), and since MAT reconstructions indicate continuously cold, low saline and densely sea ice covered surface waters, it seems likely that the terminations of the HEs were characterized by heavy ice production, causing the brine induced $\delta^{18}O$ shifts.

The Bølling-Allerød (BA; ~14.7-12.9 cal ka BP) and the Younger Dryas (YD; ~12.9-11.6 cal ka BP) are not obvious in the northwest Labrador Sea record. The sea surface reconstructions and Npl-$\delta^{18}O$ values show no clear indications for warmer conditions corresponding to the BA. Consequently, there is no evidence for cooling related to the YD (Fig. 1.5b). From around 14 to 13 cal ka BP, though, increased concentrations of dinocysts (Fig. 1.3) coupled with the highest calculated sedimentation rates in the core (Fig. 1.2) might suggest enhanced productivity. This interval could thus represent slightly improved conditions during the BA. Very low palynomorph concentrations (Fig. 1.3) coupled with a peak in coarse fraction content during a brief episode between ~12.8 and ~12.5 cal ka BP (245-216 cm; Fig. 1.2) suggest higher detrital input likely related to ice-rafting activity, which might thus constitute the local signature of the early YD. However, there is no evidence for a significant change in sea surface conditions prior to ~12.2 cal ka BP. The high Npl-$\delta^{13}C$ values prior to ~12.2 cal ka BP (Fig. 1.5b) could indicate an enhanced ventilation rate of the subsurface water mass (e.g., Ravelo and Hillaire-Marcel, 2007). However the dense

sea ice cover would inhibit vertical convection. Veum et al. (1992) and Bauch et al. (2001) also observed an increase in Npl-$\delta^{13}C$ in the GIN Seas during the YD, matching a similar trend in benthic-$\delta^{13}C$. They considered it as the result of intermediate water formation caused by vertical convection during the YD cooling. We are thus tempted to assign the ~12.4-12.2 ka $\delta^{13}C$-peak in PC04 with the inflow of an intermediate component of the North Atlantic Deep Water produced in the GIN Seas during an interval marked by dense sea ice cover and strong stratification between the cold and diluted surface water layer in the Labrador Sea and warmer North Atlantic water. The $\delta^{18}O$ and $\delta^{13}C$ profiles in core PC04 are comparable to those from the more thoroughly dated P094 at Orphan Knoll (Fig. 1.1; Clarke et al., 1999; de Vernal and Hillaire-Marcel, 2000). However unlike P094, PC04 and other adjacent cores (Rashid et al., 2011) do not have a carbonate peak defining H0 making it difficult to estimate the timing of the YD (e.g., Pearce et al., 2013) and the shift in oceanic regime.

### 1.5.2 The deglaciation phase (ca. 12.2-8.3 cal ka BP)

Dinocyst species associated with the phototrophic productivity in subpolar-temperate waters, such as *Spiniferites* spp., *Pentapharsodinium dalei, Nematosphaeropsis labyrinthus* and *Impagidinium sphaericum* (e.g., Rochon et al., 1999), occurred in significant numbers at about 12.2 cal ka BP (Fig. 1.4), thus marking the end of full glacial conditions in the northwest Labrador Sea. A similar shift at the glacial-interglacial transition has been reported from the Labrador slope core P021 (de Vernal et al., 2001). Therefore this transition seems to be regionally consistent, and its timing, around 12.2 cal ka BP is well constrained from the record of core PC04.

The dinocyst assemblages of the 12.2-8.3 ka interval contain species characteristic of temperate waters (cf. above), but also taxa typical of seasonal sea ice cover such as

*Islandinium minutum*. Therefore, the overall assemblages suggest strong seasonal gradients of temperatures. Accordingly, MAT reconstructions indicate that surface water conditions dramatically changed at 12.2 ka from very cold and quasi-perennial sea ice covered, to cool, fresher, and ice free for most of the year (Fig. 1.5b). The reduced salinity is associated with meltwater fluxes from the LIS (e.g., Dyke et al., 2004). It was accompanied by strong stratification of the upper water masses and resulted in low thermal inertia of the surface layer, which is consistent with large seasonal gradients of temperature in the surface layer marked by warm summers and freezing conditions in winter (cf. also Solignac et al., 2004).

During the deglaciation phase, the $\delta^{13}C$ values in Npl remained light until the final phase of the deglaciation (Fig. 1.5b). This indicates a lack of ventilation of the subsurface water mass (e.g., Ravelo and Hillaire-Marcel, 2007). The isotopic and dinocyst data together illustrate highly stratified upper water masses in the Labrador Sea during the deglaciation as previously shown by de Vernal and Hillaire-Marcel (2006). This stratification prevented vertical convection and intermediate water formation at a regional scale.

Although the sea surface conditions reconstructed from the PC04 dinocyst record fluctuated slightly throughout the deglacial phase, there is one prominent interval around 10.4 cal ka BP. MAT reconstructions are marked by minimum salinity values coupled with relatively high winter SST and less than two months per year of sea ice cover (Fig. 1.5b), indicating continued stratification. The isotopes of Npl suggest an influx of a warmer, more ventilated subsurface water mass. The timing of this shift roughly coincides with a retreat in the Hudson Strait Ice Stream (Dyke and Prest, 1987) between the Gold Cove Advance (~11.4-11.0 cal ka BP; Andrews et al., 1999) and the Nobel Inlet Advance (~10.2-9.5 cal ka BP; Jennings et al., 1998). Nearly simultaneously, the Northwest Passage became fully deglaciated (by ~10.3 ka; cf. Dyke, 2004) and Nares Strait began to open (~10.6 cal ka BP; England et al., 2006).

The deglaciation of northeastern Canada would have been fostered by climate warming due to maximum summer insolation (Berger and Loutre, 1991). Therefore ~10.4 cal ka BP marks an interval of increased stratification due to intense meltwater input from the LIS and Arctic channels, and possibly a high subsurface inflow of NEADW in response to its enhanced overflow from the Nordic Seas during the early Holocene (e.g., Weaver and Hillaire-Marcel, 2004; see also Levac et al., 2001; Lloyd et al., 2005; Knudsen et al., 2005). The warmer sea surface conditions reflect the maximum warming of the early Holocene Thermal Optimum observed in other records from the Northwest Atlantic (de Vernal and Hillaire-Marcel, 2006).

### 1.5.3 The Postglacial phase (~8.3 cal ka BP to present)

The averaged reconstruction for the ~8.3 cal ka BP layer assemblages suggests both warm winter and summer SSTs (Fig. 1.5b). Four of the 9 samples comprising the 36-85 cm interval contain specimens of the warm water species *S. mirabilis* (cf. Rochon et al. 1999). Assuming these specimens are not reworked, the assemblage might indicate some advection of North Atlantic waters to the northern Labrador Sea. Mild sea surface conditions, along with the negligible changes in the subsurface isotope values, correlate with other records from the Labrador Sea (Hillaire-Marcel et al., 2007) indicating a barely visible impact of the final drainage of glacial Lake Agassiz on surface and subsurface waters.

After ~8.3 cal ka BP, the dinocyst assemblages were dominated by *O. centrocarpum* (>60%) with few remaining heterotrophic taxa, which suggest relatively warm winter and cool summer SSTs and thus a reduced seasonal temperature gradient (Figs. 1.4, 1.5b; Rochon et al., 1999). They also indicate increased salinity, and decreased sea ice extent. Such sea surface conditions are attributed to reduced meltwater from the breakup of the LIS, which had retreated by more than 90% by ~7.5 cal ka BP (Dyke,

2004). Less meltwater resulted in reduced stratification thus giving way to winter convection and ventilation of the intermediate water mass, as shown by the switch to high $\delta^{13}C$ values in the subsurface dwelling Npl. This regime shift may be associated with inception of intermediate LSW production, as initially documented in core P094 at Orphan Knoll (Hillaire-Marcel et al., 2001) upon the demise of the LIS. A strengthened Irminger Current (IC) as it was suggested from dinocyst data in the eastern Labrador Sea (P013, Fig. 1.1; Solignac et al., 2004, 2006) would have contributed to enhanced supply of saltier water to the western Labrador Sea and promoted winter convection. This was the second major post-glacial reorganization of surface and subsurface conditions in the northwest Labrador Sea.

The Holocene record of PC04 is characterized by a poor temporal resolution between ca 8 and 4 cal ka BP, preventing detailed interpretation of regional changes for this interval. The upper part of the sequence spanning the last 4000 years has a better resolution and permits some interpretations about the regional paleoceanography. Sea surface conditions were relatively warm at ca 4-3 cal ka BP (Fig. 1.5a), which coincides with the Holocene Thermal Maximum in terrestrial climate records described by Kaufman et al. (2004) and with the northward most migration of marine mollusks along Baffin Island coastlines reported much earlier by Andrews (1972). After ~2.0 cal ka BP, the dinocyst-based reconstructions from core PC04 indicate colder, less saline sea surface conditions with increased ice cover (Fig. 1.5a). The $^{13}C$-depleted and $^{18}O$-enriched Npl suggest more stratified subsurface waters, possibly related to a weakened IC. These conditions could have developed as the results of enhanced flux of cooler, fresher Arctic surface water from the Canadian Arctic Archipelago (CAA) to the Labrador Current. Levac et al. (2001) associated similar sea surface conditions in northern Baffin Bay to an increase in Arctic water flux through Nares Strait. Jennings et al. (2011) also documented an increase in Polar Water in the EGC relative to a decrease in the contribution of Irminger water. Therefore, the recent trend towards colder, less saline surface waters in the northwest

Labrador Sea suggests that there is an increase in Arctic outflow with a strengthened Baffin Island Current and weakened IC, coinciding with the Neoglacial cooling of the northeast Canadian coast (Miller et al., 2005).

## 1.6 Conclusions

Palynological analyses and foraminiferal isotopic analyses of a core from the outlet of Hudson Strait in the deep northwest Labrador Sea revealed that the regional hydrography has been strongly influenced by meltwater discharge from the LIS and/or freshwater fluxes from the Arctic. Several features are singular to the site. Firstly, proximal LIS margin conditions were maintained until ~12.2 cal ka BP. This glacial phase was characterized by quasi-perennial sea ice conditions, with episodes of sea ice break up and extreme sea ice formation at the termination of Heinrich Events. Secondly, both the BA and YD climatic events were not clearly recorded. Thirdly, during the local deglacial interval from ca. 12.2 to 8.3 cal ka BP, meltwater from the retreating LIS contributed to low sea surface salinity, as low as 28 in the surface water, which resulted in a strong stratification that prevented convective mixing. This allowed a strong summer warming with SST reaching up to 11°C and reduced sea ice cover (down to 3 months per year). As a consequence, the habitat of the planktic foraminifer Npl, which requires salinity above 34 to develop (e.g., Spindler and Dieckmann, 1986; Bergami et al., 2009), was displaced towards the deeper end of the pycnocline with the intermediate water mass where such conditions could be found. This behavior would thus account for the departure of isotopic records in planktics from values in agreement with temperatures and salinities of the surface water layer recorded by dinocysts. Finally, one may interpret the complicated paleoceanography of the area as a response to the combined influences of the thermal

conditions in the North Atlantic, the local ice history and the late opening of the Canadian Arctic channels. Therefore, the major paleoceanographic reorganizations observed in the northwest Labrador Sea at ca. 12.2 and 8.3 cal ka BP are regionally consistent but have no analogue elsewhere. This again highlights the strong regionalism characterizing the North Atlantic oceanographic response to climatic changes (Solignac et al., 2004, 2006; de Vernal and Hillaire-Marcel, 2006).

Acknowledgements

This paper is a contribution to the Past4Future project of the 7th Framework Program of the European Commission. Support from the *Ministère du Développement Économique, Innovation et Exportation* (MDEIE) and *Fonds Québécois de Recherche sur la Nature et les Technologies* (FQRNT) is acknowledged. Special thanks to the Canadian Foundation for Climate and Atmospheric Sciences (CFCAS), Natural Resources Canada (NRCan), and the Natural Sciences and Engineering Research Council of Canada (NSERC) for their financial support of the HU2008029 expedition in the Labrador Sea. Special thanks to Owen Brown, Rob Fensome, Peta Mudie, and Graham Williams at NRCan (Bedford Institute of Oceanography) for their in kind support of laboratory equipment, to Pierre Francus (INRS) for the CAT-scan images, and to Maryse Henry and Jean-François Hélie for their help and expertise in the GEOTOP laboratories. We are also grateful to the reviewers who provided useful and constructive comments on the manuscript.

# REFERENCES

Andrews, J.T., 1972. Recent and fossil growth rates of marine bivalves, Canadian Arctic, and Late-Quaternary Arctic marine environments. Palaeogeography, Palaeoclimatology, Palaeoecology 11 (3), 157-176.

Andrews, J.T., Tedesco, K., 1992. Detrital carbonate-rich sediments, northwestern Labrador Sea: implications for ice-sheet dynamics and iceberg rafting (Heinrich) events in the North Atlantic. Geology 20 (12), 1087-1090.

Andrews, J.T., Erlenkeuser, H., Tedesco, K., Aksu, A.E., Jull, A.J., 1994a. Late Quaternary (stage 2 and 3) meltwater and Heinrich events, northwest Labrador Sea. Quaternary Research 41 (1), 26-34.

Andrew, J.T., Tedesco, K., Briggsa, W.M., Evans, L.W., 1994b. Sediments, sedimentation rates, and environments, southeast Baffin Shelf and northwest Labrador Sea, 8 - 26 ka. Canadian Journal of Earth Sciences 31 (1), 90-103.

Andrews, J.T., Jennings, A.E., Kerwin, M., Kirby, M., Manley, W., Miller, G.H., Bond, G., MacLean, B., 1995. A Heinrich-like event, H-0 (DC-0): Source(s) for detrital carbonate in the North Atlantic during the Younger Dryas chronozone. Paleoceanography 10 (5), 943-952.

Andrews, J.T., Kirby, M.E., Aksu, A., Barber, D.C., Meese, D., 1998. Late Quaternary detrital carbonate (dc-) layers in Baffin Bay marine sediments (67°–74° n): correlation with Heinrich events in the North Atlantic? Quaternary Science Reviews 17 (12), 1125-1137.

Andrews, J.T., Keigwin, L., Hall, F., Jennings, A.E., 1999. Abrupt deglaciation events and Holocene palaeoceanography from high-resolution cores, Cartwright Saddle, Labrador Shelf, Canada. Journal of Quaternary Science 14 (5), 383-397.

Andrews, J.T., Barber, D.C., Jennings, A.E., Eberl, D.D., Maclean, B., Kirby, M.E., Stoner, J.S., 2012. Varying sediment sources (Hudson Strait, Cumberland Sound, Baffin Bay) to the NW Labrador Sea slope between and during Heinrich events 0 to 4. Journal of Quaternary Science 27, 475-484.

Barber, D.C., Dyke, A., Hillaire-Marcel, C., Jennings, A.E., Andrews, J.T., Kerwin, M.W., Bilodeau, G., McNeely, R., Southon, J., Morehead, M.D., Gagnonk, J.-M., 1999. Forcing of the cold event of 8,200 years ago by catastrophic drainage of Laurentide lakes. Nature 400 (6742), 344-348.

Bard, E., 2001. Paleoceanographic implications of the difference in deep-sea sediment mixing between large and fine particles. Paleoceanography 16 (3), 235-239.

Bauch, H.A., Erlenkeuser, H., Spielhagen, R.F., Struck,U., Matthiessen, J., Thiede, J., Heinemeier, J., 2001. A multiproxy reconstruction of the evolution of deep and surface waters in the subarctic Nordic seas over the last 30,000 yr. Quaternary Science Reviews 20 (4), 659-678.

Bé, A.W.H., Tolderlund, D.S., 1971. Distribution and ecology of planktonic foraminifera. In: Funnell, B.M., Riedel, W.R., (eds), The micropaleontology of oceans. Cambridge University Press, London.

Bergami, C., Capotondi, L., Langone, L., Giglio, F., Ravaioli, M., 2009. Distribution of living planktonic foraminifera in the Ross Sea and the Pacific sector of the Southern Ocean (Antarctica). Marine Micropaleontology 73 (1), 37-48.

Berger, A.L., Loutre, M.F., 1991. Insolation values for the climate of the last 10 million years. Quaternary Science Reviews 10 (4), 297-317.

Berger, W.H., Johnson, R.F., 1978. On the thickness and the $^{14}C$ age of the mixed layer in deep sea carbonates. Earth and Planetary Science Letters 41 (2), 223-227.

Campbell, D.C., de Vernal, A., and shipboard party. 2009: CGS Hudson Expedition 2008029: Marine geology and paleoceanography of Baffin Bay and adjacent areas, Nain, NL to Halifax, NS, August 28-September 23. Geological Survey of Canada, Open File 5989.

Carstens, J., Hebbeln, G., Wefer, G., 1997. Distribution of planktic foraminifera at the ice margin in the Arctic (Fram Strait). Marine Micropaleontology 29, 257-269.

Cheng, W., Rhines, P.B., 2004. Response of the overturning circulation to high-latitude fresh-water perturbations in the North Atlantic Climate Dynamics 22, 359-372.

Clarke, G.K.C., Marshall, S.J., Hilllaire-Marcel, C., Bilodeau, G., Veiga-Pires, C., 1999. A glaciological perspective on Heinrich events. In: Clark, P.U., Webb, R.S., Keigwin, L.D. (Eds.), Mechanisms of Global Climate Change at Millennial Time Scales. Geophysical Monograph Series, vol. 112.

Cuny, J., Rhines, P.B., Niiler, P.P., Bacon, S., 2002. Labrador Sea boundary currents and the fate of the Irminger Sea Water. Journal of Physical Oceanography 32 (2), 627-647.

Curry, B., Lee, C.M., Petrie, B., 2011. Volume, Freshwater, and Heat Fluxes through Davis Strait, 2004-05*. Journal of Physical Oceanography 41 (3), 429-436.

de Vernal, A., Hillaire-Marcel, C., 2000. Sea-ice cover, sea-surface salinity and halo-thermocline structure of the northwest North Atlantic: modern versus full glacial conditions. Quaternary Science Reviews 19 (1), 65-85.

de Vernal, A., Hillaire-Marcel, C., 2006. Provincialism in trends and high frequency changes in the northwest North Atlantic during the Holocene. Global Planetary Change 54 (3), 263- 290.

de Vernal, A., Larouche, A., Richard, P.J.H., 1987. Evaluation of palynomorph concentrations: do the aliquot and the marker-grain methods yield comparable results? Pollen et Spores 29 (2-3), 291-303.

de Vernal, A., Bilodeau, G., Hillaire-Marcel, C., Kasou, N., 1992. Quantitative assessment of carbonate dissolution in marine sediments from foraminifer linings vs. shell ratios: example from Davis Strait, NW North Atlantic. Geology 20 (6), 527-530.

de Vernal, A., Rochon, A., Turon, J.-L., Matthiessen, J., 1997. Organic-walled dinoflagellate cysts: palynological tracers of sea-surface conditions in middle to high latitude marine environments. GEOBIOS 30 (7), 905-920.

de Vernal, A., Henry, M., Bilodeau, G., 1999. Technique de préparation et d'analyse en micropaléontologie. Les Cahiers du GEOTOP, Université du Québec à Montréal, 3, unpublished report.

de Vernal, A., Hillaire-Marcel, C., Turon, J.-L., Matthiessen, J., 2000. Reconstruction of sea-surface temperature, salinity, and sea-ice cover in the northern North Atlantic during the last glacial maximum based on dinocyst assemblages. Canadian Journal of Earth Sciences 37 (5), 725-750.

de Vernal, A., Henry, M., Matthiessen, J., Mudie, P.J., Rochon, A., Boessenkool, K., Eynaud, F., Grøsfjeld, K., Guiot, J., Hamel, D., Harland, R., Head, M.J., Kunz-Pirrung, M., Levac, E., Loucheur, V., Peyron, O., Pospelova, V., Radi, T., Turon, J.-L., Voronina, E., 2001. Dinoflagellate cyst assemblages as tracers of sea surface conditions in the northern North Atlantic, Arctic and sub-arctic seas: the new "n=677" database and application for quantitative paleoceanographical reconstruction. Journal of Quaternary Science 16 (7), 681-699.

de Vernal, A., Eynaud, F., Henry, M., Hillaire-Marcel, C., Londeix, L., Mangin, S., Matthiessen, J., Marret, F., Radi, T., Rochon, A., Solignac, S., Turon, J.L., 2005. Reconstruction of sea surface conditions at middle to high latitudes of the Northern

Hemisphere during the Last Glacial Maximum (LGM) based on dinoflagellate cyst assemblages. Quaternary Science Reviews 24 (7), 897-924.

de Vernal, A., Hillaire-Marcel, C., Solignac, S., Radi, T., Rochon, A., 2008. Reconstructing sea-ice conditions in the Arctic and subarctic prior to human observations. In: Weaver, E. (ed), Arctic Sea ice Decline: Observations, Projections, Mechanisms, and Implications. AGU Monograph Series 180, 27-45.

de Vernal, A., Rochon, A., 2011. Dinocysts as tracers of sea-surface conditions and sea-ice cover in polar and subpolar environments. In IOP Conference Series: Earth and Environmental Science Vol. 14 (1), p. 012007. IOP Publishing.

de Vernal, A., Rochon, A., Fréchette, B., Henry, M., Radi, T., Solignac, S., 2013. Reconstructing past sea ice cover of the Northern hemisphere from dinocyst assemblages: status of the approach. Quaternary Science Reviews, in press.

Dyke, A.S., Prest, V.K., 1987. Late Wisconsinan and Holocene history of the Laurentide ice sheet. Geographie physique et Quaternaire 41 (2), 237-263.

Dyke, A.S., 2004. An outline of the deglaciation of North America with emphasis on central and northern Canada. In: Ehlers, J., Gibbard, P.L., (eds), Quaternary Glaciations, Extent and Chronology. Part II. North America. Developments in Quaternary Science, vol. 2b. Elsevier, Amsterdam.

England, J., Atkinson, N., Bednarski, J., Dyke, A.S., Hodgson, D.A., Ó Cofaigh, C., 2006. The Innuitian Ice Sheet: configuration, dynamics and chronology. Quaternary Science Reviews 25 (7), 689-703.

Forcino, F.L., 2012. Multivariate assessment of the required sample size for community paleoecological research. Palaeogeography, Palaeoclimatology, Palaeoecology 315-316, 134-141.

Gelderloos, R., Straneo, F., Katsman, C.A., 2012. Mechanisms behind the Temporary Shutdown of Deep Convection in the Labrador Sea: Lessons from the Great Salinity Anomaly Years 1968-71. Journal of Climate 25 (19), 6743-6755.

Goosse, H., Fichefet, T., Campin, J.-M., 1997. The effects of the water flow through the Canadian Archipelago in a global ice–ocean model. Geophysical Research Letters 24 (12), 1507-1510.

Head, M.J., Harland, R., Matthiessen, J., 2001. Cold marine indicators of the late Quaternary: The new dinoflagellate cyst genus Islandinium and related morphotypes. Journal of Quaternary Science 16 (7), 621-636.

Hélie, J.-F., 2009. Elemental and stable isotopic approaches for studying the organic and inorganic carbon components in natural samples. In Deep-Sea to Coastal Zones: Methods - Techniques for Studying Paleoenvironments. IOP Conference Series: Earth and Environmental Science 5.

Hesse, R., Khodabakhsh, S., 1998. Depositional facies of the late Pleistocene Heinrich events in the Labrador Sea. Geology 26, 103-106.

Hilbrecht, H., 1996. Extant planktic foraminifera and the physical environment in the Atlantic and Indian Oceans: an atlas based on Climap and Levitus (1982) data. Geologische Institut der Eidgen, Technischen Hochschule und der Universitat Zurich. Neue Folge: Zurich.

Hillaire-Marcel, C., Bilodeau, G., 2000. Instabilities in the Labrador Sea water mass structure during the last climatic cycle. Canadian Journal of Earth Sciences 37 (5), 795-809.

Hillaire-Marcel, C., de Vernal, A., 2008. Stable isotope clue to episodic sea ice formation in the glacial North Atlantic. Earth and Planetary Science Letters 268 (1), 143-150.

Hillaire-Marcel, C., de Vernal, A., Bilodeau, G., Wu, G., 1994. Isotope stratigraphy, sedimentation rates, deep circulation, and carbonate events in the Labrador Sea during the last ~200 ka. Canadian Journal of Earth Science 31 (1), 63-89.

Hillaire-Marcel, C., de Vernal, A., Bilodeau, G., Weaver, A.J., 2001. Absence of deep water formation in the Labrador Sea during the last interglacial periods. Nature 410 (6832), 1073-1077.

Hillaire-Marcel, C., de Vernal, A., Polyak, L., Darby, D., 2004. Size-dependent isotopic composition of planktic foraminifers from Chukchi Sea vs. NW Atlantic sediments-implications for the Holocene paleoceanography of the western Arctic. Quaternary Science Reviews 23 (3), 245-260.

Hillaire-Marcel, C., de Vernal, A., Piper, D.J.W., 2007. Lake Agassiz Final drainage event in the northwest North Atlantic. Geophysical Research Letters 34 (15), L15601.

Hiscott, R.N., Aksu, A.E., Mudie, P.J., Parsons, D.F., 2001. A 340,000 year record of ice rafting, palaeoclimatic fluctuations, and shelf-crossing glacial advances in the southwestern Labrador Sea. Global and Planetary Change 28 (1), 227-240.

Jennings, A.E., Manley, W.F., Maclean, B., Andrews, J.T., 1998. Marine evidence for the last glacial advance across eastern Hudson Strait, eastern Canadian Arctic. Journal of Quaternary
Science 13 (6), 501-514.

Jennings, A., Andrews, J., Wilson, L., 2011. Holocene environmental evolution of the SE Greenland Shelf North and South of the Denmark Strait: Irminger and East Greenland current interactions. Quaternary Science Reviews 30 (7), 980-998.

Kaufman, D.S., et al., 2004. Holocene thermal maximum in the western Arctic (0–180°W). Quaternary Science Reviews 23 (5-6), 529-560.

Knudsen, K.L., Stabell, B., Seidenkrantz, M.-S., Eiriksson, J., Blake Jr., W., 2008. Deglacial and Holocene conditions in northernmost Baffin Bay: sediments, foraminifera, diatoms and stable isotopes. Boreas 37 (3), 346-376.

Kucera, M., 2007. Planktonic foraminifera as tracers of past oceanic environments. In: Hillaire-Marcel, C., de Vernal, A. (eds), Proxies in Late Cenozoic Paleoceanography. Elsevier, The Netherlands, pp. 213-262.

Lazier, J.R.N., 1973. The renewal of Labrador Sea Water. Deep Sea Research 20 (4), 341-353.

Levac, E., de Vernal, A., Blake, W., 2001. Sea surface conditions in northernmost Baffin Bay during the Holocene: palynological evidence. Journal of Quaternary Science 16 (4), 353-363.

Lewis, C.F.M., Miller, A.A.L., Levac, E., Piper, D.J.W., Sonnichsen, G.V., 2012. Lake Agassiz outburst age and routing by Labrador Current and the 8.2 cal ka cold event. Quaternary International 260, 83-97.

Lloyd, J.M., Park, L.A., Kuijpers, A., Moros, M., 2005. Early Holocene palaeoceanography and deglacial chronology of Disko Bugt, west Greenland. Quaternary Science Reviews 24 (14), 1741-1755.

Maccali, J., Hillaire-Marcel, C., Carignan, J., Reisberg, L.C., 2013. Geochemical signatures of sediments documenting Arctic sea-ice and water mass export through Fram Strait since the Last Glacial Maximum. Quaternary Science Reviews 64, 136-151.

Matthews, J., 1969. The assessment of a method for the determination of absolute pollen frequencies. New Phytologist 68 (1), 161-166.

McAndrews, J.H., Berti, A.A., Norris, G., 1973. Key to the Quaternary pollen and spores of the great Lakes region. Life Science Miscellaneous Publications, Royal Ontario Museum, Toronto, Canada.

Miller, G.H., Wolfe, A.P., Briner, J.P., Sauer, P.E., Nesje, A., 2005. Holocene glaciation and climate evolution of Baffin Island, Arctic Canada. Quaternary Science Reviews 24 (14), 1703-1721.

Moore, P.D., Webb, J.A., Collinson, M.E., 1991. Pollen Analysis, 2nd edition. Blackwell Scientific Publications, Oxford.

Pearce, C., Seidenkrantz, M.S., Kuijpers, A., Massé, G., Reynisson, N.F., Kristiansen, S.M., 2013. Ocean lead at the termination of the Younger Dryas cold spell. Nature Communications 4, 1664.

Radi, T., de Vernal, A., 2008. Dinocysts as proxy of primary productivity in mid-high latitudes of the Northern Hemisphere. Marine Micropaleontology 68 (1), 84-114.

Ramsey, C.B., 2008. Deposition models for chronological records. Quaternary Science Reviews 27 (1), 42-60.

Rashid, H., Piper, D.J.W., 2007. The extent of ice on the continental shelf off Hudson Strait during Heinrich events 1-3. Canadian Journal of Earth Sciences 44, 1537-1549.

Rashid, H., Hesse, R., Piper, D.J.W., 2003. Origin of unusually thick Heinrich layers of ice-proximal regions of the northwest Labrador Sea. Earth and Planetary Science Letters 208, 319-336.

Rashid, H., Piper, D.J.W., Flower, B.P., 2011. The role of Hudson Strait outlet in Younger Dryas sedimentation in the Labrador Sea. In: Rashid, H., Polyak, L., Mosley-Thompson, E. (Eds.), Abrupt Climate Change: Mechanisms, Patterns, and Impacts. AGU Geophysical Monograph Series 193, pp. 93-110. Washington, DC.

Ravelo, A.C., Hillaire-Marcel, C., 2007. The use of oxygen and carbon isotopes of foraminifera in paleoceanography. In: Hillaire-Marcel, C., de Vernal, A. (eds), Proxies in Late Cenozoic Paleoceanography. Elsevier, The Netherlands, pp. 735-764.

Reimer, P.J., Baillie, M.G.L., Bard, E., Bayliss, A., Beck, J.W., Blackwell, P.G., Ramsey, C.B., Buck, C.E., Burr, G.S., Edwards, R.L., Friedrich, M., Grootes, P.M., Guilderson, T.P., Hajdas, I., Heaton, T.J., Hogg, A.G., Hughen, K.A., Kaiser, K.F., Kromer, B., McCormac, F.G., Manning, S.W., Reimer, R.W., Richards, D.A., Southon, J.R., Talamo, S., Turney, C.S.M., van der Plicht, J., Weyhenmeyer, C.E.,

2009. INTCAL 09 and MARINE09 radiocarbon age calibration curves, 0-50,000 years Cal BP. Radiocarbon 51, 1111-1150.

Rochon, A., de Vernal, A., 1994. Palynomorph distribution in recent sediments from the Labrador Sea. Canadian Journal of Earth Sciences 31 (1), 115-127.

Rochon, A., de Vernal, A., Turon, J.-L., Matthiessen, J., Head, M.J., 1999. Distribution of dinoflagellate cyst assemblages in surface sediments from the North Atlantic Ocean and adjacent basins and quantitative reconstruction of sea surface parameters. American Association of Stratigraphic Palynologists, Contribution Series No. 35.

Serreze, M.C., Barrett, A.P., Slater, A.G., Woodgate, R.A., Aagaard, K., Lammers, R.B., Steele, M., Moritz, R., Meredith, M., Lee, C.M., 2006. The large-scale freshwater cycle of the Arctic.
Journal of Geophysical Research 111 (C11), C11010.

Simstich, J., Sarnthein, M., Erlenkeuser, H., 2003. Paired d18O signals of *Neogloboquadrina pachyderma* (s) and *Turborotalita quinqueloba* show thermal stratification structure in Nordic Seas. Marine Micropaleontology 48, 107-125.

Solignac, S., de Vernal, A., Hillaire-Marcel, C., 2004. Holocene sea surface conditions in the North Atlantic-contrasted trends and regimes between the eastern and western sectors (Labrador Sea vs. Iceland Basin). Quaternary Science Reviews 23 (3), 319-334.

Solignac, S., Giraudeau, J., de Vernal, A., 2006. Holocene sea surface conditions in the western North Atlantic: Spatial and temporal heterogeneities. Paleoceanography 21 (2), PA2004.

Spindler, M., Dieckmann, G.S., 1986. Distribution and Abundance of the Planktic Foraminifer
Neogloboquadrina pachyderma in Sea Ice of the Weddell Sea (Antarctica). Polar Biology 5 (3), 185-191.

Stoner, J.S., Channell, J.E.T., Hillaire-Marcel, C., 1995. Late Pleistocene relative geomagnetic paleointensity from the deep Labrador Sea: Regional and global correlations. Earth and Planetary Science Letters 134 (3), 237-252.

Stoner, J.S., Channell, J.E.T., Hillaire-Marcel, C., 1996. The magnetic signature of rapidly deposited detrital layers from the deep Labrador Sea: Relationship to North Atlantic Heinrich layers. Paleoceanography 11 (3), 309-325.

Veum, T., Jansen, E., Arnold, M., Beyer, I., Duplessy, J.-C., 1992. Water mass exchange between the North Atlantic and the Norwegian Sea during the past 28,000 years. Nature 356 (6372), 783-785.

Wadley, M.R., Bigg, G.R., 2002. Impact of flow through the Canadian Archipelago and Bering Strait on the North Atlantic and Arctic circulation: An ocean modelling study. Quarterly Journal of the Royal Meteorological Society 128 (585), 2187-2203

Weaver, A., Hillaire-Marcel, C., 2004. Global warming and the next ice-age. Science 304, 400-402.

Wendeberg, M., Richter, J.M., Rothe, M., Brand, W.A., 2011. δ18O anchoring to VPDB: calcite digestion with 18O-adjusted ortho-phosphoric acid. Rapid Communications in Mass Spectrometry 25 (7), 851-860.

Wu, Y.S., Tang, C.L., 2011. Atlas of ocean currents in eastern Canadian waters. Canadian
Technical Report of Hydrography and Ocean Sciences no. 271.

Yashayaev, I., 2007. Hydrographic changes in the Labrador Sea, 1960–2005. Progress in Oceanography 73, 242–276.

Yashayaev, I., Loder, J.W., 2009. Enhanced production of Labrador Sea Water in 2008. Geophysical Research Letters 36 (1), L01606.

Figures

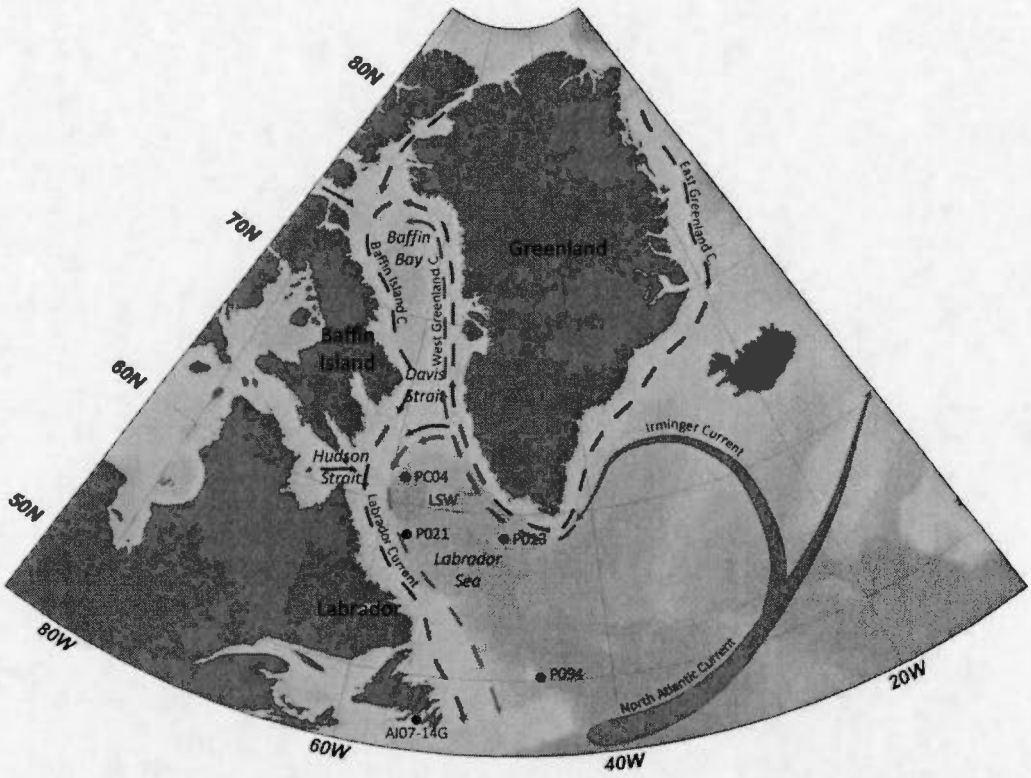


Figure 1.1. Map indicating PC04 coring location (895 cm long piston core; 61.46 °N, 58.04 °W; 2163 m water depth), with surface currents (North Atlantic Current (NAC), Irminger Current (IC), East Greenland Current (EGC), West Greenland Current (WGC), Baffin Island Current (BIC), and Labrador Current (LC)). Neighboring cores P013, P021, P094 and AI07-14G are also displayed. Labrador Sea Water (LSW) is formed in the Labrador Sea approximately at the location indicated by the hatched oval.

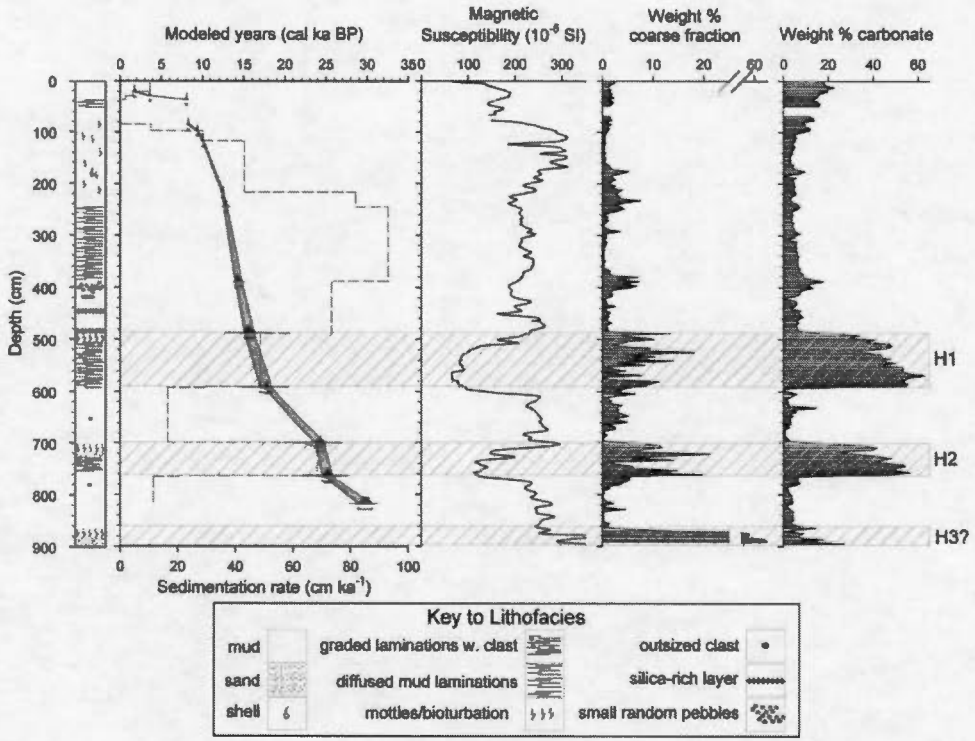


Figure 1.2. Age vs. depth relationship for core PC04 based on lithology, magnetic susceptibility, weight % coarse fraction, weight % carbonate, and $^{14}$Cdates listed in Table 1.1. These parameters assisted in the establishment of Heinrich Events H1, H2 and possibly H3 identified as the hatched intervals. The rapidly deposited H1 and H2 provided prior information for the age model in the form of boundaries (solid horizontal lines). Two separate models were produced before and after the interval of rapid accumulation during the drainage of Lake Agassiz (e.g., Barber et al., 1999; Hillaire-Marcel et al., 2007). The sedimentation rates are represented by the dashed lines.

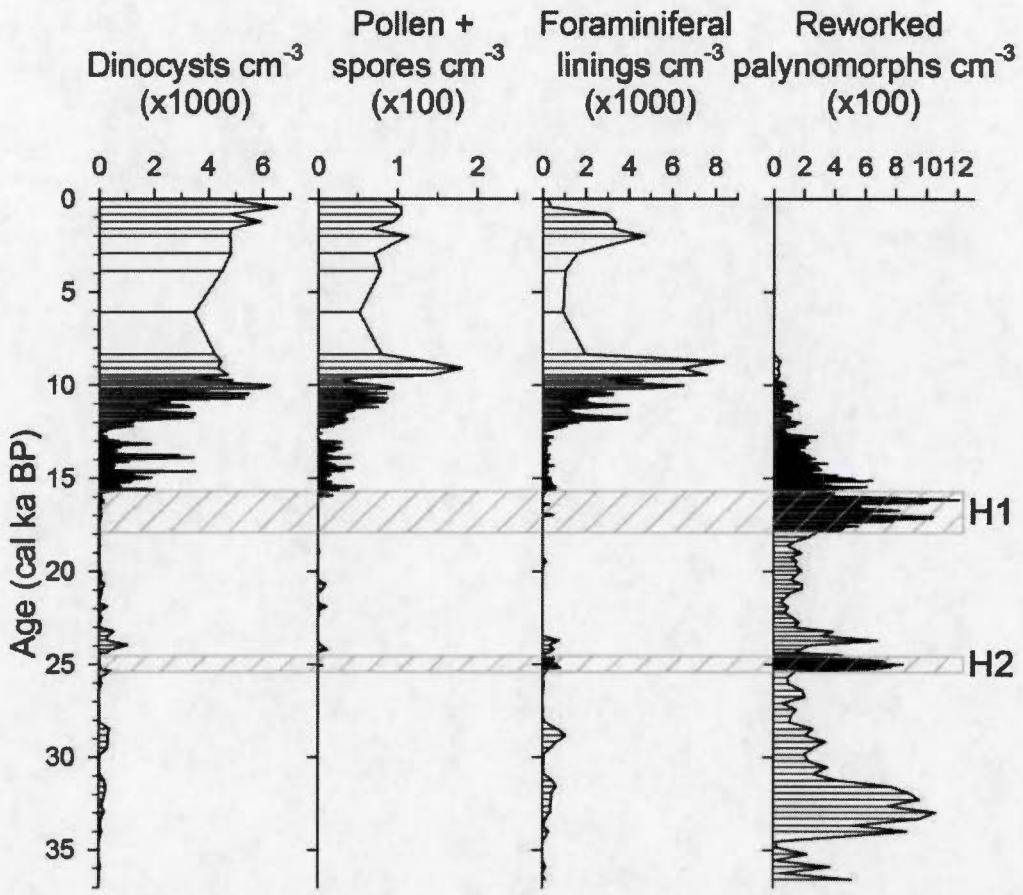


Figure 1.3. Concentrations of dinocysts, pollen and spores, foraminifer linings, and reworked palynomorphs expressed in number of specimen per $cm^3$ of sediment for the last ~36,600 years in core PC04. Peaks of reworked palynomorphs are temporally correlated to Heinrich Events H1 and H2 as identified as the hatched intervals.

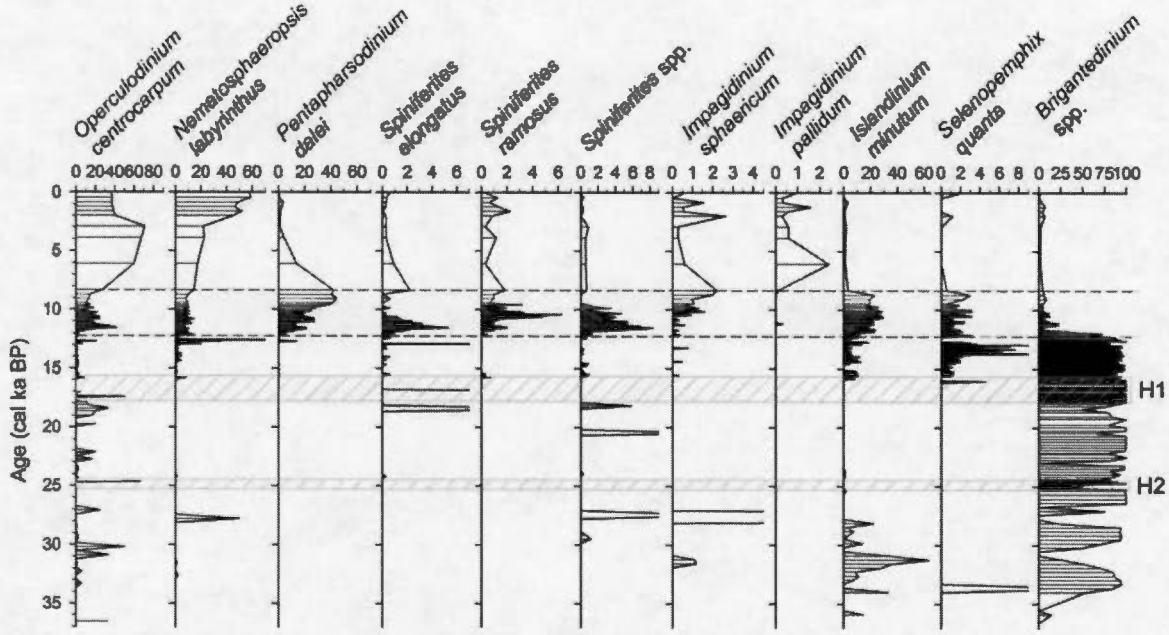


Figure 1.4. Relative abundance (percentage) of the main dinocyst taxa in core PC04 for the last ~36,600 years (note the variable percentage scales). The complete assemblage and tabulation can be found on the GEOTOP website (http://www.geotop.ca). Ecostratigraphic units are separated by a dashed line. Heinrich Events H1 and H2 are identified as the hatched intervals.

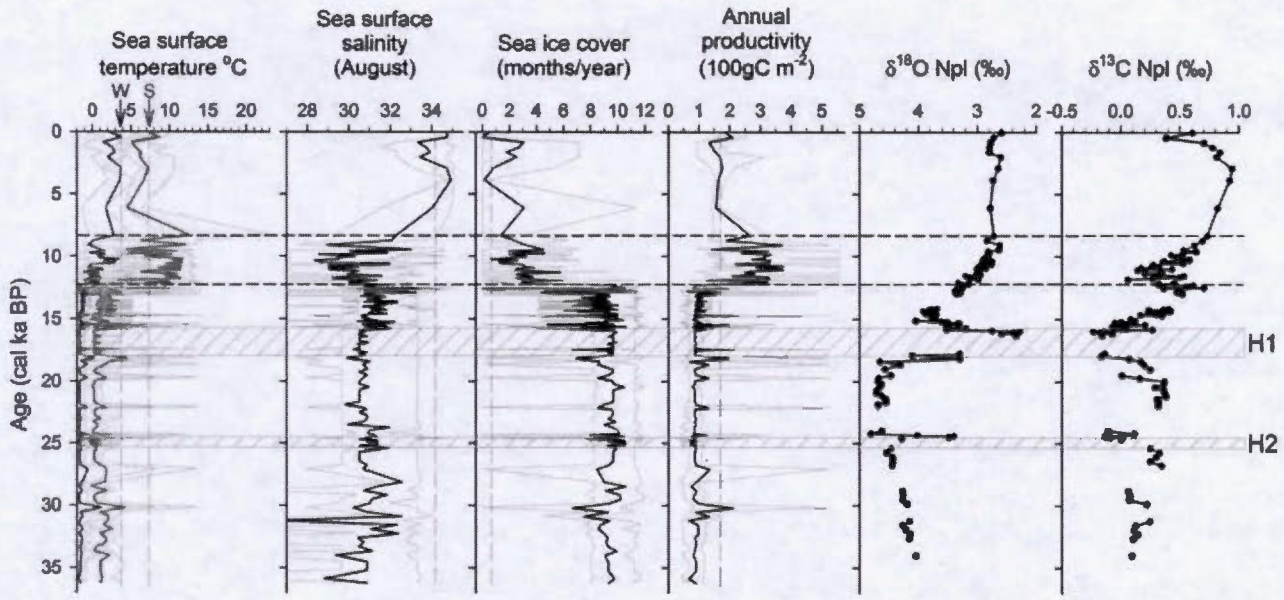


Figure 1.5a. Reconstruction of sea surface conditions covering the past ~36,600 years from dinocyst assemblages and the oxygen and carbon stable isotopes of *Neogloboquadrina pachyderma* left-coiled (Npl) of core PC04. Sea surface temperatures (SST) in winter (w) and summer (s) are represented by blue and pink curves respectively. The lighter blue and pink curves correspond to maximum and minimum SSTs possible as calculated from a set of 5 modern analogues. Sea surface salinity, sea ice cover and annual productivity are represented by black (most probable values) and gray lines (minimum and maximum possible). Modern values of winter and summer sea surface temperature, sea surface salinity and sea ice cover, as provided by the NODC and NSIDC, are indicated by the vertical dashed lines. Ecostratigraphic units are separated by a horizontal dashed line. Heinrich Events H1 and H2 are identified as the hatched intervals.

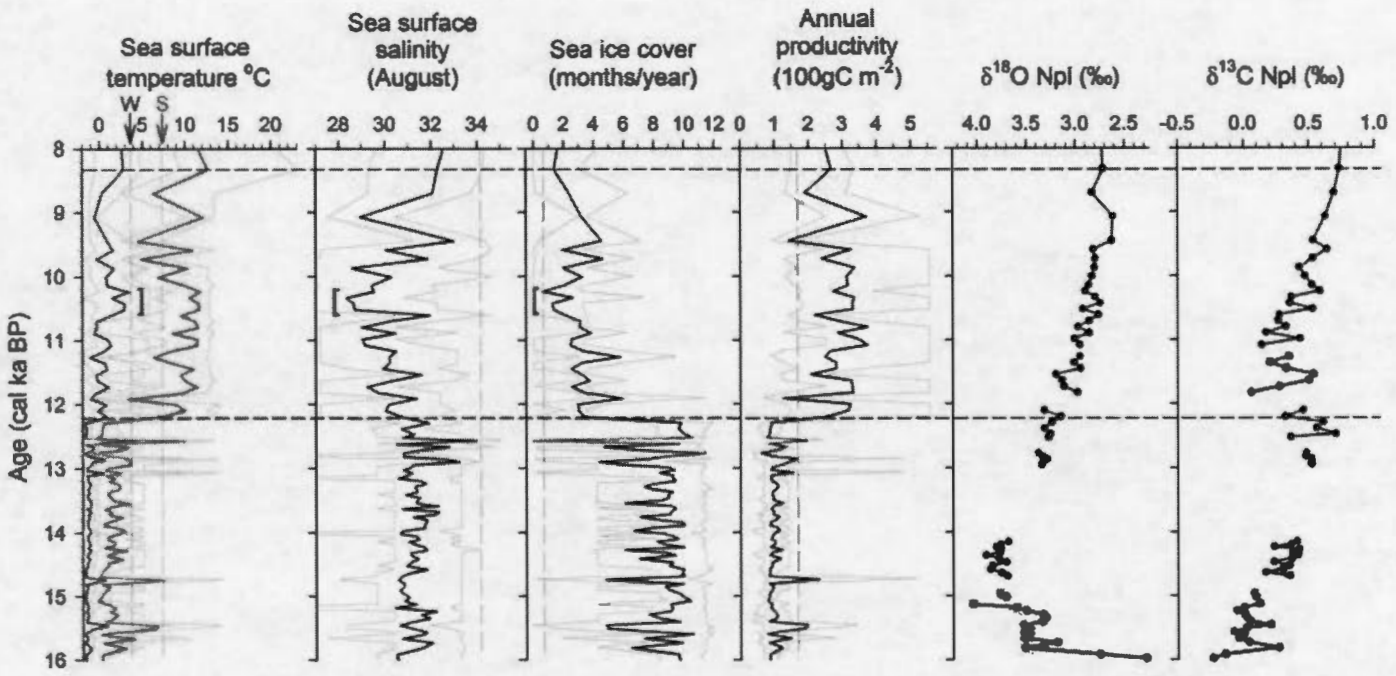


Figure 1.5b Reconstruction of sea surface conditions for the interval spanning 16-8 ka. from dinocyst assemblages and the oxygen and carbon stable isotopes of *Neogloboquadrina pachyderma* left-coiled (Npl) of core PC04. Sea surface temperatures (SST) in winter (w) and summer (s) are represented by blue and pink curves respectively. The lighter blue and pink curves correspond to maximum and minimum SSTs possible as calculated from a set of 5 modern analogues. Sea surface salinity, sea ice cover and annual productivity are represented by black (most probable values) and gray lines (minimum and maximum possible). Modern values of winter and summer sea surface temperature, sea surface salinity and sea ice cover, as provided by the NODC and NSIDC, are indicated by the vertical dashed lines. Ecostratigraphic units are separated by a horizontal dashed line. Red brackets identify the ~10.4 cal ka BP extreme climate event (see text).

Table

Table 1.1. Radiocarbon dates from planktonic foraminifers (*Neogloboquadrina pachyderma* left-coiled).

| Depth (cm) | CAMS/ NOSAMS (OS) Laboratory number [a] | AMS-$^{14}$C ages (years BP)[b] | Calibrated age interval (2σ) (cal years BP)[c] | Modeled age interval (2σ) (cal years BP)[d] | Modeled age median (cal years BP) |
|---|---|---|---|---|---|
| 20-21 | CAMS-153491 | 2,370 ± 60 | 2,151-1,841 | 2,159-1,828 | 1,998 |
| 28-29 | OS-96931 | 3,880 ± 25 | 3,953-3,750 | 3,953-3,751 | 3,850 |
| 36-37* | CAMS-155459 | 7,845 ± 30 | 8,416-8,181 | 8,418-8,179 | 8,319 |
| 68-69* | CAMS-155461 | 7,975 ± 35 | 8,416-8,181 | n/a | n/a |
| 84-85* | CAMS-155462 | 7,735 ± 30 | 8,416-8,181 | 8,441-8,196 | 8,335 |
| 96-97 | CAMS-153492 | 8,780 ± 60 | 9,544-9,302 | 9,540-9,300 | 9,447 |
| 116-117 | CAMS-155463 | 9,290 ± 30 | 10,218-10,033 | 10,218-10,009 | 10,147 |
| 216-217 | CAMS-153493 | 10,990 ± 45 | 12,630-12,380 | 12,620-12,375 | 12,473 |
| 244-245 | CAMS-153494 | 11,400 ± 120 | 13,128-12,636 | 13,071-12,635 | 12,816 |
| 388-389 | CAMS-153495 | 12,700 ± 60 | 14,878-13,952 | 14,871-14,010 | 14,363 |
| 488-489 | CAMS-153496 | 13,360 ± 60 | 16,207-15,076 | 16,359-15,191 | 15,734 |
| 592-593 | CAMS-153497 | 15,120 ± 60 | 18,445-17,615 | 18,447-17,614 | 17,898 |
| 704-705 | CAMS-153498 | 20,860 ± 170 | 24,922-23,932 | 24,907-23,928 | 24,407 |
| 764-765 | OS-96934 | 21,600 ± 160 | 25,906-24,903 | 25,903-24,919 | 25,353 |
| 816-817 | CAMS-153499 | 25,400 ± 370 | 30,687-29,105 | 30,655-29,005 | 29,848 |

[a] The analyses were made at Lawrence Livermore National Laboratory (CAMS) or the National Ocean Sciences AMS Facility (NOSAMS).
[b] Radiocarbon age was calculated using the Libby half-life of 5568 years and corrected with a $\delta^{13}C$ of -25‰.
* Three $^{14}C$ ages were averaged (7852 ± 55) prior to calibration due to their association with the rapid sediment accumulation during the final drainage of glacial lake Agassiz some 8.4 cal ka ago (e.g. Barber et al., 1999; Hillaire-Marcel et al., 2007).
[c] A marine reservoir correction of 400 years was applied with no additional correction (ΔR), and the ages converted to calibrated years using Oxcal 4.2 (Ramsey, 2008) and the Marine09 (Reimer et al., 2009) calibration curve.
[d] The ages were modeled using Oxcal 4.2 (Ramsey, 2008). Modeled ages marked n/a indicate the interval was not used in the age model.

CHAPTER II

# Paleohydrography of Baffin Bay during the last climatic cycle from planktic and benthic foraminiferal records

Olivia T. Gibb[1], Claude Hillaire-Marcel[1], and Anne de Vernal[1]

[1]GEOTOP Research Center, CP. 8888 Succ Centre Ville, Montréal, QC H3C 3P8, Canada

This chapter will be submitted for publication in *Paleoceanography*

Abstract

Baffin Bay is a semi-enclosed basin through which nearly 50% of Arctic freshwater towards the North Atlantic Ocean. Its paleoceanography over the last glacial cycle remains imperfectly established: low biogenic production, poor carbonate preservation, and high terrigenous inputs have hampered paleoceanographic reconstructions. The recent establishment of an age-depth model spanning the last ~116 ka from detailed paleomagnetic measurements in a deep Baffin Bay core (HU2008-029-016PC) has provided the incentive to look deeper into the microfossil content of the core and measure the isotopic composition ($\delta^{18}O$ and $\delta^{13}C$) of foraminifera when present. Three size fractions of the planktic foraminifera *Neogloboquadrina pachyderma* left-coiled (Npl) and two species of benthic foraminifera (*Cassidulina neoteretis* and *C. reniforme*) were hand-picked for isotopic measurements. Almost similar $\delta^{18}O$ values in the benthic and planktic species suggest no stratification between the intermediate and bottom water masses. Episodes marked by high $\delta^{18}O$ values (>+4‰ vs VPDB) occurred during Marine Isotope Stages (MIS) 5d, 3 and the MIS 2/1 transition, likely in response to the advection of saline Atlantic water. The absence of dinocysts during these intervals points toward extremely low productivity and a perennial sea ice cover. Most other samples yield $\delta^{18}O$-Npl values ranging +2.6 to +3.6‰, some matching dinocyst occurrences. These samples suggest intervals of slight breakup of the perennial sea ice cover, thus slightly milder conditions. This new record suggests a harsh, ice-covered environment throughout most of the last glacial cycle, interspersed with occasional penetration of Atlantic water under both cooler (stadial) and warmer (interstadial) intervals.

## 2.1 Introduction

Baffin Bay is a semi-enclosed basin connecting the Arctic and Atlantic oceans (Fig. 2.1). The flow is restricted by sills, allowing cold Arctic surface waters to enter via Lancaster Sound (125 m), Jones Sound (190 m), and Nares Strait (220 m) in the north, and warmer intermediate waters from the Atlantic to enter via Davis Strait (640 m) in the south. During glacial periods, Baffin Bay was surrounded by the Innuitian (IIS), Laurentide (LIS) and Greenland Ice Sheets (GIS), with the GIS extending onto the shelf (Briner et al., 2003, 2006; Dyke, 2004; England et al., 2006; Funder et al., 2011; Ó Cofaigh et al., 2013) further restricting flow. As oceanic circulation is intimately related with ice sheet dynamics and because its location is ideal for investigating the past ice sheet history, Baffin Bay is a basin deserving special attention. However, the Baffin Bay sedimentary record is not ideal for paleoceanographic reconstruction due to the rarity of microfossils and the difficulty to set chronostratigraphies (e.g., Aksu 1983; de Vernal et al., 1987a; Hillaire-Marcel et al., 1989). Variable sedimentation rates during glacial periods due to high detrital inputs related to glacial erosion from surrounding ice sheets adds difficulty (Simon et al., 2012 and refs therein). Moreover, the lack of calcareous foraminifera for radiocarbon dating and the establishment of $\delta^{18}O$ stratigraphy has been the primary hindrance (Aksu and Piper, 1979; Aksu, 1981, 1983; Mudie and Aksu, 1984; de Vernal et al., 1987a; Hillaire-Marcel et al., 1989; Scott et al., 1989). Low concentrations of foraminifera have been explained by dilution due to high sedimentation rates (Scott et al., 1989), low salinities and low productivity due to harsh, ice covered conditions (Hillaire-Marcel et al., 1989), carbonate dissolution (Aksu, 1983), or a combination of these factors (Hillaire-Marcel et al., 1989). The rarity of calcareous foraminiferal tests in Holocene sediments from Baffin Bay is due to a shallow lysocline and dissolution of calcium carbonate at depths > 900 m (Aksu 1983; Osterman and Nelson, 1989; de Vernal et al., 1992; Schröeder-Adams and Van

Rooyen, 2011). These conditions have been associated with the inflow of Pacific waters, through the Canadian Arctic channels, with low carbonate saturation states (Azetsu-Scott et al., 2010), in addition to high biogenic productivity in the North Water polynya responsible for organic matter oxidation at the bottom of Baffin Bay (e.g., de Vernal et al., 1992; Hamel et al., 2002). In sediments predating the Holocene, when Baffin Bay was not subjected to these conditions due to severe ice cover, preservation of calcium carbonate resulted in sporadic occurrence of calcareous foraminiferal tests. Although low foraminiferal abundance remains an issue, isotopic analyses of smaller samples and temporally associating their values with changes in oceanographic circulation is now possible. Recently, based on detailed paleomagnetic data, Simon et al. (2012) have proposed a chronostratigraphical scheme spanning the last 115 ka in core HU2008-029-016 (PC16, Fig. 2.1), which was collected near the Ocean drilling Program (ODP) Site 645 (cf. Arthur et al., 1987; Hillaire-Marcel et al., 1989). This provided an opportunity to revisit the foraminiferal stable isotopes as proxies of paleoceanographic conditions during the late Pleistocene.

Piston core HU2008-029-016PC (henceforth PC16) used for the present study was collected within 0.5 km of core 85-027-016, the site survey core for ODP Site 645 (Fig. 2.1). It was analysed by Hillaire-Marcel et al. (1989) for carbon and oxygen isotope compositions of the planktic foraminifera *Neogloboquadrina pachyderma* left-coiled (Npl) with a sample size of ~50 foraminiferal tests, which constituted a limitation. Samples containing fewer specimens were not plotted or discussed due to large possible analytical offsets in the isotopic analysis of small samples and to possible bias due to the presence of reworked foraminifera. Baffin Bay sediments consist largely of Paleozoic carbonates (Hiscott et al., 1989) eroded and deposited as detrital carbonate by the Laurentide and Innuitian Ice Sheets (Simon et al., 2014). Any detrital carbonate material within foraminiferal tests could bias the measured isotopic composition and result in misleading offsets (Hodell and Curtis, 2008). The

early interpretations of the $\delta^{18}$O-Npl signal from the discontinuous records of Baffin Bay, which included a large range in values, were based on direct correlation with the global marine isotope stratigraphy (Aksu, 1983; Aksu and Mudie, 1985). These interpretations were revised by de Vernal et al. (1987a) who argued that low $\delta^{18}$O-Npl values represent episodic depletions with meltwater inputs instead of interglacial stages. Such an interpretative scheme involving episodic dilution was also used for low $\delta^{18}$O signals in the Labrador Sea (Hillaire-Marcel et al., 1994; Hillaire-Marcel and Bilodeau, 2000; Rasmussen et al., 2003). However, it has recently been suggested that the low $\delta^{18}$O-Npl values in the Labrador Sea might reflect the sinking of isotopically depleted brines at Npl habitat depths, usually along the pycnocline between the more or less diluted surface water layer and the intermediate to deep water masses, due to sea ice production (Hillaire-Marcel and de Vernal, 2008).

Based on technical and conceptual progresses made during the last decades for $\delta^{18}$O measurement in foraminifers, we revisit the last climatic cycle isotope data from Baffin Bay using the new chonostratigraphy of core PC16 (Simon et al., 2012). The carbon and oxygen isotopic compositions of planktic and benthic foraminifera were analysed using fewer tests with a mass spectrometer set up for small $CO_2$ volume measurements. The planktic Npl, which is most commonly found in cold, saline (~34) waters along the pycnocline (Bé and Tolderlund, 1971; Hilbrecht, 1996; Carstens et al., 1997; Volkmann and Menshc, 2001; Simstich et al., 2003; Pados and Spielhagen, 2014) but can also be found near the surface within the chlorophyll maximum under permanent sea ice cover (Volkmann and Mensch, 2001; Pados and Spielhagen, 2014; Xiao et al., 2014), can be used as a proxy for changes in the subsurface water mass. Since planktic foraminiferal size and shell density increase with depth in the water column (Bauch et al., 1997; Volkmann, 2000; Volkmann and Mensch, 2001; Hillaire-Marcel et al., 2004; Xiao et al., 2014), isotopic analyses were performed on three size fractions to assess temperature-salinity (i.e., density) gradients at Npl-habitat depths. Benthic foraminifera were also analysed to assess bottom water conditions and

stratification between Npl-habitat and bottom water masses (e.g., Hillaire-Marcel and Bilodeau, 2000). Special attention has also been paid to possible offsets in foraminiferal oxygen and carbon isotopic values due to contamination with detrital glacially-produced carbonate flours, abundant in deep Baffin Bay sediments. In parallel, palynological analyses were conducted to provide an estimate of the sea surface conditions including temperature, salinity, sea ice cover and productivity from dinocysts, erosion and subsequent deposition from pre-Quaternary palynomorphs, and benthic productivity or degree of carbonate dissolution from the organic linings of benthic foraminifera (e.g., de Vernal et al., 1992). The relative changes in dinocyst abundances will be used as an index of changes in paleoproductivity in the basin. This updated record should provide new insights on paleoceanographical changes in Baffin Bay throughout the last glacial cycle.

### 2.1.1 Modern hydrography

Baffin Bay consists of water from the Arctic and the Atlantic, that are partly stratified into four water masses, with a reverse thermocline between surface and deeper water masses (see Cuny et al., 2002, 2005, and Tang et al., 2004 for details listed below). In the upper part of the water column, the West Greenland Current (WGC) flowing northward results from the mixing of cold low salinity East Greenland Current (EGC; Arctic waters through Fram Strait) with the warm saline waters of the Irminger Current (IC; a westward branch of the North Atlantic Current) which lies above the IC. Once the WGC reaches northern Baffin Bay, it turns west and is cooled by Arctic water from Nares Strait, Lancaster Sound, and Jones Sound. In the western Baffin Bay, this cold (< 0°C), low salinity (< 34) surface water mass flowing south forms the Baffin Island Current (BIC) and extends to 300 m depth before heading south and exiting through western Davis Strait. Underlying the surface water, the Baffin Bay Intermediate Water (BBIW) reaches depths of 800 m. It is warmer and more saline

than the surface layer as it is mainly composed of warm Atlantic water following the WGC path that enters through eastern Davis Strait. At the base, it mixes with some Arctic Intermediate Water (AIW) that passes through Nares Strait (Bourke et al., 1989). The Baffin Bay Deep Water (BBDW) cools with depths reaching 1800 m, due to the sinking of cold brines, and the Baffin Bay Bottom Water (BBBW) covers the deepest areas of the Bay. The mechanism through which the bottom waters are formed remains unknown. Bourke et al. (1989) have suggested that BBBW is a combination of cold, saline brine-convected water formed in winter in northern Baffin Bay. Tan and Strain (1980) have used the $\delta^{18}O$-salinity relationship to show that BBBW could be a combination of sea ice produced brines and deeper water from the Labrador Sea. Sea ice cover in Baffin Bay is currently seasonal (~10 months per year). Ice formation begins in September in the northwest reaches of Baffin Bay and expands southeast until it reaches complete ice cover in March (Tang et al., 2004). Sea ice melt begins in April in the southeast. Sea ice concentrations and seasonal duration are usually lower in the east due to the warmer WGC, and interannual variability is coupled to winter air temperatures and wind.

## 2.2 Material and methods

Core HU2008-029-016 (PC16) is a 741 cm long piston core from deep Baffin Bay (Fig. 2.1; 70°46.14 N, -64°65.77 W; 2063 m; Campbell et al., 2009). The coring site is within close proximity to ODP Site 645 and 85-027-016, which is useful for correlating with previous records. Some of the physical properties of PC16 were compiled by Simon et al. (2012) including stratigraphic log indicating grain size and sedimentary features, as well as the Baffin Bay Detrital Carbonate (BBDC) layers. The core consists of four sedimentary facies. The first is a brown to dark brown silty

mud found in the upper most part of the core (~post-glacial section). Below, three facies are seen in alternation. They include i) an "olive clay" facies, which is composed of brownish black and olive-black silty to clayey muds, ii) a "detrital carbonate" facies (cf. the BBDC layers), which consists of carbonate-rich, yellowish-brown to dark brown very poorly sorted muds with gravel and sand, and iii) a "low detrital carbonate" facies with olive gray to dark gray muds containing poorly sorted sands as well as low amounts of gravel and sand (Simon et al., 2012). The chronostratigraphy of this core (Simon et al., 2012) is based on the correlation of the high-resolution magnetic paleointensity record to regional and global paleointensity curves, and is placed on the GISP2 age scale. The age model correlates well with three radiocarbon dates, two geomagnetic excursions, and with other regional records (Simon et al., 2012). Linear interpolation between tie points used in the age-depth model is used to plot proxy data against age.

Subsampling of 1 cm slices for microfossils was initially performed at 8 cm intervals, which provides an average time resolution of 1.2 ka. The subsamples were sieved at 106 μm and the coarse fraction was kept for further sieving and hand-picking of foraminiferal tests, wheras the fraction < 106 μm was reserved for palynological preparation. *N. pachyderma* (sinistral) left-coiled (Npl) dominates the planktic foraminiferal population as expected from a core collected from Arctic waters (cf. Kucera, 2007). Only rare specimens of *Neogloboquadrina pachyderma* (dextral), *Globigerina bulloides*, and *Turborotalia quinqueloba* were also observed. Thus Npl was the only species analysed for the stable isotopic compositions of oxygen and carbon. Although the samples were initially processed and picked for foraminifera at 8 cm intervals, the sampling resolution was increased in intervals of foraminiferal abundance. On average, 20 Npl specimens were picked from the > 106 μm fraction after rinsing and sieving with water. The clean Npl were sieved into size-classes of 106-150, 150-250, and >250 μm size when present.

Detrital carbonates are abundant in Baffin Bay (Aksu and Piper, 1987). Because foraminiferal tests are often filled with fine detrital material that could potentially be a contamination source, we addressed the possible effect of imperfect cleaning on their isotopic composition. Observation of Npl specimens under scanning electron microscope (SEM) after an initial differentiation under binocular microscope (x10) confirmed the occurrence of clays size particles within their tests (Figs. 2.2a,b). Due to the low numbers of foraminifera, cleaning methods including ultra sonic bath or breaking the tests open were not possible, therefore cleaning process only included rinsing the samples with water while sieving. Therefore "clean" samples contain Npl free of impurities (Fig. 2.2a), and "dirty" samples consist of Npl with tests containing clay sized particles (Fig. 2.2b). From within three samples, "clean" and "dirty" Npl were picked from the 150-250 μm size fraction and analysed to assess possible biases due to contamination by detrital carbonate. In order to estimate the isotopic bias due to the clay sized detrital carbonate from within the tests, the $\delta^{13}C$ and $\delta^{18}O$ were also measured in the < 10 μm size fraction of bulk sediment.

Benthic foraminifera were analysed for their oxygen and carbon isotopic composition in samples also containing Npl. Intervals containing abundant benthic foraminifera were rare and there is no species common throughout the core. However, *Cassidulina neoteretis* and *Cassidulina reniforme*, which occur in many samples were collected and analysed. Due to low numbers, all size fractions were used although some bias on the isotopic composition cannot be totally discarded (Barras et al., 2010). No correction for global ice volume or vital effects was made on the benthic $\delta^{18}O$ and $\delta^{13}C$ since the results are used to document relative changes in water mass within the same records. *C. neoteretis* and *C. reniforme* likely precipitate their test in equilibrium with respect to $\delta^{18}O$, and since they are both infaunal species they depict a $\delta^{13}C$ offset, which has been estimated at about -1.5‰ (for *C. reniforme* see Erbs-Hansen et al., 2013; for *C. neoteretis* see Husum and Hald, 2004). In order to remove

any potential bias due to organic carbon from within the benthic foraminifers, their tests were roasted in a 200°C oven under vacuum for one hour.

All isotopic analyses were conducted at GEOTOP with a MulticarbTM preparation device coupled to an IsoPrimeTM isotope ratio mass spectrometer after acidification with 102% orthophosphoric acid (Wendeberg et al., 2011). The isotopic composition was measured relative to the international reference, the Vienna Pee Dee Belemnite (VPDB), using the conventional "δ-per mil" notation. Reference (NBS 19, IAEA) and working (UQ6 carbonate; Hillaire-Marcel et al., 2004) standards were used for each analytical run as a measure of reproducibility which is better than ±0.05‰ at ±1 σ level (Hillaire-Marcel et al., 2004). Four replicate samples (three Npl and one *C. neoteretis*) were analysed to assess the homogeneity of the foraminiferal isotopic populations (Table 2.1). This was performed by picking two aliquots of ~20 Npl from each sample and analysing both for $\delta^{18}O$ and $\delta^{13}C$. The samples can be replicated within a standard deviation of 0.50‰ for $\delta^{18}O$ and 0.22‰ for $\delta^{13}C$. This is a degree of magnitude greater than the reproducibility of the standard material, which indicates that distinct Npl generations, produced under variable conditions, are mixed in the sediment.

Each sample for palynological analysis consists of a 5 $cm^3$ subsample of sediment from a 1 cm thick section of the core. Each subsample was rinsed through > 106 and < 10 μm mesh sieves. The material was processed according to the methods described by de Vernal et al. (1999). The organic residue is mounted onto a slide with Kaiser's glycerol gelatin and examined for both modern and pre-Quaternary dinoflagellate cysts (dinocysts) and pollen and spores, in addition to the organic linings of foraminiferal tests. Each species of dinocyst was identified following the nomenclature provided by Rochon et al. (1999), de Vernal et al. (2001), and Head et al. (2001). Total numbers of dinocysts were tabulated and concentrations per $cm^3$ were calculated using the marker-grain method (Matthews, 1969) which provides an

accuracy of ±10% for a 95% confidence interval (de Vernal et al., 1987b). Due to the high amounts of mineral remaining in the residue, slide mounting and examination was difficult and lengthy. Therefore palynological analysis was performed on 24 samples. The intervals were chosen to represent each sedimentary facies described above and varied amounts of detrital carbonate (Simon et al., 2012).

## 2.3 Results

### 2.3.1 Possible bias in isotopic data due to detrital carbonate

An assessment of possible isotopic biases in foraminifera preserved in detrital carbonate-rich sediments was made by comparing the $\delta^{18}O$ and $\delta^{13}C$ of clean Npl specimens, with those of dirty Npl, and of the sediment (Table 2.2, Fig. 2.2c). Three dirty samples were chosen based on the extensive amount of clay on and within the foraminiferal tests (Figs. 2.2a,b). The percentage of detrital carbonate (Table 2.2) was calculated from the percentage of calcite and dolomite, including calcareous foraminifera (Simon et al., 2014) and percentage of inorganic carbon (Nuttin and Hillaire-Marcel, 2015). Along with images showing the detrital clays, the SEM provided the elemental composition of the particles from which we can interpret their mineralogy. The detrital particles are clay minerals, with rare larger particles of quartz, feldspar, and dolomite. The sediment sample at 300.5 cm contains low carbonate content (~ 5% based on samples at 296.5 and 304.5 cm), while the sediment samples at 472.5 cm and 720.5 cm are from detrital carbonate layers and contain high carbonate percentages (30 and 20%). The $\delta^{18}O$ values of the detrital carbonate material range -5.79 to -3.12‰, and the $\delta^{13}C$ values range between -1.55 and -0.25‰. Although the analyses were done on bulk sediment that may also

contained isotopically heavier biogenic carbonate (foraminifera), the lower $\delta^{18}O$ values are similar to those analysed on individual detrital carbonate sand sized grains (Hodell and Curtis, 2008). Otherwise, the difference between the $\delta^{18}O$ and $\delta^{13}C$ of Npl and the detrital carbonate was >6.38 and >0.84‰ respectively. The largest isotopic difference between dirty and clean samples for is -0.34‰ for $\delta^{18}O$ and -0.24‰ for $\delta^{13}C$.

### 2.3.2 Stable isotopes of foraminifera

Planktic (Npl) and benthic foraminifera are not present throughout the core (Fig. 2.4c,d). Maximum abundances of Npl in the 150-250 μm size fraction reach ~740 specimens $cm^{-3}$, but most samples contain about 200 specimens $cm^{-3}$ or less. The benthic foraminifers reach a maximum concentration of 211 specimens $cm^{-3}$. Both planktic and benthic foraminifera are found within 92% of the samples, however 20% of those contain very low concentrations (<10 tests $cm^{-3}$).

The size fraction with the highest abundance of Npl is 150-250 μm. Hence the carbon and oxygen stable isotope composition measured in Npl from the 150-250 μm size fraction were used to develop the main isotope curves for the core (Table 2.3, Fig. 2.3). Due to the variability in Npl abundance, the curve is discontinuous. The $\delta^{18}O$ values range between 1.69 and 4.82‰, with most values varying between 2.5 and 4.0‰. Three intervals marked by particularly high $\delta^{18}O$ values (> 4‰) are centered at around 108-115, 95, and 48-50 ka BP. One interval marked by particularly light $\delta^{18}O$ values (<2.5‰) is recorded between 98 and 105 ka BP. The $\delta^{13}C$ values range from -0.23 to 0.66‰ and are variable throughout the record.

Npl specimens from the 106-150 and >250 μm size fractions were also analysed when possible to assess temperature and salinity (thus density) gradients within Npl-

habitat. Although the offsets between these and the 150-250 μm size fraction are not consistent regarding positive or negative offsets, on average, there is a positive relationship between test size and its $\delta^{18}O$ and $\delta^{13}C$ values (Table 2.3, Fig. 2.3), especially when comparing the smaller size range (106-150) to larger ones. The offsets between the values in the 150-250 μm size fraction and the 106-150 and >250 μm size fractions for both $\delta^{18}O$ and $\delta^{13}C$ are 0.32 and 0.23‰, and 0.49 and 0.20‰, respectively.

Only 35% of the samples containing enough planktic foraminifers for stable isotope measurement also contain benthic foraminifers yielding isotope values (Table 2.3, Figs. 2.4a,b). The $\delta^{18}O$ values in benthic foraminifers range from 2.89 to 4.83‰ and the $\delta^{13}C$ values from -1.41 to 0.01‰. The differences in $\delta^{18}O$ values between the benthic and planktic samples are small in most samples, except at about 112 and 13 ka BP where they reach 0.85‰, with one value reaching 1.60‰ at 13.2 ka BP. The differences in $\delta^{13}C$ values vary from 0 to -1.40‰, with very a small offset at around 13 ka BP, a larger one at ~112 ka BP, and the largest one at 48.5 ka BP.

### 2.3.3 Palynology

Palynological analyses were performed on 24 samples from PC16 (Table 2.4). Concentrations of modern palynomorphs are generally low, with 10 samples containing dinocysts (up to 854 $cm^{-3}$; Fig. 2.4c) and only 2 samples containing pollen and spores of < 50 $cm^{-3}$. The analysis of TWC16, the trigger core collected with piston core PC16, indicated that the concentrations of dinocysts remained very low until after the deglaciation and establishment of postglacial conditions (Steinhauer, 2012). The dinocysts in PC16 were mainly identified from the bottom half of the core (Fig. 2.4e). In samples containing > 10 cysts $cm^{-3}$, the dominant species include the

heterotrophic species *Brigantedinium* spp. and *Islandinium minutum* (> 88%) in addition to rare specimens of the phototrophic species *Operculodinium centrocarpum* at 288.5, 560.5 and 592.5 cm. Reworked pre-Quaternary palynomorphs are abundant (up to 3717 $cm^{-3}$) and include pollen, spores, dinocysts and acritarchs which originate from the Paleozoic-Mesozoic sediments of the Canadian Arctic (e.g., Hiscott et al., 2001). The organic linings of benthic foraminifers mainly occur in low concentrations but are relatively abundant in a few samples and reach 1174 linings $cm^{-3}$ (Fig. 2.4f).

### 2.3.4 Comparison with 85-027-016

It is noteworthy that the planktic and benthic foraminiferal abundance and $\delta^{18}O$ and $\delta^{13}C$ records of core HU-2008-029-016 (Fig. 2.4) are very similar to those of core 85-027-016 (P1985; Figs. 2.5a,b; cf. Hillaire-Marcel et al., 1989; Scott et al., 1989). There is a slight offset in depth, but the same general trends and variations are recorded. The foraminiferal abundances reported for core P1985 are over double those of PC16 due to different sampling practices (Figs. 2.5c,d). The total planktic population was counted in P1985 in the 212-250 μm size fraction and the benthics, including agglutinated species, were counted in the >63 μm size fraction. The foraminifera reported in PC16 include >106 μm benthics and the 150-250 μm Npl. The $\delta^{18}O$ and $\delta^{13}C$ Npl values of P1985 have a slight negative offset with respect to PC16, possibly up to 0.5‰. The overall palynological assemblages and abundances of core PC16 appear comparable with those of P1985 (Hillaire-Marcel et al., 1989) (Fig. 2.5e). Dinocyst concentrations in P1985 are generally low with < 50 cysts $cm^{-3}$ between 50 and 450 cm and below 730 cm. The remainder of the core contains samples of concentrations > 50 cysts $cm^{-3}$. Similarly to PC16, the dominant species identified in P1985 include *I. minutum* and *Brigantedinium* spp. along with some occurrences of *Spiniferites elongatus*. The comparison of core PC16 with P1985 has

demonstrated that the isotopic analyses and microfossil assessments are robust from Baffin Bay sediments, despite the discontinuous record.

## 2.4 Discussion

### 2.4.1 Possible bias in isotopic data due to detrital carbonate

The dirty vs clean Npl have a slight offset with respect to both oxygen and carbon isotopes (Table 2.2, Fig. 2.2c). Interestingly, the sample with the least amount of carbonate produced the largest isotopic offset with respect to both $\delta^{18}O$ and $\delta^{13}C$, while only one of the two samples with higher carbonate content affected the $\delta^{13}C$. Also, the SEM elemental analysis indicated that the fine grained sediment within the foraminiferal test was in fact clay minerals with larger detrital carbonate grains. This suggests that although sediments in Baffin Bay can contain high amounts of detrital carbonate, only a slight fraction may be entering the Npl once they are buried. Regardless, the isotopic offset of ~0.3‰ in both oxygen and carbon fall within the statistical scatter of isotopic compositions of Npl-assemblage mixing generations (Table 2.1) and the excursions in the Npl record (Figs 2.3, 2.4). The isotopic offsets among replicate samples might be partly due to variable detrital carbonate contamination, but more importantly to the mixing of generations produced under distinct environmental conditions: a mixing to be expected under such low productivity conditions. Improved methods allow for smaller sample sizes of 20 tests rather than samples of 100 tests collected from P1985. A smaller sample thus allows for more stringent subsampling which would produce samples with less detrital carbonate. However it may be the mixing of generations in a larger sample size that is

liable for the lighter values in P1985 relative to PC16 rather than the presence of isotopically light detrital carbonate (Figs. 2.4, 2.5). Therefore it seems that any fine grained sediment that may enter foraminiferal tests during burial does not necessarily affect its isotopic composition, and if it does, the offset seems insignificant considering the dispersal of values throughout the record.

### 2.4.2 Size dependent isotopic composition of Npl

The positive relationship between Npl test size and $\delta^{13}C$ is consistent with what has been shown from studies in western Arctic and northwest North Atlantic (Aksu and Vilks, 1988; Hillaire-Marcel et al., 2004). This relationship, however, differs from the expected negative relationship implying that larger tests living at greater depth are characterized by low $\delta^{13}C$ corresponding to decreasing $\delta^{13}C$ of dissolved inorganic carbon (DIC) with depth, which is usually attributed to organic matter oxidation rates and metabolic effects of Npl (Aksu and Vilks, 1988; Ravelo and Hillaire-Marcel, 2007). In Baffin Bay, as in the Arctic Ocean or the northwest North Atlantic, the positive test size and $\delta^{13}C_{Npl}$ values could be related to higher calcite precipitation rates in juvenile specimens (cf. Hillaire-Marcel et al., 2004).

There is slight variable offset between Npl test size and $\delta^{18}O$. It is however within the scatter observed for any given sample, and is thus not large enough to infer stratification within the intermediate water mass. Therefore it appears that episodes of Npl production correspond to relatively uniform subsurface water mass conditions in Baffin Bay during the last 116 ka.

### 2.4.3 Isotope values of planktic (Npl) vs benthic foraminifera

Intervals with isotopic data in both planktic and benthic foraminifera are approximately dated at 13, 46-50, and 110-115 ka BP (cf. hatched intervals in Fig. 2.4), which correspond to the Marine Isotope Stage (MIS) 2/1 transition, early MIS 3, and MIS 5d. Taking into account the heterogeneity of samples, the possible effect of detrital carbonate, and the large ranges of $\delta^{18}O$ values throughout the core, the isotopic composition of benthic and planktic foraminifers are remarkably comparable. This suggests that there was no stratification between the intermediate and bottom water masses during these intervals. However, the planktic vs benthic $\delta^{13}C$ values present singularities. On one hand, the ~ 13 ka interval shows nearly similar values, when one would expect a much lighter carbon in the benthic tests due to the oxidation of isotopically light organic carbon in the sediment. One must infer here that productivity was so low in Baffin Bay during this interval, that organic carbon ($C_{org}$) fluxes at the sea floor were very low as well (Fig. 2.4g). Both, the 46-50 and 110-115 ka BP intervals show lighter carbon isotope values in benthics. Much higher organic matter fluxes to the sea floor might be inferred during these intervals (e.g., Ravelo and Hillaire-Marcel, 2007). This could have been particularly the case of the 110-115 ka BP interval which follows the last interglacial (MIS 5e). During MIS 5e, warmer regional climate (e.g. Fréchette et al., 2006) led to higher primary productivity on land and at sea, with $C_{org}$ fluxes to the sea floor comparing to those of the Holocene (Hillaire-Marcel et al., 1989; Steinhauer, 2012; see also the small increase in dinocyst concentrations in Fig. 2.4c). However, there is no corresponding $C_{org}$ peak during this interval (Fig. 2.4g). One may suppose here that most of the fresh organic matter sedimented during the interval has been totally diagenetically decomposed (e.g., Muzuka and Hillaire-Marcel, 1999). The difference in $\delta^{13}C$ values of Npl and benthic at 46-50 ka BP, is much larger (~ 1.5‰), without any specific indication for enhanced primary productivity (Fig. 2.4). A shift of such magnitude has been reported in

benthic foraminifera that precipitated their carbonate test in porewaters marked by $\delta^{13}C$ altered by methane seeps (e.g., Mackensen et al., 2006; Ouellet-Bernier et al., 2014). Although Baffin Bay Bottom Water is currently methane depleted (Punshon et al., 2014), elevated levels could have been present 50 ka ago as they were some 8 ka ago, based on Ouellet-Bernier et al. (2014).

### 2.4.4 Past productivity and paleoceanographical conditions

The concurrence of planktic and benthic foraminifera at about 13, 46-50, and 110-115 ka BP suggests conditions ideal for carbonate preservation, and an influx of nutrients and organic detritus to both the intermediate and deep-water masses. The intervals marked by a biogenic (microfossil) component throughout PC16 are not consistent among the epipelagic (dinoflagellates), mesopelagic (planktic foraminifera), and benthic communities (Fig. 2.4). The mesopelagic and benthic foraminifers occur together in most intervals, but most often without dinocysts, indicator of epipelagic productivity, except for the interval prior to 108 ka BP. This is also the case with P1985, where peaks in dinocyst abundance are interspersed between peaks in foraminiferal abundance (Fig. 2.5). The lack of dinocysts during the most recent two $^{18}O$-enriched intervals suggests perennial sea ice cover preventing primary productivity. Therefore the benthic and planktic foraminifera were likely living in waters characterised by inputs of nutrients and organic detritus from a lateral source rather than from vertical fluxes. The foraminifera have very high $\delta^{18}O$ values, typical of the cold, saline water of glacial intervals, similar to those from the Labrador Sea and northwest North Atlantic throughout the last glacial period (Hillaire-Marcel and Bilodeau, 2000; Rasmussen et al., 2003). Cold conditions during the two most recent intervals (red hatched intervals Fig. 2.6) also occurred in Greenland during the stadials visible in the GISP2 $\delta^{18}O$ ice core record (Fig. 2.6d). Therefore we suggest

advection of saline Atlantic water during periods of continued ice cover over Baffin Bay, at least during the intervals marked by high $\delta^{18}O$ values in both planktic and benthic foraminifera (~13, 46-50 and 110-115 ka BP).

Samples barren or nearly barren (<10 tests $cm^{-3}$) in foraminifera (Fig. 2.4) can be interpreted as intervals of nil productivity due to very dense ice cover preventing any biological activity, and/or of shallow lysocline resulting in calcium carbonate dissolution. Some of these samples are also characterized by concentrations of dinocysts and organic linings of foraminifers which suggest epipelagic and benthic productivity during episodes marked by carbonate dissolution in Baffin Bay similar as during the Holocene (Fig. 2.4; de Vernal et al., 1992).

All things considered, the micropaleontological data from Baffin Bay reflect very low productivity during most of the last climatic cycle, which can be associated with dense sea ice cover similar to that observed in the central Arctic Ocean (de Vernal et al., 2008; Polyak et al., 2013). It is of note that the intervals spanning from 70 to 60 ka and from 40 to 20 ka, contain very low concentrations of organic and calcareous microfossils indicating low marine productivity (Fig. 2.4). These intervals, which partly match MIS 4 and the late MIS 3 to MIS 2, respectively, could have been marked by total isolation of Baffin Bay from the Atlantic Ocean, as well as the Arctic Ocean. Total isolation caused by an ice shelf in Baffin Bay during the last climate cycle has been proposed by several authors (cf. Hulbe, 1997; Hulbe et al., 2004; Shaffer et al., 2004; Marcott et al., 2011; Petersen et al., 2013). These intervals also correspond to those marked by the lowest isotopic values in the GISP2 Greenland ice core which correlates to highest ice volume and lowest sea level (Fig. 2.6; Stuiver and Grootes, 2000).

Between the $^{18}O$-enriched and barren intervals described above, episodes with lower $\delta^{18}O$ values in Npl (< 3.4‰) are recorded (Fig. 2.4). Similar values were reported for Labrador Sea cores and associated with meltwater pulses during Heinrich Events (Hillaire-Marcel et al., 1994; Hillaire-Marcel and Bilodeau, 2000; Rasmussen et al., 2003) and more recently associated with isotopically light brine rejection due to subsequent enhancement of sea ice formation (Hillaire-Marcel and de Vernal, 2008). Due to the discontinuity and low temporal resolution of the Baffin Bay record, it is difficult to interpret with confidence the low-$\delta^{18}O$ value intervals. Core PC16 yielded two samples, at ~ 105 and ~ 44 ka BP, where $^{18}O$-depleted Npl are associated with high dinocyst occurrence, indicating some epipelagic productivity (Fig. 2.4). In core P1985, these samples are likely identified at 330 and 714 cm, among only two others at 44 and 525 cm (Fig. 2.5). The dinocyst taxa recovered (*I. minutum* and *Brigantedium* spp.) are associated with harsh conditions and dense sea ice cover (e.g., de Vernal et al., 2013). Other samples with lower $\delta^{18}O$ values contain little to no dinocysts, which also indicates harsh conditions and suggest quasi-perennial sea ice cover (cf. de Vernal et al., 2005). Thus the lowermost $\delta^{18}O$-Npl values probably reflect isotopically-light brine influence at Npl depth habitat, thus sea ice production during episodes with at least a short seasonal opening of sea ice cover. Npl production through advection of North Atlantic waters below perennial sea ice cover in Baffin Bay might have been possible as well. However, such conditions should have led to very low Npl abundances. Npl produced under such conditions might as well present low $\delta^{18}O$ values, in relation with i) the amount of isotopically light brines mixed by this North Atlantic water mass during its earlier transit along the north-west North Atlantic sea ice margin, and ii) the temperature of this water mass. As a matter of fact, most of these light $\delta^{18}O$-Npl intervals, which are hatched in grey in Fig. 2.6, coincide with Greenland interstadials as shown by the GISP2 record (Fig. 6b). They also match enhanced weight % contribution of Eastern Baffin Island terrigenous supplies in the cored sequence (Fig. 2.6c; Simon et al., 2014). Simon et al. (2014) linked the related ice sheet calving and melting off Eastern Baffin Island to

subsurface warming in Baffin Bay, caused by increased circulation of a modern-like West Greenland Current (Holland et al., 2008).

## 2.5 Conclusion

The re-examination of Baffin Bay records first aimed at verifying that the $\delta^{18}O$ and $\delta^{13}C$ records are robust then at revisiting the paleoceanographic interpretation based on the chronostratigraphy provided by Simon et al. (2012). The isotopic analysis of clean vs dirty Npl has revealed that if there can be a small isotopic departure due to contamination by $^{18}O$-depleted fine detrital carbonate, an effect that would be indistinguishable due the exceptionally large scatter of $\delta^{18}O$ values depicted by Npl-populations in Baffin Bay sediments. The data also showed that the isotopic record of core PC16 is comparable to that of core 85-027-016 collected at almost the same location, more than 23 years earlier. Despite slightly heavier values in PC16, the two records demonstrate the robustness of the Baffin Bay isotope stratigraphy.

The paleoceanographic reconstructions have revealed intervals of different oceanic environements. Very low microfossil abundances characterize most of the MIS 2 and 4 intervals. Coupled with low concentrations of organic linings, this indicates that carbonate dissolution cannot be the primary cause. Harsh, ice covered environments with oceanographic conditions unsuitable for primary productivity, thus foraminiferal production, are more likely. Core PC16 is marked by episodes of high planktic and benthic $\delta^{18}O$ values at about 13, 46-50 and 108-115 ka BP. The lack of offsets between plantic and benthic $^{18}O$-contents suggests the presence of a homogeneous subsurface water mass down to the sea floor. These $^{18}O$-enriched intervals date from MIS 5d, 3, and the 2/1 transition. They are tentatively linked to advection of saline Atlantic water in Baffin Bay, below a thick sea ice cover (indicated by the absence of

dinocysts thus the total collapse of primary productivity). Relatively lower $\delta^{18}$O-Npl values were recorded during MIS 5c and 5a, as well as during MIS 3 and the MIS 2/1 transition. Some of these light isotopic excursions are associated with an abundance of dinocysts, indicating periods of summer productivity, but still under seasonally very dense sea ice conditions, as indicated by the dinocyst assemblage composition. A few other intervals with low $\delta^{18}$O-Npl values match warm Greenland interstadials and are thought to be linked to incursions of Atlantic water into Baffin Bay. These updated stable isotope records from Baffin Bay presented here provided new information about the paleohydrography of Baffin Bay throughout the last glacial cycle. Information from complementary proxies revealed essential to propose drastically distinct processes, leading to similar $^{18}$O-shifts in the record. These records have also identified the importance of North Atlantic water on microfossil abundance.

Acknowledgements

Support from the *Ministère du Développement Économique, Innovation et Exportation* (MDEIE) and *Fonds Québécois de Recherche sur la Nature et les Technologies* (FQRNT) is acknowledged. Special thanks to the Canadian Foundation for Climate and Atmospheric Sciences (CFCAS), Natural Resources Canada (NRCan), and the Natural Sciences and Engineering Research Council of Canada (NSERC) for their financial support of the HU2008029 expedition in the Labrador Sea. Special thanks to Maryse Henry and Jean-François Hélie for their help and expertise in the GEOTOP laboratories.

# REFERENCES

Aksu, A.E., 1981. Late Quaternary stratigraphy, paleoenvironments and sedimentation history of Baffin Bay and Davis Strait. Ph.D. thesis, Dalhousie University, Halifax, N.S.

Aksu, A.E., 1983. Holocene and Pleistocene dissolution cycles in deepsea cores of Baffin Bay and Davis Strait: paleoceanographic implications. Marine Geology 53, 331-348.

Aksu, A.E., Piper, D.J.W., 1979. Baffin Bay in the past 100,000 yr. Geology 7, 245-248.

Aksu, A.E., Mudie, P.J., 1985. Late Quaternary stratigraphy and paleoecology of northwest Labrador Sea. Marine Micropaleontology 9 (6), 537-557.

Aksu, A.E., Vilks, G., 1988. Stable isotopes in planktonic and benthic foraminifera from Arctic Ocean surface sediments. Canadian Journal of Earth Sciences 25 (5), 701-709.

Arthur, M.A., Srivastava, S.P., Kaminski, M., Jarrard, R., Osler, J., 1989. Seismic stratigraphy and history of deep circulation and sediment drift development in Baffin Bay and the Labrador Sea. *In*: Srivastava, S. P., Arthur, M., Clement, B., et al., (eds), Proceedings of the Ocean Drilling Program, Scientific Results, Vol. 105. Ocean Drilling Program, College Station, TX.

Azetsu-Scott, K., Clarke, A., Falkner, K., Hamilton, J., Jones, E.P., Lee, C., Petrie, B., Prinsenberg, S., Starr, M., Yeats, P., 2010. Calcium carbonate saturation states in the waters of the Canadian Arctic Archipelago and the Labrador Sea. Journal of Geophysical Research: Oceans 115 (C11).

Barras, C., Duplessy, J.C., Geslin, E., Michel, E., Jorissen, F.J., 2010. Calibration of $\delta^{18}O$ of laboratory-cultured deep-sea benthic foraminiferal shells in function of temperature. Biogeosciences Discussions 7 (1), 335-350.

Bauch, D., Carstens, J., Wefer, G. 1997. Oxygen isotope composition of living Neogloboquadrina pachyderma (sin.) in the Arctic Ocean. Earth and Planetary Science Letters 146 (1), 47-58.

Bé, A.W.H., Tolderlund, D.S., 1971. Distribution and ecology of planktonic foraminifera. In: Funnell, B.M., Riedel, W.R., (eds), The micropaleontology of oceans. Cambridge University Press, London.

Bourke, R.H., Addison,V.G., Paquette, R.G., 1989. Oceanography of Nares Strait and northern Baffin Bay in 1986 with emphasis on deep and bottom water formation, Journal of Geophysical Research, 94, 8289– 8302.

Briner, J.P., Miller, G.H., Davis, P.T., Bierman, P.R., Caffee, M., 2003. Last Glacial Maximum ice sheet dynamics in Arctic Canada inferred from young erratics perched on ancient tors. Quaternary Science Reviews 22, 437-444.

Briner, J.P., Miller, G.H., Davis, P.T., Finkel, R.C., 2006. Cosmogenic radionuclides from fiord landscapes support differential erosion by overriding ice sheets. Geological Society of America Bulletin 118, 406–420.

Campbell, D.C., and shipboard party. 2009: CGS Hudson Expedition 2008029: Marine geology and paleoceanography of Baffin Bay and adjacent areas, Nain, NL to Halifax, NS, August 28-September 23. Geological Survey of Canada, Open File 5989.

Carstens, J., Hebbeln, G., Wefer, G., 1997. Distribution of planktic foraminifera at the ice margin in the Arctic (Fram Strait). Marine Micropaleontology 29, 257-269.

Cuny, J., Rhines, P.B., Niiler, P.P., Bacon, S., 2002. Labrador Sea boundary currents and the fate of the Irminger Sea Water. Journal of Physical Oceanography 32 (2), 627-647.

Cuny, J., Rhines, P.B., Kwok, R., 2005. Davis Strait volume, freshwater and heat fluxes. Deep Sea Research Part I: Oceanographic Research Papers 52 (3), 519-542.

de Vernal, A., Hillaire-Marcel, C., Aksu, A.E., Mudie, P.J., 1987a. Palynostratigraphy and chronostratigraphy of Baffin Bay deep sea cores: climatostratigraphic implications. Palaeogeography, palaeoclimatology, palaeoecology, 61, 97-105.

de Vernal, A., Larouche, A., Richard, P.J.H., 1987b. Evaluation of palynomorph concentrations: do the aliquot and the marker-grain methods yield comparable results? Pollen et Spores 29 (2–3), 291–303.

de Vernal, A., Bilodeau, G., Hillaire-Marcel, C., Kassou, N., 1992. Quantitative assessment of carbonate dissolution in marine sediments from foraminifer linings vs. shell ratios: Davis Strait, northwest North Atlantic. Geology 20 (6), 527-530.

de Vernal, A., Henry, M., Bilodeau, G., 1999. Technique de préparation et d'analyse en micropaléontologie. Les Cahiers du GEOTOP, Université du Québec à Montréal, 3, Unpublished report.

de Vernal, A., Henry, M., Matthiessen, J., Mudie, P.j., Rochon, A., Boessenkool, K., Eynaud, F., Grøsfjeld, K., Guiot, J., Hamel, D., Harland, R., Head, M.j., Kunz-pirrung, M., Levac, E., Loucheur, V., Peyron, O., Pospelova, V., Radi, T., Turon, J.-L., Voronina, E., 2001. dinoflagellate cyst assemblages as tracers of sea-surface conditions in the northern North Atlantic, Arctic and sub-arctic seas: the new "n=677" database and application for quantitative paleoceanographical reconstruction. Journal of Quaternary Science 16, 681-699.

de Vernal, A., Eynaud, F., Henry, M., Hillaire-Marcel, C., Londeix, L., Mangin, S., Matthiessen, J., Marret, F., Radi, T., Rochon, A., Solignac, S., Turon, J.L., 2005. Reconstruction of sea surface conditions at middle to high latitudes of the Northern Hemisphere during the Last Glacial Maximum (LGM) based on dinoflagellate cyst assemblages. Quaternary Science Reviews 24 (7), 897-924.

de Vernal, A., Hillaire-Marcel, C., Solignac, S., Radi, T., Rochon, A., 2008. Reconstructing sea ice conditions in the Arctic and sub-Arctic prior to human observations. Arctic Sea ice Decline: Observations, Projections, Mechanisms, and Implications, 27-45.

de Vernal, A., Rochon, A., Fréchette, B., Henry, M., Radi, T., Solignac, S., 2013. Reconstructing past sea ice cover of the Northern hemisphere from dinocyst assemblages: status of the approach. Quaternary Science Reviews 79, 122-134.

Dyke, A.S., 2004. An outline of the deglaciation of North America with emphasis on central and northern Canada. In: Ehlers, J., Gibbard, P.L., (eds), Quaternary Glaciations, Extent and Chronology. Part II. North America. Developments in Quaternary Science, vol. 2b. Elsevier, Amsterdam.

England, J., Atkinson, N., Bednarski, J., Dyke, A.S., Hodgson, D.A., Ó Cofaigh, C., 2006. The Innuitian Ice Sheet: configuration, dynamics and chronology. Quaternary Science Reviews 25 (7), 689-703.

Erbs-Hansen, D.R., Knudsen, K.L., Olsen, J., Lykke-Andersen, H., Underbjerg, J.A., Sha, L., 2013. Paleoceanographical development off Sisimiut, West Greenland, during the mid-and late Holocene: A multiproxy study. Marine Micropaleontology 102, 79-97.

Fréchette, B., Wolfe, A.P., Miller, G.H., Richard, P.J., de Vernal, A., 2006. Vegetation and climate of the last interglacial on Baffin Island, Arctic Canada.Palaeogeography, Palaeoclimatology, Palaeoecology 236 (1), 91-106.

Funder, S., Kjeldsen, K.K., Kjær, K.H., Ó Cofaigh, C., 2011. The Greenland Ice Sheet during the past 300,000 years: A review. Developments in Quaternary Science 15, 699-713.

Hamel, D., de Vernal, A., Gosselin, M., Hillaire-Marcel, C., 2002. Organic-walled microfossils and geochemical tracers: sedimentary indicators of productivity changes in the North Water and northern Baffin Bay during the last centuries. Deep Sea Research Part II: Topical Studies in Oceanography 49 (22), 5277-5295.

Head, M.J., Harland, R., Matthiessen, J., 2001. Cold marine indicators of the late Quaternary: The new dinoflagellate cyst genus Islandinium and related morphotypes. Journal of Quaternary Science 16 (7), 621-636.

Hilbrecht, H., 1996. Extant planktic foraminifera and the physical environment in the Atlantic and Indian Oceans: an atlas based on Climap and Levitus (1982) data. Geologische Institut der Eidgen, Technischen Hochschule und der Universitat Zurich. Neue Folge: Zurich.

Hillaire-Marcel, C., de Vernal, A., Aksu, A., Macko, S., 1989. High-resolution isotopic and micropaleontological studies of upper Pleistocene sediments at ODP Site 645, Baffin Bay. *In*: Srivastava, S. P., Arthur, M., Clement, B., et al., (eds), Proceedings of the Ocean Drilling Program, Scientific Results, Vol. 105. Ocean Drilling Program, College Station, TX.

Hillaire-Marcel, C., de Vernal, A., Bilodeau, G., Wu, G., 1994. Isotope stratigraphy, sedimentation rates, deep circulation, and carbonate events in the Labrador Sea during the last -200 ka. Canadian Journal of Earth Science 31, 63-89.

Hillaire-Marcel, C., Bilodeau, G., 2000. Instabilities in the Labrador Sea water mass structure during the last climatic cycle. Canadian Journal of Earth Sciences 37 (5), 795-809.

Hillaire-Marcel, C., de Vernal, A., Polyak, L., Darby, D., 2004. Size-dependent isotopic composition of planktic foraminifers from Chukchi Sea vs. NW Atlantic sediments-implications for the Holocene paleoceanography of the western Arctic. Quaternary Science Reviews 23 (3), 245-260.

Hillaire-Marcel, C., de Vernal, A., 2008. Stable isotope clue to episodic sea ice formation in the glacial North Atlantic. Earth and Planetary Science Letters 268, 143-150.

Hiscott, R.N., Aksu, A.E., Nielsen, O.B., 1989. Provenance and dispersal patterns, Pliocene-Pleistocene section at Site 645, Baffin Bay. *In*: Srivastava, S. P., Arthur, M., Clement, B., et al., (eds), Proceedings of the Ocean Drilling Program, Scientific Results, Vol. 105. Ocean Drilling Program, College Station, TX.

Hiscott, R.N., Aksu, A.E., Mudie, P.J., Parsons, D.F., 2001. A 340,000 year record of ice rafting, palaeoclimatic fluctuations, and shelf-crossing glacial advances in the southwestern Labrador Sea. Global and Planetary Change 28 (1), 227-240.

Hodell, D.A., Curtis, J.H., 2008. Oxygen and carbon isotopes of detrital carbonate in North Atlantic Heinrich Events. Marine Geology 256 (1), 30-35.

Holland, D.M., Thomas, R.H., de Young, B., Ribergaard, M.H., Lyberth, B., 2008. Acceleration of Jakobshavn Isbrae triggered by warm subsurface ocean waters. Nature Geoscience 1 (10), 659-664.

Hulbe, C.L., 1997. An ice shelf mechanism for Heinrich layer production. Paleoceanography 12, 711-717.

Hulbe, C.L., MacAyeal, D.R., Denton, G.H., Kleman, J., Lowell, T.V., 2004. Catastrophic ice shelf breakup as the source of Heinrich event icebergs. Paleoceanography 19 (1).

Husum, K., Hald, M., 2004. A continuous marine record 8000-1600 cal. yr BP from the Malangenfjord, north Norway: foraminiferal and isotopic evidence. The Holocene 14 (6), 877-887.

Kucera, M., 2007. Planktonic foraminifera as tracers of past oceanic environments. In: Hillaire-Marcel, C., de Vernal, A. (eds), Proxies in Late Cenozoic Paleoceanography. Elsevier, The Netherlands, pp. 213-262.

Laskar, J., Robutel, P., Joutel, F., Gastineau, M., Correia, A.C.M., Levrard, B., 2004. A long-term numerical solution for the insolation quantities of the Earth. Astronomy & Astrophysics 428 (1), 261-285.

Mackensen, A., Wollenburg, J., Licari, L., 2006. Low $\delta^{13}C$ in tests of live epibenthic and endobenthic foraminifera at a site of active methane seepage. Paleoceanography, 21 (2).

Marcott, S.A., Clark, P.U., Padman, L., Klinkhammer, G.P., Springer,A.R., Liu, Z., Otto-Bliesner, B.L., Carlsone, A.E., Ungererc, A., Padmanc, J., Hee, F., Chengh, J., Schmittnerc, A., 2011. Ice-shelf collapse from subsurface warming as a trigger for Heinrich events. Proceedings of the National Academy of Sciences 108 (33), 13415-13419.

Matthews, J., 1969. The assessment of a method for the determination of absolute pollen frequencies. New Phytologist 68, 161-166.

Mudie, P.J., Aksu, A.E., 1984. Palaeoclimate of Baffin Bay from 300,000-year record of foraminifera, dinoflagellates and pollen. Nature 312, 630-634.

Muzuka, A.N., Hillaire-Marcel, C., 1999. Burial rates of organic matter along the eastern Canadian margin and stable isotope constraints on its origin and diagenetic evolution. Marine Geology 160 (3), 251-270.

Nuttin, L., Hillaire-Marcel, C., 2015. U-and Th-series isotopes in deep Baffin Bay sediments: Tracers of detrital sources and of contrasted glacial/interglacial sedimentary processes. Marine Geology 361 (1), 1-10.

Ó Cofaigh, C., Dowdeswell, J.A., Jennings, A.E., Hogan, K.A., Kilfeather, A., Hiemstra, J.F. Noormets, R., Evans, J., McCarthy, D.J., Andrews, J.T., Lloyd, J.M., Moros, M., 2013. An extensive and dynamic ice sheet on the West Greenland shelf during the last glacial cycle. Geology 41 (2), 219-222.

Osterman, L.E. and Nelson, A.R., 1989. Latest Quaternary and Holocene paleoceanography of the eastern Baffin Island continental shelf, Canada: benthic foraminiferal evidence. Canadian Journal of Earth Science 26, 2236-2248.

Ouellet-Bernier, M.-M., de Vernal, A., Hillaire-Marcel, C., 2014. Paleoceanographic changes of Disko Bugt area West Greenland during the Holocene. The Holocene 24 (11), 1573-1583.

Pados, T., Spielhagen, R.F., 2014. Species distribution and depth habitat of recent planktic foraminifera in Fram Strait, Arctic Ocean. Polar Research, 33.

Petersen, S.V., Schrag, D.P., Clark, P.U., 2013. A new mechanism for Dansgaard-Oeschger cycles. Paleoceanography 28, 1-7.

Polyak, L., Best, K.M., Crawford, K.A., Council, E.A., St-Onge, G., 2013. Quaternary history of sea ice in the western Arctic Ocean based on foraminifera. Quaternary Science Reviews 79, 145-156.

Punshon, S., Azetsu-Scott, K., Lee, C.M., 2014. On the distribution of dissolved methane in Davis Strait, North Atlantic Ocean. Marine Chemistry 161, 20-25.

Rasmussen, T.L., Oppo, D.W., Thomsen, E., Lehman, S.J., 2003. Deep sea records from the southeast Labrador Sea: Ocean circulation changes and ice-rafting events during the last 160,000 years. Paleoceanography 18 (1), 1018.

Ravelo, A.C., Hillaire-Marcel, C., 2007. The use of oxygen and carbon isotopes of foraminifera in paleoceanography. In: Hillaire-Marcel, C., de Vernal, A. (eds), Proxies in Late Cenozoic Paleoceanography. Elsevier, The Netherlands, pp. 735-764.

Rochon, A., de Vernal, A., Turon, J.-L., Matthiessen, J., and Head, M.J. 1999. Distribution of dinoflagellate cyst assemblages in surface sediments from the North Atlantic Ocean and adjacent basins and quantitative reconstruction of sea-surface parameters. American Association of Stratigraphic Palynologists, Contribution Series No. 35.

Schröeder-Adams, C.J., Van Rooyen, D., 2011. Response of Recent Benthic Foraminiferal Assemblages to Contrasting Environments in Baffin Bay and the Northern Labrador Sea, Northwest Atlantic. Arctic, 317-341.

Scott, D.B., Mudie, P.J., de Vernal, A., Hillaire-Marcel, C., Baki, V., MacKinnon, K.D., Medioli, F.S., Mayer, L., 1989. Lithostratigraphy, biostratigraphy, and stable-isotope stratigraphy of cores from ODP Leg 105 site surveys, Labrador Sea and Baffin Bay. *In*: Srivastava, S. P., Arthur, M., Clement, B., et al., (eds), Proceedings of the Ocean Drilling Program, Scientific Results, Vol. 105. Ocean Drilling Program, College Station, TX.

Shaffer, G., Olsen, S.M., Bjerrum, C.J., 2004. Ocean subsurface warming as a mechanism for coupling Dansgaard-Oeschger climate cycles and ice-rafting events. Geophysical Research Letters 31 (24).

Simon, Q., St-Onge, G., Hillaire-Marcel, C., 2012. Late Quaternary chronostratigraphic framework of deep Baffin Bay glaciomarine sediments from high-resolution paleomagnetic data. Geochemistry, Geophysics, Geosystems 13 (11).

Simon, Q., Hillaire-Marcel, C., St-Onge, G., Andrews, J.T., 2014. North-eastern Laurentide, western Greenland and southern Innuitian ice stream dynamics during the last glacial cycle. Journal of Quaternary Science 29 (1), 14-26.

Simstich, J., Sarnthein, M., Erlenkeuser, H., 2003. Paired d18O signals of *Neogloboquadrina pachyderma* (s) and *Turborotalita quinqueloba* show thermal stratification structure in Nordic Seas. Marine Micropaleontology 48, 107-125.

Steinhauer, S., 2012. Postglacial paleoceanography of central Baffin Bay from palynological tracers. Master's thesis, Université du Québec à Montréal, Montréal, Canada.

Stoner, J.S., Channell, J.E.T., Hillaire-Marcel, C., Kissel, C., 2000. Geomagnetic paleointensity and environmental record from Labrador Sea core MD95-2024: global marine sediment and ice core chronostratigraphy for the last 110 kyr. Earth and Planetary Science Letters 183 (1), 161-177.

Stuiver, M., Grootes, P.M., 2000. GISP2 oxygen isotope ratios. Quaternary Research 53 (3), 277-284.

Tan, F.C., Strain, P.M., 1980. The distribution of sea ice meltwater in the Eastern Canadian Arctic. Journal of Geophysical Research 85, 1925–1932.

Tang, C.C.L., Ross, C.K., Yao, T., Petrie, B., DeTracey, B.M., Dunlap, E., 2004. The circulation, water masses and sea-ice of Baffin Bay. Progress in Oceanography 63, 183-228.

Volkmann, R. 2000. Planktic foraminifers in the outer Laptev Sea and the Fram Strait—modern distribution and ecology. The Journal of Foraminiferal Research 30 (3), 157-176.

Volkmann, R., Mensch, M., 2001. Stable isotope composition ($\delta^{18}O$, $\delta^{13}C$) of living planktic foraminifers in the outer Laptev Sea and the Fram Strait.Marine Micropaleontology 42 (3), 163-188.

Wendeberg, M., Richter, J.M., Rothe, M., Brand, W.A., 2011. δ18O anchoring to VPDB: calcite digestion with $^{18}O$-adjusted ortho-phosphoric acid. Rapid Communications in Mass Spectrometry 25 (7), 851-860.

Xiao, W., Wang, R., Polyak, L., Astakhov, A., Cheng, X., 2014. Stable oxygen and carbon isotopes in planktonic foraminifera Neogloboquadrina pachyderma in the Arctic Ocean: An overview of published and new surface-sediment data. Marine Geology 352, 397-408.

Figures

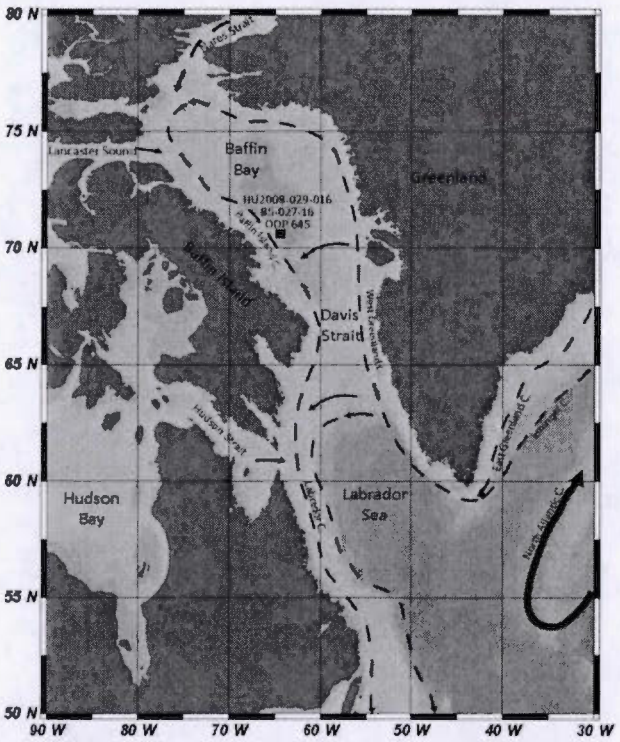


Figure 2.1. Map indicating the coring location of piston core HU2008-029-016PC, site survey core 85-027-016PC, and ODP Site 645. The following surface currents are also displayed: North Atlantic Current (NAC), Irminger Current (IC), East Greenland Current (EGC), West Greenland Current (WGC), Baffin Island Current (BIC), and Labrador Current (LC).

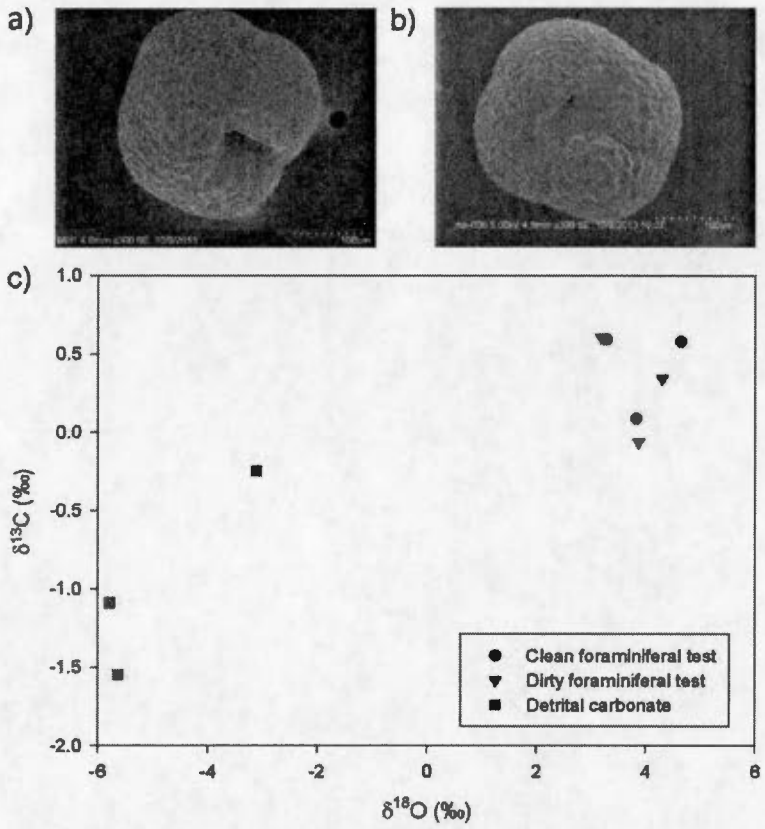


Figure 2.2. Assessment of possible bias in isotopic composition due to detrital carbonate. Scanning electron microscope (SEM) images of (a) "clean" (free of impurities) and (b) "dirty" (containing clay sized particles which may contain detrital carbonate) planktic foraminifera *Neogloboquadrina pachymerma* sinistral (left coiling; Npl). Carbon ($\delta^{13}C$) vs oxygen ($\delta^{18}O$) isotopic composition in permil of the 150-250 μm size fraction of Npl and of < 10 μm bulk sediment (representing detrital carbonate) (c), where colours represent different samples.

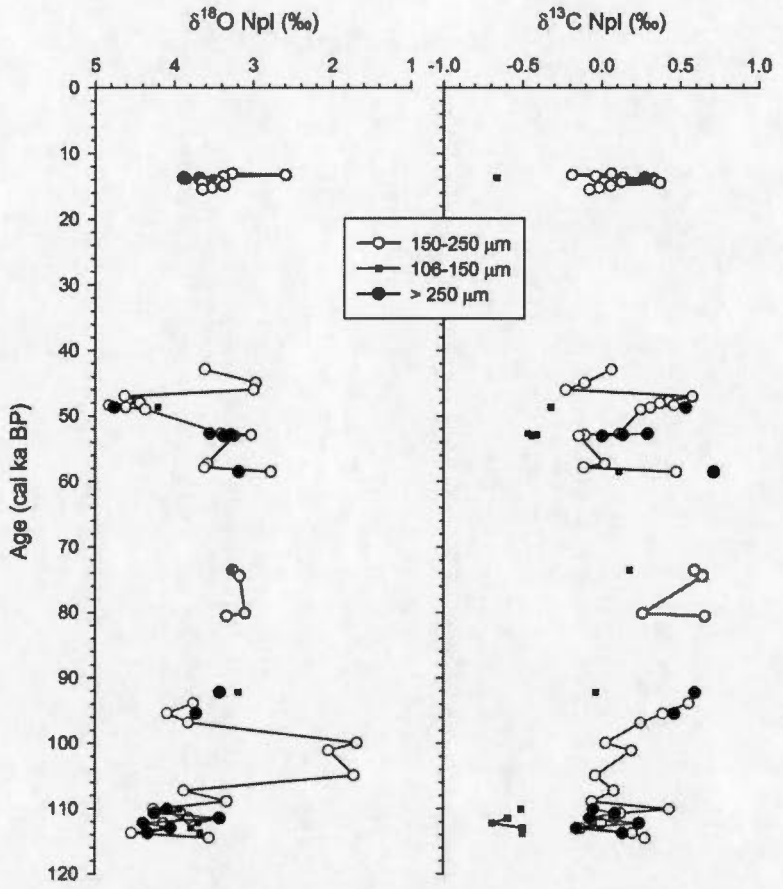


Figure 2.3. Carbon ($\delta^{13}C$) and oxygen ($\delta^{18}O$) isotopic composition in permil of the 106-150, 150-250, and >250 µm size fractions of the planktic foraminifera *Neogloboquadrina pachyderma* sinistral (left coiling; Npl).

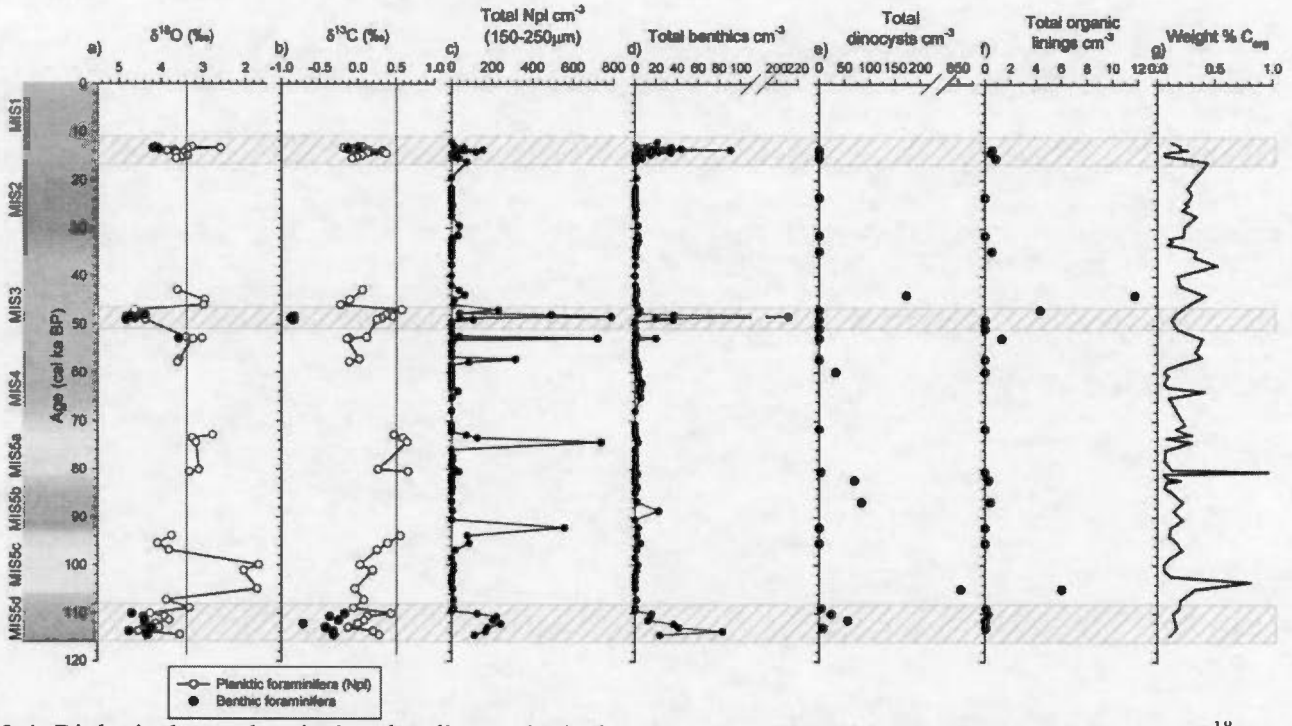


Figure 2.4. Biological, geochemical and sedimentological parameters collected in core PC16. (a) Oxygen ($\delta^{18}O$) isotopic composition in permil of the 150-250 µm size fraction of the planktic foraminifera *Neogloboquadrina pachyderma* sinistral (left coiling; Npl) and benthic foraminifera (species listed in Table 2.3). (b) Carbon ($\delta^{13}C$) isotopic composition of Npl and benthic foraminifera. (c) Total numbers per $cm^3$ of the 150-250 µm size fraction of Npl. (d) Total numbers per $cm^3$ of all size fractions of benthic foraminifera. (e) Concentrations of dinocysts per $cm^3$. (f) Concentrations of organic linings per $cm^3$. (g) The weight percent (%) organic carbon ($C_{org}$) content. The hatched intervals indicate the $^{18}O$-enriched values of both planktic and benthic foraminifera.

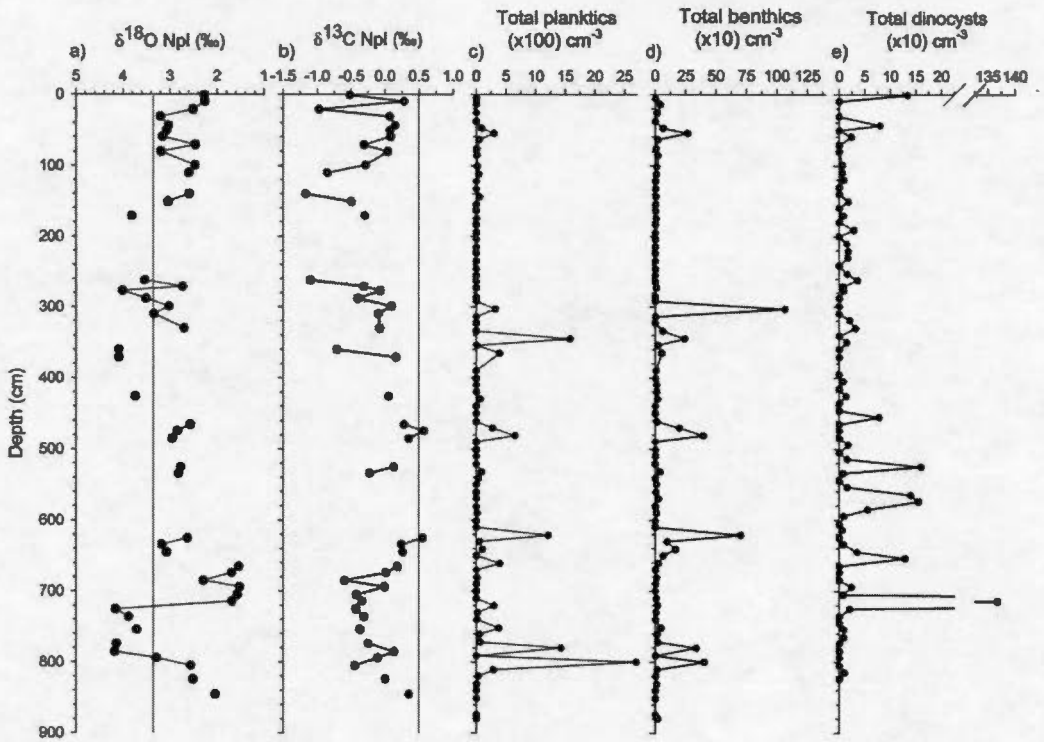


Figure 2.5. Biological and geochemical parameters collected in core 85-029-016. (a) Oxygen ($\delta^{18}O$) isotopic composition in permil of the 150-250 μm size fraction of the planktic foraminifera *Neogloboquadrina pachyderma* sinistral (left coiling; Npl; Hillaire-Marcel et al., 1989). (b) Carbon ($\delta^{13}C$) isotopic composition of Npl (Hillaire-Marcel et al., 1989). (c) Total numbers per $cm^3$ of planktic foraminifera (Scott et al., 1989). (d) Total numbers per $cm^3$ of benthic foraminifera (Scott et al., 1989). (e) Concentrations of dinocysts per $cm^3$ (Hillaire-Marcel et al., 1989).

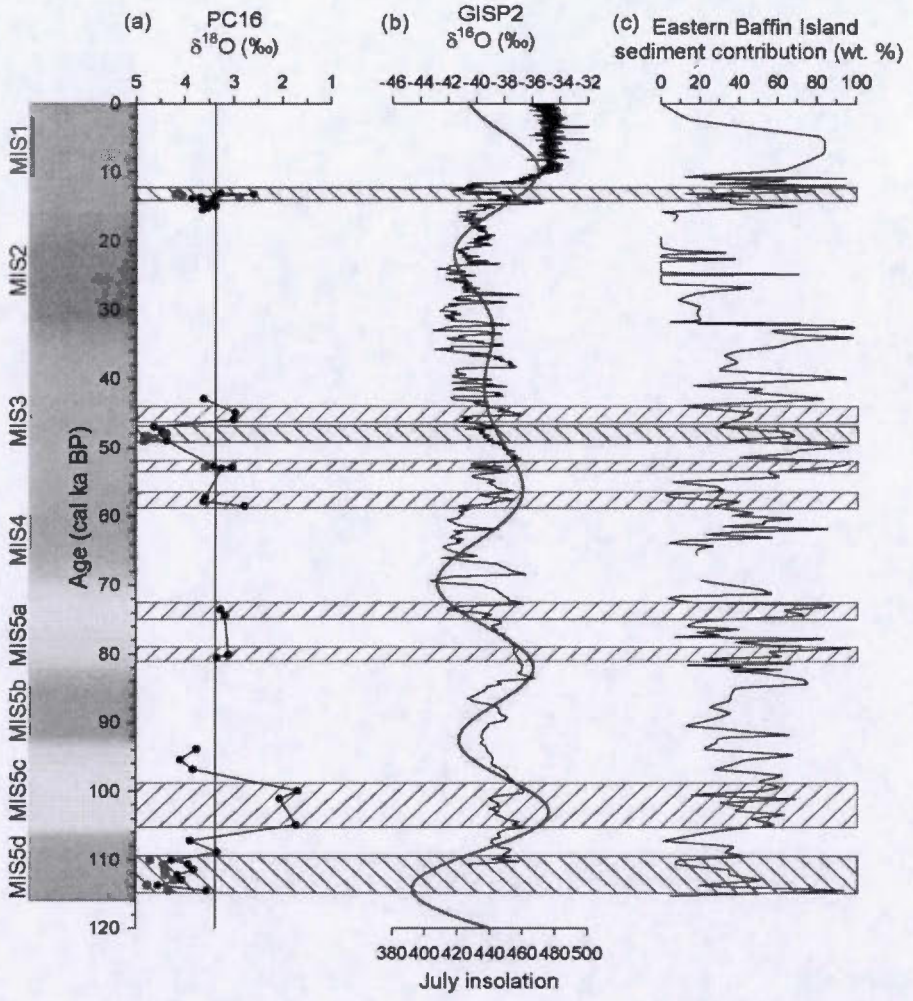


Figure 2.6. Comparison of the PC16 $\delta^{18}O$ record with other surrounding records. (a) Core PC16 oxygen ($\delta^{18}O$) isotopic composition in permil of the 150-250 μm size fraction of the planktic foraminifera *Neogloboquadrina pachymerma* sinistral (left coiling; Npl) in black and benthic foraminifera (species listed in Table 2.3) in red. Grey hatched intervals indicate lighter $\delta^{18}O$ values and red hatched intervals indicate $^{18}O$-enriched values. (b) GISP2 $\delta^{18}O$ (‰) ice core record (Stuiver and Grootes, 2000) and July insolation (Laskar et al., 2004). (c) Eastern Baffin Island sediment contribution in weight % as estimated from sediment provenance in PC16 (Simon et al., 2014).

Tables

Table 2.1. Replicate samples of oxygen ($\delta^{18}O$) and carbon ($\delta^{13}C$) isotopic composition in permil the 150-250 μm size fraction of the planktic foraminifera *Neogloboquadrina pachyderma* sinistral (left coiling; Npl) and of the benthic foraminifera *Cassidulina neoteretis*.

| Sample midpoint (cm) | Species of foraminifera | $\delta^{18}O$ | | | | $\delta^{13}C$ | | | |
|---|---|---|---|---|---|---|---|---|---|
| | | run 1 | run 2 | Average value | Standard deviation | run 1 | run 2 | Average value | Standard deviation |
| 76.5 | *C. neoteretis* | 3.84 | 4.25 | 4.05 | 0.29 | -0.19 | -0.06 | -0.13 | 0.09 |
| 76.5 | 150-250 μm Npl | 3.02 | 3.73 | 3.38 | 0.50 | -0.19 | 0.11 | -0.04 | 0.21 |
| 328.5 | 150-250 μm Npl | 2.86 | 3.20 | 3.03 | 0.24 | -0.26 | 0.04 | -0.11 | 0.22 |
| 480.5 | 150-250 μm Npl | 2.98 | 3.37 | 3.17 | 0.27 | 0.53 | 0.75 | 0.64 | 0.16 |

Table 2.2. Oxygen ($\delta^{18}O$) and carbon ($\delta^{13}C$) isotopic composition in permil of calcite in clean (uncontaminated) and dirty (contaminated) of the 150-250 μm size fraction of the planktic foraminifera *Neogloboquadrina pachyderma* sinistral (left coiling; Npl) and of < 10 μm bulk sediment (detrital carbonate).

| Sample midpoint (cm) | weight % carbonate | $\delta^{18}O$ | | | | $\delta^{13}C$ | | | |
|---|---|---|---|---|---|---|---|---|---|
| | | Clean | Dirty | Dirty-clean | Detrital carbonate | Clean | Dirty | Dirty-clean | Detrital carbonate |
| 300.5 | ~ 5 | 4.63 | 4.28 | -0.34 | -3.12 | 0.58 | 0.34 | -0.24 | -0.25 |
| 472.5 | 30.2 | 3.26 | 3.17 | -0.09 | -5.64 | 0.59 | 0.60 | 0.01 | -1.55 |
| 720.5 | 20.8 | 3.81 | 3.85 | 0.04 | -5.79 | 0.08 | -0.07 | -0.15 | -1.09 |

Table 2.3. Oxygen ($\delta^{18}O$) and carbon ($\delta^{13}C$) isotopic composition in permil of the three size fractions (106-150, 150-250, >250 μm) of the planktic foraminifera *Neogloboquadrina pachyderma* sinistral (left coiling; Npl), and of the benthic foraminifera. The analysed benthic foraminiferal species is listed where cn = *Cassidulina neoteretis* and cr = *Cassidulina reniforme*, and tests were picked from all size fractions.

| midpoint (cm) | Age (ka BP) | $\delta^{18}O$ 106-150 | $\delta^{18}O$ 150-250 | $\delta^{18}O$ >250 | $\delta^{13}C$ 106-150 | $\delta^{13}C$ 150-250 | $\delta^{13}C$ >250 | Benthic species | Benthic $\delta^{18}O$ | Benthic $\delta^{13}C$ | B-P $\delta^{18}O$ | B-P $\delta^{13}C$ |
|---|---|---|---|---|---|---|---|---|---|---|---|---|
| 68.5 | 13.05 | | 3.27 | | | 0.06 | | cn | 4.13 | 0.01 | 0.85 | -0.05 |
| 72.5 | 13.25 | | 2.59 | | | -0.19 | | cn | 4.19 | -0.13 | 1.60 | 0.06 |
| 76.5 | 13.45 | | 3.38 | | | -0.04 | | cn | 4.05 | -0.13 | 0.67 | -0.09 |
| 80.5 | 13.66 | 3.51 | 3.68 | 3.89 | -0.66 | 0.13 | 0.27 | cn | 2.89 | -0.57 | -0.79 | -0.70 |
| 82.5 | 13.81 | | 3.85 | | | 0.33 | | | | | | |
| 86.5 | 14.11 | | 3.67 | | | 0.34 | | | | | | |
| 88.5 | 14.26 | | 3.45 | | | 0.13 | | | | | | |
| 90.5 | 14.42 | | 3.65 | | | 0.37 | | | | | | |
| 96.5 | 14.87 | | 3.37 | | | 0.06 | | | | | | |
| 100.5 | 15.17 | | 3.52 | | | -0.02 | | | | | | |
| 104.5 | 15.47 | | 3.64 | | | -0.08 | | | | | | |
| 112.5 | 16.24 | | | | | | | | | | | |

| midpoint (cm) | Age (ka BP) | $\delta^{18}O$ | | | $\delta^{13}C$ | | | Benthic species | Benthic | | B-P | B-P |
|---|---|---|---|---|---|---|---|---|---|---|---|---|
| | | 106-150 | 150-250 | >250 | 106-150 | 150-250 | >250 | | $\delta^{18}O$ | $\delta^{13}C$ | $\delta^{18}O$ | $\delta^{13}C$ |
| 284.5 | 42.88 | | 3.61 | | | 0.06 | | | | | | |
| 288.5 | 43.90 | | | | | | | | | | | |
| 292.5 | 44.94 | | 2.97 | | | -0.11 | | | | | | |
| 296.5 | 45.97 | | 2.99 | | | -0.23 | | | | | | |
| 300.5 | 46.99 | | 4.63 | | | 0.58 | | | | | | |
| 304.5 | 47.67 | | 4.46 | | | 0.43 | | | | | | |
| 306.5 | 48.00 | | 4.43 | | | 0.37 | | cr | 4.38 | -1.03 | -0.05 | -1.40 |
| 308.5 | 48.33 | | 4.82 | | | 0.46 | | cr | 4.76 | -0.84 | -0.06 | -1.30 |
| 310.5 | 48.67 | 4.21 | 4.61 | 4.76 | -0.32 | 0.31 | 0.53 | cr | 4.63 | -0.88 | 0.01 | -1.19 |
| 312.5 | 49.00 | | 4.37 | | | 0.25 | | cr | 4.83 | -0.84 | 0.47 | -1.09 |
| 327.5 | 52.68 | 3.39 | 3.40 | 3.55 | -0.47 | 0.12 | 0.29 | | | | | |
| 328.5 | 52.85 | 3.40 | 3.03 | 3.28 | -0.41 | -0.11 | 0.13 | cr | 3.58 | -1.41 | 0.55 | -1.30 |
| 329.5 | 53.03 | 3.37 | 3.25 | 3.37 | -0.44 | -0.14 | 0.00 | | | | | |
| 356.5 | 57.25 | | 3.58 | | | 0.02 | | | | | | |
| 360.5 | 57.83 | | 3.62 | | | -0.11 | | | | | | |
| 464.5 | 58.50 | 3.21 | 2.78 | 3.19 | 0.11 | 0.47 | 0.71 | | | | | |

| midpoint (cm) | Age (ka BP) | $\delta^{18}O$ | | | $\delta^{13}C$ | | | Benthic species | Benthic | | B-P | B-P |
|---|---|---|---|---|---|---|---|---|---|---|---|---|
| | | 106-150 | 150-250 | >250 | 106-150 | 150-250 | >250 | | $\delta^{18}O$ | $\delta^{13}C$ | $\delta^{18}O$ | $\delta^{13}C$ |
| 472.5 | 73.51 | 3.29 | 3.26 | | 0.18 | 0.59 | | | | | | |
| 480.5 | 74.40 | | 3.17 | | | 0.64 | | | | | | |
| 520.5 | 80.09 | | 3.10 | | | 0.26 | | | | | | |
| 528.5 | 80.53 | | 3.33 | | | 0.66 | | | | | | |
| 616.5 | 92.18 | 3.19 | | 3.42 | -0.04 | | 0.59 | | | | | |
| 624.5 | 93.86 | | 3.75 | | | 0.55 | | | | | | |
| 632.5 | 95.41 | | 4.09 | 3.72 | | 0.39 | 0.46 | | | | | |
| 640.5 | 96.82 | | 3.82 | | | 0.25 | | | | | | |
| 656.5 | 99.93 | | 1.69 | | | 0.03 | | | | | | |
| 664.5 | 101.09 | | 2.05 | | | 0.19 | | | | | | |
| 688.5 | 104.91 | | 1.72 | | | -0.04 | | | | | | |
| 696.5 | 107.21 | | 3.88 | | | 0.08 | | | | | | |
| 704.5 | 108.89 | | 3.33 | | | -0.06 | | | | | | |
| 712.5 | 110.06 | 3.94 | 4.26 | 4.09 | -0.51 | 0.43 | -0.05 | cn | 4.70 | -0.17 | 0.44 | -0.61 |
| 716.5 | 110.69 | | 3.92 | 4.25 | | 0.12 | 0.09 | cn | 4.42 | -0.37 | 0.50 | -0.49 |
| 720.5 | 111.45 | 3.43 | 3.81 | 3.42 | -0.59 | 0.08 | -0.07 | cn | 4.39 | -0.25 | 0.58 | -0.34 |

| midpoint (cm) | Age (ka BP) | $\delta^{18}O$ | | | $\delta^{13}C$ | | | Benthic species | Benthic | | B-P | B-P |
|---|---|---|---|---|---|---|---|---|---|---|---|---|
| | | 106-150 | 150-250 | >250 | 106-150 | 150-250 | >250 | | $\delta^{18}O$ | $\delta^{13}C$ | $\delta^{18}O$ | $\delta^{13}C$ |
| 724.5 | 112.21 | 3.69 | 4.13 | 4.39 | -0.69 | 0.00 | 0.24 | cn | 4.38 | -0.71 | 0.24 | -0.71 |
| 728.5 | 112.97 | 3.79 | 4.05 | 4.04 | -0.50 | -0.13 | -0.16 | cn | 4.21 | -0.42 | 0.16 | -0.29 |
| 732.5 | 113.73 | 3.67 | 4.54 | 4.33 | -0.50 | 0.20 | 0.14 | cn | 4.76 | -0.32 | 0.22 | -0.52 |
| 736.5 | 114.49 | | 3.55 | | | 0.28 | | cn | 4.32 | -0.31 | 0.77 | -0.59 |

Table 2.4. Concentrations of dinocysts, reworked palynomorphs, and organic linings in number of specimens per $cm^3$.

| Depth (cm) | Age (ka BP) | Dinocysts | Pollen + spores | Reworked palynomorphs | Organic linings |
|---|---|---|---|---|---|
| 80.5 | 13.66 | 0 | 0 | 522 | 58 |
| 88.5 | 14.26 | 0 | 0 | 16 | 49 |
| 104.5 | 15.47 | 0 | 0 | 1155 | 87 |
| 152.5 | 23.59 | 0 | 0 | 78 | 0 |
| 208.5 | 31.48 | 0 | 0 | 1008 | 0 |
| 248.5 | 34.79 | 0 | 0 | 1293 | 54 |
| 288.5 | 43.90 | 172 | 0 | 466 | 1174 |
| 300.5 | 46.99 | 0 | 0 | 511 | 432 |
| 312.5 | 49.00 | 0 | 0 | 91 | 0 |
| 320.5 | 50.86 | 0 | 0 | 3717 | 0 |
| 328.5 | 52.85 | 0 | 0 | 165 | 133 |
| 356.5 | 57.25 | 0 | 0 | 552 | 0 |
| 376.5 | 59.88 | 32 | 0 | 40 | 0 |
| 448.5 | 71.57 | 0 | 0 | 210 | 0 |
| 528.5 | 80.53 | 3 | 0 | 79 | 0 |
| 560.5 | 82.27 | 70 | 0 | 139 | 29 |
| 592.5 | 86.77 | 84 | 18 | 461 | 42 |
| 616.5 | 92.18 | 0 | 0 | 57 | 0 |
| 632.5 | 95.41 | 0 | 0 | 73 | 0 |
| 688.5 | 104.91 | 854 | 46 | 854 | 600 |
| 704.5 | 108.89 | 4 | 0 | 599 | 8 |
| 712.5 | 110.06 | 24 | 0 | 339 | 24 |

| Depth (cm) | Age (ka BP) | Dinocysts | Pollen + spores | Reworked palynomorphs | Organic linings |
|---|---|---|---|---|---|
| 720.5 | 111.45 | 57 | 0 | 302 | 0 |
| 728.5 | 112.97 | 7 | 0 | 438 | 7 |

# CHAPTER III

## Diachronous evolution of sea surface conditions in the Labrador Sea and Baffin Bay since the last deglaciation

Olivia T. Gibb[1], Sarah Steinhauer[1], Bianca Fréchette[1], Anne de Vernal[1], and Claude Hillaire-Marcel [1]

[1]GEOTOP Research Center, CP. 8888 Succ Centre Ville, Montréal, QC H3C 3P8, Canada

This chapter is accepted for publication in *The Holocene*

Abstract

Assessing changes in sea surface conditions due to the effects of past freshwater outflow through Baffin Bay and Davis Strait to the Labrador Sea, hereafter referred to as the Baffin Bay corridor, is relevant in understanding the variability in Labrador Sea Water (LSW) formation. Here, regional changes in oceanographic circulation and sea surface conditions are reconstructed based on organic-walled dinoflagellate cyst (dinocyst) assemblages from four cores collected from deep, central sites of the Baffin Bay corridor. All cores exhibit a major shift in dinocyst assemblages since the late glacial period. This shift consists of a change from a polar-subpolar heterotrophic species assemblage tolerating cold and near permanent ice-covered conditions, to assemblages characterized by a higher diversity and the occurrence of phototrophic taxa associated with mild conditions. Sea surface reconstructions from the modern analogue technique display a shift from harsh, quasi-perennial ice cover to warmer summer sea surface temperatures and a seasonal sea ice. South of the Davis Strait sill, this regime shift occurred at ca. 11.9 cal ka BP due to the influence of North Atlantic waters. Baffin Bay, however, remained densely sea ice covered until about 7.4 cal ka BP, when these warmer waters penetrated into Baffin Bay and mixed with the West Greenland Current (WGC). This mixing was facilitated by the retreat of the Greenland and Laurentide Ice Sheet (LIS) margins. A major change in Labrador Sea surface conditions occurred nearly at about the same time (~7.6 cal ka BP) when the strong stratification of surface waters weakened due to the reduction in meltwater supplies from the LIS finally allowing winter convection and the inception of LSW formation. All these new records demonstrate large amplitude fluctuations in sea surface conditions tightly controlled by the relative strengths and shifts of the warmer WGC and colder Baffin Island Current.

## 3.1 Introduction

Arctic outflow through the Baffin Bay corridor, consisting of Baffin Bay, Davis Strait and the Labrador Sea, provides a significant contribution of freshwater to the North Atlantic, as shown by both observations and modeling studies (Aksenov et al., 2010; Curry et al., 2011; Serreze et al., 2006). Changes in the Arctic's hydrological cycle due to the ongoing global warming is expected to modify the export of freshwater from the Arctic to the Labrador Sea, leading to a more stratified upper ocean, which may inhibit convective mixing and the formation of an intermediate water mass (Cheng and Rhines, 2004; Goosse et al., 1997; Wadley and Bigg, 2002). From this viewpoint, documenting late- to postglacial changes in sea surface conditions and productivity, linked to variations in freshwater flow and oceanic circulation through the Baffin Bay corridor, may help comprehend their evolution in areas downstream from the Arctic Ocean.

Monitoring past changes of sea surface conditions through the Baffin Bay corridor since the deglaciation has been undertaken almost exclusively using paleoceanographic records from nearshore areas such as Disko Bugt (e.g., Andresen et al., 2010), Nares Strait (e.g., Levac et al., 2001) and Lancaster Sound (e.g., Ledu et al., 2008). Such records, unlike those of offshore sites, have high temporal resolution due to high sedimentation rates influenced by glacial erosion, but mainly reflect local atmospheric and hydrographic conditions (e.g., Erbs-Hansen et al., 2013; Seidenkrantz et al., 2008). As illustrated here, deeper sites off the shelf break yield records representative of large-scale changes in surface water conditions in response to the regional ocean dynamics rather than to coastal processes, but they offer a much lesser time resolution due to lower sedimentation rates.

Baffin Bay is a difficult environment for paleoceanographic studies due to inherent challenges of the setting of a chronostratigraphy in deep-sea sedimentary sequences. Low sedimentation rates characterize interglacial stages (< 10 cm $ka^{-1}$) in comparison to high rates during glacial periods (e.g., Simon et al., 2012; Srivastava et al., 1989). Additionally, at depths greater than 900 m, calcium carbonate dissolution occurs in Holocene sediments due to low carbonate saturation states (Azetsu-Scott et al., 2010) and oxidation of organic matter related to high productivity thus preventing radiocarbon dating of calcareous microfossils (Aksu 1983; de Vernal et al., 1992; Osterman and Nelson, 1989; Schröeder-Adams and Van Rooyen, 2011). Carbonate dissolution also makes it impossible to use foraminiferal assemblages as paleoceanographic proxies, and thus to derive oxygen and carbon stable isotope records for potential chronological correlations.

Cores from central Baffin Bay (TWC16), eastern Baffin Bay (CC70), southern Davis Strait (TWC08), and the northwest Labrador Sea (CC04) were collected along the Baffin Bay corridor during the HU2008-029 cruise (Fig. 3.1; Campbell et al. 2009). Despite the above methodological difficulties, they were analysed with the aim to provide an assessment of past sea surface conditions since the last deglaciation, and more specifically, to document the effects of freshwater fluxes from surrounding ice sheets and the Arctic on sea surface temperatures and sea ice cover between the Arctic and North Atlantic oceans.

### 3.1.1 Modern hydrographic setting and location of core sites

The surface and subsurface waters of the Baffin Bay corridor form a counter clockwise gyre influenced by northward flowing, warm high-salinity Atlantic waters, and by southward flowing cold low-salinity Arctic waters (Fig. 3.1) (see Buch,

1990/2000; Cuny et al., 2002, 2005; Ribergaard et al., 2008; Tang et al., 2004 for details listed below). Along the West Greenland shelf, the West Greenland Current (WGC) carries cool, less saline Arctic water from the East Greenland Current that has been slightly modified by warmer, more saline Atlantic water. The Atlantic water is carried through the western branch of the Irminger Current (IC), which flows below ~100 m down to ~800 m along the West Greenland shelf and slope.

Upon reaching northern Baffin Bay, the surface component of the WGC (upper 300 m) mixes with cold, less saline Arctic water that enters via Nares Strait, Lancaster Sound, and Jones Sound and becomes the Baffin Island Current (BIC). Some warmer Arctic Intermediate water of Atlantic origin passes over the sills of Nares Strait and combines with the Irminger component of the WGC that has recirculated in Baffin Bay to form the Baffin Bay Intermediate Water. The BIC follows the Baffin Island coast on the continental shelf and slope. Baffin Bay Deep and Bottom waters cool with depth and cover the deepest areas of the Bay. The BIC flows south along Baffin Island through Davis Strait into the northwest Labrador Sea. Finally, it mixes with colder, fresher Arctic water exiting Hudson Strait to form the Labrador Current (LC). Along the eastern Canadian shelf and upper slope, the surface layer of the LC overlies the WGC branch that has extended westward near Davis Strait and circulated through the gyre. Below the LC lies the Labrador Sea Water (LSW), which is formed by the sinking of dense waters when cooled in winter (Lazier, 1973). LSW reaches depths up to 2500 m and lies above the North East Atlantic Deep Water and the Denmark Strait Overflow Water (Yashayaev, 2007).

Sea ice cover along the Baffin Bay corridor is variable, ranging from 0 to > 10 months per year, thus with a concentration ranging from 0 to about 90%. Ice starts forming in northwest Baffin Bay in September and extends southwestward to form a complete sea ice cover by March (Tang et al., 2004; Wang et al., 1994), occasionally reaching the northwest Labrador Sea. The warm WGC prevents sea ice formation

along the southwestern Greenland coast and reduces the sea ice extent in eastern Baffin Bay. In opposition, the cold and stratified LC fosters sea ice growth along the Newfoundland and Labrador shelf. In Baffin Bay, sea ice begins to melt in April in the North Water Polynya and along the Greenland coast, moving westward until ice-free conditions occur, normally in August and September. A large interannual variability of sea ice cover is coupled to the strong seasonality in air temperatures and wind patterns (Tang et al., 2004).

An oceanic front is a constricted zone of increased productivity and nutrients due to a significant horizontal gradient in water mass properties such as sea surface temperature and salinity (Belkin et al., 2009). Two polar fronts are present in the study area (Fig. 3.1), both separating cold, low salinity polar current from warmer, more saline current. The Labrador Shelf-Slope Front (LSSF), which is situated on the NW Labrador/SW Baffin Island slope, is associated with the LC, and the West Greenland Current Front (WGCF) follows the western edge of the WGC (Belkin et al., 2009, supp. material). The location of these polar fronts is dependent on the strength of the LC and WGC.

## 3.2 Methods

The four sites used in this study were cored during the HU2008029 cruise aboard the CCGS Hudson (Fig. 3.1). Site information, core lengths and sampling intervals are listed in Table 3.1. Trigger cores TWC04, TWC08, and TWC70 were analysed for this study and core TWC16 was analysed by Steinhauer (2012). Two core composites were created in order to extend the Holocene trigger core records into the deglacial interval: CC04 in the northwest Labrador Sea combines TWC04 with the data from PC04 reported in Gibb et al. (2014), and CC70 in eastern Baffin Bay combines

TWC70 with data from PC70 reported in Jennings et al. (2014). Core descriptions, photographs, and onboard measurements including magnetic susceptibility are found in the cruise report (Campbell et al., 2009).

The chronostratigraphy was established based on radiocarbon dates from biogenic remains. Cores TW70 and PC70 were marked by poor biogenic carbonate preservation and very rare occurrence of foraminifer shells but contained mollusc shells and seaweed which permitted to obtain radiocarbon dates (Jennings et al., 2014). The radiocarbon dates from cores TWC04, TWC08, and TWC16 were derived from planktonic foraminiferal populations that consist of > 95 % *Neogloboquadrina pachyderma* left-coiled (Npl). Radiocarbon ages were calculated using the Libby half-life of 5568 years and normalized to a $\delta^{13}C$ of -25‰. The ages were then converted to calibrated years BP based on OxCal 4.2 (Bronk Ramsey, 2008), using the Marine13 calibration curve of Reimer et al. (2013). No additional correction ($\Delta R$) was applied.

The number of radiocarbon dates from cores TWC04 and TWC70 was sufficient to create age-depth models. The calibrated ages in core TWC70 were combined with those of PC70 (Jennings et al., 2014) then modeled in OxCal to create the age-depth model for the composite CC70 sequence (Table 3.2, Fig. 3.2). The core collection date of 2008 (-58 cal ka BP) was assigned to -15 cm in TWC70, which is offset from its corresponding box core based on physical properties. For consistency with CC04 and other records from deeper sites, the $\Delta R$ used by Jennings et al. (2014) was not used in the age-depth model for CC70. Cores TWC04 and PC04 (Gibb et al., 2014) were modeled individually then spliced at 8.3 cal ka BP for the composite CC04 sequence (Table 3.2, Fig. 3.2). For the purpose of this paper, data from CC04 will only be reported for the last 15 cal ka BP but core PC04 extends to ~36 cal ka BP (Gibb et al., 2014). Physical properties including diffuse spectral reflectance (CIE L*a*b*) values and photographs from the box core and trigger core (Campbell et al.,

2009) were used to determine that the TWC04 core top was undisturbed, assigning an age of 2008 AD (-58 cal a BP) to 0 cm of CC04. The calibrated ages were reported as the modeled median cal. age BP. Linear interpolation between each modeled date was used to calculate the age-depth relationship when plotting proxy data against age and sedimentation rates.

Due to the absence of radiocarbon chronologies in the Baffin Bay/Davis Strait records, the geochemical properties and micropaleontological content of the representative cores TWC16 and TWC08 were tentatively correlated with cores CC70 and CC04 from eastern Baffin Bay and northern Labrador Sea respectively. Ice rafted deposition, calcium carbonate content, dinoflagellate cyst (dinocyst) assemblages, and the dinocyst-based sea surface reconstructions are used for correlations.

Each sample used for dinocyst analysis consists of a 5 $cm^3$ subsample of sediment from a 1 cm thick section. Core length and sampling interval are listed in Table 3.1. The subsamples were rinsed through 106 μm and 10 μm mesh sieves. Weight percent coarse fraction was calculated from the dried > 106 μm size fraction from the dinocyst preparations. This makes a representative proxy for ice-rafted deposition (IRD) because it mainly consists of detrital material and low abundance of light biological remains (microfossils). The 10 to 106 μm size fraction was processed according to the method described by de Vernal et al. (1999). The organic residue was mounted onto a slide with Kaiser's glycerol gelatin and examined for dinocysts. Dinocyst species were identified following the nomenclature provided by de Vernal et al. (2001), Head et al. (2001), Radi et al. (2013) and Rochon et al. (1999). Dinocysts were tabulated and concentrations were calculated using the marker-grain method (Matthews, 1969), which provides an accuracy of ±10 % for a 95 % confidence interval (de Vernal et al., 1987). Relative percent abundance of the dinocyst taxa in assemblage for each sample was calculated based on identifying a

minimum of 300 cysts whenever possible. These counts were also used for further statistical analyses including principal component analysis on percentage data (PCA) to determine assemblage zones in each core, and the application of the modern analogue technique (MAT) to reconstruct sea surface conditions. Sea surface temperature (SST) in summer and winter, sea surface salinity (SSS) in summer, sea ice cover expressed as the number of months per year with a sea ice concentration > 50 %, and primary productivity (gC $m^{-2}$) were reconstructed with MAT following the procedure described by de Vernal et al. (2005). MAT was applied using the updated "modern" dinocyst database of the Northern Hemisphere that includes 1492 sites and 66 taxa (see database at http://www.geotop.ca; de Vernal et al., 2013a), using scripts prepared by Guiot (CEREGE, France) for the software R (http://cran.r-project.org/). We calculated the most probable conditions from the average of the 5 best analogues weighted inversely by their distance, and the variance provided upper and lower boundaries. Methods for the validation tests and error calculations were made after splitting of the data sets as described by de Vernal et al. (2013a). The error of prediction was established at ± 1.4 months per year for sea ice cover, ± 1.2°C and ± 1.6°C for winter and summer SSTs, respectively, and ± 2.6 for SSS. The error of prediction of SSS is high because the database includes low salinity environments (down to 5 psu), where surface salinity is particularly variable. When considering only the > 30 and > 33 salinity domains, the summer SSS errors of prediction are ±1.3 and ±0.8 psu, respectively.

## 3.3 Results

The four cores used in this study were collected from very distinct regions as shown by their water depth and corresponding modern sea surface conditions (Table 3.1).

Summarized core descriptions are listed here however greater detail and photographs can be found in the cruise report (Campbell et al., 2009). The radiocarbon dates, their calibrated ages, publication reference and laboratory identification are listed for each core in Table 3.2. The modeled age intervals and modeled median age (cal ka BP) for CC04 and CC70 are also listed in Table 3.2; their age-depth models and sedimentation rates are shown in Fig. 3.2. The physical description, chronology, dinocyst assemblage, PCA, and MAT reconstruction for each core are described below.

### 3.3.1 CC04 - The northwest Labrador Sea (Figs. 3.3a,b)

The CC04 record presented here extends to ~15.0 cal ka BP with sedimentation rates varying between 3.5 and 93.1 cm $ka^{-1}$. The piston core PC04 contains massive, dark grey silty clay from ~15 to 8.3 cal ka BP (436 to 60 cm), with diffuse laminations from ~15 to 12.9 cal ka BP (436 to 251 cm), and a mottled texture with bioturbation from (251 to 70 cm; i.e., after 12.9 cal ka BP). A layer of pebbles has been found and dated at ~14.5 cal ka BP (410 to 390 cm) (Gibb et al., 2014). The trigger core (TWC04), which spans about the last 7.8 cal ka BP, consists of massive, hemipelagic dark grey silty clay. Core CC04 contains up to 9 weight percent coarse fraction (> 106 μm; considered here as IRD), prior to ~11.3 cal ka BP (Fig. 3.3a).

The dinocyst concentrations vary from as low as 5 up to 10,000 cysts $cm^{-3}$ through the core. The dinocyst concentrations and assemblages of CC04 are plotted relative to age from ~15 cal ka BP to present (Fig. 3.3b). From ~15 to 11.9 cal ka BP, the assemblages are dominated by up to 100% *Brigantedinium* spp., but may include up to 18% *Islandinium minutum*. From ~11.9 to 7.6 cal ka BP, *Brigantedinium* spp. is significantly reduced (< 41%) whereas *I. minutum* increases up to 29%, and several other species occur in significant number. They include *Operculodinium centrocarpum* (8-40%), *Nematosphaeropsis labyrinthus* (7-14%), as well as the cysts

of *Pentapharsodinium dalei* (11-58%), which becomes the dominant species by ~8.5 cal ka BP. *I. minutum* nearly disappears after ~7.6 cal ka BP and the cysts of *P. dalei* (4-36%) also decrease, while *O. centrocarpum* (43-75%), accompanied by *N. labyrinthus* (5-33%) becomes the dominant species until ~2.4 cal ka BP. After ~2.4 cal ka BP, *O. centrocarpum* (down to 20%) is replaced by *N. labyrinthus* (up to 63%) as the dominant species. The other accompanying taxa have low relative abundance (< 10%) throughout the core.

The first component (PC1) of the PCA identified four assemblage zones in CC04, which account for 79.2% of the total variance, while PC2 accounted for 8.9% (Fig. 3.3b). The lower interval, from ~15 to 11.9 cal ka BP is characterized by the quasi-exclusive dominance of *Brigantedinium* spp., a heterotrophic taxon often associated with harsh, ice covered conditions (de Vernal et al., 1997, 2001, 2013a,b; Gibb et al., 2014; Rochon et al., 1999). The second interval, from ~11.9 to 7.6 cal ka BP, marks the increase in *I. minutum* and the occurrence of phototrophic species such as *O. centrocarpum* and *N. labyrinthus,* which are often associated with the North Atlantic Drift (Rochon et al., 1999). The cyst of *P. dalei*, as the dominant species in this interval, suggests large seasonal gradients of temperature due to strongly stratified surface waters (Rochon et al., 1999; Solignac et al., 2006). The interval from ~7.6 to 2.4 cal ka BP is dominated by *O. centrocarpum* indicating warmer, temperate conditions. The upper interval from 2.4 cal ka BP to present is characterized by the dominance of *N. labyrinthus*.

The sea surface conditions in CC04 appear to vary significantly throughout the record (Fig. 3.3a). To clearly display the trends in variability, a 5-point running mean was added to the sea surface reconstructions. Three of the four PCA assemblage zones are identifiable in these reconstructions. Overall, winter SST ranged from -1.8 to 5.3°C, summer SST from -0.8 to 13.3°C, salinity from 28.4 to 35.0, sea ice cover between 0 and 11.4 months per year, and productivity between 61 and 374 gC $m^{-2}$. The interval

between ~15 and 11.9 cal ka BP records cold, nearly perennially ice-covered conditions. Between ~11.9 and 7.6 cal ka BP, winter SSTs increase slightly to an average of 0.8°C, while summer SSTs greatly increase to an average of 9°C. This interval recorded i) the lowest salinity with a minimum of 28.4 at around 10.4 cal ka BP, ii) the highest annual productivity, and iii) a reduced sea ice cover averaging about 3 months per year. After ~7.6 cal ka BP, the salinity increase to ~34 and winter SSTs increase slightly to an average of 3.5°C. Summer SSTs decrease slightly, yet fluctuate greatly between 6 and 10°C.

### 3.3.2 TWC08 – Davis Strait (Figs. 3.4a,b)

Core TWC08 consists of massive dark greyish brown silty clays with some mud clasts and high proportions of IRD, which peak to 50% at 35 cm (Fig. 3.4a). The core has a calibrated age at 104-105 cm of 19.4 cal ka BP and one at 136-137 cm of 20.6 cal ka BP, suggesting high sedimentation rates during the glacial period. This core is affected by carbonate dissolution above theses intervals and therefore no Holocene age model was derived. Chronological interpretation was made from the piston core collected with TWC08 (PC08) by Andrews et al. (2014) who discussed in detail the geochemical data used to correlate TWC08 and PC08 with other dated records from the area. The cores are primarily correlated using sediment provenance of mineralogical and carbonate contents. The most recent detrital carbonate event (DC0) found between 60 and 25 cm in TWC08 and at the core top of PC08 was tentatively correlated with other records and assigned an age from approximately 13 to 10.5 cal ka BP (Andrews et al., 2012, 2014; Simon et al., 2014). The maximum percentage of IRD in TWC08 at 34 cm (Fig. 3.4a) indicates a large influx of icebergs into southern Davis Strait. This peak occurs during DC0, suggesting icebergs were exiting Baffin Bay between about 13 and 10.5 cal ka BP. Considering the lack of biogenic carbonate

and suggested chronology by Andrews et al. (2014), it is reasonable to assume that the Holocene is comprised within the upper 34 cm of TWC08.

Dinocyst concentrations are very low (< 500 cysts $cm^{-3}$) in the lower interval analyzed, which likely precedes the Holocene (Fig. 3.4b). They increase from 35.5 to 22 cm to reach values of 5000 cysts $cm^{-3}$ and fluctuate between 5000 and 10,000 cysts $cm^{-3}$ in the upper part of the core. The dinocyst assemblages are dominated by the heterotrophic species *I. minutum* (24-57%) and *Brigantedinium* spp. (10-65%), which have their highest abundances below 35.5 cm. In the upper 35.5 cm of the core, there is a change in relative abundance in the accompanying taxa. The cysts of *P. dalei* (0-30%) and *O. centrocarpum* (0-17%) are more abundant between 35.5 and 24 cm, and *N. labyrinthus* (0-34%) is more abundant above 24 cm. The other accompanying taxa have low relative abundance (< 10%) throughout the core.

The PC1 scores change from positive to negative at 35.5 cm and account for 79.9% of the variance (Fig. 3.4b). Similarly to core CC04, the PCA scores are influenced by the shift from heterotrophic to phototrophic species indicating a shift toward warmer conditions. PC2, explaining 11.1% of the variance, is primarily reflecting the change in assemblage at 24 cm from *P. dalei* and *O. centrocarpum* to *N. labyrinthus*.

The MAT results show cold conditions and dense sea ice cover for about 8 months/yr below 33.5 cm (Fig. 3.4a). A shift to warmer SSTs (up to 11°C), reduced salinity (down to 30), seasonal sea ice (3.0-6.5 months/yr), and increased productivity (up to 270 gC $m^{-2}$) is recorded between 33.5 and 24 cm. Above 24 cm, recurring cold summer conditions and a slight increase in sea ice cover are recorded.

### 3.3.3 CC70 – eastern Baffin Bay (Figs. 3.5a,b)

The CC70 record extends to ~12.8 cal ka BP with sedimentation rates ranging between 11.4 and 101.6 cm $ka^{-1}$ (Fig. 3.2). The core was previously described by Jennings et al. (2014) for sedimentological content and by St-Onge and St-Onge (2014) for magnetic properties. It depicts four distinct intervals. The base of the composite core (piston core) at ~12.1 cal ka BP (421 cm) to ~11.2 cal ka BP (376 cm) consists of dark gray muds with high amounts of pebbles and sand, and IRD (> 106 μm) amounting up to 85% (Fig. 3.5a). Between ~11.2 and 10.6 cal ka BP (376 and 326 cm), the sediment consists of bioturbated silty mud with shells, pebbles, vertical burrows, and Fe-rich dolomites from northern Baffin Bay (see Jennings et al., 2014). IRD and bioturbation are not visible in the interval from ~10.6 to ~9.2 cal ka BP which consists of massive silty clay. After ~9.2 cal ka BP, from 223 cm to the top of the composite core, the sediment consists of bioturbated mud. Two sand intervals are present at ~2.7 cal ka BP (100-110 cm) and ~1.2 cal ka BP (48-52 cm).

The concentrations of dinocysts in core CC70 range from very low (35 cysts $cm^{-3}$) to very high (56,000 cysts $cm^{-3}$) with the lowest values measured at the bottom of the core (Fig. 3.5b). Prior to ~7.4 cal ka BP, the dinocyst assemblage mainly consists of the heterotrophic species *I. minutum* and *Brigantedinium* spp. (> 90%). *O. centrocarpum* (50-75%) dominates after ~7.4 cal ka BP with accompanying taxa that include *Nematospaeropsis labyrinthus*, *Spiniferites elongatus* and the cysts of *P. dalei*.

Based on the scores of the first two components of the PC analysis in CC70, two assemblage zones have been identified (Fig. 3.5b). The scores for PC2 (21.5% of the total variance) identify a shift in the relative abundance of *I. minutum* and *Brigantedinium* spp. at ~9.5 cal ka BP. The PC1 scores (77.3% of the total variance)

mark a shift at ~7.4 cal ka BP, representing the change in dominant species from heterotrophic to *O. centrocarpum* and other phototrophic taxa. Hence, the change indicates a shift from species which tolerate cold conditions with dense sea ice (de Vernal et al., 1997, 2001, 2013a,b; Gibb et al., 2014; Rochon et al., 1999) to milder conditions associated with the North Atlantic Current (Rochon et al., 1999).

The two shifts identified by the PCA are distinguishable in the sea surface reconstructions, particularly through the salinity and sea ice cover records (Fig. 3.5a). Before ~7.4 cal ka BP, sea surface conditions are reconstructed as cold, with extensive sea ice cover. The shift at ~9.5 cal ka BP distinguishes a regime marked by low salinity (28.0 on average) and quasi-perennial ice cover from a regime with higher salinity (31.7 on average) and seasonal sea ice cover of about 8 months per year, without clear change in SSTs. After ~7.4 cal ka BP, there is an increase in summer SST from 2.5 up to 9.5°C, an increase in salinity toward values between 32 and 34, while sea ice cover decrease to seasonal extent from 1 to 6 months per year. Productivity increased slightly to an average of 160 gC $m^{-2}$. Although the records show highly variable values, the smoothed data suggests a trend towards milder conditions throughout the Holocene.

### 3.3.4 TWC16 – central Baffin Bay (Figs. 3.6a,b)

Core TWC16 contains laminated silty clays with abundant IRD (Fig. 3.6a) and mud clasts from the bottom to 16 cm downcore. Above 16 cm, the occurrence of IRD and clasts is signigicantly diminished. A colour change from grey (bottom) to brown (top) occurs at 50 cm. Core TWC16 yielded one calibrated age of 13.3 cal ka BP at 56-57 cm. This was the uppermost possible date due to carbonate dissolution above.

Therefore it is assumed that the upper 56 cm of TWC16 span the deglacial and postglacial periods in central Baffin Bay.

The samples contain rare dinocysts except in the upper 10 cm, where their concentrations gradually increase to 1260 cysts $cm^{-3}$ (Fig. 3.6b). The dinocyst assemblage is dominated by 70-80% *Impagidinium pallidum* from the core bottom to 16 cm, where it is replaced by *O. centrocarpum*. When either of these two species dominates an assemblage marked by low species diversity, the assemblage is associated with cool-cold open ocean conditions (Rochon et al., 1999). In the lower part of the record, *I. pallidum* is accompanied by *I. minutum*. The overall assemblage reflects low productivity and harsh conditions (cf. Steinhauer, 2012). In the upper 17 cm of the sequence, the disappearance of heterotrophic species and increase in diversity of phototrophic taxa, which include *Spiniferites* spp., *N. labyrinthus* and *Impagidinium sphaericum,* illustrate the onset of milder conditions (Rochon et al., 1999).

Two assemblage zones have been identified based on the scores from PC1, which accounts for 92.7% of the total variance (Fig. 3.6b). The zones are divided at 17.5 cm by the shift in dominant species, from *I. pallidum* to *O. centrocarpum,* in addition to the occurrence of accompanying taxa.

The sea surface reconstructions demonstrate a regime shift at 17.5 cm (Fig. 3.6a). The lower zone corresponds to cold conditions with about 8 months per year of sea ice cover. The conditions warm throughout the upper interval, with a significant reduction in sea ice cover and summer SST and salinity reaching maximums of 9°C and 34.7, respectively.

As pointed out by Steinhauer (2012), the sea surface reconstructions of the upper part of the core do not reflect conditions of recent decades. There is a large discrepancy

between reconstructed sea surface conditions from the topmost sample and the modern hydrographic data, which average 3.2°C and -1.1°C in summer and winter respectively, with salinity of 29.9, sea ice cover for 9 months per year, and 57 gC $m^{-2}$ of productivity (Table 3.1). Actually, the top cm of core TWC016 possibly integrates several hundred years of sedimentation if we take into account the very low postglacial sedimentation rates (Simon et al., 2012) and mixing by bioturbation as shown from $^{210}Pb$ and $^{137}Cs$ data (Steinhauer, 2012). Alternatively, the preservation of dinocysts in the upper part of the core might be questioned since the assemblages are lacking the taxa that are most susceptible to degradation due to oxidation such as *Brigantedinium* spp. The aerobic degradation of the more labile cysts of heterotrophic species has been documented by Zonneveld et al. (1997, 2001, 2007). However, deep Baffin Bay is currently a low [$O_2$] environment (3.2-3.5 ml/l; Aksu, 1983; Schröder-Adams and Van Rooyen, 2011). Although we cannot totally discard the possibility of selective preservation of dinocysts, the occurrence of subpolar taxa leading to reconstruct mild conditions is significant. Hence, we do not think that there is a major bias in the reconstruction and we rather consider that the top centimeter does not represent modern conditions as it likely integrates at least several centuries of sedimentation. In this case, the discrepancy between estimated sea surface conditions from dinocyst assemblages and the recent hydrography would reflect a cooling trend during the latest Holocene.

## 3.4 Discussion

Dinocyst assemblages and the application of MAT allowing reconstruction of sea surface reconstructions reflect the shift from cold, quasi-perennial sea ice cover to warmer conditions with seasonal ice cover at all four sites. According to the chronology in radiocarbon dated cores CC04 and CC70 (Fig. 3.2), this shift towards mild postglacial conditions occurred in a time transgressive manner, around 11.9 cal ka BP in the northwest Labrador Sea and 7.4 cal ka BP in Baffin Bay. The northern Labrador Sea and Davis Strait cores CC04 (Fig. 3.3a) and TWC08 (Fig. 3.4a) also recorded variation in salinity reflecting changes in freshwater-meltwater discharges during the deglaciation and resulting in changes in oceanographic regimes. These changes are discussed below in reference to the available chronostratigraphic information, to assess the timing of events in the Baffin Bay-Labrador Sea corridor during the Holocene.

### 3.4.1 Deglaciation and breakup of quasi-perennial sea ice cover

In the northwest Labrador Sea core CC04, very low dinocyst concentrations and the almost exclusive occurrence of the heterotrophic species *Brigantedinium* spp. and *I. minutum* characterize the record prior to ~11.9 cal ka BP (Fig. 3.3b). Such an assemblage can be associated with harsh conditions (de Vernal et al., 1997, 2001, 2013a,b; Gibb et al., 2014; Rochon et al., 1999) and led to the reconstruction of very cold sea surface conditions with quasi-perennial sea ice cover (Fig. 3.3a). After 11.9 cal ka BP, the appearance of phototrophic taxa suggests milder conditions that can be associated with the influence of North Atlantic waters. In particular, the occurrence of cysts of *P. dalei* suggests large seasonal gradients of temperature, from freezing in winter to mild in summer, due to low thermal inertia in stratified surface waters

(Rochon et al., 1999; Solignac et al., 2006). The increase in summer SSTs coincides with the onset of relatively warm air temperatures on Baffin Island as reconstructed from chironomid and pollen in lake records (e.g. Briner et al., 2006; Fréchette and de Vernal, 2009). This early Holocene thermal optimum inland occurred during the high insolation phase of the Holocene (Berger and Loutre, 1991) which was also marked by meltwater discharges from the retreating Laurentide Ice Sheet (LIS) that probably resulted in low surface water salinity and stratification of the upper water mass. Deglaciation in the Baffin and Labrador sectors of the LIS accelerated after the Younger Dryas (YD), as recorded regionally at ~12.9-11.6 cal ka BP (Andrews et al., 1995a; Dyke, 2004; Jennings et al., 1996; Kaplan and Miller, 2003). It was accompanied by rapid retreat of the Baffin Island coastal outlet glaciers between 12 and 10 cal ka BP (Briner et al., 2009). During the deglaciation of the northeast LIS, there were a few ice advances including the Gold Cove advance (~11.3-11.0 cal ka BP; Kaufman et al., 1993) and the Noble Inlet advance (~10.0-9.5 cal ka BP; Stravers et al., 1992) in Hudson Strait. There were also ice advances on Baffin Island during the Cockburn substage (~9.5-8.5 cal ka BP; Andrews and Ives, 1978) and possibly the 8.2 ka event (Miller et al., 2005; Young et al., 2012). During the deglaciation, meltwater discharges no doubt played a role in the variability of sea surface conditions notably with regard to salinity and its role on surface water stratification, especially after ~11.9 cal ka BP. The regime shift at about 11.9 cal ka BP is thus represented by the change from a quasi-perennially ice covered glacial phase to a seasonally ice covered deglacial phase.

The changes in sea surface conditions reconstructed from the Davis Strait core TWC08 (Fig. 3.4a) are very similar to those of CC04 (Fig. 3.3a), which is consistent given the location of core TW08 on the southern side of the Davis Strait sill in the northernmost part of the Labrador Sea. The TWC08 record can thus be correlated with that of CC04 based on the carbonate peak and IRD corresponding to DC0 (60-25cm ≈ 13-10.5 cal ka BP; cf. Andrews et al., 2014). On these grounds, it is

reasonable to propose that the transition at 34 cm in TWC08 may correspond to the major regime shift recorded at ~11.9 cal ka BP in core CC04.

The sedimentological record of the eastern Baffin Bay core CC70 suggests that the site was proximal to the ice margin from 12.2 to about 11.4 cal ka BP, with high IRD content reflecting ablation by ice calving from the adjacent Greenland Ice Sheet (GIS) margin (Jennings et al., 2014). Low dinocyst concentration, exclusive dominance of heterotrophic species, the reconstruction of low SST and salinity together suggest low productivity and quasi-perennial sea ice cover likely due to the ablating GIS margin and related meltwater discharge (Figs 3.5a,b). At ~9.5 cal ka BP, the reconstruction of higher salinity and slight decrease in sea ice cover correspond to the reduction of ice ablation material (cf. Jennings et al., 2014), which indicates the diminution of proximal GIS ablation activities in eastern Baffin Bay. This change occurred after the rapid retreat of the GIS ice margin at the head of Disko Bugt by ~10.3 cal ka BP (Lloyd et al., 2005; Long and Roberts, 2003).

There are other paleoceanographic records from Baffin Bay that permit to estimate the timing of the breakup of permanent sea ice cover. Unfortunately these records are restricted to the surrounding shelves where sea ice dynamics may differ due to local influences related to the GIS and LIS margins, or to the North Water polynya (e.g. Hamel et al., 2002). The dinocyst assemblages in core P009 from Lancaster Sound in northwest Baffin Bay (Fig. 3.1) recorded the breakup of quasi-perennial ice at ~9.6 cal ka BP (Ledu et al., 2008) while cores 008P and 012P from northern Baffin Bay recorded it around 10.5 cal ka BP (Levac et al., 2001). Indirect proxies other than dinocysts were used for inferences about the transition from very dense to seasonal sea ice cover in Baffin Bay. Benthic foraminifera from northern (cores 008P and 012P) and western Baffin Bay suggest change from perennial to seasonal ice cover between 10.9 and 9.2 cal ka BP (Knudsen et al., 2008; Osterman and Nelson, 1989). Perennial sea ice breakup between 10.3 and 9.2 cal ka PB has been inferred from

molluscs, driftwood and midges (Bennike, 2004; Dyke et al., 1996; Funder 1990; Funder and Weidick, 1991). Lastly, glacial geomorphology indicates that the flow of Arctic water through Nares Strait commenced by ~10.6 cal ka BP which fully deglaciated between 9.0 and 8.3 cal ka BP (England et al., 2006; Jennings et al., 2011b), and through Lancaster Sound channeling the Canadian Arctic Archipelago starting after the YD to ~9.0 cal ka BP (Dyke, 1999). Although not directly related to sea surface conditions, these proxies suggest that the Baffin Bay coastal regions experienced the breakup of permanent sea ice between 10.5 and 9.0 cal ka BP. The CC70 record marks the breakup in eastern Baffin Bay at ~9.5 cal ka BP which fits within the time frame set by other records.

### 3.4.2 Transition towards full interglacial conditions around 7.5 cal ka BP

The dominance of phototrophic taxa (*O. centrocarpum*, *N. labyrinthus*, and the cysts of *P. dalei*), which can be associated with a strengthening of the warmer North Atlantic Drift (Rochon et al., 1999), dates from ~7.6 cal ka BP in core CC04 and possibly core TWC08 (Figs. 3.3b, 3.4b), and from ~7.4 cal ka BP in core CC70 (Fig. 3.5b). The sea surface reconstructions from core CC04 in the northwest Labrador Sea indicate an increase in winter SST, decrease in summer SST and increase in SSS (Fig. 3.3a). The reduced seasonal gradients in temperature and increase in salinity suggest reduced stratification of the upper water masses likely related to decreased meltwater discharge from the LIS. The regime shift at ~7.6 cal ka BP occurs when more than 90% of the LIS had retreated (Dyke, 2004), after the Hudson Strait deglaciation (Andrews et al., 1995b; Kerwin, 1996) and the subsequent drainage of glacial lakes Agassiz and Objiway (Barber et al., 1999) at 8.4 cal ka BP. However, the shift slightly predates the collapse of the ice cap of Foxe Basin at ~7.0 cal ka BP (Briner et al., 2009; Miller et al., 2005).

The main change in salinity recorded in the northern Labrador Sea that corresponds to reduced stratification coupled with increased advection of North Atlantic water would have fostered convective mixing of the upper water column during winter initiating LSW formation and modern circulation in the northwest North Atlantic (cf. also de Vernal and Hillaire-Marcel, 2006; Hillaire-Marcel et al., 2001). The advection of Atlantic water and reorganization within the Labrador Sea is also apparently started at 7.7 cal ka BP off southwest Greenland in cores DA04-41P and -31P (Seidenkrantz et al., 2013), and ~7.6 cal ka BP south of Davis Strait in cores CC04, TWC/P021 (Fig. 3.1; de Vernal et al., 2001, 2013b), P094 (Orphan Knoll; Solignac et al., 2004) and possibly TWC08. Hence the overall data from northern Labrador Sea and Davis Strait suggest an important regional shift in sea surface conditions at ~7.6 cal ka BP with a transition towards modern postglacial conditions.

The species assemblages and MAT reconstructions also permit to identify a shift at ~7.4 cal ka BP in eastern Baffin Bay core CC70 is as an increase in SSTs and further reduction of seasonal extent of sea ice cover. The sea surface conditions after the shift are related to the strengthened Atlantic inflow through Davis Strait into Baffin Bay with the WGC. At this time, the GIS reached maximum postglacial retreat within the Isfjord (Briner et al., 2010; Young et al., 2011), possibly related to the increased strength of the WGC (Holland et al., 2008; Young et al., 2011). Also in core CC70, Jennings et al. (2014) identified foraminiferal species indicative of warmer intermediate water from ~7.5 cal ka BP, which they attributed to an increased influence of Atlantic water and retreat of the GIS and LIS. There are now a few records that have revealed a shift due to surface and subsurface warming related to a strengthened WGC in Baffin Bay around 7.5 cal ka BP, many focusing around Disko Bugt. Similarly to CC70, core MSM343300 at the southwestern edge of Disko Bugt (Fig. 3.1) contains heterotrophic species that dominate the assemblages prior to ~7.3 cal ka BP followed by the appearance of species associated with the North Atlantic

water influence (Ouellet-Bernier et al., 2014). Benthic foraminiferal assemblages also recorded the strengthening of the North Atlantic component in subsurface waters in Disko Bugt area, at 7.3 cal ka BP in core MSM343300 (Perner et al., 2013), and between 7.7 and 7.5 cal ka BP in the nearshore cores DA00-04P and -06P (Seidenkrantz et al., 2013) (Fig. 3.1). The extremely low dinocyst concentrations that characterize most of central Baffin Bay core TWC16 indicate low productivity due to quasi-perennial ice cover (Fig. 3.6a,b). Heterotrophic species that tolerate heavy sea ice formation are present. The most striking feature is the dominance of *I. pallidum*, which is an oligotrophic species currently found at high abundance in cold, open ocean environments such as the eastern Greenland Sea (Bonnet et al., 2010; de Vernal et al., 2001; Rochon et al., 1999). Accordingly, the sea surface reconstructions with analogues selected from this area reflect very cold conditions and low productivity which is coupled with nearly perennial sea ice cover due to the presence of heterotrophic taxa throughout most of the interval. The shift at 17.5 cm towards warmer sea surface temperatures with ice-free conditions at core top is the result in the change from an assemblage dominated by *I. pallidum* to an assemblage with higher diversity of subpolar taxa. From 17.5 to 8 cm, the change in dinocyst assemblages reflects warming sea surface conditions. For the upper 8 cm of the core, likely because of the occurrence of *I. sphaericum*, most modern analogues are from the Barents and southeastern Greenland Seas, which led to reconstruct relatively warm and saline sea surface conditions, with summer SSTs of about 8°C, salinity around 34 and sea ice restricted to winter. Such assemblages mark the establishment of full interglacial conditions in Baffin Bay. The change recorded from 17.5 cm in central Baffin Bay might correlate with the shift recorded at 7.4 cal ka BP in the eastern Baffin Bay.

### 3.4.3 Changes in sea surface conditions during the mid- and late Holocene

In the Baffin Bay cores, the dinocyst assemblage composition above the transition recorded at ca. 7.5 cal ka BP is relatively uniform. However, in core CC04 from the northern Labrador Sea, there is a significant shift in dinocyst assemblage at ~2.4 cal ka BP as clearly shown from the PC analysis. It is associated with a change in species dominance, from *O. centrocarpum* to *N. labyrinthus* (Fig. 3.3b). However, it does not correspond to a major change in reconstructed sea surface conditions, which only show a slight diminution in summer SSTs and seasonal gradients of temperatures (Fig. 3.3a). In modern sediments of the reference database, *N. labyrinthus* appears to be cosmopolitan in the North Atlantic, often dominating the assemblage along the Irminger Current (Boessenkool et al., 2001; Marret et al., 2004; Rochon et al., 1999). It has also been associated with the mixing of cold Arctic waters of EGC or LC with warm North Atlantic waters of the IC or WGC (Rochon et al., 1999), and was positively correlated with nutrient levels (Devillers and de Vernal, 2000). These conditions correspond to those recorded along the Labrador Shelf-Slope Front (LSSF), which is currently located northwest of CC04 (Fig. 3.1; Belkin et al., 2009). Therefore the change in the dinocyst assemblage might reflect southward and/or eastward shift of the polar front during the course of the late Holocene with a strengthened BIC. A late Holocene increase in Arctic water outflow through the Canadian Arctic Archipelago into Baffin Bay, including Nares Strait and Lancaster Sound, is supported by slight changes in dinocyst assemblages corresponding to a cooling trend (Ledu et al., 2008; Levac et al., 2001). Therefore an increase in *N. labyrinthus* and dinocyst concentrations coupled with fluctuations in sea surface conditions in the northwest Labrador Sea (and possibly other areas along the IC), may be interpreted as reflecting the core's proximity to the polar front linked to an increase in Arctic water outflow and a strengthened BIC and LC.

One of the most prominent feature of late Holocene paleoclimate in the northwest Atlantic is a cooling trend that has been associated with Neoglaciation. Ice advance of the GIS occurred during the late Holocene (Briner et al., 2010; Long and Roberts, 2003). Surface and subsurface cooling along coastal West Greenland over the last ~4 ka have been attributed to varying strength in the Atlantic (IC) vs Arctic (EGC) components of the WGC (Andresen et al., 2011; Erbs-Hansen et al., 2013; Lloyd, 2007; Møller et al., 2006; Moros et al., 2006; Perner et al., 2013; Ouellet-Bernier et al., 2014; Seidenkrantz et al., 2007, 2008). Temperature fluctuations in those records were associated with the Medieval Warm Period and Little Ice Age. The sea surface conditions reconstructed at our sites also show fluctuations during the last 3 ka but they do not necessarily correlate with other records, nor are their trends consistent. In contrast to Neoglacial cooling, the average sea surface conditions in core CC70 increase by approximately 1.5°C after ~3.1 cal ka BP (Fig. 3.6b), suggesting an increased contribution of the Atlantic component to the WGC. Coupled with lower salinities between ~1.9 and 0.9 cal ka BP, the slightly higher SSTs can also suggest summer warming due to increased stratification and reduced thermal inertia in the surface layer. Similarly, reconstructions based on dinocyst assemblages in core MSM343300 indicate phases of warmer temperatures and lower salinities, which are attributed to increased meltwater from the GIS during intervals of warmer WGC flux (Fig. 3.7; Ouellet-Bernier et al., 2014). The variations in sea surface conditions in CC70 do not seem to be perfectly in phase with those recorded in core MSM343300, which is more directly influenced by the WGC.

Actually, the sea surface salinity records from these two areas appear to be negatively correlated (Fig. 3.7), suggesting that fluctuations in the salinity nearshore may have little influence offshore. Core CC70 is located ~155 km west of the Greenland coast within the BIC-WGC frontal zone (Fig. 3.1; Belkin et al., 2009; Curry et al., 2011; Fisheries and Oceans Canada, 2012) with a modern summer SST and salinity of 3.6°C and 32.8, and 6.2 months per year of sea ice cover (Table 3.1). Its postglacial

assemblages are characterized by phototrophic taxa and dominant *O. centrocarpum* (Fig. 3.6a), which is typical of open ocean conditions. In contrast, core MSM343300 is located ~15 km west of the Greenland coast on the southern flank of the opening of Disko Bugt (Fig. 3.1) with a modern summer SST and salinity of 4.4°C and 32.9 respectively with about 4 months per year of sea ice cover. Hence dinocyst assemblages are largely dominated by *I. minutum* and reflect a neritic environment. The reconstructed sea surface conditions of CC70 throughout the postglacial appear to be about 5°C colder, 1 unit of salinity higher, and characterized by slightly more extensive sea ice cover than in core MSM343300 (Fig. 3.7). Thus the surface waters at the coastal site (MSM343300) show greater ability to warm in summer due to lower thermal inertia and the more direct influence of the WGC (and EGC) than sites offshore toward central Baffin Bay (CC70), which are under the influence of the cyclonic ocean gyre mixing BIC with WGC and being responsible for lower stratification.

## 3.5 Conclusion

Despite difficulties to establish chronostratigraphical schemes, poor preservation due to biogenic carbonates and low postglacial sedimentation rates, the Holocene records from the Baffin Bay, Davis Strait and northern Labrador Sea presented here provide some insight into the postglacial paleoceanographical reorganisation in the northwest North Atlantic. These records are mostly based on dinocyst assemblages. They illustrate strong regionalism in the dinocyst distribution, but yield a consistent picture of the main paleoceanographical changes. South of Davis Strait, the breakup of perennial sea ice and onset of relatively warm sea surface conditions began ~11.9 cal ka BP with dinocyst records that indicate the strengthening of the Atlantic component of the WGC. In Baffin Bay, the breakup of perennial sea ice began after

~9.5 cal ka BP and the regime shift to warmer sea surface temperatures occurred later, at about 7.5 cal ka BP. The onset of warmer conditions in Baffin Bay seems also to be a response to a strengthened North Atlantic component of the WGC and to relate with the final retreat of the LIS and GIS. Therefore the early to mid-Holocene optimum, identified as the intensification of the North Atlantic Current (de Vernal and Hillaire-Marcel, 2006), occurred diachronously north of the Labrador Sea, in the Baffin Bay, the delayed establishment of full postglacial conditions being likely related to late glacial retreat in the northeast LIS possibly caused by limited exchanges through the narrow Davis Strait. The timing of changes in Baffin Bay is coherent with reduction of meltwater-freshwater export to the Labrador Sea, which likely contributed to higher salinity and density favorable for convective mixing and the formation of LSW. Beyond the major change recorded at around 7.5 cal ka BP, paleoceanographic assessment from dinocyst assemblages in cores from the Baffin Bay corridor suggests that sea surface conditions experienced spatial and temporal variability throughout the postglacial, responding to large scale changes in the open oceanic regime. This variability seems also to be related to fluctuations in the position of the polar front that constitutes a boundary between inflowing North Atlantic water and outflowing Arctic water.

Acknowledgements

This paper is a contribution to the Past4Future project of the 7th Framework Program of the European Commission. Special thanks Maryse Henry for her help and expertise in the Micropaleontology and Marine Palynology Laboratory – GEOTOP, and to Helen Gillespie, Susan Fudge, and Danny Boyce at Memorial University for their in kind support of laboratory equipment. We are also grateful to the reviewers who provided useful and constructive comments on the manuscript.

Funding

Support from the *Ministère du Développement Économique, Innovation et Exportation* (MDEIE) and *Fonds Québécois de Recherche sur la Nature et les Technologies* (FQRNT) is acknowledged. Special thanks to the Canadian Foundation for Climate and Atmospheric Sciences (CFCAS), Natural Resources Canada (NRCan), and the Natural Sciences and Engineering Research Council of Canada (NSERC) for their financial support of the HU2008029 expedition in the Labrador Sea.

# REFERENCES

Aksenov Y, Bacon S, Coward AC and Holliday NP (2010) Polar outflow from the Arctic Ocean: A high resolution model study. *Journal of Marine Systems* 83(1): 14-37.

Aksu AE (1983) Holocene and Pleistocene dissolution cycles in deep-sea cores of Baffin Bay and Davis Strait: Palaeoceanographic implications. *Marine Geology* 53(4): 331-348.

Andersen C, Koc N and Moros, M (2004) A highly unstable Holocene climate in the subpolar North Atlantic: evidence from diatoms. *Quaternary Science Reviews* 23: 2155-2166.

Andresen CS, McCarthy DJ, Dylmer CV, Seidenkrantz MS, Kuijpers A and Lloyd JM (2011) Interaction between subsurface ocean waters and calving of the Jakobshavn Isbræ during the late Holocene. *The Holocene* 21(2): 211-224.

Andrews JT and Ives JD (1978) Cockburn'' nomenclature and the Late Quaternary history of the eastern Canadian Arctic. *Arctic Alpine Research* 10, 617-633.

Andrews JT, Jennings AE, Kerwin M, Kirby M, Manley W, Miller GH, Bond G and MacLean B (1995a). A Heinrich-like event, H-0 (DC-0): Source (s) for detrital carbonate in the North Atlantic during the Younger Dryas Chronozone. *Paleoceanography* 10(5), 943-952.

Andrews JT, MacLean B, Kerwin M, Manley W, Jennings AE, and Hall F (1995b). Final stages in the collapse of the Laurentide Ice Sheet, Hudson Strait, Canada, NWT: 14 C AMS dates, seismics stratigraphy, and magnetic susceptibility logs. *Quaternary Science Reviews* 14(10), 983-1004.

Andrews JT, Barber DC, Jennings AE, Eberl DD, Maclean B, Kirby ME and Stoner JS (2012) Varying sediment sources (Hudson Strait, Cumberland Sound, Baffin Bay) to the NW Labrador Sea slope between and during Heinrich events 0 to 4. *Journal of Quaternary Science* 27: 475-484.

Andrews JT, Gibb OT, Jennings AE and Simon Q (2014) Variations in the provenance of sediment from ice sheets surrounding Baffin Bay during MIS 2 and 3 and export to the Labrador Shelf Sea: site HU2008029-0008 Davis Strait. *Journal of Quaternary Science* 29(1): 3-13.

Azetsu-Scott K, Clarke A, Falkner K, Hamilton J, Jones EP, Lee C, Petrie B, Prinsenberg S, Starr M and Yeats P (2010) Calcium carbonate saturation states in the waters of the Canadian Arctic Archipelago and the Labrador Sea. *Journal of Geophysical Research: Oceans* 115(C11).

Barber DC, Dyke A, Hillaire-Marcel C, Jennings AE, Andrews JT, Kerwin MW, Bilodeau G, McNeely R, Southon J, Morehead MD and Gagnon JM (1999). Forcing of the cold event of 8,200 years ago by catastrophic drainage of Laurentide lakes. *Nature* 400(6742), 344-348.

Belkin IM, Cornillon PC and Sherman K (2009). Fronts in large marine ecosystems. *Progress in Oceanography* 81(1): 223-236.

Bennike O (2004) Holocene sea-ice variations in Greenland: onshore evidence. *The Holocene* 14(4): 607-613.

Boessenkool KP, Van Gelder MJ, Brinkhuis H and Troelstra SR (2001) Distribution of organic-walled dinoflagellate cysts in surface sediments from transects across the Polar Front offshore southeast Greenland. *Journal of Quaternary Science* 16(7): 661-666.

Bonnet S, de Vernal A, Hillaire-Marcel C, Radi T and Husum K (2010) Variability of sea-surface temperature and sea-ice cover in the Fram Strait over the last two millennia. *Marine Micropaleontology* 74: 59-74.

Bronk Ramsey C (2008) Deposition models for chronological records. *Quaternary Science Reviews* 27(1): 42-60.

Briner JP, Michelutti N, Francis DR, Miller GH, Axford Y, Wooller MJ and Wolfe AP (2006). A multi-proxy lacustrine record of Holocene climate change on northeastern Baffin Island, Arctic Canada. *Quaternary Research* 65(3), 431-442.

Briner JP, Davis PT and Miller GH (2009) Latest Pleistocene and Holocene glaciation of Baffin Island, Arctic Canada: key patterns and chronologies. *Quaternary Science Reviews* 28(21), 2075-2087.

Briner JP, Stewart HAM, Young NE, Philipps W and Losee S (2010) Using proglacial-threshold lakes to constrain fluctuations of the Jakobshavn Isbræ ice margin, western Greenland, during the Holocene. *Quaternary Science Reviews* 29(27): 3861-3874.

Buch E, (1990/2000). A monograph on the Physical Oceanography of the Greenland Waters. Greenland Fisheries Research Institute Report, (reissued in 2000 as Danish Meteorological Institute, Scientific report, 00-12), 405 pp.

Campbell DC, de Vernal A and shipboard party 2009: CGS Hudson Expedition 2008029: Marine geology and paleoceanography of Baffin Bay and adjacent areas Nain NL to Halifax NS August 28-September 23. Geological Survey of Canada, Open File 5989.

Castañeda IS, Smith LM, Kristjánsdóttir GB and Andrews JT (2004) Temporal changes in Holocene $\delta^{18}O$ records from the northwest and central North Iceland Shelf. *Journal of Quaternary Science* 19: 321-334.

Cheng W and Rhines PB (2004) Response of the overturning circulation to high-latitude fresh-water perturbations in the North Atlantic. *Climate Dynamics* 22: 359-372.

Cuny J, Rhines PB, Niiler PP and Bacon S (2002) Labrador Sea boundary currents and the fate of the Irminger Sea Water. *Journal of Physical Oceanography* 32(2): 627-647.

Cuny J, Rhines PB and Kwok R (2005) Davis Strait volume freshwater and heat fluxes. *Deep Sea Research Part I: Oceanographic Research Papers* 52(3): 519-542.

Curry B, Lee CM and Petrie B (2011) Volume Freshwater and Heat Fluxes through Davis Strait 2004-05*. *Journal of Physical Oceanography* 41(3): 429-436.

de Vernal A and Hillaire-Marcel C (2006) Provincialism in trends and high frequency changes in the northwest North Atlantic during the Holocene. *Global Planetary Change* 54(3): 263- 290.

de Vernal A, Larouche A and Richard PJH (1987) Evaluation of palynomorph concentrations: do the aliquot and the marker-grain methods yield comparable results? *Pollen et Spores* 29(2-3): 291-303.

de Vernal A, Bilodeau G, Hillaire-Marcel C and Kassou N (1992) Quantitative assessment of carbonate dissolution in marine sediments from foraminifer linings vs shell ratios: Davis Strait northwest North Atlantic. *Geology* 20(6): 527-530.

de Vernal A, Rochon A, Turon JL and Matthiessen J (1997) Organic-walled dinoflagellate cysts: palynological tracers of sea-surface conditions in middle to high latitude marine environments. *Geobios* 30(7): 905-920.

de Vernal A, Henry M and Bilodeau G (1999) Technique de préparation et d'analyse en micropaléontologie. Les Cahiers du GEOTOP Université du Québec à Montréal 3, unpublished report.

de Vernal A, Henry M, Matthiessen J, Mudie PJ, Rochon A, Boessenkool K, Eynaud F, Grøsfjeld K, Guiot J, Hamel D, Harland R, Head MJ, Kunz-Pirrung M, Levac E, Loucheur V, Peyron O, Pospelova V, Radi T, Turon J-L and Voronina E (2001) Dinoflagellate cyst assemblages as tracers of sea surface conditions in the northern North Atlantic Arctic and sub-arctic seas: the new ''n=677'' database and application for quantitative paleoceanographical reconstruction. *Journal of Quaternary Science* 16(7): 681-699.

de Vernal A, Eynaud F, Henry M, Hillaire-Marcel C, Londeix L, Mangin S, Matthiessen J, Marret F, Radi T, Rochon A, Solignac S and Turon JL (2005) Reconstruction of sea surface conditions at middle to high latitudes of the Northern Hemisphere during the Last Glacial Maximum (LGM) based on dinoflagellate cyst assemblages. *Quaternary Science Reviews* 24(7): 897-924.

de Vernal A, Rochon A, Fréchette B, Henry M, Radi T and Solignac S (2013a) Reconstructing past sea ice cover of the Northern hemisphere from dinocyst assemblages: status of the approach. *Quaternary Science Reviews* 79: 122-134.

de Vernal A, Hillaire-Marcel C, Rochon A, Fréchette B, Henry M, Solignac S and Bonnet S (2013b) Dinocyst-based reconstructions of sea ice cover concentration during the Holocene in the Arctic Ocean the northern North Atlantic Ocean and its adjacent seas. *Quaternary Science Reviews* 79: 111-121.

Devillers R and de Vernal A (2000) Distribution of dinoflagellate cysts in surface sediments of the northern North Atlantic in relation to nutrient content and productivity in surface waters. *Marine Geology* 166(1): 103-124.

Dyke AS (2004) An outline of the deglaciation of North America with emphasis on central and northern Canada In: Ehlers J Gibbard PL (eds) Quaternary Glaciations Extent and Chronology Part II North America Developments in Quaternary Science vol 2b. Amsterdam: Elsevier.

Dyke A (1999). Last glacial maximum and deglaciation of Devon Island, Arctic Canada: support for an Innuitian ice sheet. *Quaternary Science Reviews* 18(3), 393-420.

Dyke AS, Dale JE and McNeely RN (1996) Marine molluscs as indicators of environmental change in glaciated North America and Greenland during the last 18 000 years. *Géographie physique et Quaternaire* 50(2): 125-184.

England J, Atkinson N, Bednarski J, Dyke AS, Hodgson DA and Ó Cofaigh C (2006) The Innuitian Ice Sheet: configuration dynamics and chronology. *Quaternary Science Reviews* 25(7): 689-703.

Erbs-Hansen DR, Knudsen KL, Olsen J, Lykke-Andersen H, Underbjerg JA and Sha L (2013) Paleoceanographical development off Sisimiut West Greenland during the mid-and late Holocene: A multiproxy study. *Marine Micropaleontology* 102: 79-97.

Fisheries and Oceans Canada (2012) Ice Navigation in Canadian Waters Icebreaking Program. Maritime Services Canadian Coast Guard Fisheries and Oceans Canada, 53 p.

Fréchette B and de Vernal A (2009) Relationship between Holocene climate variations over southern Greenland and eastern Baffin Island and synoptic circulation pattern. *Climate of the Past* 5: 347-359.

Funder S and Weidick A (1991) Holocene boreal molluscs in Greenland—palaeoceanographic implications. *Palaeogeography Palaeoclimatology Palaeoecology* 85(1): 123-135.

Funder S (ed) 1990 Late Quaternary stratigraphy and glaciology in the Thule area Meddelelser om Gronland. *Geoscience* 22: 63p.

Gibb OT, Hillaire-Marcel C and de Vernal A (2014) Oceanographic regimes in the northwest Labrador Sea since Marine Isotope Stage 3 based on dinocyst and stable isotope proxy records. *Quaternary Science Reviews* 92: 269-279.

Goosse H, Fichefet T and Campin J-M (1997) The effects of the water flow through the Canadian Archipelago in a global ice–ocean model. *Geophysical Research Letters* 24(12): 1507-1510.

Hamel D, de Vernal A, Gosselin M and Hillaire-Marcel C (2002) Organic-walled microfossils and geochemical tracers: sedimentary indicators of productivity changes in the North Water and northern Baffin Bay (High Arctic) during the last centuries. *Deep Sea Research II* 49: 5277-5295.

Head MJ, Harland R and Matthiessen J (2001) Cold marine indicators of the late Quaternary: The new dinoflagellate cyst genus Islandinium and related morphotypes. *Journal of Quaternary Science* 16(7): 621-636.

Hillaire-Marcel C, de Vernal A, Bilodeau G and Weaver AJ (2001) Absence of deep water formation in the Labrador Sea during the last interglacial period. *Nature* 410: 1073-1077.

Holland DM, Thomas RH, de Young B, Ribergaard MH and Lyberth B (2008) Acceleration of Jakobshavn Isbrae triggered by warm subsurface ocean waters. *Nature Geoscience* 1(10): 659-664.

Jennings AE, Tedesco KA, Andrews JT and Kirby ME (1996). Shelf erosion and glacial ice proximity in the Labrador Sea during and after Heinrich events (H-3 or 4 to H-0) as shown by foraminifera. Geological Society, London, Special Publications, 111(1), 29-49.

Jennings A, Andrews J and Wilson L (2011a) Holocene environmental evolution of the SE Greenland Shelf North and South of the Denmark Strait: Irminger and East Greenland current interactions. *Quaternary Science Reviews* 30(7): 980-998.

Jennings AE, Sheldon C, Cronin TM, Francus P, Stoner J, and Andrews J (2011b) The Holocene history of Nares Strait: Transition from glacial bay to Arctic-Atlantic throughflow. *Oceanography* 24(3): 26-41,

Jennings AE, Walton ME, Ó Cofaigh C, Kilfeather A, Andrews JT, Ortiz JD, de Vernal A and Dowdeswell JA (2014) Paleoenvironments during Younger Dryas-Early Holocene retreat of the Greenland Ice Sheet from outer Disko Trough central west Greenland. *Journal of Quaternary Science* 29(1): 27-40.

Kaplan MR and Miller GH (2003) Early Holocene delevelling and deglaciation of the Cumberland Sound region, Baffin Island, Arctic Canada. *Geological Society of America Bulletin* 115, 445-462.

Kaufman DS, Miller GH, Stravers JA and Andrews JT (1993). Abrupt early Holocene (9.9-9.6 ka) ice-stream advance at the mouth of Hudson Strait, Arctic Canada. *Geology* 21(12), 1063-1066.

Kaufman DS et. al. (2004) Holocene thermal maximum in the western Arctic (0–180°W). *Quaternary Science Reviews* 23(5-6): 529-560.

Kerwin MW (1996). A regional stratigraphic isochron (ca. 8000 14 C yr BP) from final deglaciation of Hudson Strait. *Quaternary Research* 46(2), 89-98.

Knudsen KL, Stabell B, Seidenkrantz M-S, Eiríksson J and Blake Jr W (2008) Deglacial and Holocene conditions in northernmost Baffin Bay: sediments foraminifera diatoms and stable isotopes. *Boreas* 37(3): 346-376.

Lazier JRN (1973) The renewal of Labrador Sea water. *Deep Sea Research* 20(4): 341-353.

Ledu D, Rochon A, de Vernal A and St-Onge G (2008) Palynological evidence of Holocene climate change in the eastern Arctic: a possible shift in the Arctic oscillation at the millennial time scale. *Canadian Journal of Earth Science* 45: 1363-1375.

Levac E, de Vernal A and Blake W (2001) Sea surface conditions in northernmost Baffin Bay during the Holocene: palynological evidence. *Journal of Quaternary Science* 16(4): 353-363.

Lloyd JM, Park LA, Kuijpers A and Moros M (2005) Early Holocene palaeoceanography and deglacial chronology of Disko Bugt west Greenland. *Quaternary Science Reviews* 24(14): 1741-1755.

Lloyd JM, Kuijpers A, Long A, Moros M and Park LA (2007) Foraminiferal reconstruction of mid- to late-Holocene ocean circulation and climate variability in Disko Bugt West Greenland. *The Holocene* 17: 1079-1091.

Long AJ, and Roberts DH (2003). Late Weichselian deglacial history of Disko Bugt, West Greenland, and the dynamics of the Jakobshavns Isbrae ice stream. *Boreas* 32(1), 208-226.

Marret F, Eiríksson J, Knudsen KL, Turon JL and Scourse JD (2004) Distribution of dinoflagellate cyst assemblages in surface sediments from the northern and western shelf of Iceland. *Review of Palaeobotany and Palynology* 128(1): 35-53.

Matthews J (1969) The assessment of a method for the determination of absolute pollen frequencies. *New Phytologist* 68(1): 161-166.

Miller GH, Wolfe AP, Briner JP, Sauer PE and Nesje A (2005). Holocene glaciation and climate evolution of Baffin Island, Arctic Canada. *Quaternary Science Reviews* 24(14), 1703-1721.

Møller HS, Jensen KG, Kuijpers A, Aagaard-Sørensen S, Seidenkrantz M-S, Endler R and Mikkelsen N (2006) Late Holocene environmental and climatic changes in Ameralik Fjord Southwest Greenland - evidence from the sedimentary record. *The Holocene* 16: 685-695.

Moros M, Jensen KG and Kuijpers A (2006) Mid-to late-Holocene hydrological and climatic variability in Disko Bugt central West Greenland. *The Holocene* 16(3): 357-367.

Ó Cofaigh C, Dowdeswell JA, Jennings AE, Hogan KA, Kilfeather A, Hiemstra JF, Noormets R, Evans J, McCarthy DJ, Andrews JT, Lloyd JM and Moros M (2013) An extensive and dynamic ice sheet on the West Greenland shelf during the last glacial cycle. *Geology* 41(2): 219-222.

Olafsdottir S, Jennings AE, Geirsdottir A, Andrews JT and Miller GH (2010) Holocene variability of the North Atlantic Irminger Current on the South- and Northwest shelf of Iceland. *Marine Micropaleontology* 77: 101-118.

Osterman LE and Nelson AR (1989) Latest Quaternary and Holocene paleoceanography of the eastern Baffin Island continental shelf Canada: benthic foraminiferal evidence. *Canadian Journal of Earth Sciences* 26: 2236-2248.

Ouellet-Bernier M-M, de Vernal A, Hillaire-Marcel C and Moros M (2014) Paleoceanographic changes of Disko Bugt area West Greenland during the Holocene. *The Holocene* 24(11): 1573-1583.

Perner K, Moros M, Jennings A, Lloyd JM and Knudsen KL (2013) Holocene palaeoceanographic evolution off West Greenland. *The Holocene* 23(3): 374-387.

Radi T and de Vernal A (2008) Dinocysts as proxy of primary productivity in mid-high latitudes of the Northern Hemisphere. *Marine Micropaleontology* 68(1): 84-114.

Radi T, Bonnet S, Cormier M-A, de Vernal A, Durantou L, Faubert E, Head MJ, Henry M, Pospelova V, Rochon A and Van Nieuwenhove N (2013). Operational taxonomy and (paleo-) autecology of round brown spiny dinoflagellate cysts from the Quaternary of high northern latitudes. *Marine Micropaleontology* 98: 41-57.

Reimer PJ, Bard E, Bayliss A, Beck JW, Blackwell PG, Ramsey CB, Buck CE, Cheng H, Edwards RL, Friedrich M, Grootes PM, Guilderson TP, Haflidason H, Hajdas I, Hatté C, Heaton TJ, Hoffman DL, Hogg AG, Hughen KA, Kaiser KF, Kromer B, Manning SW, Niu M, Reimer RW, Richards DA, Scott EM, Southon JR, Staff RA, Turney CSM and van der Plicht J (2013) IntCal13 and Marine13 radiocarbon age calibration curves 0–50000 years cal BP. *Radiocarbon* 55(4): 1869-1887.

Ribergaard MH, Olsen SM, Mortensen J (2008) Oceanographic Investigations off West Greenland 2007. In: NAFO SCR Doc. 08/3, Scientific Council Meeting, June 2008.

Rochon A, de Vernal A, Turon J-L, Matthiessen J and Head MJ (1999) Distribution of dinoflagellate cyst assemblages in surface sediments from the North Atlantic Ocean and adjacent basins and quantitative reconstruction of sea surface parameters. *American Association of Stratigraphic Palynologists Contribution* Series No 35.

Schröeder-Adams CJ and Van Rooyen D (2011) Response of Recent Benthic Foraminiferal Assemblages to Contrasting Environments in Baffin Bay and the Northern Labrador Sea Northwest Atlantic. *Arctic* 317-341.

Seidenkrantz M-S, Aagaard-Sørensen S, Sulsbrück H, Kuijpers A, Jensen KG and Kunzendorf H (2007) Hydrography and climate of the last 4400 years in a SW Greenland fjord: implications for Labrador Sea palaeoceanography. *Holocene* 17(3): 387–401.

Seidenkrantz M-S, Roncaglia L, Fischel A, Heilmann-Clausen C, Kuijpers A and Moros M (2008) Variable North Atlantic climate seesaw patterns documented by a late Holocene marine record from Disko Bugt West Greenland. *Marine Micropaleontology* 68: 66-83.

Seidenkrantz M-S, Ebbesen H, Aagaard-Sørensen S, Moros M, Lloyd JM, Olsen J, Knudsen MF and Kuijpers A (2013) Early Holocene large-scale meltwater discharge from Greenland documented by foraminifera and sediment parameters. *Palaeogeography Palaeoclimatology Palaeoecology* 391: 71-81.

Serreze MC, Barrett AP, Slater AG, Woodgate RA, Aagaard K, Lammers RB, Steele M, Moritz R, Meredith M and Lee CM (2006) The large-scale freshwater cycle of the Arctic. *Journal of Geophysical Research* 111(C11): C11010.

Simon Q, St-Onge G and Hillaire-Marcel C (2012) Late Quaternary chronostratigraphic framework of deep Baffin Bay glaciomarine sediments from high-resolution paleomagnetic data. *Geochemistry Geophysics Geosystems* 13(11).

Simon Q, Hillaire-Marcel C, St-Onge G and Andrews JT (2014) North-eastern Laurentide western Greenland and southern Innuitian ice stream dynamics during the last glacial cycle. *Journal of Quaternary Science* 29(1): 14-26.

Solignac S, de Vernal A and Hillaire-Marcel C (2004) Holocene sea surface conditions in the North Atlantic-contrasted trends and regimes between the eastern and western sectors (Labrador Sea vs Iceland Basin). *Quaternary Science Reviews* 23(3): 319-334.

Solignac S, Giraudeau J and de Vernal A (2006) Holocene sea surface conditions in the western North Atlantic: Spatial and temporal heterogeneities. *Paleoceanography* 21(2): PA2004.

Srivastava SP, Arthur M and Clement B et al (eds) 1989 Proceedings of the Ocean Drilling Program Scientific Results, Vol 105, Ocean Drilling Program College Station TX.

Steinhauer S (2012) Postglacial paleoceanography of central Baffin Bay from palynological tracers. Master's thesis Université du Québec à Montréal, Montréal Canada.

St-Onge M-P and St-Onge G **(2014)** Environmental changes in Baffin Bay during the Holocene based on the physical and magnetic properties of sediment cores. *Journal of Quaternary Science* 29(1): 41-56.

Stravers JA, Miller GH and Kaufman DS (1992). Late glacial ice margins and deglacial chronology for southeastern Baffin Island and Hudson Strait, eastern Canadian Arctic. *Canadian Journal of Earth Sciences* 29(5), 1000-1017

Tang CCL, Ross CK, Yao T, Petrie B, DeTracey BM and Dunlap E (2004) The circulation water masses and sea-ice of Baffin Bay. *Progress in Oceanography* 63: 183-228.

Wadley MR and Bigg GR (2002) Impact of flow through the Canadian Archipelago and Bering Strait on the North Atlantic and Arctic circulation: An ocean modelling study. *Quarterly Journal of the Royal Meteorological Society* 128(585): 2187-2203.

Wang J, Mysak LA and Ingram RG (1994) Interannual variability of sea-ice cover in Hudson Bay Baffin Bay and the Labrador Sea. *Atmosphere-ocean* 32(2): 421-447.

Yashayaev I (2007) Hydrographic changes in the Labrador Sea 1960–2005. *Progress in Oceanography* 73: 242–276.

Young NE, Briner JP, Stewart HA, Axford Y, Csatho B, Rood DH and Finkel RC (2011) Response of Jakobshavn Isbræ, Greenland, to Holocene climate change. *Geology* 39(2): 131-134.

Young NE, Briner JP, Rood DH and Finkel RC (2012). Glacier extent during the Younger Dryas and 8.2-ka event on Baffin Island, Arctic Canada. *Science* 337(6100), 1330-1333.

Zonneveld KAF, Versteegh GJM and de Lange GJ (1997) Preservation of organic walled dinoflagellate cysts in different oxygen regimes: a 10000 years natural experiment. *Marine Micropaleontology* 29: 393-405.

Zonneveld KAF, Versteegh GJM and de Lange GJ (2001) Palaeoproductivity and post-depositional aerobic organic matter decay reflected by dinoflagellate cyst assemblages of the Eastern Mediterranean S1 sapropel. *Marine Geology* 172: 181-195.

Zonneveld KA, Bockelmann F and Holzwarth U (2007) Selective preservation of organic-walled dinoflagellate cysts as a tool to quantify past net primary production and bottom water oxygen concentrations. *Marine Geology* 237(3): 109-126.

Figures

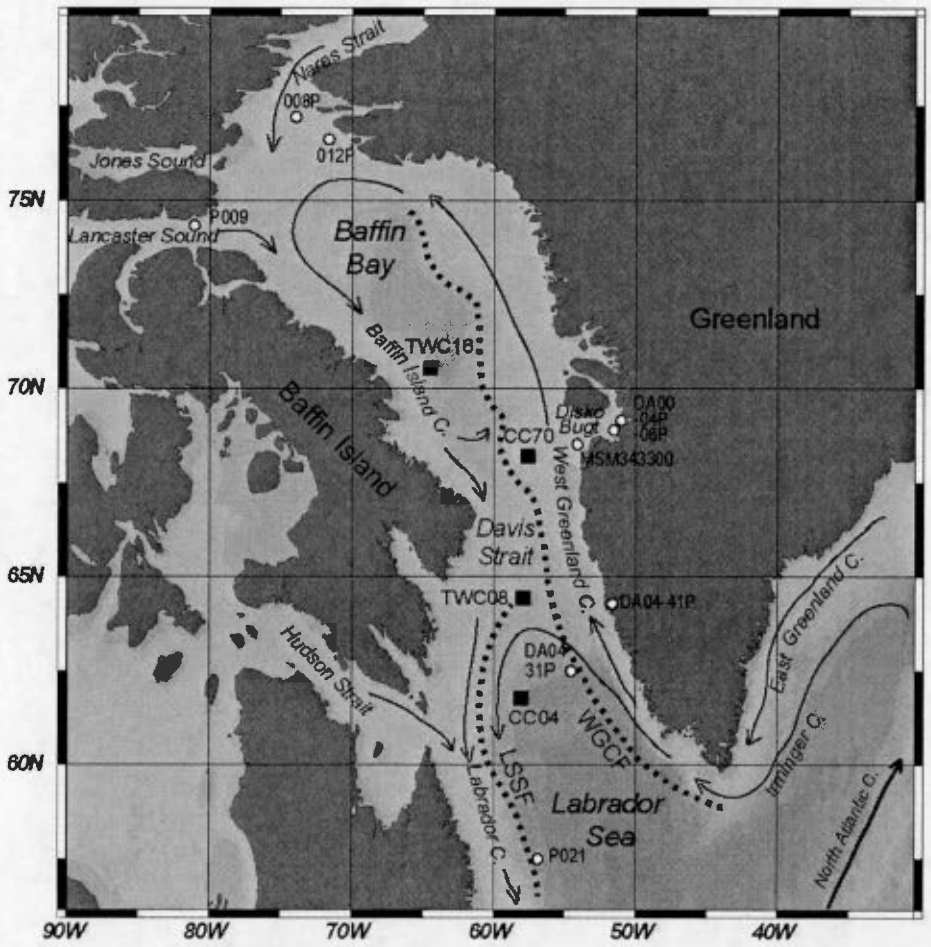


Figure 3.1. Map indicating sampling locations for cores CC04, TWC08, TWC16, and CC70, which are used in this study, as well as other cores mentioned in the text (008P, 012P, DA00-04P, DA00-06P, DA04-31P, DA04-41P, MSM343300, P009, P021). Surface currents are also displayed including the North Atlantic Current (NAC), Irminger Current (IC), East Greenland Current (EGC), West Greenland Current (WGC), Baffin Island Current (BIC), and Labrador Current (LC). The appoximate location of the West Greenland Current Front (WGCF) and the Labrador Shelf-Slope Front (LSSF) are shown as dotted lines (after Belkin et al., 2009).

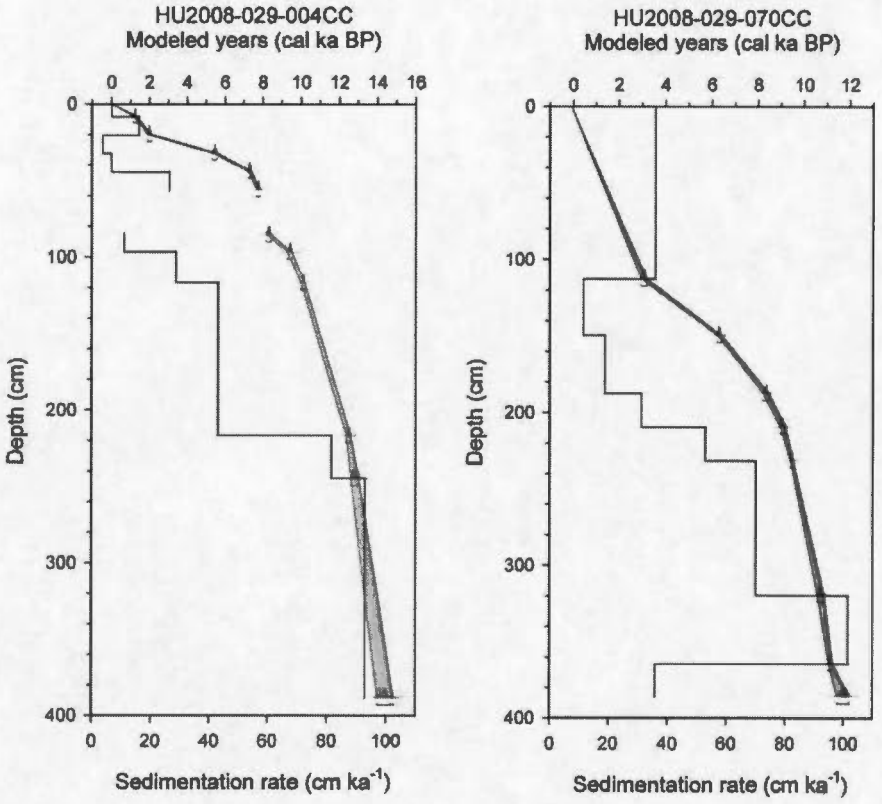


Figure 3.2. Age vs. depth relationship for core CC04 (a) and CC70 (b) based on the calibrated $^{14}C$ ages listed in Table 3.1. The age-depth model is shown in purple and blue and the sedimentation rates are represented by the black lines. The age-depth model for core CC04 (a) is in two sections, with core PC04 in blue and TWC04 in purple.

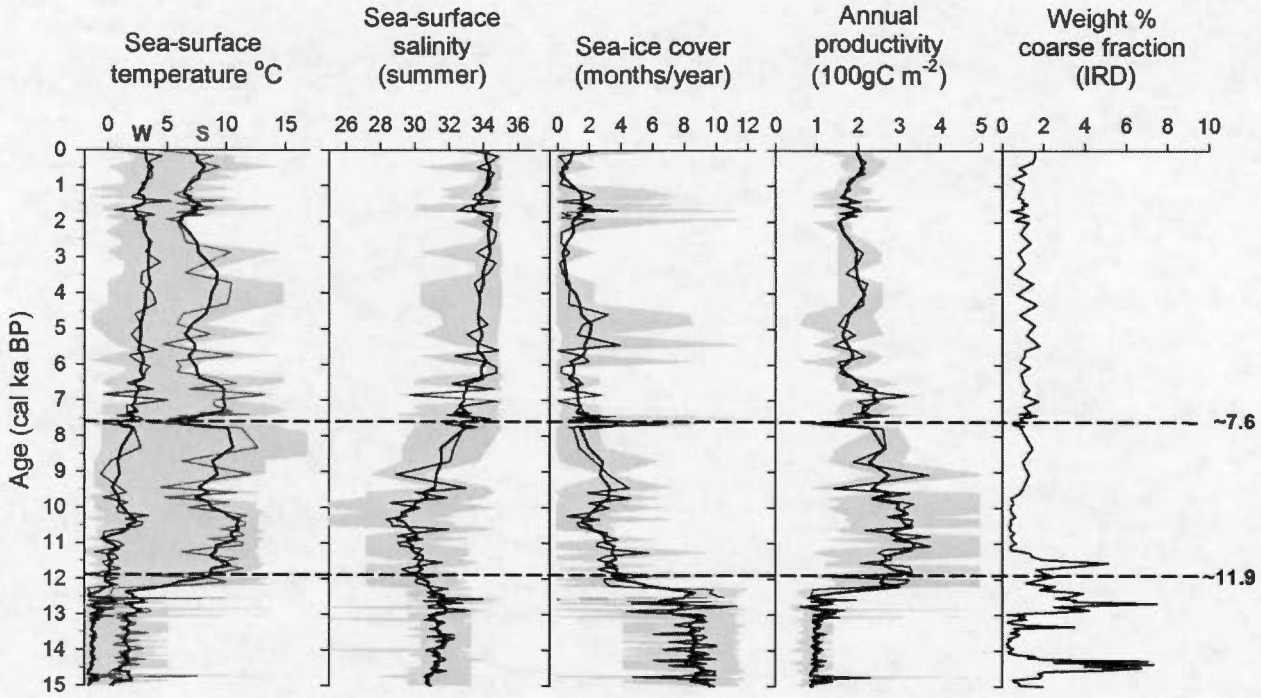


Figure 3.3a. Core CC04 - reconstruction of sea surface conditions from dinocyst assemblages and the weight percent coarse fraction (>106 μm, mostly representative of ice rafted debris - IRD) plotted vs age (cal ka BP). Sea surface temperatures (SST) in winter (w) and summer (s) are represented by blue and pink curves respectively. The lighter blue and pink curves correspond to possible maximum and minimum SSTs calculated from a set of 5 modern analogues. Sea surface salinity, sea ice cover and annual productivity are represented by thin black (most probable values) and grey shading (minimum and maximum). The thick black lines represent a 5-point running mean. Ecostratigraphic units identified by the principal component analyses and sea surface reconstructions are separated by a horizontal dashed line.

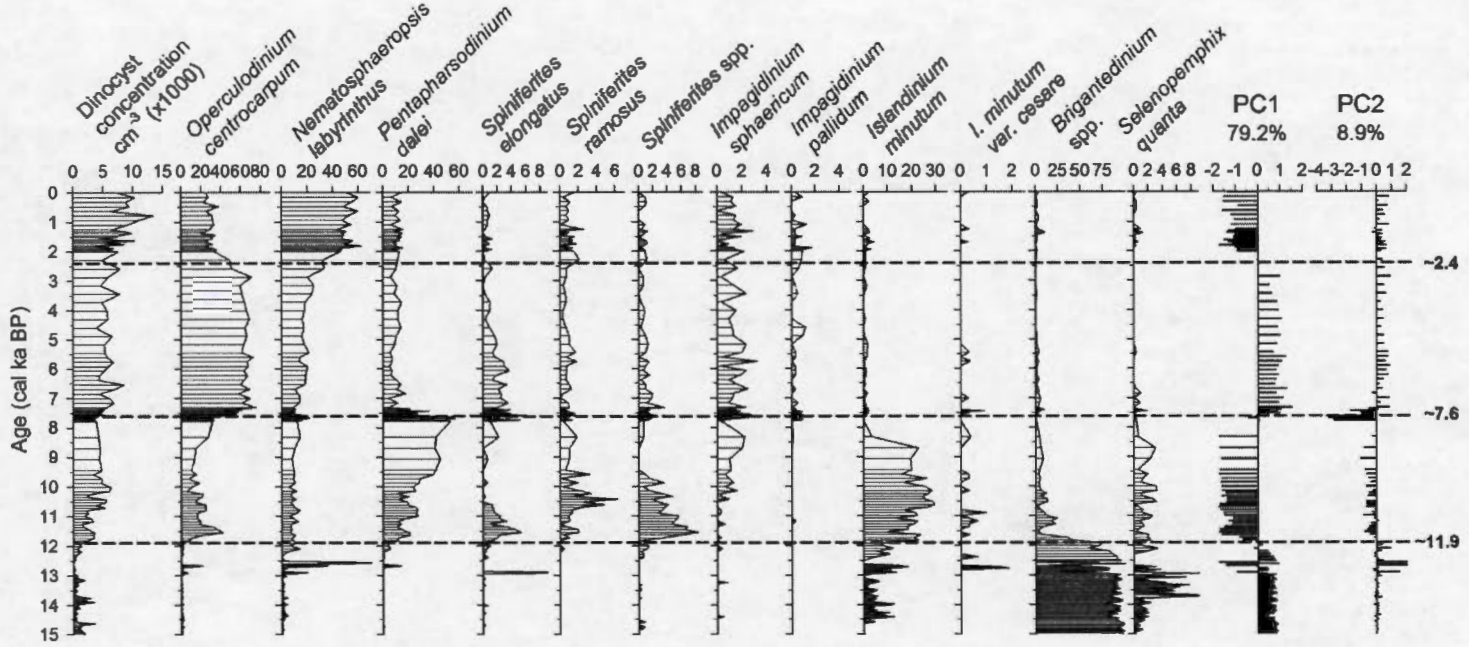


Figure 3.3b. Core CC04 - concentrations of dinocysts expressed as number of specimen per $cm^3$ of sediment, relative abundance (percentage) of the main dinocyst taxa, and scores for principal components (PC) 1 and 2 are plotted vs age (cal ka BP). The complete dinocyst dataset can be found on the GEOTOP website (http://www.geotop.ca). Ecostratigraphic units identified by the principal component analyses are separated by a dashed line, and marked with ages.

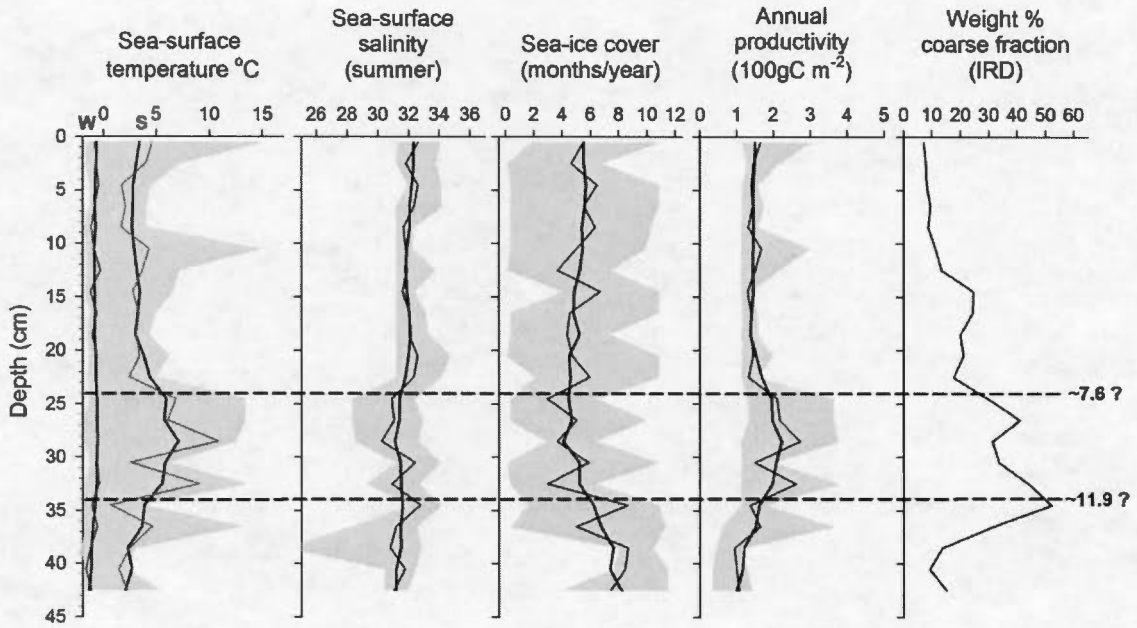


Figure 3.4a. Core TWC08 - reconstruction of sea surface conditions from dinocyst assemblages and the weight percent coarse fraction (>106 μm, mostly representative of ice rafted debris – IRD) plotted vs depth (cm). Sea surface temperatures (SST) in winter (w) and summer (s) are represented by blue and pink curves respectively. The lighter blue and pink curves correspond to possible maximum and minimum SSTs calculated from a set of 5 modern analogues. Sea surface salinity, sea ice cover and annual productivity are represented by thin black (most probable values) and grey shading (minimum and maximum). The thick black lines represent a 5-point running mean. Ecostratigraphic units identified by the principal component analyses and sea surface reconstructions are separated by a horizontal dashed line and identified by an inferred age (?) in cal ka BP.

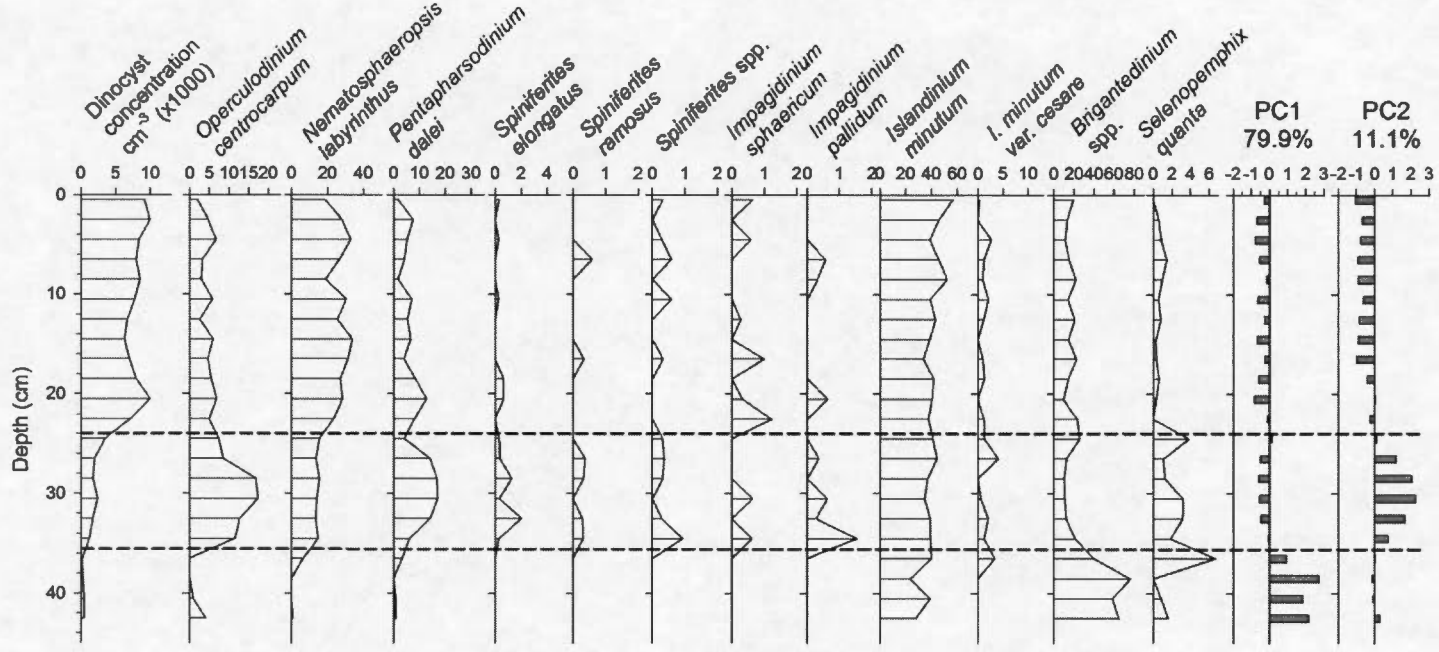


Figure 3.4b. Core TWC08 - concentrations of dinocysts expressed as number of specimen per $cm^3$ of sediment, relative abundance (percentage) of the main dinocyst taxa, and scores for principal components (PC) 1 and 2 are plotted vs depth (cm). The complete dinocyst dataset can be found on the GEOTOP website (http://www.geotop.ca). Ecostratigraphic units identified by the principal component analyses are separated by a dashed line.

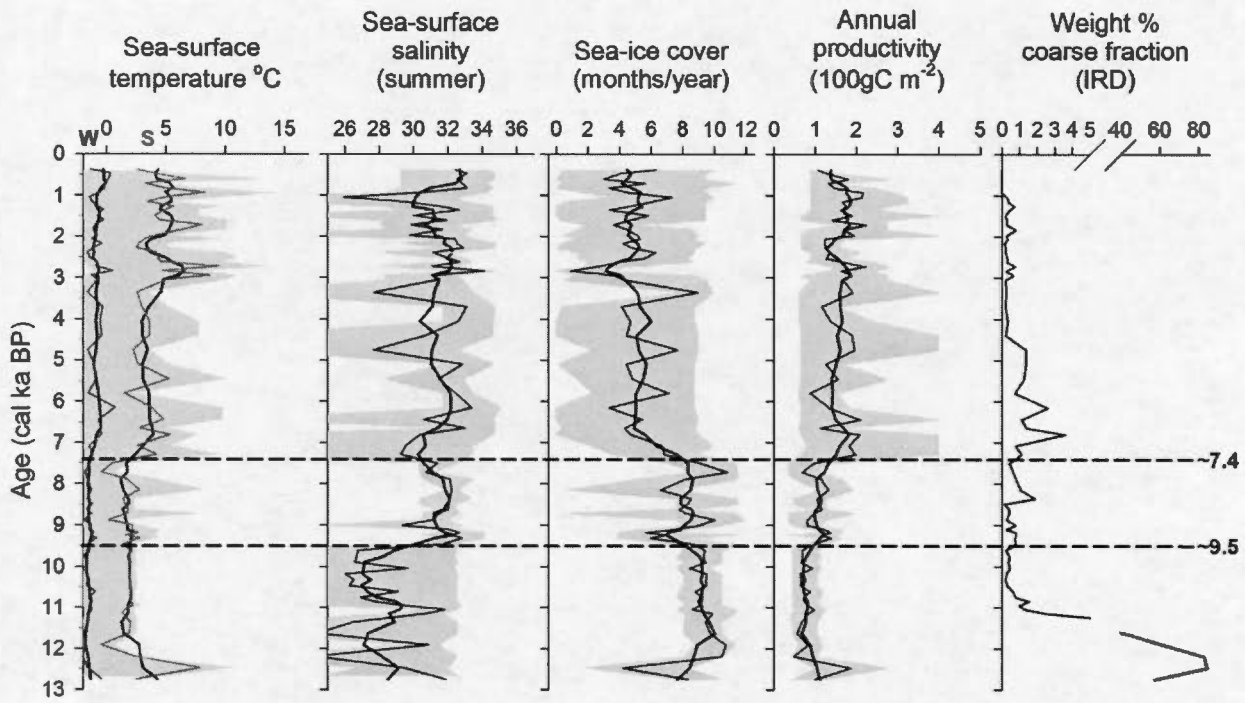


Figure 3.5a. Core CC70 - reconstruction of sea surface conditions from dinocyst assemblages and the weight percent coarse fraction (>106 μm, mostly representative of ice rafted debris – IRD) plotted vs age (cal ka BP). Sea surface temperatures (SST) in winter (w) and summer (s) are represented by blue and pink curves respectively. The lighter blue and pink curves correspond to possible maximum and minimum SSTs calculated from a set of 5 modern analogues. Sea surface salinity, sea ice cover and annual productivity are represented by thin black (most probable values) and grey shading (minimum and maximum). The thick black lines represent a 5-point running mean. Ecostratigraphic units identified by the principal component analyses and sea surface reconstructions are separated by a horizontal dashed line.

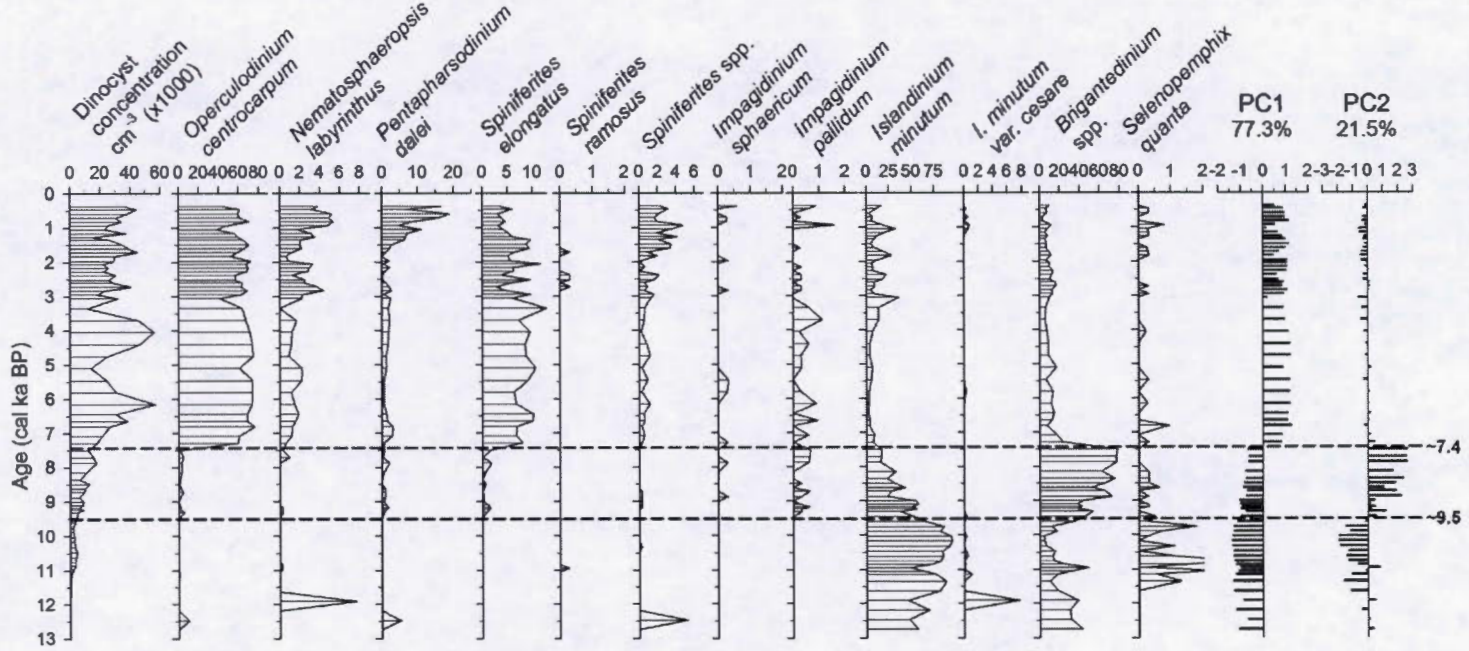


Figure 3.5b. Core CC70 - concentrations of dinocysts expressed as number of specimen per $cm^3$ of sediment, relative abundance (percentage) of the main dinocyst taxa, and scores for principal components (PC) 1 and 2 are plotted vs age (cal ka BP). The complete dinocyst dataset can be found on the GEOTOP website (http://www.geotop.ca). Ecostratigraphic units identified by the principal component analyses are separated by a dashed line.

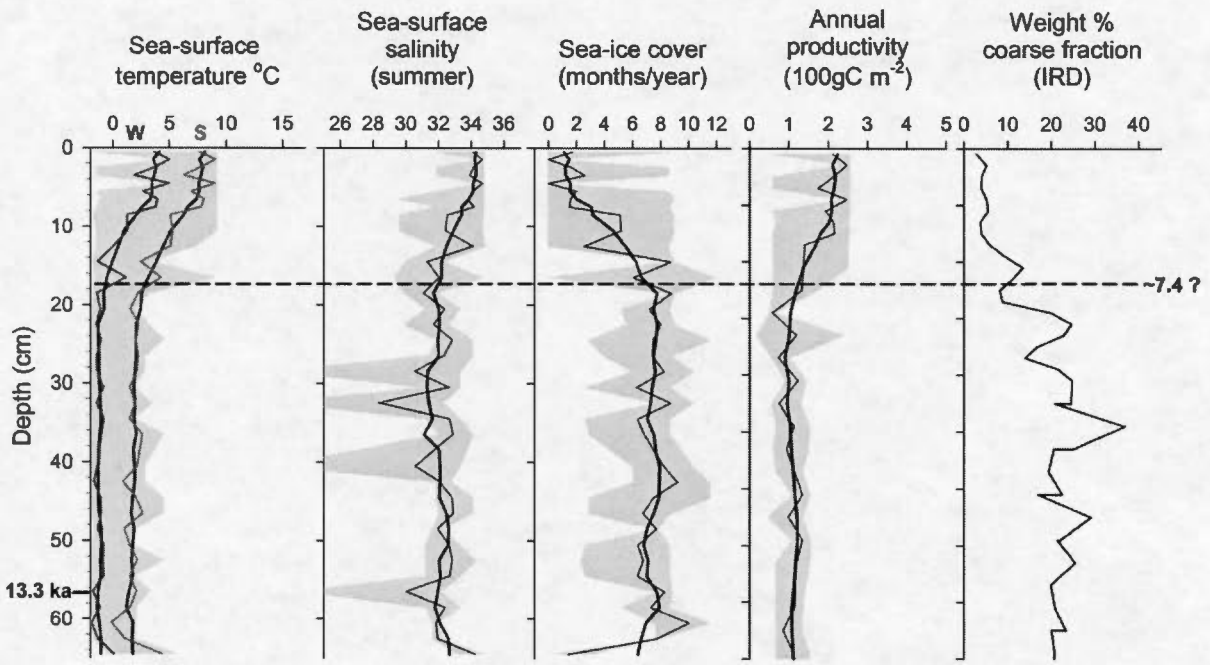


Figure 3.6a. Core TWC16 - reconstruction of sea surface conditions from dinocyst assemblages and the weight percent coarse fraction (>106 μm, mostly representative of ice rafted debris – IRD) plotted vs depth (cm). Sea surface temperatures (SST) in winter (w) and summer (s) are represented by blue and pink curves respectively. The lighter blue and pink curves correspond to possible maximum and minimum SSTs calculated from a set of 5 modern analogues. Sea surface salinity, sea ice cover and annual productivity are represented by thin black (most probable values) and grey shading (minimum and maximum). The thick black lines represent a 5-point running mean. Ecostratigraphic units identified by the principal component analyses and sea surface reconstructions are separated by a horizontal dashed line and identified by an inferred age (?) in cal ka BP.

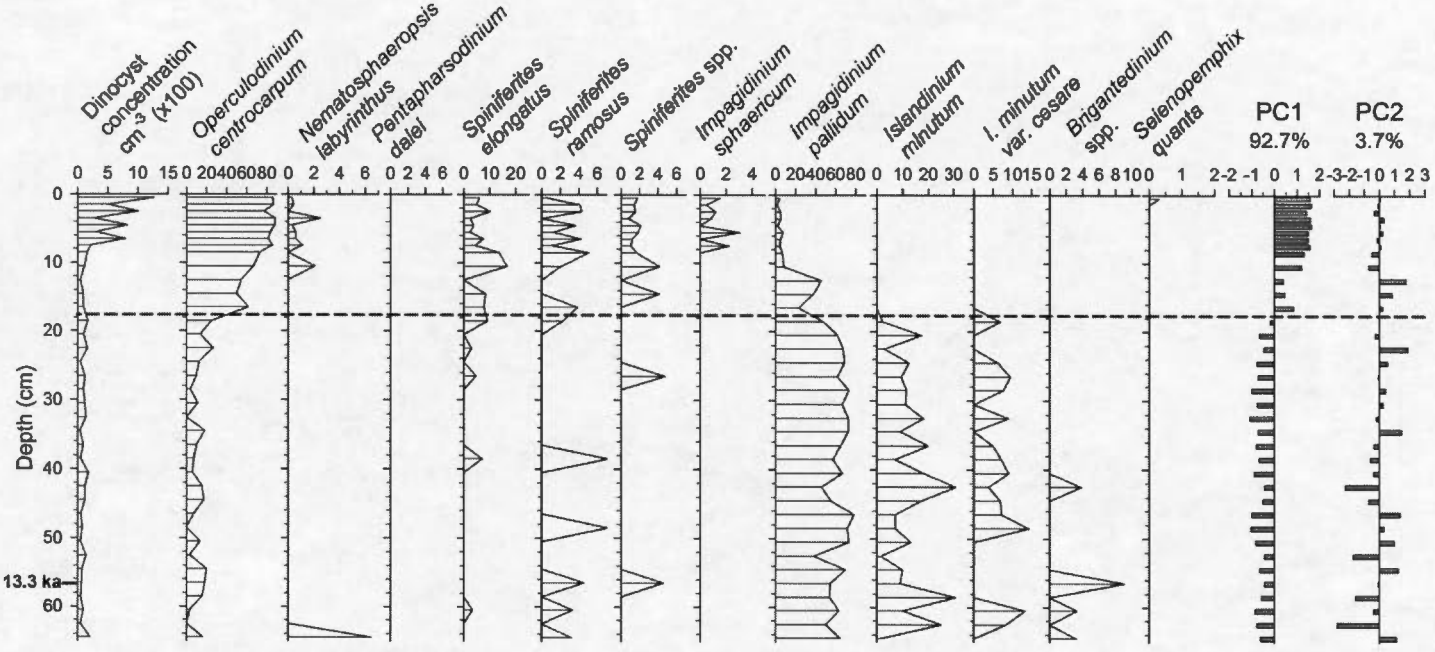


Figure 3.6b. Core TWC16 - concentrations of dinocysts expressed as number of specimen per $cm^3$ of sediment, relative abundance (percentage) of the main dinocyst taxa, and scores for principal components (PC) 1 and 2 are plotted vs depth (cm). The complete dinocyst dataset can be found on the GEOTOP website (http://www.geotop.ca). Ecostratigraphic units identified by the principal component analyses are separated by a dashed line.

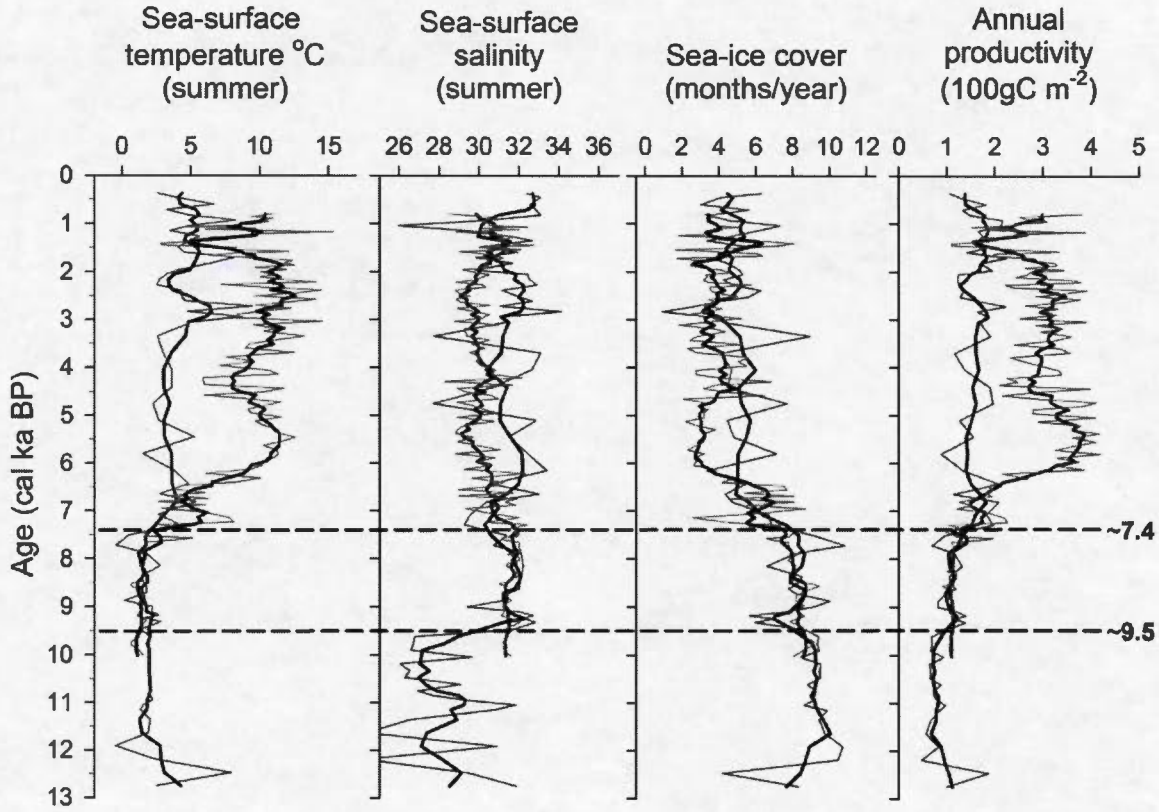


Figure 3.7. Reconstructions of sea surface temperature and salinity in summer, sea ice cover and annual productivity from dinocyst assemblages of cores CC70 (blue) and MSM343300 (red; Ouellet-Bernier et al., 2014) plotted vs age (cal ka BP). The thick black lines represent a 5-point running mean. Ecostratigraphic units for core CC70 identified by the principal component analyses and sea surface reconstructions are separated by a horizontal dashed line.

Tables

Table 3.1. List of cores used in this study with core location (latitude and longitude), water depth (m), core length (cm), and sampling interval. Also listed are the modern sea surface conditions (sea surface temperature (SST) in winter (w) and summer (s), sea surface salinity (SSS), months per year of sea ice cover (SIC), and gC $m^{-2}$ of annual productivity (prod)) for each location provided by the NODC and NSIDC.

| Core ID | Core location | Lat (°N) | Long (°W) | Water depth (m) | Modern sea surface conditions | | | | | Core sampling | | |
|---|---|---|---|---|---|---|---|---|---|---|---|---|
| | | | | | SST (s) | SST (w) | SSS | SIC | Prod | Core ID | Length (cm) | Interval |
| CC04 | northwest Labrador Sea | 61.4639 | 58.0365 | 2674 | 7.31 | 3.72 | 34.16 | 0.72 | 167.89 | TWC04 | 56 | 1 cm |
| TWC 08 | southern Davis Strait | 64.3931 | 58.1347 | 857 | 4.17 | 0.21 | 32.58 | 4.44 | 53.33 | TWC08 | 156 | 2 cm to 43 cm |
| TWC 16 | central Baffin Bay | 70.4619 | 64.6578 | 2063 | 3.21 | -1.10 | 29.92 | 8.98 | 56.83 | TWC16 | 155 | 1 cm to 8 cm, 2 cm to 64 cm |
| CC70 | western Greenland | 68.2279 | 57.6175 | 444 | 3.58 | -1.68 | 32.76 | 6.18 | 113.65 | TWC70 | 208 | 4 cm |

Table 3.2. Radiocarbon dates for the cores in this study. Refer to reference list for more details on previously published dates.

| Core name and depth interval (cm) | Laboratory identifier | AMS-$^{14}$C ages (years BP) | Calibrated age interval (2σ) (cal years BP) | Calibrated median age (cal years BP) | Modeled age interval (2σ) (cal years BP) | Modeled median age (cal years BP) | Reference |
|---|---|---|---|---|---|---|---|
| **TWC04** | | | | | | | |
| 8-9 | CAMS-155456 | 1,690 ± 35 | 1,170-1,314 | 1,250 | 1,170-1,315 | 1,249 | this paper |
| 20-21 | OS-96929 | 2,380 ± 25 | 1,921-2,102 | 2,008 | 1,923-2,101 | 2,009 | this paper |
| 32-33 | CAMS-155457 | 5,085 ± 35 | 5,323-5,552 | 5,448 | 5,323-5,551 | 5,447 | this paper |
| 44-45 | OS-96930 | 6,790 ± 35 | 7,245-7,403 | 7,318 | 7,245-7,403 | 7,317 | this paper |
| 56-57 | CAMS-155458 | 7,315 ± 30 | 7,680-7,860 | 7,776 | 7,681-7,860 | 7,775 | this paper |
| **PC04** | | | | | | | |
| *84-85 | CAMS-155462 | 7,735 ± 30 | 8,416-8,181 | 8,319 | 8,441-8,196 | 8,335 | Gibb et al., 2014 |
| 96-97 | CAMS-153492 | 8,780 ± 60 | 9,544-9,302 | 9,451 | 9,540-9,300 | 9,447 | Gibb et al., 2014 |
| 116-117 | CAMS-155463 | 9,290 ± 30 | 10,218-10,033 | 10,150 | 10,218-10,009 | 10,147 | Gibb et al., 2014 |
| 216-217 | CAMS-153493 | 10,990 ± 45 | 12,630-12,380 | 12,520 | 12,620-12,375 | 12,473 | Gibb et al., 2014 |

| Core name and depth interval (cm) | Laboratory identifier | AMS-$^{14}$C ages (years BP) | Calibrated age interval (2σ) (cal years BP) | Calibrated median age (cal years BP) | Modeled age interval (2σ) (cal years BP) | Modeled median age (cal years BP) | Reference |
|---|---|---|---|---|---|---|---|
| 244-245 | CAMS-153494 | 11,400 ± 120 | 13,128-12,636 | 12,881 | 13,071-12,635 | 12,816 | Gibb et al., 2014 |
| 388-389 | CAMS-153495 | 12,700 ± 60 | 14,878-13,952 | 14,226 | 14,871-14,010 | 14,363 | Gibb et al., 2014 |
| **TWC08** | | | | | | | |
| 104-105 | GRL 1897-S | 16,460 ± 110 | 19,043-19,651 | 19,370 | | | Andrews et al., 2014 |
| 136-137 | GRL 1898-S | 17,480 ± 80 | 20,351-20,850 | 20,597 | | | Andrews et al., 2014 |
| **TWC16** | | | | | | | |
| 56-57 | CAMS-146826 | 11,800 ± 40 | 13,167-13,383 | 13,276 | | | Steinhauer, 2012 |
| **TWC70** | | | | | | | |
| 97-98 | AA-84709 | 3,252 ± 37 | 2,760-3,021 | 2,887 | 2,757-3,014 | 2,882 | Jennings et al., 2013 |
| 134-135 | SUERC-25670 | 5,913 ± 39 | 6,035-6,295 | 6,198 | 6,033-6,286 | 6,190 | Jennings et al., 2013 |
| 172 | AA-84710 | 7,898 ± 54 | 8,072-8,359 | 8,229 | 8,061-8,346 | 8,218 | Jennings et al., 2013 |
| 194-195 | SUERC-3058 | 8,464 ± 40 | 8,693-9,019 | 8,887 | 8,694-9,008 | 8,879 | Jennings et al., 2013 |

| Core name and depth interval (cm) | Laboratory identifier | AMS-$^{14}$C ages (years BP) | Calibrated age interval (2σ) (cal years BP) | Calibrated median age (cal years BP) | Modeled age interval (2σ) (cal years BP) | Modeled median age (cal years BP) | Reference |
|---|---|---|---|---|---|---|---|
| **PC70** | | | | | | | |
| 55-56 | SUERC-30590 | 7,501±41 | 9,238-9,470 | 9,363 | 9,222-9,462 | 9,345 | Jennings et al., 2013 |
| 142-144.5 | AA-84711 | 7,501±42 | 10,438-10,733 | 10,590 | 10,430-10,705 | 10,574 | Jennings et al., 2013 |
| 188-189 | AA-84713 | 7,501±43 | 10,834-11,175 | 11,035 | 10,885-11,175 | 11,054 | Jennings et al., 2013 |
| 209-211 | AA-84714 | 7,501±44 | 11,250-11,775 | 11,497 | 11,240-11,731 | 11,460 | Jennings et al., 2013 |

[a] The analyses were made at the following institutions:
CAMS = Lawrence Livermore National Laboratory's Center for Accelerator Mass Spectrometry
OS = The National Ocean Sciences Accelerator Mass Spectrometry Facility, Woods Hole Oceanographic Institute
AA = NSF-Arizona Accelerator Mass Spectrometry Laboratory
SUERC = Scottish Universities Environmental Research Centre

[b] Radiocarbon age was calculated using the Libby half-life of 5568 years and corrected with a $\delta^{13}C$ of -25‰.

[c] A marine reservoir correction of 400 years was applied with no additional correction (ΔR), and the ages converted to calibrated years using Oxcal 4.2 (Ramsey, 2008) and the Marine13 (Reimer et al., 2013) calibration curve.

[d] The ages were modeled using Oxcal 4.2 (Ramsey, 2008).

* The $^{14}$C date used in the calibration and age-model is an average of three dates (7852 ± 55 years BP) representing the final drainage of glacial lake Agassiz (refer to Gibb et al., 2014 for further detail).

# CONCLUSION

The central problematic of my thesis is the importance of ocean circulation in past, present and future climate. In the Canadian Arctic, the Baffin Bay corridor deserves particular attention due to its role in Arctic freshwater outflow, its range in environment and oceanic conditions throughout a glacial cycle, and its lack of previously analyzed paleoceanographic records. To fill this knowledge gap in a key region, a transect of cores was collected from the corridor from which paleoceanographic records were reconstructed. The focus was to document the variability in oceanographic conditions through the Baffin Bay corridor over the last glacial cycle while correlating them with regional and basin scale oceanographic and climate records. In three research chapters, my goal was to address the three objectives presented in the introduction. The results demonstrate that the Baffin Bay corridor is in fact a unique environment. Surrounded by ice sheets during the glacial interval, this area was insulated from the North Atlantic current, which delayed the breakup of permanent sea ice cover and the establishment of full "interglacial conditions" in the central areas of Baffin Bay and the northwest Labrador Sea. Ice sheet melt had a dramatic effect on the sea surface and subsurface conditions of these confined basins, creating a very stratified upper water mass with seasonal sea ice and strong seasonal gradients in temperature. The Davis Strait sill seemed to play a role by delaying the progressive deglaciation from the northwest Labrador Sea to Baffin Bay. These deglacial changes are not only unique, but are completely decoupled from those in the Northern North Atlantic. Further, the Holocene records demonstrate that the coring location was paramount in separating coastal from regional changes in oceanic conditions by revealing the interaction between the warmer, more saline West Greenland Current (WGC) and cooler, less saline Baffin Island Current (BIC). Unfortunately, these sites have the disadvantage of low temporal resolution which

created difficulties in correlating the records with those of the late Holocene climate fluctuations on a basin scale. Therefore, while these results can be used for modeling large scale changes in oceanographic conditions due to Arctic freshwater outflow or warming on long time scales, they are constrained to low resolution.

I also proposed to address the limitations of paleoceanographic research from a site that has experienced such persistently cold, ice covered conditions, to provide a baseline documenting the variety and quality of information that can be extracted. I report that the most restricting parameters are chronology and lack of microfossils for proxy reconstructions of ocean parameters. However, the Baffin Bay core does provide a record of intervals of Atlantic water advection and intervals of quasi-perennial to seasonal sea ice cover. This information is of great significance for research conducted on the dynamics of surrounding ice sheets. Specifically, this record suggests that Atlantic water advection may affect ice stream retreat (O'Cofaigh et al., 2013; Simon et al., 2014).

My thesis consists of three research chapters with a record spanning the last ~36 ka from the northwest Labrador Sea, the last ~115 ka from central Baffin Bay, and higher resolution records focusing on the deglacial and Holocene (last ~15 ka) from a transect of cores from the northwest Labrador Sea, Davis Strait, and eastern and central Baffin Bay. Due to the inherent difficulties of paleoceanographic research in this region, not all objectives were met in all areas due to limitations of data. While the individual research Chapters provide details of my results, here I provide an account of how the objectives, and the specific goals, were used to address the central problematic and some of the challenges inherent in using proxy records to reconstruct past ocean conditions in these areas.

Objective 1: Reconstruct sea surface conditions including summer and winter temperatures, salinity, productivity, and sea ice cover as they respond to changes in climate, the subsurface water mass, and meltwater input.

In central Baffin Bay, intermittent periods of perennial sea ice cover throughout most of the glacial interval inhibited primary production within the surface water mass, which resulted in barren samples. Intervals containing low dinocyst abundances were episodic and reflected seasonal breakup. However the record was also sparse due to the few numbers of palynological samples analysed. The low abundance of dinocysts was known from the analysis of P1985. Due to lengthy palynological processing protocols analysis of Baffin Bay sediments (see future work section below), I chose to select samples throughout the core to create a subset associated with a variety of different parameters. These parameters include presence/absence of planktic and benthic foraminifera and a range of their stable isotope values, and varying percentages of ice rafted debris (IRD) and detrital carbonate content (Simon et al., 2014). This subset of samples does provide an assessment of the amount of sea ice cover during various intervals of colder and warmer subsurface conditions.

Dinocyst concentrations in the northwest Labrador Sea were also very low prior to deglaciation, which indicated perennial to quasi-perennial sea ice cover, especially when considering the species that were present. Sea surface reconstructions were quantitatively weak but reflected harsh conditions nonetheless. Large amounts of meltwater from the three surrounding ice sheets during the deglacial interval were evident in the reconstructions with low salinities and strong seasonal gradients of temperature. Unexpectedly, the dramatic shift from glacial to deglacial conditions

recorded in the northwest Labrador Sea overshadowed the Bølling-Allerød and Younger Dryas events, which are easily identified in the Northern North Atlantic.

Postglacial sea surface conditions were successfully reconstructed at all four sites within the Baffin Bay corridor due to increased productivity within seasonally open seas. These records demonstrated large fluctuations controlled by the relative strengths and shifts of the warmer, more saline WGC and colder, less saline BIC. The climate events of the Holocene, which can be correlated with surrounding coastal records, were not identifiable within the records I analysed. This suggests that sites beyond the shelf provide an opportunity for analysis of the variability of ocean currents independent of local climate.

Although Baffin Bay dinocysts were sufficiently abundant through the postglacial for the application of the modern analogue technique, the reconstructions toward the top of the core did not reflect modern conditions (Steinhauer, 2012). The lack of heterotrophic species might reflect possible degradation due to oxidation (Zonneveld et al., 1997, 2001, 2007), or bioturbation of sediments with very low accumulation rates as shown by $^{210}$Pb and $^{137}$Cs dating (Steinhauer, 2012). The shift in dominant species suggests that sea surface conditions improved postglacially, regarless of the amount of change, likely in accordance with those in eastern Baffin Bay.

Objective 2: Characterize temporal variability in relative temperature, salinity, and dissolved inorganic carbon of the subsurface water mass due to the advection of other water masses, changes in sea ice cover, and stratification and/or ventilation throughout the water column.

My focus on re-investigating the paleoceanographic record in Baffin Bay (Chapter 2) was intended to overcome some of the limitations of creating stable isotope records from foraminiferal tests. Although the lack of foraminifera due to low productivity in a predominantly ice covered environment was known and unavoidable, I have shown that the planktic-$\delta^{18}O$ records, from PC16 and from the core analysed in the 1980s, are robust. Also, the addition of benthic $\delta^{18}O$ and $\delta^{13}C$ values contributed substantially to the paleoceanographic record, indicating a single, cold subsurface water mass. Although the Baffin Bay record is discontinous, the values represent intervals of Atlantic water advection during both stadials and interstadials of the last glacial interval.

A relatively complete planktic stable isotope record was produced from the northwest Labrador Sea (PC04 described in Chapter 1). Intervals without stable isotope values occurred during the glacial interval as a result of low foraminiferal concentrations, likely due to dense sea ice cover, lack of nutrient rich Atlantic water, or very high sedimentation rates. Objective 2 was instrumental in identifying sea ice formation during Heinrich Events, inflow of an intermediate component of the NADW produced in the GIN Seas during the Younger Dryas, and the shift from a stratified to ventilated subsurface at the onset of LSW formation at the onset of the postglacial. Unfortunately, the benthic foraminiferal abundances were very low throughout the core and were therefore not collected for isotopic analyses. However, as shown by the isotopic analyses in Baffin Bay (Chapter 2), valuable information can be extracted from a discontinuous record and therefore it may be of interest to do so as complementary future study using core PC04.

Finally, an isotope record was also created for TWC04 but it wasn't used in Chapter 3 since no other records were available for correlation (Appendix B, Table 6). This was because the Holocene sediments at the three other sites in this thesis were subjected to carbonate dissolution.

Objective 3: Spatially and temporally correlate changes in paleoceanographic conditions among sites throughout the Baffin Bay corridor and with other records from the North Atlantic to identify associations with oceanic circulation and climate.

Establishing a chronology should be the first analysis for the study of marine sediment cores. The dissolution of calcareous foraminifera in the Baffin Bay and Davis Strait cores was known prior to paleoceanographic analysis. Fortunately, bivalve shells and seaweed were preserved in the eastern Baffin Bay core (CC70) and yielded radiocarbon data. This core, located well within the WGC, was instrumental in the correlation of the transect of cores. Cores TWC08 and CC04 were tentatively correlated based on dinocyst assemblages and sea surface reconstructions. For the reasons provided in Chapter 3, it seems likely these records are correlated but it is impossible to know if they are concomitant. However, the timing of the deglaciation and establishment of modern sea surface conditions in Davis Strait probably occurred after the changes in the northwest Labrador Sea, and before similar events took place in eastern Baffin Bay. This diachronous evolution toward seasonal sea ice cover from the northwest Labrador Sea to eastern Baffin Bay is evident, but a chronology is required in core TWC08 in order to constrain the timing. The execution of objective 3 has shown how dinocyst assemblages and sea surface reconstructions can contribute to establishing relative chronological order.

Future work

Addressing the limitations of Baffin Bay for paleoceanographic research required the re-analysis of Baffin Bay sediments. Most of the micropaleontological methods have remained the same over the last 30 years, but a few concerns arose during the preparations and analyses. The following are some suggestions that would advance paleoceanographic research using microfossils as proxies in harsh ocean environments.

In Chapter 2, planktic foraminiferal tests filled with fine detrital material were found and avoided while picking for isotopic analyses. This was due to the high amounts of detrital carbonate in Baffin Bay sediments (Hiscott et al., 1989), which suggested that the foraminiferal isotopic values could be offset due to the isotopically light detrital carbonate material (Hodell and Curtis, 2008). I therefore attempted two different methods to remove the sediment. The first was by ultrasonication, but it was either not efficient enough or too efficient and began to dissolve the tests. The second was to first break the tests open then quickly ultrasonicate and rinse each one, but too much material was lost. Due to low abundances, the latter was not an option and therefore I was encouraged to perform an analytical test of the possible offset caused by detrital carbonate contamination within planktic foraminiferal tests. Fortunately, the results indicated little offset relative to the replicate samples. However, I would suggest the need to establish a method that can efficiently clean the inner chambers of foraminiferal tests, especially for $^{14}C$ dating.

Difficulties with palynological analyses were also encountered with Baffin Bay sediments. Processing includes digestion with alternating hydrochloric acid (HCl) which removes calcium carbonate ($CaCO_3$), and hydrofluoric acid (HF) which removes silicates ($SiO_2$). After processing, the residue should only contain organic material such as palynomorphs and organic detritus. The Baffin Bay residues contained high amounts of mineral, originally assumed to be undigested silica. After further digestions without success, I now hypothesised that the remaining mineral is fluorite. Fluorite is calcium fluoride ($CaF_2$) that could have formed when remaining $Ca^{+2}$ ions from the dissociated $CaCO_3$ bonds with the dissociated HF. An attempt was made to separate the organic residue from the mineral with some success. The problem with a residue containing mineral is caused by obstructed palynomorphs by minerals in thick microscope slides, and by palynomorphs being diluted in the sample. This particularly poses a problem in Baffin Bay where concentrations are already extremely low. Therefore slides were made by concentrating the organic matter, and several slides were analysed to count a significant number of marker grains. In future processing, I suggest rinses possibly while sieving between each acid digestion to remove any remaining ions.

I have also developed an interest in studying carbonate dissolution. Benthic foraminiferal linings found in the palynological sample reflect carbonate dissolution. However, it remains uncertain whether the tests dissolved in situ (ocean) or after the sediments were cored and brought to the surface and depressurised. There is also concern about storage and processing methods. During the HU2008-029 cruise, we collected surface sediment samples consisting of the top (cm) layer of sediment from boxcores (Campbell et al., 2009). The samples were stained with rose Bengal and preserved in ethanol. Live and dead benthic foraminifera were found in the deep Baffin Bay surface sediments. Therefore it would be worth investigating the potential of foraminiferal test preservation within the subsurface sediment layers.

A few other research areas of interest emerge from my studies. Site selection for core collection to complement this work is important. Future work in the Baffin Bay corridor should consist of the analysis of cores strategically collected for optimal chronology and temporal resolution. Ideally, future cores would be similar to PC70 in eastern Baffin Bay, which have higher sedimentation rates resulting in higher temporal resolution, are above the lysocline preserving carbonate tests, and yet are a significant distance away from coastal influence. A comparison between cores collected well within the BIC and the WGC may offer more information in terms of timing and intensity of the relative contribution of currents. A transect of cores perpendicular to the Baffin Island or West Greenland shelf may provide such an environment. It will also demonstrate the impact of coastal processes and climate.

## Summary

Until now, the paleoceanographic development of the Baffin Bay corridor over the last glacial cycle had been largely unknown. I have contributed new paleoceanographic research both spatially and temporally to fill this knowledge gap and I have shown how microfossils can be an effective tool for the study of oceanographic circulation in the harshest of conditions. My reassessment of a deep Baffin Bay record has shown the potential and limitations of reconstructions in a harsh, ice covered environment. Foraminiferal isotope records revealed intervals of the advection of Atlantic water into the Bay during the glacial, which contributes to the study of surrounding glacial activity. Sea surface reconstructions of the northwest Labrador Sea revealed delayed response to deglaciation and the dramatic response to glacial melt. Baffin Bay remained ice covered until postglacial conditions were

established throughout the corridor, which consisted of seasonal sea ice cover and the onset of Labrador Sea Water formation. Late Holocene sea surface conditions were variable, and likely reflect oceanic circulation rather than climate. These reconstructions will contribute to future research in this area including other paleoceanographic reconstructions and ice stream activity, and provide a baseline for analysing the impacts of glacial-interglacial climate change.

# APPENDIX A

Dinocyst taxonomy

ACHO *Achomosphaera* spp., Evitt 1963
BSPP *Brigantedinium* species identified to the genus level, Reid 1977
BCAR *Brigantedinium cariacoense*, (Wall 1967) Lentin and Williams 1993
BSIM *Brigantedinium simplex*, Wall 1965 ex Lentin and Williams 1993
EKAR *Echinidinium karaense*, Head et al., 2001
IACU *Impagidinium aculeatum*, (Wall 1967) Lentin and Williams 1981
IPAL *Impagidinium pallidum*, Bujak 1984
IPAR *Impagidinium paradoxum*, (Wall 1967) Stover and Evitt 1978
IPAT *Impagidinium patulum*, (Wall 1967) Stover and Evitt 1978
ISPH *Impagidinium sphaericum*, (Wall 1967) Lentin and Williams 1981
ISTR *Impagidinium strialatum*, (Wall 1967) Stover and Evitt 1978
ISPP *Impagidinium* species identified to the genus level
IMIN *Islandinium minutum*, (Harland and Reid in Harland et al. 1980) Head et al. 2001
IMIC *Islandinium* var. *cezare*, (de Vernal et al., 1989, Rochon et al., 1999) Head et al., 2001
LMAC *Lingulodinium machaerophorum*, (Deflandre and Cookson 1955) Wall 1967
NLAB *Nematosphaeropsis labyrinthus*, (Ostenfeld 1903) Reid 1974
OCEN *Operculodinium centrocarpum sensu*, Wall and Dale 1966
OCSS *Operculodinium centrocarpum sensu* – short processes, Wall and Dale 1966
OARC *Operculodinium centrocarpum sensu* – Arctic morphotype, (Wall and Dale 1966) de Vernal et al., 2001
PDAL Cyst of *Pentapharsodinium dalei*, Indelicato and Loeblich III 1986
PERI Miscellaneous congruentidiacean cysts

PRET *Pyxidinopsis reticulate*, (McMinn and Sun 1994) Marret and de Vernal 1997
PARC *Protoperidinium americanum* (Gran and Braarud 1935) Balech 1974
SNEP *Selenopemphix nephroides*, (Benedek 1972) Benedek and Sarjeant 1981
SQUA *Selenopemphix quanta* s.l., includes *Selenopemphix quanta* (Bradford 1975) Matsuoka 1985 and cysts of *Protoperidinium nudum* (Meunier 1919) Balech 1974
SELO *Spiniferiles elongatus*, Reid 1974
SFRI *Spiniferiles frigidus*, Harland and Reid in Harland et al., 1980

SMIR *Spiniferites mirabilis* s.l., includes *Spiniferites mirabilis* (Rossignol 1967) Sarjeant 1970, and *Spiniferites hyperacanthus* (Deflandre and Cookson 1955) Cookson and Eisenack 1974

SRAM *Spiniferites ramosus* s.l., includes *Spiniferites ramosus* (Ehrenberg 1838) Mantell 1854, and *Spiniferites bulloideus* (Deflandre et Cookson 1955) Sarjeant 1970

SSPP *Spiniferites* species only identifiable to the genus level

TAPP *Trinovantedinium applanatum*, (Bradford 1977) Bujak and Davies 1983

APPENDIX B

Data tables

Table B.1 Core PC04 Palynolomorph concentrations

| Depth (cm) | Dinocysts $cm^{-3}$ | Pollen $cm^{-3}$ | Spores $cm^{-3}$ | Reworked palynomorphs $cm^{-3}$ | Organic linings $cm^{-3}$ |
|---|---|---|---|---|---|
| 0.5 | 4632 | 28 | 56 | 0 | 237 |
| 4.5 | 6507 | 21 | 83 | 0 | 396 |
| 8.5 | 4787 | 59 | 45 | 0 | 2973 |
| 12.5 | 5896 | 78 | 16 | 0 | 3372 |
| 16.5 | 4807 | 67 | 0 | 0 | 3313 |
| 20.5 | 4801 | 42 | 70 | 0 | 4702 |
| 24.5 | 4823 | 28 | 42 | 0 | 1612 |
| 28.5 | 4499 | 65 | 13 | 0 | 1043 |
| 32.5 | 3445 | 32 | 21 | 0 | 948 |
| 36.5 | 4239 | 45 | 35 | 0 | 1974 |
| 40.5 | 1595 | 46 | 20 | 0 | 419 |
| 44.5 | 4558 | 147 | 59 | 0 | 3881 |
| 48.5 | 2590 | 46 | 54 | 0 | 536 |
| 68.5 | 1499 | 35 | 56 | 0 | 1129 |
| 72.5 | 2288 | 45 | 23 | 15 | 2077 |
| 76.5 | 2287 | 30 | 30 | 15 | 2775 |
| 80.5 | 2499 | 16 | 24 | 0 | 2523 |
| 84.5 | 2231 | 14 | 43 | 7 | 2746 |
| 88.5 | 4482 | 45 | 89 | 45 | 8356 |
| 92.5 | 4273 | 111 | 70 | 28 | 6417 |
| 96.5 | 4721 | 39 | 104 | 39 | 7590 |
| 100.5 | 3383 | 22 | 32 | 32 | 2715 |
| 104.5 | 4879 | 0 | 31 | 0 | 4650 |
| 108.5 | 4676 | 30 | 15 | 61 | 3431 |
| 112.5 | 6291 | 39 | 39 | 77 | 6522 |
| 116.5 | 6004 | 57 | 38 | 0 | 5032 |
| 120.5 | 2887 | 9 | 35 | 53 | 1580 |
| 124.5 | 2190 | 26 | 6 | 58 | 1816 |

| Depth (cm) | Dinocysts $cm^{-3}$ | Pollen $cm^{-3}$ | Spores $cm^{-3}$ | Reworked palynomorphs $cm^{-3}$ | Organic linings $cm^{-3}$ |
|---|---|---|---|---|---|
| 128.5 | 5489 | 52 | 34 | 17 | 3269 |
| 132.5 | 5448 | 34 | 17 | 68 | 3207 |
| 136.5 | 3876 | 12 | 37 | 61 | 1607 |
| 140.5 | 5307 | 52 | 35 | 52 | 2071 |
| 144.5 | 2107 | 32 | 13 | 32 | 1112 |
| 148.5 | 2602 | 68 | 17 | 118 | 2103 |
| 152.5 | 1830 | 39 | 6 | 67 | 2267 |
| 156.5 | 3121 | 40 | 0 | 161 | 3973 |
| 160.5 | 3264 | 54 | 22 | 119 | 2747 |
| 164.5 | 1355 | 17 | 12 | 42 | 1177 |
| 168.5 | 1755 | 17 | 29 | 120 | 926 |
| 172.5 | 2717 | 26 | 9 | 44 | 1341 |
| 176.5 | 3517 | 12 | 12 | 12 | 1571 |
| 180.5 | 3387 | 34 | 0 | 80 | 2228 |
| 184.5 | 3419 | 11 | 0 | 110 | 3915 |
| 188.5 | 2244 | 30 | 7 | 103 | 3618 |
| 192.5 | 1063 | 32 | 0 | 77 | 1186 |
| 196.5 | 1240 | 24 | 8 | 175 | 1639 |
| 200.5 | 577 | 9 | 5 | 93 | 428 |
| 204.5 | 1239 | 12 | 8 | 139 | 1092 |
| 208.5 | 566 | 0 | 0 | 61 | 700 |
| 212.5 | 300 | 0 | 0 | 64 | 426 |
| 216.5 | 235 | 0 | 0 | 80 | 127 |
| 220.5 | 111 | 0 | 0 | 83 | 28 |
| 224.5 | 5 | 0 | 5 | 43 | 14 |
| 228.5 | 7 | 0 | 0 | 85 | 14 |
| 232.5 | 19 | 0 | 0 | 157 | 18 |
| 236.5 | 219 | 0 | 0 | 209 | 270 |
| 240.5 | 155 | 0 | 0 | 285 | 475 |
| 244.5 | 295 | 0 | 0 | 221 | 310 |
| 248.5 | 164 | 0 | 0 | 214 | 232 |
| 252.5 | 31 | 0 | 2 | 226 | 63 |
| 256.5 | 189 | 0 | 0 | 170 | 187 |
| 260.5 | 661 | 0 | 0 | 191 | 89 |
| 264.5 | 732 | 24 | 0 | 161 | 249 |
| 268.5 | 248 | 30 | 0 | 236 | 89 |
| 272.5 | 1458 | 20 | 0 | 158 | 341 |
| 276.5 | 1880 | 22 | 0 | 217 | 347 |
| 280.5 | 1131 | 11 | 0 | 196 | 138 |

| Depth (cm) | Dinocysts $cm^{-3}$ | Pollen $cm^{-3}$ | Spores $cm^{-3}$ | Reworked palynomorphs $cm^{-3}$ | Organic linings $cm^{-3}$ |
|---|---|---|---|---|---|
| 284.5 | 676 | 11 | 3 | 116 | 114 |
| 288.5 | 654 | 9 | 3 | 135 | 171 |
| 292.5 | 794 | 17 | 11 | 205 | 199 |
| 296.5 | 381 | 22 | 8 | 129 | 115 |
| 300.5 | 289 | 18 | 7 | 84 | 88 |
| 304.5 | 328 | 1 | 0 | 166 | 147 |
| 308.5 | 642 | 17 | 5 | 158 | 195 |
| 312.5 | 307 | 3 | 3 | 125 | 157 |
| 316.5 | 105 | 7 | 2 | 183 | 91 |
| 320.5 | 307 | 4 | 0 | 203 | 102 |
| 324.5 | 582 | 11 | 0 | 155 | 125 |
| 328.5 | 1326 | 6 | 0 | 174 | 174 |
| 332.5 | 2933 | 0 | 0 | 220 | 335 |
| 336.5 | 1398 | 14 | 5 | 238 | 178 |
| 340.5 | 1397 | 9 | 0 | 202 | 125 |
| 344.5 | 3453 | 41 | 0 | 183 | 193 |
| 348.5 | 2017 | 13 | 0 | 271 | 310 |
| 352.5 | 775 | 10 | 3 | 223 | 195 |
| 356.5 | 810 | 10 | 0 | 213 | 175 |
| 360.5 | 645 | 6 | 0 | 194 | 142 |
| 364.5 | 1076 | 3 | 0 | 230 | 224 |
| 368.5 | 308 | 7 | 2 | 167 | 90 |
| 372.5 | 309 | 17 | 0 | 353 | 105 |
| 376.5 | 440 | 9 | 3 | 170 | 252 |
| 380.5 | 557 | 18 | 4 | 277 | 272 |
| 384.5 | 537 | 9 | 2 | 247 | 511 |
| 388.5 | 98 | 7 | 0 | 202 | 125 |
| 392.5 | 434 | 44 | 0 | 295 | 252 |
| 396.5 | 525 | 15 | 2 | 243 | 214 |
| 400.5 | 421 | 14 | 9 | 312 | 77 |
| 404.5 | 620 | 17 | 17 | 222 | 205 |
| 408.5 | 3514 | 11 | 0 | 258 | 269 |
| 412.5 | 1066 | 13 | 0 | 246 | 141 |
| 416.5 | 1236 | 0 | 0 | 209 | 157 |
| 421.5 | 916 | 16 | 0 | 418 | 177 |
| 424.5 | 1244 | 14 | 0 | 349 | 126 |
| 428.5 | 1441 | 0 | 0 | 323 | 150 |
| 432.5 | 1923 | 0 | 0 | 496 | 347 |
| 436.5 | 1492 | 5 | 5 | 530 | 372 |

| Depth (cm) | Dinocysts $cm^{-3}$ | Pollen $cm^{-3}$ | Spores $cm^{-3}$ | Reworked palynomorphs $cm^{-3}$ | Organic linings $cm^{-3}$ |
|---|---|---|---|---|---|
| 440.5 | 601 | 0 | 0 | 385 | 101 |
| 444.5 | 1181 | 0 | 0 | 649 | 329 |
| 448.5 | 1144 | 14 | 4 | 261 | 409 |
| 452.5 | 711 | 14 | 0 | 272 | 315 |
| 456.5 | 582 | 3 | 0 | 279 | 350 |
| 460.5 | 694 | 13 | 0 | 382 | 493 |
| 464.5 | 424 | 20 | 0 | 373 | 435 |
| 468.5 | 812 | 39 | 5 | 610 | 608 |
| 472.5 | 591 | 17 | 4 | 463 | 416 |
| 476.5 | 635 | 14 | 2 | 370 | 591 |
| 480.5 | 2008 | 13 | 13 | 320 | 227 |
| 484.5 | 847 | 18 | 0 | 328 | 241 |
| 488.5 | 211 | 2 | 0 | 359 | 158 |
| 492.5 | 30 | 5 | 0 | 396 | 25 |
| 497.5 | 82 | 5 | 14 | 309 | 55 |
| 500.5 | 79 | 0 | 0 | 560 | 10 |
| 504.5 | 45 | 0 | 0 | 865 | 12 |
| 508.5 | 136 | 0 | 0 | 1213 | 0 |
| 512.5 | 147 | 0 | 0 | 719 | 6 |
| 516.5 | 174 | 0 | 0 | 1005 | 11 |
| 520.5 | 0 | 0 | 0 | 314 | 314 |
| 524.5 | 60 | 0 | 0 | 568 | 0 |
| 528.5 | 39 | 0 | 0 | 510 | 0 |
| 532.5 | 75 | 0 | 0 | 658 | 0 |
| 536.5 | 38 | 0 | 0 | 827 | 0 |
| 540.5 | 46 | 0 | 0 | 646 | 0 |
| 544.5 | 92 | 0 | 0 | 598 | 14 |
| 548.5 | 0 | 0 | 0 | 485 | 513 |
| 552.5 | 87 | 0 | 0 | 1043 | 8 |
| 556.5 | 58 | 0 | 0 | 1035 | 15 |
| 560.5 | 25 | 0 | 0 | 717 | 4 |
| 564.5 | 34 | 0 | 0 | 783 | 0 |
| 568.5 | 4 | 0 | 0 | 415 | 0 |
| 572.5 | 7 | 0 | 0 | 294 | 0 |
| 576.5 | 9 | 0 | 0 | 552 | 0 |
| 580.5 | 29 | 0 | 0 | 423 | 0 |
| 584.5 | 0 | 0 | 0 | 459 | 13 |
| 588.5 | 18 | 0 | 0 | 433 | 0 |
| 592.5 | 20 | 0 | 0 | 284 | 20 |

| Depth (cm) | Dinocysts $cm^{-3}$ | Pollen $cm^{-3}$ | Spores $cm^{-3}$ | Reworked palynomorphs $cm^{-3}$ | Organic linings $cm^{-3}$ |
|---|---|---|---|---|---|
| 596.5 | 29 | 0 | 0 | 233 | 7 |
| 600.5 | 11 | 0 | 0 | 145 | 0 |
| 604.5 | 25 | 0 | 0 | 91 | 0 |
| 610.5 | 11 | 2 | 0 | 184 | 0 |
| 614.5 | 9 | 0 | 0 | 113 | 0 |
| 618.5 | 0 | 0 | 0 | 152 | 170 |
| 622.5 | 21 | 0 | 0 | 145 | 30 |
| 626.5 | 47 | 0 | 0 | 183 | 17 |
| 630.5 | 83 | 0 | 0 | 150 | 12 |
| 634.5 | 42 | 0 | 0 | 112 | 10 |
| 638.5 | 189 | 0 | 10 | 189 | 10 |
| 642.5 | 97 | 7 | 0 | 186 | 0 |
| 646.5 | 94 | 0 | 0 | 110 | 0 |
| 650.5 | 50 | 0 | 0 | 75 | 8 |
| 654.5 | 12 | 0 | 0 | 47 | 0 |
| 658.5 | 295 | 11 | 0 | 97 | 0 |
| 662.5 | 19 | 0 | 0 | 78 | 0 |
| 664.5 | 25 | 0 | 2 | 86 | 0 |
| 668.5 | 104 | 0 | 0 | 132 | 16 |
| 672.5 | 33 | 0 | 0 | 168 | 5 |
| 676.5 | 0 | 0 | 0 | 131 | 0 |
| 680.5 | 522 | 0 | 0 | 392 | 0 |
| 684.5 | 325 | 0 | 0 | 318 | 0 |
| 688.5 | 282 | 0 | 0 | 679 | 758 |
| 692.5 | 1043 | 3 | 0 | 247 | 307 |
| 696.5 | 466 | 1 | 11 | 177 | 526 |
| 700.5 | 316 | 0 | 0 | 147 | 339 |
| 704.5 | 56 | 0 | 0 | 249 | 143 |
| 708.5 | 16 | 0 | 0 | 423 | 122 |
| 712.5 | 88 | 0 | 0 | 459 | 124 |
| 716.5 | 0 | 0 | 0 | 123 | 144 |
| 720.5 | 11 | 0 | 0 | 230 | 53 |
| 724.5 | 4 | 0 | 0 | 508 | 567 |
| 728.5 | 17 | 0 | 0 | 651 | 229 |
| 732.5 | 12 | 0 | 0 | 736 | 485 |
| 736.5 | 0 | 0 | 0 | 285 | 100 |
| 740.5 | 14 | 0 | 0 | 621 | 573 |
| 744.5 | 27 | 0 | 0 | 849 | 697 |
| 748.5 | 56 | 0 | 6 | 695 | 651 |

| Depth (cm) | Dinocysts $cm^{-3}$ | Pollen $cm^{-3}$ | Spores $cm^{-3}$ | Reworked palynomorphs $cm^{-3}$ | Organic linings $cm^{-3}$ |
|---|---|---|---|---|---|
| 752.5 | 29 | 0 | 0 | 778 | 467 |
| 756.5 | 0 | 0 | 0 | 712 | 809 |
| 760.5 | 79 | 0 | 0 | 674 | 280 |
| 764.5 | 424 | 0 | 0 | 150 | 188 |
| 768.5 | 34 | 0 | 0 | 90 | 9 |
| 772.5 | 89 | 0 | 0 | 104 | 70 |
| 776.5 | 7 | 0 | 0 | 191 | 34 |
| 780.5 | 0 | 0 | 0 | 207 | 18 |
| 784.5 | 7 | 0 | 0 | 62 | 16 |
| 788.5 | 20 | 0 | 0 | 149 | 34 |
| 792.5 | 17 | 0 | 0 | 117 | 17 |
| 796.5 | 20 | 0 | 0 | 106 | 121 |
| 800.5 | 366 | 0 | 0 | 261 | 680 |
| 804.5 | 321 | 0 | 0 | 209 | 1069 |
| 808.5 | 319 | 0 | 0 | 342 | 689 |
| 812.5 | 301 | 0 | 0 | 259 | 377 |
| 816.5 | 43 | 0 | 0 | 202 | 59 |
| 820.5 | 8 | 0 | 0 | 233 | 58 |
| 824.5 | 0 | 0 | 0 | 357 | 37 |
| 828.5 | 16 | 0 | 0 | 262 | 60 |
| 832.5 | 197 | 0 | 0 | 420 | 463 |
| 836.5 | 232 | 0 | 0 | 772 | 636 |
| 840.5 | 213 | 0 | 0 | 896 | 436 |
| 844.5 | 160 | 0 | 0 | 959 | 420 |
| 848.5 | 96 | 0 | 0 | 748 | 376 |
| 852.5 | 186 | 0 | 0 | 1061 | 377 |
| 856.5 | 67 | 0 | 0 | 960 | 159 |
| 860.5 | 48 | 0 | 0 | 522 | 48 |
| 864.5 | 94 | 0 | 0 | 879 | 299 |
| 870.5 | 0 | 0 | 0 | 24 | 35 |
| 874.5 | 0 | 0 | 0 | 24 | 8 |
| 878.5 | 0 | 0 | 0 | 222 | 25 |
| 882.5 | 4 | 0 | 0 | 8 | 12 |
| 886.5 | 54 | 0 | 0 | 369 | 162 |
| 890.5 | 0 | 0 | 0 | 45 | 7 |
| 894.5 | 14 | 0 | 0 | 513 | 132 |

Table B.2.Core PC04 weight percent (%) ice rafted debris (IRD), weight percent (%) carbonate, and the carbon and oxygen stable isotopes (VPDB) ($\delta^{13}C$ and $\delta^{18}O$) of *Neogloboquadrina pachyderma* lef-coiled (Npl).

| Depth (cm) | wt% IRD | wt% carbonate | $\delta^{13}C$ ‰ | $\delta^{18}O$ ‰ |
|---|---|---|---|---|
| 0.5 | 2.52 | 18.03 | 0.61 | 2.58 |
| 4.5 | 2.21 | 17.90 | 0.38 | 2.72 |
| 8.5 | 1.43 | 18.78 | 0.70 | 2.78 |
| 12.5 | 1.02 | 22.47 | 0.78 | 2.79 |
| 16.5 | 1.71 | 19.27 | 0.84 | 2.79 |
| 20.5 | 1.31 | 19.34 | 0.81 | 2.60 |
| 24.5 | 1.93 | 15.91 | 0.94 | 2.64 |
| 28.5 | 1.41 | 15.59 | 0.92 | 2.73 |
| 32.5 | 2.23 | 14.66 | 0.82 | 2.78 |
| 36.5 | 1.10 | 12.78 | 0.71 | 2.68 |
| 40.5 | 2.08 | 15.24 | 0.85 | 2.66 |
| 44.5 | 1.82 | 16.13 | 0.77 | 2.69 |
| 48.5 | 1.24 | 15.80 | 0.90 | 2.67 |
| 68.5 | 1.49 | 11.69 | 0.64 | 2.72 |
| 72.5 | 1.54 | 13.17 | 0.88 | 2.77 |
| 76.5 | 1.86 | 13.76 | 0.61 | 2.70 |
| 80.5 | 0.47 | 7.97 | 0.65 | 2.83 |
| 84.5 | 1.74 | 9.75 | 0.59 | 2.74 |
| 88.5 | 1.01 | 9.35 | 0.69 | 2.83 |
| 92.5 | 1.31 | 11.87 | 0.62 | 2.62 |
| 96.5 | 1.01 | 11.40 | 0.53 | 2.63 |
| 100.5 | 0.87 | 7.38 | 0.64 | 2.82 |
| 104.5 | 0.44 | 4.33 | 0.53 | 2.80 |
| 108.5 | 0.55 | 5.58 | 0.43 | 2.81 |
| 112.5 | 0.39 | 5.32 | 0.47 | 2.83 |
| 116.5 | 0.48 | 5.00 | 0.52 | 2.87 |
| 120.5 | 0.63 | 4.06 | 0.58 | 2.90 |
| 124.5 | 0.41 | 4.45 | 0.37 | 2.80 |
| 128.5 | 0.44 | 4.89 | 0.35 | 2.75 |
| 132.5 | 0.37 | 4.33 | 0.53 | 2.92 |
| 136.5 | 0.38 | 3.62 | 0.28 | 2.77 |
| 140.5 | 0.58 | 4.03 | 0.26 | 2.86 |

| Depth (cm) | wt% IRD | wt% carbonate | $\delta^{13}C$ ‰ | $\delta^{18}O$ ‰ |
|---|---|---|---|---|
| 144.5 | 0.43 | 3.16 | 0.32 | 2.97 |
| 148.5 | 0.50 | 3.02 | 0.17 | 2.86 |
| 152.5 | 0.68 | 2.73 | 0.43 | 3.01 |
| 156.5 | 0.40 | 3.29 | 0.14 | 2.96 |
| 160.5 | 0.44 | 2.83 | | |
| 164.5 | 1.37 | 4.55 | 0.35 | 2.96 |
| 168.5 | 1.44 | 4.01 | 0.20 | 3.01 |
| 172.5 | 1.99 | 5.77 | 0.33 | 2.95 |
| 176.5 | 5.15 | 9.49 | 0.54 | 3.20 |
| 180.5 | 3.49 | 6.95 | 0.50 | 3.14 |
| 184.5 | 1.65 | -1.14 | 0.27 | 3.12 |
| 188.5 | 2.04 | 5.34 | 0.06 | 2.98 |
| 192.5 | 2.51 | 4.05 | | |
| 196.5 | 1.78 | 4.55 | | |
| 200.5 | 1.19 | 4.50 | 0.46 | 3.32 |
| 204.5 | 2.56 | 5.10 | 0.32 | 3.15 |
| 208.5 | 1.83 | 4.83 | 0.61 | 3.24 |
| 212.5 | 3.93 | 4.38 | 0.56 | 3.32 |
| 216.5 | 3.26 | 5.47 | 0.70 | 3.26 |
| 220.5 | 2.61 | 5.53 | 0.36 | 3.28 |
| 224.5 | 3.57 | 3.50 | | |
| 228.5 | 3.43 | 3.00 | | |
| 232.5 | 7.48 | 3.66 | | |
| 236.5 | 4.56 | 4.47 | | |
| 240.5 | 2.50 | 6.83 | 0.48 | 3.38 |
| 244.5 | 3.56 | 7.21 | 0.48 | 3.34 |
| 248.5 | 4.21 | 6.37 | 0.52 | 3.29 |
| 252.5 | 3.17 | 4.17 | | |
| 256.5 | 1.47 | 3.75 | 0.52 | 3.35 |
| 260.5 | 0.24 | 4.14 | | |
| 264.5 | 1.12 | 3.81 | | |
| 268.5 | 0.82 | 3.70 | | |
| 272.5 | 1.18 | 3.69 | | |
| 276.5 | 0.49 | 4.54 | | |
| 280.5 | 0.25 | 4.17 | | |
| 284.5 | 0.55 | 4.30 | | |
| 288.5 | 1.12 | 4.86 | | |
| 292.5 | 3.48 | 5.07 | | |
| 296.5 | 0.59 | 7.40 | | |

| Depth (cm) | wt% IRD | wt% carbonate | $\delta^{13}C$ ‰ | $\delta^{18}O$ ‰ |
|---|---|---|---|---|
| 300.5 | 0.80 | 4.93 | | |
| 304.5 | 0.70 | 4.81 | | |
| 308.5 | 0.40 | 1.65 | | |
| 312.5 | 0.84 | 5.94 | | |
| 316.5 | 0.75 | 5.85 | | |
| 320.5 | 0.55 | 5.20 | | |
| 324.5 | 0.29 | 6.06 | | |
| 328.5 | 0.43 | 5.35 | | |
| 332.5 | 0.28 | 6.45 | | |
| 336.5 | 0.22 | 6.10 | | |
| 340.5 | 0.36 | 7.05 | | |
| 344.5 | 0.26 | 6.35 | | |
| 348.5 | 0.54 | 6.36 | | |
| 352.5 | 0.47 | 6.48 | | |
| 356.5 | 0.29 | 6.64 | | |
| 360.5 | 0.37 | 6.42 | | |
| 364.5 | 0.78 | 7.57 | | |
| 368.5 | 1.60 | 6.91 | 0.41 | 3.69 |
| 372.5 | 1.27 | 8.19 | 0.36 | 3.77 |
| 376.5 | 2.08 | 8.93 | 0.23 | 3.81 |
| 380.5 | 7.05 | 9.29 | 0.42 | 3.77 |
| 384.5 | 2.51 | 12.58 | 0.37 | 3.77 |
| 388.5 | 7.32 | 17.55 | 0.41 | 3.92 |
| 392.5 | 3.99 | 12.01 | 0.36 | 3.79 |
| 396.5 | 6.72 | 11.16 | 0.23 | 3.71 |
| 400.5 | 5.15 | 13.17 | 0.35 | 3.85 |
| 404.5 | 2.05 | 8.58 | 0.30 | 3.87 |
| 408.5 | 1.75 | 7.19 | 0.17 | 3.76 |
| 412.5 | 1.95 | 7.35 | 0.35 | 3.70 |
| 416.5 | 1.85 | 5.33 | | |
| 421.5 | 0.54 | -2.26 | | |
| 424.5 | 0.60 | 5.37 | | |
| 428.5 | 0.86 | 5.83 | | |
| 432.5 | 0.83 | 5.74 | 0.08 | 3.77 |
| 436.5 | 2.54 | 5.07 | 0.09 | 3.71 |
| 440.5 | 0.37 | 3.04 | | |
| 444.5 | 0.88 | 7.70 | 0.12 | 4.05 |
| 448.5 | 1.48 | 6.98 | 0.01 | 3.60 |
| 452.5 | 1.08 | 7.60 | -0.05 | 3.50 |

| Depth (cm) | wt% IRD | wt% carbonate | $\delta^{13}C$ ‰ | $\delta^{18}O$ ‰ |
|---|---|---|---|---|
| 456.5 | 1.26 | 8.83 | 0.01 | 3.33 |
| 460.5 | 0.93 | 6.95 | 0.03 | 3.31 |
| 464.5 | 0.90 | 5.96 | 0.05 | 3.34 |
| 468.5 | 1.91 | 6.98 | 0.21 | 3.53 |
| 472.5 | 0.93 | 5.04 | 0.02 | 3.47 |
| 476.5 | 0.84 | 6.25 | -0.07 | 3.52 |
| 480.5 | 1.23 | 6.53 | 0.00 | 3.47 |
| 484.5 | 0.59 | 8.44 | -0.04 | 3.52 |
| 488.5 | 13.46 | 24.88 | 0.04 | 3.19 |
| 492.5 | 2.56 | 34.29 | 0.27 | 3.52 |
| 497.5 | 8.95 | 29.08 | -0.14 | 2.75 |
| 500.5 | 10.28 | 41.50 | -0.23 | 2.28 |
| 504.5 | 5.00 | 36.15 | -0.18 | 2.39 |
| 508.5 | 3.75 | 47.39 | -0.08 | 2.58 |
| 512.5 | 1.80 | 48.48 | | |
| 516.5 | 9.44 | 45.96 | -0.16 | 2.33 |
| 520.5 | 8.23 | 36.80 | | |
| 524.5 | 18.14 | 35.82 | | |
| 528.5 | 4.30 | 43.84 | | |
| 532.5 | 10.55 | 43.65 | | |
| 536.5 | 4.21 | 48.03 | | |
| 540.5 | 13.94 | 43.75 | | |
| 544.5 | 2.59 | 50.28 | | |
| 548.5 | 8.27 | 41.77 | | |
| 552.5 | 0.34 | 53.44 | | |
| 556.5 | 2.43 | 53.57 | | |
| 560.5 | 4.54 | 52.91 | | |
| 564.5 | 0.14 | 56.59 | | |
| 568.5 | 8.08 | 62.97 | | |
| 572.5 | 0.06 | 56.12 | | |
| 576.5 | 1.39 | 54.42 | | |
| 580.5 | 11.21 | 52.78 | | |
| 584.5 | 9.71 | 55.58 | | |
| 588.5 | 8.34 | 54.98 | -0.14 | 3.30 |
| 592.5 | 5.05 | 6.12 | -0.17 | 4.10 |
| 596.5 | 3.91 | -1.98 | 0.07 | 3.30 |
| 600.5 | 2.38 | 2.49 | 0.17 | 4.65 |
| 604.5 | 6.46 | 5.79 | 0.20 | 4.31 |
| 610.5 | 1.38 | 3.14 | 0.25 | 4.57 |

| Depth (cm) | wt% IRD | wt% carbonate | $\delta^{13}C$ ‰ | $\delta^{18}O$ ‰ |
|---|---|---|---|---|
| 614.5 | 1.23 | 1.45 | | |
| 618.5 | 1.87 | 1.69 | 0.01 | 4.47 |
| 622.5 | 1.31 | 2.38 | 0.16 | 4.68 |
| 626.5 | 3.95 | 1.66 | 0.37 | 4.69 |
| 630.5 | 2.88 | 14.75 | 0.36 | 4.63 |
| 634.5 | 3.33 | 4.08 | 0.29 | 4.66 |
| 638.5 | 2.95 | 5.54 | 0.36 | 4.71 |
| 642.5 | 3.98 | 3.38 | 0.37 | 4.72 |
| 646.5 | 5.17 | 4.07 | 0.38 | 4.62 |
| 650.5 | 2.45 | 3.16 | 0.31 | 4.56 |
| 654.5 | 3.55 | 2.91 | 0.32 | 4.55 |
| 658.5 | 4.93 | 3.20 | 0.32 | 4.69 |
| 662.5 | 1.95 | 3.35 | | |
| 664.5 | 0.80 | 1.02 | | |
| 668.5 | 2.47 | 2.71 | | |
| 672.5 | 2.46 | 1.14 | | |
| 676.5 | 0.58 | 0.75 | | |
| 680.5 | 0.21 | 0.79 | | |
| 684.5 | 1.01 | 1.01 | | |
| 688.5 | 0.29 | 1.34 | | |
| 692.5 | 0.27 | 2.43 | -0.11 | 4.62 |
| 696.5 | 0.23 | 2.48 | 0.11 | 4.81 |
| 700.5 | 7.99 | 18.99 | 0.00 | 4.02 |
| 704.5 | 11.05 | 36.26 | -0.13 | 3.40 |
| 708.5 | 11.90 | 41.68 | -0.09 | 3.48 |
| 712.5 | 7.68 | 39.99 | | |
| 716.5 | 6.34 | 24.33 | | |
| 720.5 | 21.48 | 32.72 | 0.00 | 4.28 |
| 724.5 | 12.94 | 41.90 | | |
| 728.5 | 5.38 | 48.48 | | |
| 732.5 | 14.20 | 44.29 | | |
| 736.5 | 0.57 | 41.32 | | |
| 740.5 | 2.67 | 53.05 | | |
| 744.5 | 5.92 | 54.46 | | |
| 748.5 | 6.03 | 49.17 | | |
| 752.5 | 14.82 | 50.80 | | |
| 756.5 | 8.01 | 56.47 | | |
| 760.5 | 19.66 | 46.63 | | |
| 764.5 | 3.46 | 7.27 | 0.25 | 4.46 |

| Depth (cm) | wt% IRD | wt% carbonate | $\delta^{13}C$ ‰ | $\delta^{18}O$ ‰ |
|---|---|---|---|---|
| 768.5 | 5.43 | 6.30 | 0.33 | 4.54 |
| 772.5 | 5.09 | 6.29 | 0.30 | 4.44 |
| 776.5 | 4.02 | 7.43 | 0.25 | 4.43 |
| 780.5 | 3.30 | 5.87 | 0.35 | 4.45 |
| 784.5 | 0.93 | 2.02 | | |
| 788.5 | 1.39 | 1.52 | | |
| 792.5 | 0.26 | 2.39 | | |
| 796.5 | 0.40 | 2.54 | | |
| 800.5 | 0.16 | 3.58 | | |
| 804.5 | 0.23 | 3.67 | 0.06 | 4.27 |
| 808.5 | 0.16 | 3.83 | 0.08 | 4.25 |
| 812.5 | 0.92 | 4.16 | 0.08 | 4.26 |
| 816.5 | 2.21 | 4.14 | 0.22 | 4.19 |
| 820.5 | 0.37 | 1.91 | | |
| 824.5 | 0.54 | 2.27 | | |
| 828.5 | 4.53 | 3.06 | | |
| 832.5 | 0.23 | 4.60 | 0.25 | 4.15 |
| 836.5 | 0.24 | 4.21 | 0.13 | 4.26 |
| 840.5 | 0.32 | 4.43 | 0.11 | 4.21 |
| 844.5 | 0.26 | 4.25 | 0.14 | 4.14 |
| 848.5 | 0.29 | 4.86 | 0.10 | 4.15 |
| 852.5 | 0.47 | 3.85 | | |
| 856.5 | 1.40 | 3.99 | | |
| 860.5 | 1.21 | 6.71 | | |
| 864.5 | 0.99 | 14.46 | 0.09 | 4.04 |
| 870.5 | 14.54 | 0.00 | | |
| 874.5 | 57.76 | 9.12 | | |
| 878.5 | 57.86 | 7.25 | | |
| 882.5 | 56.21 | 6.11 | | |
| 886.5 | 63.74 | 17.70 | | |
| 890.5 | 64.76 | 7.10 | | |
| 894.5 | 34.35 | 27.36 | | |

Table B.3.a. Core PC04 dinocyst species assemblage, (Part A). Species acronyms are found in Appendix A. Note. This table has two parts (A and B) that are at the same depths but with different species.

| Depth (cm) | Acho | Iacu | Ipal | Ipar | Ipat | Isph | Istr | Ispp | Lmac | Nlab | Ocen | Pret | Selo | Sram |
|---|---|---|---|---|---|---|---|---|---|---|---|---|---|---|
| **0.5** | 0 | 0 | 3 | 0 | 0 | 2 | 0 | 2 | 0 | 194 | 119 | 0 | 2 | 1 |
| **4.5** | 0 | 0 | 1 | 0 | 0 | 0 | 0 | 1 | 0 | 183 | 117 | 0 | 1 | 4 |
| **8.5** | 0 | 0 | 1 | 0 | 0 | 5 | 0 | 0 | 0 | 159 | 118 | 0 | 1 | 2 |
| **12.5** | 0 | 0 | 6 | 0 | 0 | 2 | 0 | 1 | 0 | 174 | 143 | 0 | 1 | 5 |
| **16.5** | 0 | 0 | 2 | 0 | 0 | 2 | 0 | 0 | 0 | 185 | 139 | 0 | 0 | 8 |
| **20.5** | 0 | 0 | 1 | 0 | 0 | 9 | 0 | 0 | 0 | 154 | 138 | 0 | 1 | 3 |
| **24.5** | 0 | 0 | 2 | 0 | 0 | 1 | 0 | 0 | 0 | 74 | 242 | 0 | 1 | 1 |
| **28.5** | 0 | 0 | 2 | 0 | 0 | 1 | 0 | 1 | 0 | 77 | 233 | 0 | 1 | 4 |
| **32.5** | 0 | 0 | 8 | 0 | 0 | 2 | 0 | 4 | 0 | 57 | 198 | 0 | 3 | 1 |
| **36.5** | 0 | 0 | 0 | 0 | 0 | 7 | 0 | 4 | 0 | 51 | 118 | 0 | 16 | 4 |
| **40.5** | 0 | 0 | 1 | 0 | 0 | 6 | 0 | 0 | 0 | 73 | 63 | 1 | 14 | 7 |
| **44.5** | 0 | 0 | 2 | 0 | 0 | 9 | 0 | 0 | 0 | 42 | 139 | 1 | 5 | 3 |
| **48.5** | 0 | 1 | 0 | 0 | 0 | 4 | 0 | 0 | 0 | 37 | 163 | 0 | 7 | 4 |
| **68.5** | 0 | 0 | 0 | 0 | 0 | 6 | 0 | 1 | 0 | 44 | 59 | 0 | 7 | 6 |
| **72.5** | 0 | 2 | 0 | 0 | 0 | 6 | 0 | 2 | 0 | 38 | 69 | 0 | 3 | 4 |
| **76.5** | 0 | 0 | 0 | 0 | 0 | 14 | 0 | 1 | 0 | 47 | 69 | 0 | 5 | 4 |
| **80.5** | 0 | 2 | 0 | 0 | 0 | 7 | 0 | 0 | 0 | 34 | 52 | 0 | 1 | 10 |
| **84.5** | 0 | 2 | 0 | 0 | 0 | 3 | 0 | 0 | 0 | 43 | 37 | 0 | 3 | 9 |
| **88.5** | 0 | 1 | 0 | 0 | 0 | 6 | 0 | 0 | 0 | 30 | 43 | 0 | 0 | 3 |
| **92.5** | 0 | 0 | 0 | 0 | 0 | 3 | 0 | 6 | 0 | 25 | 42 | 0 | 2 | 3 |
| **96.5** | 0 | 0 | 0 | 0 | 0 | 4 | 0 | 0 | 0 | 34 | 37 | 0 | 0 | 2 |
| **100.5** | 0 | 0 | 0 | 0 | 0 | 2 | 0 | 1 | 0 | 31 | 48 | 0 | 0 | 10 |
| **104.5** | 0 | 1 | 0 | 0 | 0 | 3 | 0 | 0 | 0 | 29 | 24 | 0 | 0 | 0 |
| **108.5** | 0 | 0 | 0 | 0 | 0 | 4 | 0 | 1 | 0 | 32 | 57 | 0 | 2 | 6 |
| **112.5** | 0 | 0 | 0 | 0 | 0 | 2 | 0 | 0 | 0 | 19 | 35 | 0 | 0 | 1 |
| **116.5** | 0 | 1 | 0 | 0 | 0 | 5 | 0 | 0 | 0 | 35 | 16 | 0 | 0 | 7 |
| **120.5** | 0 | 1 | 0 | 0 | 0 | 1 | 0 | 0 | 0 | 23 | 72 | 0 | 0 | 11 |
| **124.5** | 0 | 0 | 0 | 0 | 0 | 1 | 0 | 0 | 0 | 27 | 72 | 0 | 1 | 4 |
| **128.5** | 0 | 1 | 0 | 0 | 0 | 3 | 0 | 0 | 0 | 35 | 51 | 0 | 0 | 20 |
| **132.5** | 0 | 1 | 0 | 0 | 0 | 0 | 0 | 0 | 0 | 21 | 47 | 0 | 0 | 8 |
| **136.5** | 0 | 0 | 0 | 0 | 0 | 0 | 0 | 2 | 0 | 29 | 78 | 0 | 4 | 15 |
| **140.5** | 0 | 0 | 0 | 0 | 0 | 0 | 0 | 1 | 0 | 30 | 74 | 0 | 4 | 7 |
| **144.5** | 0 | 0 | 0 | 0 | 0 | 1 | 0 | 0 | 0 | 47 | 81 | 0 | 5 | 4 |
| **148.5** | 0 | 0 | 0 | 0 | 0 | 1 | 0 | 0 | 0 | 35 | 49 | 0 | 5 | 4 |
| **152.5** | 0 | 0 | 0 | 0 | 0 | 0 | 0 | 0 | 0 | 19 | 54 | 0 | 8 | 3 |
| **156.5** | 0 | 0 | 0 | 0 | 0 | 0 | 0 | 0 | 0 | 29 | 52 | 0 | 7 | 3 |
| **160.5** | 1 | 2 | 1 | 0 | 0 | 0 | 0 | 3 | 0 | 39 | 60 | 0 | 10 | 3 |

| Depth (cm) | Acho | Iacu | Ipal | Ipar | Ipat | Isph | Istr | Ispp | Lmac | Nlab | Ocen | Pret | Selo | Sram |
|---|---|---|---|---|---|---|---|---|---|---|---|---|---|---|
| **164.5** | 2 | 1 | 0 | 0 | 0 | 2 | 0 | 0 | 0 | 24 | 60 | 0 | 3 | 0 |
| **168.5** | 0 | 1 | 0 | 0 | 0 | 0 | 0 | 0 | 0 | 22 | 99 | 0 | 10 | 2 |
| **172.5** | 0 | 3 | 0 | 0 | 0 | 0 | 0 | 0 | 0 | 24 | 115 | 0 | 14 | 6 |
| **176.5** | 0 | 1 | 0 | 0 | 0 | 0 | 0 | 0 | 0 | 19 | 127 | 0 | 16 | 6 |
| **180.5** | 0 | 2 | 0 | 0 | 0 | 0 | 0 | 0 | 0 | 31 | 63 | 0 | 7 | 1 |
| **184.5** | 0 | 0 | 0 | 1 | 0 | 1 | 1 | 0 | 0 | 25 | 33 | 0 | 6 | 3 |
| **188.5** | 0 | 0 | 0 | 0 | 0 | 0 | 0 | 1 | 0 | 28 | 23 | 0 | 4 | 0 |
| **192.5** | 0 | 2 | 0 | 0 | 0 | 0 | 0 | 0 | 0 | 31 | 4 | 0 | 0 | 0 |
| **196.5** | 0 | 0 | 0 | 0 | 0 | 0 | 0 | 0 | 0 | 21 | 6 | 0 | 3 | 0 |
| **200.5** | 0 | 0 | 0 | 1 | 0 | 1 | 0 | 2 | 0 | 36 | 4 | 0 | 1 | 1 |
| **204.5** | 0 | 2 | 0 | 0 | 0 | 0 | 0 | 0 | 0 | 16 | 3 | 0 | 1 | 0 |
| **208.5** | 0 | 0 | 0 | 0 | 0 | 0 | 0 | 0 | 0 | 2 | 2 | 0 | 0 | 0 |
| **212.5** | 0 | 0 | 0 | 0 | 0 | 0 | 0 | 0 | 1 | 0 | 0 | 0 | 1 | 0 |
| **216.5** | 0 | 0 | 0 | 0 | 0 | 0 | 0 | 0 | 0 | 1 | 0 | 0 | 0 | 0 |
| **220.5** | 0 | 0 | 0 | 0 | 0 | 0 | 0 | 0 | 0 | 1 | 0 | 0 | 0 | 0 |
| **224.5** | 0 | 0 | 0 | 0 | 0 | 0 | 0 | 0 | 0 | 1 | 0 | 0 | 0 | 0 |
| **228.5** | 0 | 0 | 0 | 0 | 0 | 0 | 0 | 0 | 0 | 0 | 0 | 0 | 0 | 0 |
| **232.5** | 0 | 0 | 0 | 0 | 0 | 0 | 0 | 0 | 0 | 5 | 3 | 0 | 0 | 0 |
| **236.5** | 0 | 0 | 0 | 0 | 0 | 0 | 0 | 0 | 0 | 3 | 0 | 0 | 0 | 0 |
| **240.5** | 0 | 0 | 0 | 0 | 0 | 0 | 0 | 0 | 0 | 2 | 1 | 0 | 0 | 0 |
| **244.5** | 0 | 0 | 0 | 0 | 0 | 0 | 0 | 0 | 0 | 0 | 0 | 0 | 0 | 0 |
| **248.5** | 0 | 2 | 0 | 0 | 0 | 0 | 0 | 0 | 0 | 0 | 1 | 0 | 0 | 0 |
| **252.5** | 0 | 0 | 0 | 0 | 0 | 0 | 0 | 0 | 0 | 3 | 1 | 0 | 2 | 0 |
| **256.5** | 0 | 0 | 0 | 0 | 0 | 0 | 0 | 0 | 0 | 3 | 3 | 0 | 0 | 0 |
| **260.5** | 0 | 0 | 0 | 0 | 0 | 0 | 0 | 0 | 0 | 1 | 1 | 0 | 0 | 0 |
| **264.5** | 0 | 0 | 0 | 0 | 0 | 0 | 0 | 0 | 0 | 3 | 0 | 0 | 0 | 0 |
| **268.5** | 0 | 0 | 0 | 0 | 0 | 0 | 0 | 0 | 0 | 0 | 0 | 0 | 0 | 0 |
| **272.5** | 0 | 1 | 0 | 0 | 0 | 0 | 0 | 0 | 0 | 2 | 1 | 0 | 1 | 0 |
| **276.5** | 0 | 0 | 0 | 0 | 0 | 0 | 0 | 0 | 0 | 0 | 0 | 0 | 0 | 0 |
| **280.5** | 0 | 0 | 0 | 0 | 1 | 0 | 0 | 0 | 0 | 2 | 0 | 0 | 0 | 0 |
| **284.5** | 0 | 0 | 0 | 0 | 0 | 2 | 0 | 0 | 0 | 3 | 1 | 0 | 0 | 0 |
| **288.5** | 0 | 0 | 0 | 0 | 0 | 0 | 0 | 0 | 0 | 5 | 2 | 0 | 0 | 0 |
| **292.5** | 0 | 0 | 0 | 0 | 0 | 0 | 0 | 0 | 0 | 4 | 2 | 0 | 1 | 0 |
| **296.5** | 0 | 0 | 0 | 0 | 0 | 0 | 0 | 0 | 0 | 1 | 0 | 0 | 0 | 0 |
| **300.5** | 0 | 0 | 0 | 0 | 0 | 0 | 0 | 0 | 0 | 1 | 1 | 0 | 0 | 0 |
| **304.5** | 0 | 0 | 0 | 0 | 0 | 0 | 0 | 0 | 0 | 2 | 1 | 0 | 0 | 0 |
| **308.5** | 0 | 0 | 0 | 0 | 0 | 0 | 0 | 0 | 0 | 3 | 2 | 0 | 0 | 0 |
| **312.5** | 0 | 0 | 0 | 0 | 0 | 0 | 0 | 0 | 0 | 4 | 3 | 0 | 0 | 0 |
| **316.5** | 0 | 0 | 0 | 0 | 0 | 0 | 0 | 0 | 0 | 0 | 0 | 0 | 0 | 0 |
| **320.5** | 0 | 0 | 0 | 0 | 0 | 0 | 0 | 0 | 0 | 2 | 0 | 0 | 0 | 0 |
| **324.5** | 0 | 0 | 0 | 0 | 0 | 0 | 0 | 0 | 0 | 0 | 0 | 0 | 0 | 0 |
| **328.5** | 0 | 0 | 0 | 0 | 0 | 0 | 0 | 0 | 0 | 0 | 3 | 0 | 0 | 0 |
| **332.5** | 0 | 0 | 0 | 0 | 0 | 0 | 0 | 0 | 0 | 15 | 3 | 0 | 0 | 0 |

| Depth (cm) | Acho | Iacu | Ipal | Ipar | Ipat | Isph | Istr | Ispp | Lmac | Nlab | Ocen | Pret | Selo | Sram |
|---|---|---|---|---|---|---|---|---|---|---|---|---|---|---|
| 336.5 | 0 | 0 | 0 | 0 | 0 | 0 | 0 | 0 | 0 | 2 | 3 | 0 | 0 | 0 |
| 340.5 | 0 | 0 | 0 | 0 | 0 | 0 | 0 | 0 | 0 | 1 | 0 | 0 | 0 | 0 |
| 344.5 | 0 | 0 | 0 | 0 | 0 | 0 | 0 | 0 | 0 | 3 | 0 | 0 | 0 | 0 |
| 348.5 | 0 | 0 | 0 | 0 | 0 | 0 | 0 | 0 | 0 | 5 | 1 | 0 | 0 | 0 |
| 352.5 | 0 | 1 | 0 | 0 | 0 | 0 | 0 | 0 | 0 | 11 | 5 | 0 | 0 | 0 |
| 356.5 | 0 | 0 | 0 | 0 | 0 | 0 | 0 | 0 | 0 | 1 | 0 | 0 | 1 | 0 |
| 360.5 | 0 | 0 | 0 | 0 | 0 | 0 | 0 | 0 | 0 | 2 | 0 | 0 | 0 | 0 |
| 364.5 | 0 | 0 | 0 | 0 | 0 | 0 | 0 | 0 | 0 | 5 | 0 | 0 | 0 | 0 |
| 368.5 | 0 | 0 | 0 | 0 | 0 | 0 | 0 | 0 | 0 | 2 | 2 | 0 | 0 | 0 |
| 372.5 | 0 | 0 | 0 | 1 | 0 | 0 | 0 | 0 | 0 | 1 | 0 | 0 | 0 | 0 |
| 376.5 | 0 | 0 | 0 | 0 | 0 | 0 | 0 | 0 | 0 | 2 | 0 | 0 | 0 | 0 |
| 380.5 | 0 | 1 | 0 | 1 | 0 | 0 | 0 | 0 | 0 | 9 | 4 | 0 | 1 | 0 |
| 384.5 | 0 | 0 | 0 | 0 | 0 | 0 | 0 | 2 | 0 | 4 | 2 | 0 | 0 | 0 |
| 388.5 | 0 | 0 | 0 | 0 | 0 | 0 | 0 | 0 | 0 | 3 | 1 | 0 | 0 | 0 |
| 392.5 | 0 | 0 | 0 | 0 | 0 | 1 | 0 | 0 | 0 | 4 | 5 | 0 | 0 | 0 |
| 396.5 | 0 | 1 | 0 | 0 | 0 | 0 | 0 | 0 | 0 | 6 | 1 | 0 | 0 | 0 |
| 400.5 | 0 | 0 | 0 | 0 | 0 | 0 | 0 | 0 | 0 | 2 | 4 | 0 | 0 | 0 |
| 404.5 | 0 | 0 | 0 | 0 | 0 | 0 | 0 | 0 | 0 | 0 | 1 | 0 | 0 | 0 |
| 408.5 | 0 | 0 | 0 | 0 | 0 | 0 | 0 | 0 | 0 | 1 | 2 | 0 | 0 | 0 |
| 412.5 | 0 | 0 | 0 | 0 | 0 | 0 | 0 | 0 | 0 | 2 | 0 | 0 | 1 | 0 |
| 416.5 | 0 | 0 | 0 | 0 | 0 | 0 | 0 | 0 | 0 | 1 | 4 | 0 | 0 | 0 |
| 421.5 | 0 | 0 | 0 | 0 | 0 | 0 | 0 | 0 | 0 | 1 | 2 | 0 | 0 | 0 |
| 424.5 | 0 | 0 | 0 | 0 | 0 | 0 | 0 | 0 | 0 | 1 | 1 | 0 | 0 | 0 |
| 428.5 | 0 | 0 | 0 | 0 | 0 | 0 | 0 | 0 | 0 | 1 | 1 | 0 | 0 | 0 |
| 432.5 | 0 | 0 | 0 | 0 | 0 | 0 | 0 | 0 | 0 | 0 | 3 | 0 | 0 | 0 |
| 436.5 | 0 | 2 | 0 | 0 | 0 | 0 | 0 | 0 | 0 | 1 | 1 | 0 | 0 | 0 |
| 440.5 | 0 | 0 | 0 | 0 | 0 | 0 | 0 | 0 | 0 | 1 | 0 | 0 | 0 | 0 |
| 444.5 | 0 | 0 | 0 | 0 | 0 | 0 | 0 | 0 | 0 | 1 | 2 | 0 | 0 | 0 |
| 448.5 | 0 | 0 | 0 | 0 | 0 | 0 | 0 | 0 | 0 | 3 | 0 | 0 | 0 | 0 |
| 452.5 | 0 | 1 | 0 | 0 | 0 | 0 | 0 | 0 | 0 | 0 | 2 | 0 | 0 | 0 |
| 456.5 | 0 | 0 | 0 | 0 | 0 | 0 | 0 | 0 | 0 | 3 | 1 | 0 | 0 | 0 |
| 460.5 | 0 | 0 | 0 | 0 | 0 | 0 | 0 | 0 | 0 | 3 | 3 | 0 | 0 | 0 |
| 464.5 | 0 | 1 | 0 | 0 | 0 | 0 | 0 | 0 | 0 | 1 | 2 | 0 | 0 | 0 |
| 468.5 | 0 | 1 | 0 | 0 | 0 | 0 | 0 | 0 | 0 | 3 | 10 | 0 | 1 | 1 |
| 472.5 | 0 | 2 | 0 | 0 | 0 | 0 | 0 | 0 | 0 | 3 | 7 | 0 | 2 | 0 |
| 476.5 | 0 | 1 | 0 | 0 | 1 | 1 | 0 | 0 | 0 | 1 | 8 | 0 | 0 | 1 |
| 480.5 | 0 | 0 | 0 | 0 | 0 | 0 | 0 | 0 | 0 | 0 | 1 | 0 | 0 | 0 |
| 484.5 | 0 | 0 | 0 | 0 | 0 | 0 | 0 | 0 | 0 | 3 | 10 | 0 | 0 | 0 |
| 488.5 | 0 | 0 | 0 | 0 | 0 | 0 | 0 | 0 | 0 | 0 | 2 | 0 | 0 | 1 |
| 492.5 | 0 | 0 | 0 | 0 | 0 | 0 | 0 | 0 | 0 | 1 | 1 | 0 | 0 | 0 |
| 497.5 | 0 | 0 | 0 | 0 | 0 | 0 | 0 | 0 | 0 | 0 | 0 | 0 | 0 | 0 |
| 500.5 | 0 | 0 | 0 | 0 | 0 | 0 | 0 | 0 | 0 | 0 | 0 | 0 | 0 | 0 |
| 504.5 | 0 | 0 | 0 | 0 | 0 | 0 | 0 | 0 | 0 | 0 | 0 | 0 | 0 | 0 |

| Depth (cm) | Acho | Iacu | Ipal | Ipar | Ipat | Isph | Istr | Ispp | Lmac | Nlab | Ocen | Pret | Selo | Sram |
|---|---|---|---|---|---|---|---|---|---|---|---|---|---|---|
| **508.5** | 0 | 0 | 0 | 0 | 0 | 0 | 0 | 0 | 0 | 0 | 0 | 0 | 0 | 0 |
| **512.5** | 0 | 0 | 0 | 0 | 0 | 0 | 0 | 0 | 0 | 0 | 0 | 0 | 0 | 0 |
| **516.5** | 0 | 0 | 0 | 0 | 0 | 0 | 0 | 0 | 0 | 0 | 0 | 0 | 0 | 0 |
| **520.5** | 0 | 0 | 0 | 0 | 0 | 0 | 0 | 0 | 0 | 0 | 0 | 0 | 0 | 0 |
| **524.5** | 0 | 0 | 0 | 0 | 0 | 0 | 0 | 0 | 0 | 0 | 0 | 0 | 0 | 0 |
| **528.5** | 0 | 0 | 0 | 0 | 0 | 0 | 0 | 0 | 0 | 0 | 0 | 0 | 0 | 0 |
| **532.5** | 0 | 0 | 0 | 0 | 0 | 0 | 0 | 0 | 0 | 0 | 0 | 0 | 0 | 0 |
| **536.5** | 0 | 0 | 0 | 0 | 0 | 0 | 0 | 0 | 0 | 0 | 0 | 0 | 0 | 0 |
| **540.5** | 0 | 0 | 0 | 0 | 0 | 0 | 0 | 0 | 0 | 0 | 0 | 0 | 0 | 0 |
| **544.5** | 0 | 0 | 0 | 0 | 0 | 0 | 0 | 0 | 0 | 0 | 0 | 0 | 1 | 0 |
| **548.5** | 0 | 0 | 0 | 0 | 0 | 0 | 0 | 0 | 0 | 0 | 0 | 0 | 0 | 0 |
| **552.5** | 0 | 0 | 0 | 0 | 0 | 0 | 0 | 0 | 0 | 0 | 1 | 0 | 0 | 0 |
| **556.5** | 0 | 0 | 0 | 0 | 0 | 0 | 0 | 0 | 0 | 0 | 0 | 0 | 0 | 0 |
| **560.5** | 0 | 0 | 0 | 0 | 0 | 0 | 0 | 0 | 0 | 0 | 0 | 0 | 0 | 0 |
| **564.5** | 0 | 0 | 0 | 0 | 0 | 0 | 0 | 0 | 0 | 0 | 0 | 0 | 0 | 0 |
| **568.5** | 0 | 0 | 0 | 0 | 0 | 0 | 0 | 0 | 0 | 0 | 0 | 0 | 0 | 0 |
| **572.5** | 0 | 0 | 0 | 0 | 0 | 0 | 0 | 0 | 0 | 0 | 1 | 0 | 0 | 0 |
| **576.5** | 0 | 0 | 0 | 0 | 0 | 0 | 0 | 0 | 0 | 0 | 0 | 0 | 0 | 0 |
| **580.5** | 0 | 0 | 0 | 0 | 0 | 0 | 0 | 0 | 0 | 0 | 0 | 0 | 0 | 0 |
| **584.5** | 0 | 0 | 0 | 0 | 0 | 0 | 0 | 0 | 0 | 0 | 0 | 0 | 0 | 0 |
| **588.5** | 0 | 0 | 0 | 0 | 0 | 0 | 0 | 0 | 0 | 0 | 0 | 0 | 0 | 0 |
| **592.5** | 0 | 0 | 0 | 0 | 0 | 0 | 0 | 0 | 0 | 0 | 1 | 0 | 0 | 0 |
| **596.5** | 0 | 1 | 0 | 0 | 0 | 0 | 0 | 0 | 0 | 0 | 2 | 0 | 0 | 0 |
| **600.5** | 0 | 0 | 0 | 0 | 0 | 0 | 0 | 0 | 0 | 0 | 2 | 0 | 1 | 0 |
| **604.5** | 0 | 0 | 0 | 0 | 0 | 0 | 0 | 0 | 0 | 0 | 1 | 0 | 0 | 0 |
| **610.5** | 0 | 0 | 0 | 0 | 0 | 0 | 0 | 0 | 0 | 0 | 1 | 0 | 0 | 0 |
| **614.5** | 0 | 0 | 0 | 0 | 0 | 0 | 0 | 0 | 0 | 0 | 0 | 0 | 0 | 0 |
| **618.5** | 0 | 0 | 0 | 0 | 0 | 0 | 0 | 0 | 0 | 0 | 0 | 0 | 0 | 0 |
| **622.5** | 0 | 0 | 0 | 0 | 0 | 0 | 0 | 0 | 0 | 0 | 1 | 0 | 0 | 0 |
| **626.5** | 0 | 0 | 0 | 0 | 0 | 0 | 0 | 0 | 0 | 0 | 0 | 0 | 0 | 0 |
| **630.5** | 0 | 0 | 0 | 0 | 0 | 0 | 0 | 0 | 0 | 0 | 0 | 0 | 0 | 0 |
| **634.5** | 0 | 0 | 0 | 0 | 0 | 0 | 0 | 0 | 0 | 0 | 0 | 0 | 0 | 0 |
| **638.5** | 0 | 0 | 0 | 0 | 0 | 0 | 0 | 0 | 0 | 0 | 0 | 0 | 0 | 0 |
| **642.5** | 0 | 0 | 0 | 0 | 0 | 0 | 0 | 0 | 0 | 0 | 0 | 0 | 0 | 0 |
| **646.5** | 0 | 0 | 0 | 0 | 0 | 0 | 0 | 0 | 0 | 0 | 0 | 0 | 0 | 0 |
| **650.5** | 0 | 0 | 0 | 0 | 0 | 0 | 0 | 0 | 0 | 0 | 0 | 0 | 0 | 0 |
| **654.5** | 0 | 0 | 0 | 0 | 0 | 0 | 0 | 0 | 0 | 0 | 0 | 0 | 0 | 0 |
| **658.5** | 0 | 0 | 0 | 0 | 0 | 0 | 0 | 0 | 0 | 0 | 1 | 0 | 0 | 0 |
| **662.5** | 0 | 0 | 0 | 0 | 0 | 0 | 0 | 0 | 0 | 0 | 1 | 0 | 0 | 0 |
| **664.5** | 0 | 0 | 0 | 0 | 0 | 0 | 0 | 0 | 0 | 0 | 2 | 0 | 0 | 0 |
| **668.5** | 0 | 0 | 0 | 0 | 0 | 0 | 0 | 0 | 0 | 0 | 0 | 0 | 0 | 0 |
| **672.5** | 0 | 0 | 0 | 0 | 0 | 0 | 0 | 0 | 0 | 0 | 1 | 0 | 0 | 0 |
| **676.5** | 0 | 0 | 0 | 0 | 0 | 0 | 0 | 0 | 0 | 0 | 0 | 0 | 0 | 0 |

| Depth (cm) | Acho | Iacu | Ipal | Ipar | Ipat | Isph | Istr | Ispp | Lmac | Nlab | Ocen | Pret | Selo | Sram |
|---|---|---|---|---|---|---|---|---|---|---|---|---|---|---|
| **680.5** | 0 | 0 | 0 | 0 | 0 | 0 | 0 | 0 | 0 | 0 | 0 | 0 | 0 | 0 |
| **684.5** | 0 | 0 | 0 | 0 | 0 | 0 | 0 | 0 | 0 | 0 | 1 | 0 | 0 | 0 |
| **688.5** | 0 | 0 | 0 | 0 | 0 | 0 | 0 | 0 | 0 | 0 | 3 | 0 | 0 | 0 |
| **692.5** | 0 | 0 | 0 | 0 | 0 | 0 | 0 | 0 | 0 | 1 | 1 | 0 | 0 | 0 |
| **696.5** | 0 | 0 | 0 | 0 | 0 | 0 | 0 | 0 | 0 | 4 | 0 | 0 | 1 | 0 |
| **700.5** | 0 | 0 | 0 | 0 | 0 | 0 | 0 | 0 | 0 | 0 | 1 | 0 | 0 | 0 |
| **704.5** | 0 | 0 | 0 | 0 | 0 | 0 | 0 | 0 | 0 | 0 | 0 | 0 | 0 | 0 |
| **708.5** | 0 | 0 | 0 | 0 | 0 | 0 | 0 | 0 | 0 | 0 | 0 | 0 | 0 | 0 |
| **712.5** | 0 | 0 | 0 | 0 | 0 | 0 | 0 | 0 | 0 | 0 | 0 | 0 | 0 | 0 |
| **716.5** | 0 | 0 | 0 | 0 | 0 | 0 | 0 | 0 | 0 | 0 | 0 | 0 | 0 | 0 |
| **720.5** | 0 | 0 | 0 | 0 | 0 | 0 | 0 | 0 | 0 | 0 | 2 | 0 | 0 | 0 |
| **724.5** | 0 | 0 | 0 | 0 | 0 | 0 | 0 | 0 | 0 | 0 | 0 | 0 | 0 | 0 |
| **728.5** | 0 | 0 | 0 | 0 | 0 | 0 | 0 | 0 | 0 | 0 | 0 | 0 | 0 | 0 |
| **732.5** | 0 | 0 | 0 | 0 | 0 | 0 | 0 | 0 | 0 | 0 | 0 | 0 | 0 | 0 |
| **736.5** | 0 | 0 | 0 | 0 | 0 | 0 | 0 | 0 | 0 | 0 | 0 | 0 | 0 | 0 |
| **740.5** | 0 | 0 | 0 | 0 | 0 | 0 | 0 | 0 | 0 | 0 | 0 | 0 | 0 | 0 |
| **744.5** | 0 | 0 | 0 | 0 | 0 | 0 | 0 | 0 | 0 | 0 | 0 | 0 | 0 | 0 |
| **748.5** | 0 | 0 | 0 | 0 | 0 | 0 | 0 | 0 | 0 | 0 | 0 | 0 | 0 | 0 |
| **752.5** | 0 | 0 | 0 | 0 | 0 | 0 | 0 | 0 | 0 | 0 | 0 | 0 | 0 | 0 |
| **756.5** | 0 | 0 | 0 | 0 | 0 | 0 | 0 | 0 | 0 | 0 | 0 | 0 | 0 | 0 |
| **760.5** | 0 | 0 | 0 | 0 | 0 | 0 | 0 | 0 | 0 | 0 | 0 | 0 | 0 | 0 |
| **764.5** | 0 | 0 | 0 | 0 | 0 | 0 | 0 | 0 | 0 | 0 | 0 | 0 | 0 | 0 |
| **768.5** | 0 | 0 | 0 | 0 | 0 | 0 | 0 | 0 | 0 | 0 | 0 | 0 | 0 | 0 |
| **772.5** | 0 | 0 | 0 | 0 | 0 | 0 | 0 | 0 | 0 | 0 | 0 | 0 | 0 | 0 |
| **776.5** | 0 | 0 | 0 | 0 | 0 | 0 | 0 | 0 | 0 | 0 | 0 | 0 | 0 | 0 |
| **780.5** | 0 | 0 | 0 | 0 | 0 | 0 | 0 | 0 | 0 | 0 | 0 | 0 | 0 | 0 |
| **784.5** | 0 | 0 | 0 | 0 | 0 | 0 | 0 | 0 | 0 | 0 | 1 | 0 | 0 | 0 |
| **788.5** | 0 | 0 | 0 | 0 | 0 | 5 | 0 | 0 | 0 | 0 | 0 | 0 | 0 | 0 |
| **792.5** | 0 | 0 | 0 | 0 | 0 | 1 | 0 | 0 | 0 | 1 | 0 | 0 | 0 | 0 |
| **796.5** | 0 | 0 | 0 | 0 | 0 | 0 | 0 | 0 | 0 | 0 | 0 | 0 | 0 | 0 |
| **800.5** | 0 | 0 | 0 | 1 | 0 | 0 | 0 | 0 | 0 | 0 | 2 | 0 | 0 | 0 |
| **804.5** | 0 | 0 | 0 | 0 | 0 | 0 | 0 | 0 | 0 | 0 | 0 | 0 | 0 | 0 |
| **808.5** | 0 | 0 | 0 | 0 | 0 | 0 | 0 | 0 | 0 | 0 | 3 | 0 | 0 | 0 |
| **812.5** | 0 | 0 | 0 | 0 | 0 | 0 | 0 | 0 | 0 | 0 | 2 | 0 | 0 | 0 |
| **816.5** | 0 | 0 | 0 | 0 | 0 | 0 | 0 | 0 | 0 | 0 | 0 | 0 | 0 | 0 |
| **820.5** | 0 | 0 | 0 | 0 | 0 | 0 | 0 | 0 | 0 | 0 | 1 | 0 | 0 | 0 |
| **824.5** | 0 | 0 | 0 | 0 | 0 | 0 | 0 | 0 | 0 | 0 | 0 | 0 | 0 | 0 |
| **828.5** | 0 | 0 | 0 | 0 | 0 | 0 | 0 | 0 | 0 | 0 | 1 | 0 | 0 | 0 |
| **832.5** | 0 | 0 | 0 | 1 | 0 | 1 | 0 | 0 | 0 | 0 | 0 | 0 | 0 | 0 |
| **836.5** | 0 | 0 | 0 | 0 | 0 | 1 | 0 | 1 | 0 | 1 | 1 | 0 | 0 | 0 |
| **840.5** | 0 | 0 | 0 | 0 | 0 | 0 | 0 | 0 | 0 | 0 | 0 | 0 | 0 | 0 |
| **844.5** | 0 | 0 | 0 | 0 | 0 | 0 | 0 | 0 | 0 | 0 | 2 | 0 | 0 | 0 |
| **848.5** | 0 | 0 | 0 | 0 | 0 | 0 | 0 | 0 | 0 | 1 | 0 | 0 | 0 | 0 |

| Depth (cm) | Acho | Iacu | Ipal | Ipar | Ipat | Isph | Istr | Ispp | Lmac | Nlab | Ocen | Pret | Selo | Sram |
|---|---|---|---|---|---|---|---|---|---|---|---|---|---|---|
| **852.5** | 0 | 0 | 0 | 0 | 0 | 0 | 0 | 0 | 0 | 0 | 0 | 0 | 0 | 0 |
| **856.5** | 0 | 0 | 0 | 0 | 0 | 0 | 0 | 0 | 0 | 0 | 1 | 0 | 0 | 0 |
| **860.5** | 0 | 0 | 0 | 0 | 0 | 0 | 0 | 0 | 0 | 0 | 0 | 0 | 0 | 0 |
| **864.5** | 0 | 0 | 0 | 0 | 0 | 0 | 0 | 0 | 0 | 0 | 0 | 0 | 0 | 0 |
| **870.5** | 0 | 0 | 0 | 0 | 0 | 0 | 0 | 0 | 0 | 0 | 0 | 0 | 0 | 0 |
| **874.5** | 0 | 0 | 0 | 0 | 0 | 0 | 0 | 0 | 0 | 0 | 0 | 0 | 0 | 0 |
| **878.5** | 0 | 0 | 0 | 0 | 0 | 0 | 0 | 0 | 0 | 0 | 0 | 0 | 0 | 0 |
| **882.5** | 0 | 0 | 0 | 0 | 0 | 0 | 0 | 0 | 0 | 0 | 0 | 0 | 0 | 0 |
| **886.5** | 0 | 0 | 0 | 0 | 0 | 0 | 0 | 0 | 0 | 0 | 0 | 0 | 0 | 0 |
| **890.5** | 0 | 0 | 0 | 0 | 0 | 0 | 0 | 0 | 0 | 0 | 0 | 0 | 0 | 0 |
| **894.5** | 0 | 0 | 0 | 0 | 0 | 0 | 0 | 0 | 0 | 0 | 1 | 0 | 0 | 0 |

Table B.3.b. Core PC04 dinocyst species assemblage, (Part B). Species acronyms are found in Appendix A. Note. This table has two parts (A and B) that are at the same depths but with different species.

| Depth (cm) | Sfri | Smir | Sspp | Pdal | Imin | Imic | Bspp | Peri | Snep | Squa | Tapp | Parc | Ekar |
|---|---|---|---|---|---|---|---|---|---|---|---|---|---|
| **0.5** | 0 | 0 | 0 | 0 | 0 | 0 | 5 | 0 | 0 | 6 | 0 | 0 | 0 |
| **4.5** | 0 | 0 | 1 | 3 | 0 | 0 | 1 | 0 | 0 | 0 | 1 | 0 | 0 |
| **8.5** | 0 | 0 | 0 | 12 | 10 | 0 | 14 | 0 | 0 | 0 | 0 | 0 | 0 |
| **12.5** | 0 | 0 | 1 | 11 | 6 | 0 | 27 | 0 | 0 | 0 | 0 | 0 | 1 |
| **16.5** | 0 | 0 | 1 | 5 | 2 | 0 | 13 | 0 | 0 | 0 | 0 | 0 | 0 |
| **20.5** | 0 | 0 | 0 | 5 | 3 | 0 | 23 | 0 | 0 | 4 | 0 | 0 | 0 |
| **24.5** | 0 | 0 | 3 | 4 | 6 | 0 | 7 | 0 | 0 | 0 | 0 | 0 | 0 |
| **28.5** | 0 | 0 | 2 | 15 | 5 | 0 | 5 | 0 | 0 | 0 | 0 | 0 | 0 |
| **32.5** | 0 | 0 | 2 | 46 | 4 | 0 | 6 | 0 | 0 | 0 | 0 | 0 | 0 |
| **36.5** | 0 | 6 | 9 | 113 | 2 | 0 | 9 | 0 | 0 | 2 | 0 | 0 | 0 |
| **40.5** | 0 | 2 | 2 | 134 | 1 | 0 | 8 | 0 | 0 | 0 | 0 | 0 | 0 |
| **44.5** | 0 | 0 | 1 | 65 | 4 | 2 | 35 | 0 | 0 | 2 | 0 | 0 | 0 |
| **48.5** | 0 | 2 | 2 | 113 | 2 | 0 | 3 | 0 | 0 | 0 | 0 | 0 | 0 |
| **68.5** | 1 | 2 | 3 | 147 | 2 | 2 | 16 | 0 | 0 | 0 | 0 | 0 | 0 |
| **72.5** | 0 | 1 | 1 | 150 | 10 | 5 | 9 | 0 | 0 | 4 | 0 | 0 | 0 |
| **76.5** | 0 | 0 | 0 | 124 | 19 | 2 | 14 | 0 | 0 | 6 | 0 | 0 | 0 |
| **80.5** | 0 | 0 | 0 | 170 | 21 | 0 | 13 | 0 | 0 | 0 | 0 | 0 | 0 |

| Depth (cm) | Sfri | Smir | Sspp | Pdal | Imin | Imic | Bspp | Peri | Snep | Squa | Tapp | Parc | Ekar |
|---|---|---|---|---|---|---|---|---|---|---|---|---|---|
| **84.5** | 0 | 1 | 1 | 157 | 32 | 0 | 17 | 0 | 0 | 3 | 0 | 0 | 0 |
| **88.5** | 0 | 0 | 0 | 123 | 69 | 0 | 18 | 0 | 0 | 9 | 0 | 0 | 0 |
| **92.5** | 0 | 0 | 0 | 138 | 60 | 0 | 26 | 1 | 0 | 7 | 0 | 0 | 0 |
| **96.5** | 0 | 0 | 0 | 149 | 72 | 0 | 16 | 46 | 0 | 2 | 0 | 0 | 0 |
| **100.5** | 0 | 0 | 3 | 123 | 50 | 1 | 10 | 30 | 0 | 6 | 0 | 0 | 0 |
| **104.5** | 0 | 0 | 5 | 93 | 84 | 1 | 17 | 58 | 0 | 4 | 0 | 0 | 0 |
| **108.5** | 0 | 0 | 11 | 86 | 51 | 0 | 12 | 44 | 0 | 3 | 0 | 0 | 0 |
| **112.5** | 0 | 0 | 2 | 77 | 83 | 0 | 14 | 83 | 0 | 10 | 0 | 0 | 0 |
| **116.5** | 0 | 0 | 5 | 79 | 90 | 1 | 18 | 48 | 0 | 10 | 0 | 0 | 0 |
| **120.5** | 0 | 0 | 11 | 36 | 88 | 0 | 39 | 42 | 0 | 3 | 0 | 0 | 0 |
| **124.5** | 0 | 0 | 16 | 69 | 84 | 0 | 20 | 41 | 0 | 4 | 0 | 0 | 0 |
| **128.5** | 0 | 0 | 6 | 39 | 80 | 0 | 40 | 36 | 0 | 8 | 0 | 0 | 0 |
| **132.5** | 0 | 0 | 9 | 63 | 93 | 0 | 42 | 27 | 0 | 10 | 0 | 0 | 0 |
| **136.5** | 0 | 0 | 13 | 62 | 93 | 0 | 13 | 9 | 0 | 0 | 0 | 0 | 0 |
| **140.5** | 0 | 0 | 11 | 79 | 82 | 0 | 6 | 10 | 0 | 2 | 0 | 0 | 0 |
| **144.5** | 0 | 0 | 11 | 89 | 54 | 0 | 19 | 11 | 0 | 4 | 0 | 0 | 0 |
| **148.5** | 0 | 0 | 8 | 79 | 66 | 3 | 30 | 25 | 0 | 3 | 0 | 0 | 0 |
| **152.5** | 0 | 0 | 18 | 90 | 73 | 0 | 38 | 16 | 0 | 8 | 0 | 0 | 0 |
| **156.5** | 0 | 0 | 17 | 56 | 42 | 1 | 73 | 24 | 0 | 7 | 0 | 0 | 0 |
| **160.5** | 0 | 0 | 15 | 36 | 68 | 2 | 51 | 13 | 0 | 2 | 0 | 0 | 0 |
| **164.5** | 0 | 0 | 15 | 45 | 68 | 1 | 72 | 29 | 0 | 4 | 0 | 0 | 0 |
| **168.5** | 0 | 0 | 21 | 33 | 56 | 1 | 28 | 30 | 0 | 4 | 0 | 0 | 0 |
| **172.5** | 0 | 0 | 20 | 46 | 57 | 0 | 12 | 11 | 0 | 2 | 0 | 0 | 0 |
| **176.5** | 0 | 0 | 25 | 62 | 29 | 0 | 9 | 5 | 0 | 1 | 0 | 0 | 0 |
| **180.5** | 0 | 0 | 18 | 63 | 71 | 1 | 21 | 14 | 0 | 6 | 0 | 0 | 0 |
| **184.5** | 0 | 0 | 11 | 36 | 65 | 0 | 108 | 13 | 1 | 6 | 0 | 0 | 0 |
| **188.5** | 0 | 0 | 2 | 36 | 69 | 0 | 125 | 9 | 0 | 7 | 0 | 1 | 0 |
| **192.5** | 0 | 0 | 0 | 11 | 23 | 0 | 219 | 11 | 0 | 2 | 0 | 0 | 0 |
| **196.5** | 0 | 0 | 4 | 13 | 24 | 0 | 221 | 10 | 0 | 3 | 0 | 0 | 0 |
| **200.5** | 0 | 0 | 3 | 14 | 30 | 0 | 146 | 2 | 0 | 8 | 0 | 0 | 0 |
| **204.5** | 0 | 0 | 1 | 3 | 17 | 0 | 255 | 8 | 0 | 6 | 0 | 0 | 0 |
| **208.5** | 0 | 0 | 1 | 0 | 16 | 0 | 127 | 0 | 0 | 0 | 0 | 0 | 0 |
| **212.5** | 0 | 0 | 1 | 1 | 8 | 1 | 136 | 1 | 0 | 0 | 0 | 0 | 0 |
| **216.5** | 0 | 0 | 0 | 0 | 1 | 0 | 78 | 5 | 0 | 0 | 0 | 0 | 0 |
| **220.5** | 0 | 0 | 0 | 0 | 0 | 0 | 19 | 0 | 0 | 0 | 0 | 0 | 0 |
| **224.5** | 0 | 0 | 0 | 0 | 0 | 0 | 0 | 0 | 0 | 0 | 0 | 0 | 0 |
| **228.5** | 0 | 0 | 0 | 0 | 0 | 0 | 1 | 0 | 0 | 0 | 0 | 0 | 0 |

| Depth (cm) | Sfri | Smir | Sspp | Pdal | Imin | Imic | Bspp | Peri | Snep | Squa | Tapp | Parc | Ekar |
|---|---|---|---|---|---|---|---|---|---|---|---|---|---|
| **232.5** | 0 | 0 | 0 | 2 | 2 | 0 | 2 | 0 | 0 | 0 | 0 | 0 | 0 |
| **236.5** | 0 | 0 | 0 | 1 | 12 | 1 | 41 | 5 | 0 | 2 | 0 | 0 | 0 |
| **240.5** | 0 | 0 | 0 | 0 | 6 | 1 | 44 | 0 | 0 | 0 | 0 | 0 | 0 |
| **244.5** | 0 | 0 | 0 | 0 | 9 | 0 | 65 | 3 | 0 | 3 | 0 | 0 | 0 |
| **248.5** | 0 | 0 | 0 | 0 | 3 | 0 | 37 | 2 | 0 | 1 | 0 | 0 | 0 |
| **252.5** | 0 | 0 | 0 | 0 | 2 | 0 | 4 | 3 | 0 | 0 | 0 | 0 | 0 |
| **256.5** | 0 | 0 | 0 | 0 | 4 | 0 | 80 | 0 | 0 | 10 | 0 | 0 | 0 |
| **260.5** | 0 | 0 | 0 | 0 | 2 | 0 | 141 | 0 | 0 | 4 | 0 | 0 | 0 |
| **264.5** | 0 | 0 | 0 | 0 | 0 | 0 | 82 | 5 | 0 | 1 | 0 | 0 | 0 |
| **268.5** | 0 | 0 | 0 | 0 | 0 | 0 | 37 | 2 | 0 | 3 | 0 | 0 | 0 |
| **272.5** | 0 | 0 | 0 | 0 | 4 | 0 | 350 | 1 | 0 | 8 | 0 | 0 | 0 |
| **276.5** | 0 | 0 | 0 | 0 | 12 | 0 | 247 | 0 | 0 | 1 | 0 | 0 | 0 |
| **280.5** | 0 | 0 | 0 | 0 | 19 | 0 | 283 | 0 | 0 | 6 | 0 | 0 | 0 |
| **284.5** | 0 | 0 | 0 | 0 | 14 | 0 | 219 | 0 | 0 | 11 | 0 | 0 | 0 |
| **288.5** | 0 | 0 | 0 | 0 | 6 | 0 | 202 | 0 | 0 | 7 | 0 | 0 | 0 |
| **292.5** | 0 | 0 | 1 | 0 | 5 | 0 | 252 | 0 | 0 | 22 | 0 | 0 | 0 |
| **296.5** | 0 | 0 | 0 | 0 | 2 | 0 | 128 | 0 | 0 | 8 | 0 | 0 | 0 |
| **300.5** | 0 | 0 | 0 | 0 | 0 | 0 | 72 | 0 | 0 | 5 | 0 | 0 | 0 |
| **304.5** | 0 | 0 | 1 | 0 | 8 | 0 | 292 | 0 | 0 | 7 | 0 | 0 | 0 |
| **308.5** | 0 | 0 | 1 | 0 | 21 | 0 | 336 | 0 | 0 | 19 | 0 | 0 | 0 |
| **312.5** | 0 | 0 | 0 | 0 | 9 | 0 | 170 | 0 | 0 | 11 | 0 | 0 | 0 |
| **316.5** | 0 | 0 | 0 | 0 | 2 | 0 | 58 | 0 | 0 | 2 | 0 | 0 | 0 |
| **320.5** | 0 | 0 | 0 | 0 | 0 | 0 | 156 | 0 | 0 | 5 | 0 | 0 | 0 |
| **324.5** | 0 | 0 | 0 | 0 | 7 | 0 | 192 | 0 | 0 | 19 | 0 | 0 | 0 |
| **328.5** | 0 | 0 | 0 | 0 | 13 | 0 | 192 | 0 | 0 | 21 | 0 | 0 | 0 |
| **332.5** | 0 | 0 | 1 | 0 | 12 | 0 | 289 | 0 | 0 | 13 | 0 | 0 | 0 |
| **336.5** | 0 | 0 | 0 | 0 | 16 | 0 | 283 | 0 | 0 | 2 | 0 | 0 | 0 |
| **340.5** | 0 | 0 | 0 | 0 | 6 | 0 | 301 | 0 | 0 | 4 | 0 | 0 | 0 |
| **344.5** | 0 | 0 | 0 | 0 | 7 | 0 | 327 | 0 | 0 | 3 | 0 | 0 | 0 |
| **348.5** | 0 | 0 | 0 | 0 | 24 | 0 | 275 | 0 | 0 | 7 | 0 | 0 | 0 |
| **352.5** | 0 | 0 | 0 | 0 | 30 | 0 | 192 | 0 | 0 | 4 | 0 | 0 | 0 |
| **356.5** | 0 | 0 | 0 | 0 | 19 | 0 | 145 | 0 | 0 | 1 | 0 | 0 | 0 |
| **360.5** | 0 | 0 | 0 | 0 | 2 | 0 | 94 | 1 | 0 | 1 | 0 | 0 | 0 |
| **364.5** | 0 | 0 | 0 | 0 | 15 | 0 | 314 | 0 | 0 | 3 | 0 | 0 | 0 |
| **368.5** | 0 | 0 | 0 | 0 | 2 | 0 | 116 | 0 | 0 | 2 | 0 | 0 | 0 |
| **372.5** | 0 | 0 | 0 | 0 | 3 | 0 | 50 | 0 | 0 | 1 | 0 | 0 | 0 |
| **376.5** | 0 | 0 | 0 | 0 | 3 | 0 | 142 | 1 | 0 | 2 | 0 | 0 | 0 |

| Depth (cm) | Sfri | Smir | Sspp | Pdal | Imin | Imic | Bspp | Peri | Snep | Squa | Tapp | Parc | Ekar |
|---|---|---|---|---|---|---|---|---|---|---|---|---|---|
| **380.5** | 0 | 0 | 0 | 0 | 33 | 0 | 252 | 4 | 0 | 6 | 0 | 0 | 0 |
| **384.5** | 0 | 0 | 0 | 0 | 16 | 0 | 268 | 0 | 0 | 5 | 0 | 0 | 0 |
| **388.5** | 0 | 0 | 0 | 0 | 5 | 0 | 56 | 2 | 0 | 0 | 0 | 0 | 0 |
| **392.5** | 0 | 0 | 0 | 0 | 26 | 0 | 165 | 0 | 0 | 4 | 0 | 0 | 0 |
| **396.5** | 0 | 0 | 0 | 0 | 13 | 0 | 290 | 0 | 0 | 3 | 0 | 0 | 0 |
| **400.5** | 0 | 0 | 0 | 0 | 0 | 0 | 133 | 6 | 0 | 2 | 0 | 0 | 0 |
| **404.5** | 0 | 0 | 1 | 0 | 5 | 0 | 104 | 0 | 0 | 1 | 0 | 0 | 0 |
| **408.5** | 0 | 0 | 0 | 0 | 1 | 0 | 307 | 1 | 0 | 1 | 0 | 0 | 0 |
| **412.5** | 0 | 0 | 0 | 0 | 0 | 0 | 312 | 0 | 0 | 2 | 0 | 0 | 0 |
| **416.5** | 0 | 0 | 1 | 1 | 0 | 0 | 134 | 0 | 0 | 1 | 0 | 0 | 0 |
| **421.5** | 0 | 0 | 1 | 0 | 0 | 0 | 162 | 5 | 0 | 0 | 0 | 0 | 0 |
| **424.5** | 0 | 0 | 0 | 0 | 0 | 0 | 84 | 2 | 0 | 1 | 0 | 0 | 0 |
| **428.5** | 0 | 0 | 0 | 0 | 0 | 0 | 180 | 0 | 0 | 1 | 0 | 0 | 0 |
| **432.5** | 0 | 0 | 0 | 0 | 0 | 0 | 185 | 6 | 0 | 0 | 0 | 0 | 0 |
| **436.5** | 0 | 0 | 0 | 0 | 2 | 0 | 294 | 0 | 0 | 1 | 0 | 0 | 0 |
| **440.5** | 0 | 0 | 0 | 1 | 0 | 0 | 122 | 0 | 0 | 1 | 0 | 0 | 0 |
| **444.5** | 0 | 0 | 0 | 0 | 3 | 0 | 144 | 0 | 0 | 1 | 0 | 0 | 0 |
| **448.5** | 0 | 0 | 1 | 1 | 31 | 0 | 284 | 1 | 0 | 3 | 0 | 0 | 0 |
| **452.5** | 0 | 0 | 1 | 0 | 24 | 0 | 277 | 0 | 0 | 4 | 0 | 0 | 0 |
| **456.5** | 0 | 0 | 0 | 0 | 19 | 0 | 163 | 0 | 0 | 2 | 0 | 0 | 0 |
| **460.5** | 0 | 0 | 0 | 0 | 20 | 0 | 185 | 0 | 0 | 0 | 0 | 0 | 0 |
| **464.5** | 0 | 0 | 1 | 1 | 12 | 0 | 173 | 0 | 0 | 2 | 0 | 0 | 0 |
| **468.5** | 0 | 0 | 1 | 2 | 26 | 0 | 252 | 9 | 0 | 4 | 0 | 0 | 0 |
| **472.5** | 0 | 1 | 3 | 2 | 34 | 0 | 257 | 0 | 0 | 3 | 0 | 0 | 0 |
| **476.5** | 0 | 0 | 1 | 0 | 31 | 0 | 254 | 5 | 0 | 3 | 0 | 0 | 0 |
| **480.5** | 0 | 0 | 2 | 0 | 8 | 0 | 283 | 7 | 0 | 0 | 0 | 0 | 0 |
| **484.5** | 0 | 0 | 2 | 3 | 18 | 0 | 292 | 3 | 0 | 0 | 0 | 0 | 0 |
| **488.5** | 0 | 0 | 0 | 0 | 6 | 0 | 130 | 0 | 0 | 0 | 0 | 0 | 0 |
| **492.5** | 0 | 0 | 0 | 0 | 1 | 0 | 9 | 0 | 0 | 0 | 0 | 0 | 0 |
| **497.5** | 0 | 0 | 0 | 0 | 0 | 0 | 36 | 0 | 0 | 0 | 0 | 0 | 0 |
| **500.5** | 0 | 0 | 0 | 0 | 0 | 0 | 16 | 0 | 0 | 0 | 0 | 0 | 0 |
| **504.5** | 0 | 0 | 0 | 0 | 0 | 0 | 21 | 0 | 0 | 1 | 0 | 0 | 0 |
| **508.5** | 0 | 0 | 0 | 0 | 0 | 0 | 21 | 0 | 0 | 0 | 0 | 0 | 0 |
| **512.5** | 0 | 0 | 0 | 0 | 0 | 0 | 24 | 0 | 0 | 0 | 0 | 0 | 0 |
| **516.5** | 0 | 0 | 0 | 0 | 0 | 0 | 32 | 0 | 0 | 0 | 0 | 0 | 0 |
| **520.5** | 0 | 0 | 0 | 0 | 0 | 0 | 0 | 0 | 0 | 0 | 0 | 0 | 0 |
| **524.5** | 0 | 0 | 0 | 0 | 0 | 0 | 19 | 0 | 0 | 0 | 0 | 0 | 0 |

| Depth (cm) | Sfri | Smir | Sspp | Pdal | Imin | Imic | Bspp | Peri | Snep | Squa | Tapp | Parc | Ekar |
|---|---|---|---|---|---|---|---|---|---|---|---|---|---|
| **528.5** | 0 | 0 | 0 | 0 | 0 | 0 | 12 | 0 | 0 | 0 | 0 | 0 | 0 |
| **532.5** | 0 | 0 | 0 | 0 | 0 | 0 | 22 | 0 | 0 | 0 | 0 | 0 | 0 |
| **536.5** | 0 | 0 | 0 | 0 | 0 | 0 | 14 | 0 | 0 | 0 | 0 | 0 | 0 |
| **540.5** | 0 | 0 | 0 | 0 | 0 | 0 | 9 | 0 | 0 | 0 | 0 | 0 | 0 |
| **544.5** | 0 | 0 | 0 | 0 | 0 | 0 | 12 | 0 | 0 | 0 | 0 | 0 | 0 |
| **548.5** | 0 | 0 | 0 | 0 | 0 | 0 | 0 | 0 | 0 | 0 | 0 | 0 | 0 |
| **552.5** | 0 | 0 | 0 | 0 | 0 | 0 | 20 | 0 | 0 | 0 | 0 | 0 | 0 |
| **556.5** | 0 | 0 | 0 | 0 | 0 | 0 | 4 | 0 | 0 | 0 | 0 | 0 | 0 |
| **560.5** | 0 | 0 | 0 | 0 | 0 | 0 | 6 | 0 | 0 | 0 | 0 | 0 | 0 |
| **564.5** | 0 | 0 | 0 | 0 | 0 | 0 | 5 | 0 | 0 | 0 | 0 | 0 | 0 |
| **568.5** | 0 | 0 | 0 | 0 | 0 | 0 | 1 | 0 | 0 | 0 | 0 | 0 | 0 |
| **572.5** | 0 | 0 | 0 | 0 | 0 | 0 | 1 | 0 | 0 | 0 | 0 | 0 | 0 |
| **576.5** | 0 | 0 | 0 | 0 | 0 | 0 | 4 | 0 | 0 | 0 | 0 | 0 | 0 |
| **580.5** | 0 | 0 | 0 | 0 | 0 | 0 | 4 | 0 | 0 | 0 | 0 | 0 | 0 |
| **584.5** | 0 | 0 | 0 | 0 | 0 | 0 | 0 | 0 | 0 | 0 | 0 | 0 | 0 |
| **588.5** | 0 | 0 | 0 | 0 | 0 | 0 | 8 | 0 | 0 | 0 | 0 | 0 | 0 |
| **592.5** | 0 | 0 | 0 | 0 | 0 | 0 | 8 | 0 | 0 | 0 | 0 | 0 | 0 |
| **596.5** | 0 | 0 | 1 | 0 | 0 | 0 | 13 | 0 | 0 | 0 | 0 | 0 | 0 |
| **600.5** | 0 | 0 | 0 | 0 | 0 | 0 | 3 | 0 | 0 | 0 | 0 | 0 | 0 |
| **604.5** | 0 | 0 | 0 | 0 | 0 | 0 | 4 | 0 | 0 | 0 | 0 | 0 | 0 |
| **610.5** | 0 | 0 | 0 | 0 | 0 | 0 | 5 | 0 | 0 | 0 | 0 | 0 | 0 |
| **614.5** | 0 | 0 | 0 | 0 | 0 | 0 | 5 | 0 | 0 | 0 | 0 | 0 | |
| **618.5** | 0 | 0 | 0 | 0 | 0 | 0 | 0 | 0 | 0 | 0 | 0 | 0 | 0 |
| **622.5** | 0 | 0 | 0 | 0 | 0 | 0 | 4 | 0 | 0 | 0 | 0 | 0 | 0 |
| **626.5** | 0 | 0 | 0 | 0 | 0 | 0 | 16 | 0 | 0 | 0 | 0 | 0 | 0 |
| **630.5** | 0 | 0 | 0 | 0 | 0 | 0 | 20 | 0 | 0 | 0 | 0 | 0 | 0 |
| **634.5** | 0 | 2 | 2 | 0 | 0 | 0 | 8 | 0 | 0 | 0 | 0 | 0 | 0 |
| **638.5** | 0 | 0 | 0 | 0 | 0 | 0 | 58 | 0 | 0 | 0 | 0 | 0 | 0 |
| **642.5** | 0 | 0 | 0 | 0 | 0 | 0 | 14 | 0 | 0 | 0 | 0 | 0 | 0 |
| **646.5** | 0 | 0 | 0 | 0 | 0 | 0 | 12 | 0 | 0 | 0 | 0 | 0 | 0 |
| **650.5** | 0 | 0 | 0 | 0 | 0 | 0 | 12 | 0 | 0 | 0 | 0 | 0 | 0 |
| **654.5** | 0 | 0 | 0 | 0 | 0 | 0 | 2 | 0 | 0 | 0 | 0 | 0 | 0 |
| **658.5** | 0 | 0 | 0 | 0 | 0 | 0 | 54 | 0 | 0 | 0 | 0 | 0 | 0 |
| **662.5** | 0 | 0 | 0 | 0 | 0 | 0 | 4 | 0 | 0 | 0 | 0 | 0 | 0 |
| **664.5** | 0 | 0 | 0 | 0 | 0 | 0 | 12 | 0 | 0 | 0 | 0 | 0 | 0 |
| **668.5** | 0 | 0 | 0 | 0 | 0 | 0 | 19 | 0 | 0 | 0 | 0 | 0 | 0 |
| **672.5** | 0 | 0 | 0 | 0 | 0 | 0 | 5 | 0 | 0 | 0 | 0 | 0 | 0 |

| Depth (cm) | Sfri | Smir | Sspp | Pdal | Imin | Imic | Bspp | Peri | Snep | Squa | Tapp | Parc | Ekar |
|---|---|---|---|---|---|---|---|---|---|---|---|---|---|
| **676.5** | 0 | 0 | 0 | 0 | 0 | 0 | 0 | 0 | 0 | 0 | 0 | 0 | 0 |
| **680.5** | 0 | 0 | 0 | 0 | 0 | 0 | 43 | 1 | 0 | 0 | 0 | 0 | 0 |
| **684.5** | 0 | 0 | 0 | 0 | 0 | 0 | 42 | 0 | 0 | 0 | 0 | 0 | 0 |
| **688.5** | 0 | 0 | 0 | 0 | 2 | 0 | 119 | 22 | 0 | 0 | 0 | 0 | 0 |
| **692.5** | 0 | 0 | 1 | 0 | 3 | 0 | 290 | 16 | 0 | 0 | 0 | 0 | 0 |
| **696.5** | 0 | 0 | 0 | 0 | 3 | 4 | 280 | 48 | 0 | 0 | 0 | 0 | 0 |
| **700.5** | 0 | 0 | 0 | 0 | 0 | 0 | 31 | 11 | 0 | 0 | 0 | 0 | 0 |
| **704.5** | 0 | 0 | 0 | 0 | 0 | 0 | 9 | 2 | 0 | 0 | 0 | 0 | 0 |
| **708.5** | 0 | 0 | 0 | 0 | 0 | 0 | 5 | 3 | 0 | 0 | 0 | 0 | 0 |
| **712.5** | 0 | 0 | 0 | 0 | 0 | 0 | 51 | 5 | 0 | 0 | 0 | 0 | 0 |
| **716.5** | 0 | 0 | 0 | 0 | 0 | 0 | 0 | 0 | 0 | 0 | 0 | 0 | 0 |
| **720.5** | 0 | 0 | 0 | 0 | 0 | 0 | 0 | 1 | 0 | 0 | 0 | 0 | 0 |
| **724.5** | 0 | 0 | 0 | 0 | 0 | 0 | 1 | 0 | 0 | 0 | 0 | 0 | 0 |
| **728.5** | 0 | 0 | 0 | 0 | 0 | 0 | 4 | 2 | 0 | 0 | 0 | 0 | 0 |
| **732.5** | 0 | 0 | 0 | 0 | 0 | 0 | 1 | 1 | 0 | 0 | 0 | 0 | 0 |
| **736.5** | 0 | 0 | 0 | 0 | 0 | 0 | 0 | 0 | 0 | 0 | 0 | 0 | 0 |
| **740.5** | 0 | 0 | 0 | 0 | 0 | 0 | 2 | 2 | 0 | 0 | 0 | 0 | 0 |
| **744.5** | 0 | 0 | 0 | 0 | 0 | 0 | 0 | 3 | 0 | 0 | 0 | 0 | 0 |
| **748.5** | 0 | 0 | 0 | 0 | 0 | 0 | 4 | 5 | 0 | 0 | 0 | 0 | 0 |
| **752.5** | 0 | 0 | 0 | 0 | 0 | 0 | 1 | 2 | 0 | 0 | 0 | 0 | 0 |
| **756.5** | 0 | 0 | 0 | 0 | 0 | 0 | 0 | 0 | 0 | 0 | 0 | 0 | 0 |
| **760.5** | 0 | 0 | 0 | 0 | 0 | 0 | 16 | 0 | 0 | 0 | 0 | 0 | 0 |
| **764.5** | 0 | 0 | 0 | 0 | 3 | 0 | 164 | 0 | 0 | 0 | 0 | 0 | 0 |
| **768.5** | 0 | 0 | 0 | 0 | 0 | 0 | 8 | 0 | 0 | 0 | 0 | 0 | 0 |
| **772.5** | 0 | 0 | 0 | 0 | 0 | 0 | 24 | 0 | 0 | 0 | 0 | 0 | 0 |
| **776.5** | 0 | 0 | 0 | 0 | 0 | 0 | 1 | 0 | 0 | 0 | 0 | 0 | 0 |
| **780.5** | 0 | 0 | 0 | 0 | 0 | 0 | 0 | 0 | 0 | 0 | 0 | 0 | 0 |
| **784.5** | 0 | 0 | 0 | 0 | 0 | 0 | 3 | 0 | 0 | 0 | 0 | 0 | 0 |
| **788.5** | 0 | 0 | 1 | 0 | 0 | 0 | 0 | 0 | 0 | 0 | 0 | 0 | 0 |
| **792.5** | 0 | 0 | 0 | 0 | 0 | 0 | 0 | 0 | 0 | 0 | 0 | 0 | 0 |
| **796.5** | 0 | 0 | 0 | 0 | 2 | 0 | 2 | 5 | 0 | 0 | 0 | 0 | 0 |
| **800.5** | 0 | 0 | 0 | 0 | 6 | 2 | 235 | 5 | 0 | 0 | 0 | 0 | 0 |
| **804.5** | 0 | 0 | 0 | 0 | 5 | 0 | 64 | 0 | 0 | 0 | 0 | 0 | 0 |
| **808.5** | 0 | 0 | 1 | 0 | 5 | 0 | 147 | 0 | 0 | 0 | 0 | 0 | 0 |
| **812.5** | 0 | 0 | 1 | 0 | 1 | 0 | 81 | 2 | 0 | 0 | 0 | 0 | 0 |
| **816.5** | 0 | 0 | 0 | 0 | 2 | 1 | 10 | 1 | 0 | 0 | 0 | 0 | 0 |
| **820.5** | 0 | 0 | 0 | 0 | 0 | 0 | 1 | 0 | 0 | 0 | 0 | 0 | 0 |

| Depth (cm) | Sfri | Smir | Sspp | Pdal | Imin | Imic | Bspp | Peri | Snep | Squa | Tapp | Parc | Ekar |
|---|---|---|---|---|---|---|---|---|---|---|---|---|---|
| **824.5** | 0 | 0 | 0 | 0 | 0 | 0 | 0 | 0 | 0 | 0 | 0 | 0 | 0 |
| **828.5** | 0 | 0 | 0 | 0 | 1 | 0 | 0 | 1 | 0 | 0 | 0 | 0 | 0 |
| **832.5** | 0 | 0 | 0 | 0 | 57 | 0 | 26 | 5 | 0 | 0 | 0 | 0 | 0 |
| **836.5** | 0 | 0 | 0 | 0 | 31 | 0 | 44 | 6 | 0 | 0 | 0 | 0 | 0 |
| **840.5** | 0 | 0 | 0 | 0 | 18 | 0 | 47 | 0 | 0 | 0 | 0 | 0 | 0 |
| **844.5** | 0 | 0 | 0 | 0 | 3 | 0 | 30 | 0 | 0 | 0 | 0 | 0 | 0 |
| **848.5** | 0 | 0 | 0 | 0 | 5 | 0 | 38 | 0 | 0 | 0 | 0 | 0 | 0 |
| **852.5** | 0 | 0 | 0 | 0 | 3 | 0 | 40 | 0 | 0 | 0 | 0 | 0 | 0 |
| **856.5** | 0 | 0 | 0 | 0 | 0 | 0 | 17 | 0 | 0 | 0 | 0 | 0 | 0 |
| **860.5** | 0 | 0 | 0 | 0 | 0 | 0 | 5 | 0 | 0 | 1 | 0 | 0 | 0 |
| **864.5** | 0 | 0 | 0 | 0 | 7 | 0 | 11 | 3 | 0 | 0 | 0 | 0 | 0 |
| **870.5** | 0 | 0 | 0 | 0 | 0 | 0 | 0 | 0 | 0 | 0 | 0 | 0 | 0 |
| **874.5** | 0 | 0 | 0 | 0 | 0 | 0 | 0 | 0 | 0 | 0 | 0 | 0 | 0 |
| **878.5** | 0 | 0 | 0 | 0 | 0 | 0 | 0 | 0 | 0 | 0 | 0 | 0 | 0 |
| **882.5** | 0 | 0 | 0 | 0 | 0 | 0 | 0 | 1 | 0 | 0 | 0 | 0 | 0 |
| **886.5** | 0 | 0 | 0 | 0 | 1 | 0 | 1 | 5 | 0 | 0 | 0 | 0 | 0 |
| **890.5** | 0 | 0 | 0 | 0 | 0 | 0 | 0 | 0 | 0 | 0 | 0 | 0 | 0 |
| **894.5** | 0 | 0 | 0 | 0 | 0 | 0 | 0 | 2 | 0 | 0 | 0 | 0 | 0 |

Table B.4.Weight percent (%) ice rafted debris (IRD) for cores TWC04, TWC08 and TWC70.

| TWC04 depth (cm) | TWC04 IRD | TWC08 depth (cm) | TWC08 IRD | TWC70 depth (cm) | TWC70 IRD |
|---|---|---|---|---|---|
| 0.5 | 1.5816 | 0.5 | 7.145 | 0.5 | |
| 1.5 | 1.5976 | 2.5 | 7.986 | 3.5 | |
| 2.5 | 1.4706 | 4.5 | 8.2331 | 8.5 | |
| 3.5 | 0.8232 | 6.5 | 9.4831 | 12.5 | |
| 4.5 | 1.1689 | 8.5 | 8.753 | 16.5 | |
| 5.5 | 0.5271 | 10.5 | 11.2379 | 20.5 | |
| 6.5 | 1.0628 | 12.5 | 13.5078 | 24.5 | 0.0072 |
| 7.5 | 0.9735 | 14.5 | 24.6856 | 28.5 | 0.0148 |
| 8.5 | 0.8085 | 16.5 | 24.408 | 32.5 | 0.0194 |
| 9.5 | 0.7943 | 18.5 | 19.9808 | 35.5 | 0.0152 |
| 10.5 | 1.044 | 20.5 | 21.116 | 40.5 | 0.0085 |
| 11.5 | 0.9555 | 22.5 | 17.6818 | 44.5 | 0.0148 |
| 12.5 | 1.2629 | 24.5 | 29.7747 | 48.5 | 0.0142 |
| 13.5 | 0.9491 | 26.5 | 41.0117 | 52.5 | 0.036 |
| 14.5 | 1.0481 | 28.5 | 31.2997 | 57.5 | 0.0111 |
| 15.5 | 0.4251 | 30.5 | 33.6882 | 60.5 | 0.0148 |
| 16.5 | 0.9794 | 32.5 | 44.1428 | 64.5 | 0.0075 |
| 17.5 | 1.284 | 34.5 | 52.207 | 68.5 | 0.0088 |
| 18.5 | 0.8076 | 36.5 | 31.5592 | 72.5 | 0.0103 |
| 19.5 | 0.6507 | 38.5 | 13.6957 | 77.5 | 0.0153 |
| 20.5 | 1.2967 | 40.5 | 9.231 | 80.5 | 0.0166 |
| 21.5 | 0.9041 | 42.5 | 15.1725 | 84.5 | 0.0154 |
| 22.5 | 1.3861 | | | 88.5 | 0.0108 |
| 23.5 | 0.7952 | | | 92.5 | 0.0328 |
| 24.5 | 1.1126 | | | 96.5 | 0.0113 |
| 25.5 | 0.611 | | | 100.5 | 0.0114 |
| 26.5 | 1.4889 | | | 104.5 | 0.0104 |
| 27.5 | 0.7178 | | | 108.5 | 0.0158 |
| 28.5 | 1.6919 | | | 112.5 | 0.0125 |
| 29.5 | 0.8434 | | | 116.5 | 0.062 |
| 30.5 | 1.5906 | | | 120.5 | 0.0595 |
| 31.5 | 1.2076 | | | 124.5 | 0.0377 |
| 32.5 | 1.8122 | | | 128.5 | 0.0306 |
| 33.5 | 1.1295 | | | 132.5 | 0.1412 |
| 34.5 | 1.0917 | | | 136.5 | 0.0409 |
| 35.5 | 0.8832 | | | 140.5 | 0.0705 |
| 36.5 | 1.345 | | | 143.5 | 0.1963 |
| 37.5 | 0.9183 | | | 148.5 | 0.0404 |
| 38.5 | 0.9835 | | | 152.5 | 0.0577 |
| 39.5 | 1.104 | | | 156.5 | 0.027 |

| TWC04 depth (cm) | TWC04 IRD | TWC08 depth (cm) | TWC08 IRD | TWC70 depth (cm) | TWC70 IRD |
|---|---|---|---|---|---|
| 40.5 | 1.333 | | | 160.5 | 0.0364 |
| 41.5 | 1.0697 | | | 163.5 | 0.04 |
| 42.5 | 1.7704 | | | 168.5 | 0.0517 |
| 43.5 | 1.0756 | | | 172.5 | 0.1157 |
| 44.5 | 1.3849 | | | 176.5 | 0.0093 |
| 45.5 | 0.8441 | | | 180.5 | 0.0217 |
| 46.5 | 1.692 | | | 183.5 | 0.0202 |
| 47.5 | 1.2976 | | | 188.5 | 0.012 |
| 48.5 | 0.8842 | | | 192.5 | 0.0364 |
| 49.5 | 0.9484 | | | 196.5 | 0.0133 |
| 50.5 | 0.9783 | | | 200.5 | 0.0363 |
| 51.5 | 0.8681 | | | 203.5 | 0.036 |
| 52.5 | 0.8218 | | | 207.5 | 0.0363 |
| 53.5 | 0.5521 | | | | |
| 54.5 | 1.0556 | | | | |
| 55.5 | 0.8916 | | | | |
| 56.5 | 0.9333 | | | | |

Table B.5. Palynomorph concentrations for TWC04.

| Depth (cm) | Dinocysts $cm^{-3}$ | Pollen $cm^{-3}$ | Spores $cm^{-3}$ | Reworked palynomorphs $cm^{-3}$ | Organic linings $cm^{-3}$ |
|---|---|---|---|---|---|
| 0.5 | 7579 | 24 | 97 | 73 | 1628 |
| 1.5 | 10313 | 0 | 67 | 335 | 1272 |
| 2.5 | 8791 | 32 | 97 | 32 | 970 |
| 3.5 | 9408 | 0 | 29 | 348 | 523 |
| 4.5 | 6339 | 0 | 0 | 165 | 186 |
| 5.5 | 13462 | 41 | 41 | 165 | 785 |
| 6.5 | 10933 | 0 | 108 | 144 | 722 |
| 7.5 | 9069 | 0 | 119 | 149 | 743 |
| 8.5 | 6473 | 0 | 42 | 167 | 1148 |
| 9.5 | 8767 | 0 | 113 | 340 | 2865 |
| 10.5 | 9784 | 32 | 0 | 159 | 5559 |
| 11.5 | 7683 | 0 | 50 | 274 | 474 |
| 12.5 | 7316 | 0 | 0 | 140 | 1917 |
| 13.5 | 4340 | 0 | 14 | 113 | 679 |
| 14.5 | 10392 | 0 | 0 | 180 | 2309 |
| 15.5 | 5222 | 16 | 31 | 157 | 1349 |
| 16.5 | 8593 | 0 | 0 | 264 | 1529 |
| 17.5 | 3532 | 12 | 46 | 81 | 796 |
| 18.5 | 6755 | 0 | 0 | 70 | 1005 |
| 19.5 | 5656 | 0 | 32 | 226 | 1260 |
| 20.5 | 7503 | 0 | 70 | 93 | 1473 |
| 21.5 | 4822 | 0 | 14 | 72 | 660 |
| 22.5 | 7901 | 0 | 26 | 234 | 702 |
| 23.5 | 5805 | 0 | 0 | 96 | 192 |
| 24.5 | 4600 | 0 | 15 | 76 | 289 |
| 25.5 | 7796 | 0 | 0 | 113 | 363 |
| 26.5 | 4830 | 0 | 0 | 141 | 423 |
| 27.5 | 5705 | 0 | 0 | 156 | 328 |
| 28.5 | 5796 | 55 | 0 | 202 | 460 |
| 29.5 | 3833 | 0 | 12 | 163 | 267 |
| 30.5 | 6456 | 0 | 0 | 297 | 765 |
| 31.5 | 5238 | 0 | 0 | 225 | 985 |
| 32.5 | 5345 | 0 | 0 | 389 | 1664 |
| 33.5 | 5699 | 0 | 76 | 400 | 1048 |
| 34.5 | 6714 | 0 | 0 | 288 | 1127 |
| 35.5 | 5843 | 0 | 19 | 192 | 1130 |
| 36.5 | 5172 | 0 | 51 | 154 | 788 |
| 37.5 | 4318 | 0 | 27 | 147 | 735 |
| 38.5 | 4336 | 0 | 26 | 132 | 633 |
| 39.5 | 8503 | 0 | 28 | 582 | 1606 |
| 40.5 | 6849 | 0 | 0 | 251 | 835 |

| Depth (cm) | Dinocysts $cm^{-3}$ | Pollen $cm^{-3}$ | Spores $cm^{-3}$ | Reworked palynomorphs $cm^{-3}$ | Organic linings $cm^{-3}$ |
|---|---|---|---|---|---|
| 41.5 | 4307 | 0 | 55 | 384 | 631 |
| 42.5 | 6150 | 0 | 57 | 566 | 585 |
| 43.5 | 6761 | 0 | 40 | 534 | 850 |
| 44.5 | 5459 | 0 | 53 | 338 | 462 |
| 45.5 | 4678 | 0 | 42 | 269 | 692 |
| 46.5 | 5183 | 0 | 83 | 400 | 1000 |
| 47.5 | 4433 | 0 | 81 | 243 | 1230 |
| 48.5 | 4759 | 0 | 15 | 212 | 1027 |
| 49.5 | 3932 | 0 | 51 | 379 | 784 |
| 50.5 | 5210 | 0 | 16 | 159 | 1112 |
| 51.5 | 2540 | 0 | 64 | 136 | 207 |
| 52.5 | 3941 | 0 | 0 | 125 | 187 |
| 53.5 | 1712 | 0 | 43 | 144 | 32 |
| 54.5 | 3623 | 0 | 0 | 47 | 141 |
| 55.5 | 1751 | 0 | 11 | 164 | 238 |
| 56.5 | 3842 | 0 | 0 | 125 | 300 |

Table B.6. Core TWC04 carbon and oxygen stable isotopes (VPDB) ($\delta^{13}C$ and $\delta^{18}O$) of *Neogloboquadrina pachyderma* lef-coiled (Npl).

| Depth (cm) | $\delta^{13}C$ ‰ | $\delta^{18}O$ ‰ |
|---|---|---|
| 0.5 | 0.81 | 2.52 |
| 1.5 | 0.69 | 2.85 |
| 2.5 | 0.84 | 2.77 |
| 3.5 | 0.83 | 2.86 |
| 4.5 | 0.76 | 2.76 |
| 5.5 | 0.72 | 2.83 |
| 6.5 | 0.84 | 2.82 |
| 7.5 | 0.79 | 2.77 |
| 8.5 | 0.81 | 2.73 |
| 9.5 | 0.83 | 2.75 |
| 10.5 | 0.83 | 2.82 |
| 11.5 | 0.80 | 2.84 |
| 12.5 | 0.90 | 2.81 |
| 13.5 | 0.97 | 2.86 |
| 14.5 | 0.87 | 2.75 |
| 15.5 | 0.86 | 2.90 |
| 16.5 | 0.76 | 2.75 |
| 17.5 | 0.87 | 2.89 |
| 18.5 | 1.00 | 2.93 |
| 19.5 | 0.93 | 2.92 |
| 20.5 | 0.85 | 2.76 |
| 21.5 | 0.69 | 2.80 |
| 22.5 | 0.85 | 2.82 |
| 23.5 | 0.85 | 2.69 |
| 24.5 | 0.88 | 2.64 |
| 25.5 | 0.96 | 2.75 |
| 26.5 | 0.96 | 2.82 |
| 27.5 | 0.97 | 2.96 |
| 28.5 | 0.93 | 2.81 |
| 29.5 | 0.92 | 2.80 |
| 30.5 | 0.93 | 2.82 |
| 31.5 | 0.87 | 2.77 |
| 32.5 | 0.90 | 2.76 |
| 33.5 | 0.86 | 2.84 |
| 34.5 | 0.77 | 2.57 |
| 35.5 | 0.93 | 2.85 |

| Depth (cm) | $\delta^{13}C$ ‰ | $\delta^{18}O$ ‰ |
|---|---|---|
| 36.5 | 0.88 | 2.73 |
| 37.5 | 0.90 | 2.91 |
| 38.5 | 0.87 | 2.76 |
| 39.5 | 0.85 | 2.87 |
| 40.5 | 0.86 | 2.71 |
| 41.5 | 0.83 | 2.81 |
| 42.5 | 0.83 | 2.76 |
| 43.5 | 0.75 | 2.72 |
| 44.5 | 0.88 | 2.80 |
| 45.5 | 0.75 | 2.89 |
| 46.5 | 0.89 | 2.85 |
| 47.5 | 0.93 | 2.93 |
| 48.5 | 0.86 | 2.79 |
| 49.5 | 0.90 | 2.85 |
| 50.5 | 0.79 | 2.73 |
| 51.5 | 0.87 | 2.94 |
| 52.5 | 0.89 | 2.85 |
| 53.5 | 0.90 | 2.87 |
| 54.5 | 0.78 | 2.93 |
| 55.5 | 0.79 | 2.89 |
| 56.5 | 0.78 | 2.89 |

Table B.7.a. Core TWC04 dinocyst species assemblage, (Part A). Species acronyms are found in Appendix A. Note. This table has two parts (A and B) that are at the same depths but with different species.

| Depth (cm) | Iacu | Ipal | Ipar | Isph | Nlab | Ocen | Ocss | Oarc | Selo | Sram | Sspp |
|---|---|---|---|---|---|---|---|---|---|---|---|
| 0.5 | 0 | 1 | 0 | 1 | 160 | 77 | 0 | 0 | 3 | 5 | 0 |
| 1.5 | 0 | 3 | 0 | 4 | 186 | 84 | 2 | 0 | 1 | 1 | 3 |
| 2.5 | 0 | 0 | 0 | 3 | 150 | 46 | 0 | 14 | 0 | 3 | 3 |
| 3.5 | 0 | 0 | 1 | 5 | 157 | 120 | 1 | 2 | 2 | 2 | 3 |
| 4.5 | 0 | 0 | 0 | 0 | 184 | 78 | 0 | 0 | 2 | 3 | 0 |
| 5.5 | 0 | 1 | 0 | 5 | 172 | 100 | 2 | 0 | 3 | 2 | 0 |
| 6.5 | 0 | 0 | 0 | 4 | 145 | 97 | 0 | 0 | 2 | 3 | 0 |
| 7.5 | 0 | 4 | 1 | 6 | 166 | 99 | 0 | 2 | 2 | 0 | 3 |
| 8.5 | 2 | 1 | 0 | 4 | 135 | 70 | 0 | 20 | 1 | 8 | 1 |
| 9.5 | 0 | 1 | 0 | 9 | 158 | 76 | 1 | 1 | 0 | 0 | 4 |
| 10.5 | 0 | 1 | 0 | 4 | 146 | 50 | 0 | 10 | 0 | 3 | 3 |
| 11.5 | 0 | 1 | 0 | 1 | 152 | 104 | 0 | 3 | 1 | 0 | 2 |
| 12.5 | 1 | 3 | 0 | 6 | 147 | 64 | 0 | 29 | 1 | 5 | 1 |
| 13.5 | 0 | 1 | 2 | 3 | 148 | 95 | 0 | 2 | 4 | 3 | 1 |
| 14.5 | 2 | 1 | 0 | 1 | 160 | 58 | 0 | 11 | 1 | 4 | 3 |
| 15.5 | 0 | 1 | 0 | 1 | 178 | 93 | 0 | 0 | 2 | 3 | 4 |
| 16.5 | 1 | 1 | 0 | 3 | 161 | 91 | 0 | 13 | 3 | 6 | 4 |
| 17.5 | 1 | 0 | 0 | 1 | 192 | 74 | 0 | 1 | 0 | 0 | 2 |
| 18.5 | 0 | 5 | 0 | 4 | 133 | 79 | 0 | 12 | 1 | 4 | 1 |
| 19.5 | 0 | 4 | 0 | 5 | 164 | 123 | 0 | 3 | 4 | 2 | 3 |
| 20.5 | 0 | 3 | 0 | 7 | 147 | 103 | 0 | 5 | 0 | 5 | 3 |
| 21.5 | 0 | 3 | 0 | 2 | 109 | 160 | 1 | 5 | 1 | 7 | 4 |
| 22.5 | 0 | 2 | 0 | 5 | 101 | 145 | 0 | 10 | 4 | 2 | 0 |
| 23.5 | 0 | 0 | 0 | 1 | 62 | 208 | 0 | 7 | 1 | 2 | 2 |
| 24.5 | 0 | 1 | 0 | 4 | 76 | 142 | 0 | 38 | 0 | 1 | 2 |
| 25.5 | 0 | 2 | 2 | 8 | 81 | 207 | 0 | 4 | 1 | 2 | 0 |
| 26.5 | 1 | 0 | 0 | 1 | 56 | 157 | 0 | 40 | 3 | 2 | 1 |
| 27.5 | 1 | 0 | 0 | 5 | 59 | 214 | 0 | 3 | 3 | 1 | 3 |
| 28.5 | 0 | 0 | 0 | 3 | 51 | 179 | 0 | 37 | 1 | 1 | 2 |
| 29.5 | 0 | 4 | 0 | 4 | 58 | 203 | 2 | 7 | 3 | 2 | 1 |
| 30.5 | 0 | 3 | 0 | 4 | 48 | 195 | 0 | 6 | 5 | 3 | 3 |
| 31.5 | 1 | 0 | 0 | 7 | 54 | 187 | 0 | 4 | 6 | 3 | 4 |
| 32.5 | 0 | 1 | 0 | 6 | 64 | 180 | 0 | 5 | 4 | 5 | 3 |

| Depth (cm) | Iacu | Ipal | Ipar | Isph | Nlab | Ocen | Ocss | Oarc | Selo | Sram | Sspp |
|---|---|---|---|---|---|---|---|---|---|---|---|
| 33.5 | 0 | 1 | 0 | 1 | 42 | 217 | 0 | 0 | 5 | 2 | 0 |
| 34.5 | 0 | 0 | 0 | 9 | 39 | 179 | 0 | 6 | 8 | 5 | 4 |
| 35.5 | 0 | 1 | 0 | 1 | 61 | 206 | 0 | 0 | 9 | 2 | 3 |
| 36.5 | 1 | 1 | 0 | 7 | 59 | 184 | 0 | 7 | 11 | 2 | 2 |
| 37.5 | 0 | 1 | 0 | 6 | 60 | 212 | 1 | 2 | 6 | 2 | 5 |
| 38.5 | 1 | 0 | 0 | 3 | 62 | 200 | 2 | 6 | 4 | 2 | 1 |
| 39.5 | 0 | 0 | 0 | 5 | 55 | 178 | 2 | 4 | 10 | 3 | 3 |
| 40.5 | 0 | 1 | 0 | 8 | 33 | 216 | 1 | 9 | 7 | 4 | 3 |
| 41.5 | 0 | 0 | 0 | 4 | 42 | 178 | 0 | 3 | 8 | 1 | 6 |
| 42.5 | 0 | 0 | 1 | 4 | 47 | 220 | 5 | 1 | 8 | 0 | 6 |
| 43.5 | 0 | 2 | 1 | 3 | 47 | 207 | 1 | 3 | 12 | 3 | 4 |
| 44.5 | 1 | 0 | 1 | 7 | 26 | 224 | 3 | 4 | 6 | 3 | 11 |
| 45.5 | 3 | 1 | 1 | 3 | 36 | 179 | 2 | 4 | 4 | 2 | 3 |
| 46.5 | 0 | 1 | 3 | 4 | 28 | 181 | 2 | 5 | 12 | 1 | 5 |
| 47.5 | 0 | 2 | 0 | 6 | 29 | 137 | 2 | 2 | 2 | 3 | 4 |
| 48.5 | 0 | 3 | 1 | 5 | 33 | 174 | 1 | 5 | 9 | 3 | 4 |
| 49.5 | 1 | 2 | 0 | 4 | 16 | 163 | 1 | 5 | 12 | 5 | 4 |
| 50.5 | 0 | 2 | 0 | 9 | 48 | 148 | 0 | 8 | 9 | 2 | 5 |
| 51.5 | 2 | 4 | 0 | 9 | 57 | 146 | 1 | 5 | 22 | 6 | 9 |
| 52.5 | 4 | 1 | 0 | 8 | 27 | 80 | 0 | 3 | 7 | 0 | 4 |
| 53.5 | 1 | 3 | 0 | 8 | 71 | 106 | 0 | 2 | 2 | 2 | 6 |
| 54.5 | 5 | 0 | 0 | 4 | 52 | 58 | 0 | 5 | 3 | 1 | 5 |
| 55.5 | 2 | 3 | 0 | 2 | 45 | 99 | 0 | 2 | 16 | 4 | 4 |
| 56.5 | 0 | 0 | 0 | 1 | 37 | 93 | 0 | 4 | 3 | 1 | 2 |

Table B.7.b. Core TWC04 dinocyst species assemblage, (Part B). Species acronyms are found in Appendix A. Note. This table has two parts (A and B) that are at the same depths but with different species.

| Depth (cm) | Pdal | Imin | Imic | Bspp | Bcar | Bsim | Squa |
|---|---|---|---|---|---|---|---|
| 0.5 | 45 | 7 | 1 | 11 | 0 | 0 | 1 |
| 1.5 | 21 | 0 | 0 | 3 | 0 | 0 | 0 |
| 2.5 | 39 | 6 | 0 | 5 | 0 | 0 | 1 |
| 3.5 | 23 | 0 | 0 | 7 | 0 | 0 | 1 |
| 4.5 | 39 | 0 | 0 | 0 | 0 | 0 | 1 |
| 5.5 | 31 | 0 | 0 | 10 | 0 | 0 | 0 |
| 6.5 | 42 | 0 | 0 | 10 | 0 | 0 | 0 |
| 7.5 | 19 | 0 | 0 | 3 | 0 | 0 | 0 |
| 8.5 | 49 | 6 | 1 | 9 | 0 | 0 | 3 |
| 9.5 | 28 | 7 | 0 | 22 | 1 | 1 | 0 |
| 10.5 | 47 | 8 | 0 | 32 | 0 | 0 | 4 |
| 11.5 | 39 | 0 | 0 | 4 | 0 | 0 | 1 |
| 12.5 | 45 | 4 | 0 | 7 | 0 | 0 | 0 |
| 13.5 | 36 | 8 | 0 | 3 | 0 | 0 | 1 |
| 14.5 | 37 | 4 | 0 | 6 | 0 | 0 | 0 |
| 15.5 | 27 | 15 | 1 | 6 | 0 | 0 | 2 |
| 16.5 | 36 | 6 | 0 | 1 | 0 | 0 | 0 |
| 17.5 | 29 | 4 | 0 | 1 | 0 | 0 | 1 |
| 18.5 | 46 | 1 | 0 | 3 | 0 | 0 | 0 |
| 19.5 | 25 | 11 | 0 | 6 | 0 | 0 | 0 |
| 20.5 | 41 | 2 | 0 | 5 | 0 | 0 | 0 |
| 21.5 | 39 | 2 | 0 | 3 | 0 | 0 | 0 |
| 22.5 | 31 | 2 | 0 | 2 | 0 | 0 | 0 |
| 23.5 | 19 | 0 | 0 | 1 | 0 | 0 | 0 |
| 24.5 | 33 | 4 | 0 | 1 | 0 | 0 | 0 |
| 25.5 | 31 | 1 | 0 | 5 | 0 | 0 | 0 |
| 26.5 | 45 | 0 | 0 | 2 | 0 | 0 | 0 |
| 27.5 | 39 | 0 | 0 | 2 | 0 | 0 | 0 |
| 28.5 | 37 | 2 | 0 | 2 | 0 | 0 | 0 |
| 29.5 | 46 | 0 | 0 | 0 | 0 | 0 | 0 |
| 30.5 | 31 | 1 | 0 | 5 | 0 | 0 | 0 |
| 31.5 | 28 | 5 | 0 | 4 | 0 | 0 | 0 |
| 32.5 | 17 | 4 | 1 | 11 | 0 | 0 | 1 |

| Depth (cm) | Pdal | Imin | Imic | Bspp | Bcar | Bsim | Squa |
|---|---|---|---|---|---|---|---|
| 33.5 | 22 | 4 | 0 | 5 | 0 | 0 | 0 |
| 34.5 | 20 | 1 | 1 | 8 | 0 | 0 | 0 |
| 35.5 | 16 | 1 | 0 | 5 | 0 | 0 | 0 |
| 36.5 | 22 | 3 | 0 | 3 | 0 | 0 | 0 |
| 37.5 | 20 | 3 | 0 | 5 | 0 | 0 | 0 |
| 38.5 | 35 | 1 | 0 | 12 | 0 | 0 | 0 |
| 39.5 | 42 | 2 | 0 | 3 | 0 | 0 | 0 |
| 40.5 | 35 | 0 | 0 | 10 | 0 | 0 | 1 |
| 41.5 | 56 | 5 | 0 | 8 | 0 | 0 | 3 |
| 42.5 | 14 | 1 | 1 | 18 | 0 | 0 | 0 |
| 43.5 | 40 | 2 | 0 | 14 | 0 | 0 | 3 |
| 44.5 | 12 | 2 | 0 | 7 | 0 | 0 | 0 |
| 45.5 | 69 | 7 | 0 | 16 | 0 | 0 | 1 |
| 46.5 | 35 | 3 | 0 | 29 | 0 | 0 | 2 |
| 47.5 | 118 | 7 | 3 | 7 | 0 | 0 | 6 |
| 48.5 | 62 | 1 | 1 | 12 | 0 | 0 | 1 |
| 49.5 | 83 | 6 | 1 | 7 | 0 | 0 | 1 |
| 50.5 | 84 | 4 | 0 | 9 | 0 | 0 | 0 |
| 51.5 | 89 | 1 | 0 | 4 | 0 | 0 | 1 |
| 52.5 | 182 | 0 | 0 | 0 | 0 | 0 | 0 |
| 53.5 | 121 | 0 | 0 | 0 | 0 | 0 | 0 |
| 54.5 | 173 | 0 | 0 | 1 | 0 | 0 | 1 |
| 55.5 | 128 | 1 | 0 | 2 | 0 | 0 | 1 |
| 56.5 | 162 | 0 | 0 | 3 | 0 | 0 | 1 |

Table B.8. Palynomorph concentrations for core TWC08.

| Depth (cm) | Dinocysts $cm^{-3}$ | Pollen $cm^{-3}$ | Spores $cm^{-3}$ | Reworked palynomorphs $cm^{-3}$ | Organic linings $cm^{-3}$ |
|---|---|---|---|---|---|
| 0.5 | 9131 | 0 | 0 | 88 | 3951 |
| 1.5 | 5885 | 0 | 0 | 58 | 3543 |
| 2.5 | 9942 | 0 | 0 | 279 | 6380 |
| 3.5 | 5070 | 0 | 0 | 82 | 3048 |
| 4.5 | 8362 | 0 | 0 | 98 | 3937 |
| 5.5 | 4283 | 0 | 0 | 56 | 2972 |
| 6.5 | 7971 | 0 | 0 | 70 | 4161 |
| 7.5 | 9157 | 0 | 0 | 162 | 6240 |
| 8.5 | 8523 | 0 | 0 | 140 | 3074 |
| 9.5 | 8124 | 0 | 0 | 186 | 5257 |
| 10.5 | 7749 | 0 | 0 | 180 | 4482 |
| 11.5 | 7911 | 0 | 0 | 50 | 4018 |
| 12.5 | 6660 | 0 | 0 | 57 | 3339 |
| 13.5 | 7612 | 0 | 0 | 148 | 5363 |
| 14.5 | 6273 | 0 | 0 | 177 | 2674 |
| 15.5 | 6069 | 0 | 0 | 178 | 2807 |
| 16.5 | 6972 | 0 | 0 | 115 | 2078 |
| 17.5 | 5198 | 0 | 0 | 117 | 2473 |
| 18.5 | 7946 | 0 | 0 | 154 | 4562 |
| 19.5 | 6662 | 0 | 66 | 175 | 3594 |
| 20.5 | 9922 | 0 | 0 | 388 | 5850 |
| 21.5 | 3669 | 0 | 23 | 196 | 1495 |
| 22.5 | 7083 | 0 | 0 | 350 | 3891 |
| 23.5 | 3159 | 0 | 0 | 103 | 1301 |
| 24.5 | 3493 | 0 | 11 | 100 | 1161 |
| 25.5 | 2546 | 0 | 0 | 84 | 865 |
| 26.5 | 1975 | 0 | 0 | 132 | 1434 |
| 27.5 | 1858 | 0 | 0 | 131 | 542 |
| 28.5 | 1771 | 0 | 0 | 113 | 852 |
| 29.5 | 2559 | 0 | 0 | 143 | 1145 |
| 30.5 | 2410 | 0 | 31 | 101 | 1221 |
| 31.5 | 2227 | 0 | 0 | 200 | 910 |
| 32.5 | 1733 | 0 | 15 | 95 | 511 |
| 34.5 | 1256 | 0 | 8 | 70 | 811 |
| 36.5 | 199 | 0 | 0 | 93 | 497 |
| 38.5 | 311 | 0 | 0 | 212 | 661 |
| 40.5 | 482 | 0 | 0 | 367 | 955 |
| 42.5 | 452 | 0 | 0 | 192 | 738 |

Table B.9.a. Core TWC08 dinocyst species assemblage, (Part A). Species acronyms are found in Appendix A. Note. This table has two parts (A and B) that are at the same depths but with different species.

| Depth (cm) | Ipal | Ipat | Isph | Nlab | Ocen | Ocss | Oarc |
|---|---|---|---|---|---|---|---|
| 0.5 | 0 | 0 | 2 | 58 | 6 | 0 | 0 |
| 1.5 | 0 | 1 | 1 | 93 | 11 | 0 | 0 |
| 2.5 | 0 | 0 | 0 | 90 | 15 | 0 | 0 |
| 3.5 | 0 | 0 | 0 | 136 | 21 | 0 | 0 |
| 4.5 | 0 | 0 | 2 | 113 | 23 | 0 | 0 |
| 5.5 | 1 | 0 | 1 | 143 | 23 | 0 | 0 |
| 6.5 | 2 | 2 | 0 | 91 | 11 | 0 | 0 |
| 7.5 | 1 | 0 | 1 | 129 | 22 | 0 | 0 |
| 8.5 | 1 | 0 | 0 | 58 | 9 | 0 | 0 |
| 9.5 | 3 | 0 | 0 | 138 | 49 | 0 | 0 |
| 10.5 | 0 | 0 | 0 | 105 | 20 | 0 | 0 |
| 11.5 | 0 | 0 | 3 | 107 | 25 | 0 | 0 |
| 12.5 | 0 | 0 | 1 | 90 | 9 | 0 | 0 |
| 13.5 | 0 | 0 | 2 | 110 | 19 | 0 | 0 |
| 14.5 | 0 | 0 | 0 | 108 | 19 | 0 | 0 |
| 15.5 | 3 | 0 | 2 | 142 | 18 | 0 | 0 |
| 16.5 | 0 | 2 | 3 | 95 | 14 | 0 | 0 |
| 17.5 | 1 | 0 | 0 | 110 | 23 | 0 | 0 |
| 18.5 | 0 | 0 | 0 | 84 | 17 | 0 | 0 |
| 19.5 | 0 | 0 | 3 | 116 | 27 | 0 | 0 |
| 20.5 | 2 | 0 | 1 | 87 | 20 | 0 | 1 |
| 21.5 | 2 | 0 | 0 | 137 | 34 | 0 | 0 |
| 22.5 | 0 | 0 | 2 | 38 | 8 | 0 | 0 |
| 23.5 | 3 | 0 | 1 | 127 | 30 | 0 | 0 |
| 24.5 | 0 | 0 | 0 | 49 | 23 | 0 | 0 |
| 25.5 | 0 | 0 | 0 | 55 | 26 | 0 | 0 |
| 26.5 | 1 | 0 | 0 | 37 | 23 | 0 | 0 |
| 27.5 | 0 | 0 | 3 | 84 | 53 | 0 | 0 |
| 28.5 | 0 | 0 | 0 | 49 | 53 | 0 | 0 |
| 29.5 | 1 | 0 | 0 | 66 | 38 | 0 | 0 |
| 30.5 | 2 | 0 | 2 | 44 | 53 | 0 | 1 |
| 31.5 | 1 | 0 | 5 | 67 | 35 | 0 | 0 |
| 32.5 | 1 | 0 | 0 | 47 | 35 | 0 | 9 |
| 34.5 | 5 | 0 | 2 | 48 | 35 | 1 | 1 |
| 36.5 | 0 | 0 | 0 | 2 | 0 | 0 | 0 |
| 38.5 | 0 | 0 | 0 | 0 | 0 | 0 | 0 |
| 40.5 | 0 | 0 | 0 | 0 | 1 | 0 | 0 |
| 42.5 | 0 | 0 | 0 | 1 | 5 | 0 | 0 |

Table B.9.b. Core TWC08 dinocyst species assemblage, (Part B). Species acronyms are found in Appendix A. Note. This table has two parts (A and B) that are at the same depths but with different species.

| Depth (cm) | Selo | Sram | Sspp | Pdal | Imin | Imic | Bspp | Squa | Tapp |
|---|---|---|---|---|---|---|---|---|---|
| 0.5 | 1 | 0 | 1 | 5 | 177 | 1 | 61 | 0 | 0 |
| 1.5 | 1 | 0 | 2 | 30 | 80 | 4 | 74 | 7 | 0 |
| 2.5 | 0 | 0 | 0 | 24 | 147 | 0 | 43 | 2 | 0 |
| 3.5 | 1 | 0 | 1 | 23 | 37 | 0 | 87 | 5 | 0 |
| 4.5 | 1 | 0 | 1 | 18 | 133 | 9 | 39 | 3 | 0 |
| 5.5 | 1 | 0 | 0 | 33 | 41 | 0 | 60 | 4 | 0 |
| 6.5 | 0 | 2 | 2 | 14 | 156 | 4 | 52 | 5 | 0 |
| 7.5 | 0 | 0 | 0 | 72 | 46 | 1 | 64 | 3 | 0 |
| 8.5 | 0 | 0 | 0 | 5 | 159 | 3 | 67 | 3 | 0 |
| 9.5 | 0 | 0 | 2 | 45 | 14 | 0 | 49 | 6 | 0 |
| 10.5 | 1 | 0 | 2 | 24 | 134 | 7 | 49 | 2 | 0 |
| 11.5 | 2 | 0 | 1 | 42 | 82 | 2 | 50 | 1 | 0 |
| 12.5 | 0 | 0 | 0 | 19 | 153 | 4 | 74 | 3 | 0 |
| 13.5 | 3 | 0 | 1 | 33 | 87 | 6 | 45 | 2 | 0 |
| 14.5 | 0 | 0 | 0 | 21 | 123 | 0 | 47 | 1 | 0 |
| 15.5 | 2 | 0 | 0 | 53 | 29 | 1 | 57 | 0 | 0 |
| 16.5 | 0 | 1 | 1 | 12 | 102 | 3 | 68 | 1 | 0 |
| 17.5 | 1 | 0 | 1 | 58 | 42 | 9 | 63 | 3 | 0 |
| 18.5 | 2 | 0 | 0 | 26 | 130 | 4 | 45 | 2 | 0 |
| 19.5 | 1 | 0 | 0 | 57 | 41 | 4 | 52 | 3 | 0 |
| 20.5 | 2 | 0 | 0 | 39 | 124 | 0 | 30 | 1 | 0 |
| 21.5 | 0 | 0 | 0 | 60 | 28 | 2 | 56 | 0 | 0 |
| 22.5 | 0 | 0 | 0 | 13 | 61 | 2 | 38 | 0 | 0 |
| 23.5 | 1 | 0 | 0 | 40 | 60 | 2 | 37 | 4 | 1 |
| 24.5 | 1 | 0 | 1 | 13 | 129 | 4 | 81 | 12 | 0 |
| 25.5 | 3 | 0 | 0 | 50 | 81 | 6 | 76 | 6 | 0 |
| 26.5 | 1 | 1 | 1 | 38 | 120 | 11 | 34 | 3 | 0 |
| 27.5 | 5 | 2 | 2 | 69 | 28 | 0 | 55 | 11 | 0 |
| 28.5 | 4 | 1 | 1 | 53 | 116 | 0 | 33 | 4 | 0 |
| 29.5 | 4 | 0 | 1 | 91 | 44 | 8 | 41 | 10 | 0 |
| 30.5 | 1 | 0 | 0 | 53 | 108 | 2 | 34 | 10 | 0 |
| 31.5 | 7 | 0 | 2 | 87 | 37 | 3 | 48 | 9 | 0 |
| 32.5 | 7 | 1 | 1 | 49 | 135 | 7 | 43 | 11 | 0 |
| 34.5 | 1 | 1 | 3 | 20 | 126 | 4 | 69 | 6 | 0 |
| 36.5 | 0 | 0 | 0 | 1 | 12 | 1 | 12 | 2 | 0 |
| 38.5 | 0 | 0 | 0 | 0 | 17 | 0 | 55 | 0 | 0 |
| 40.5 | 0 | 0 | 0 | 1 | 44 | 0 | 66 | 1 | 0 |
| 42.5 | 0 | 0 | 0 | 1 | 35 | 0 | 81 | 2 | 0 |

Table B.10. Palynomoprh concentrations for core TWC70.

| Depth (cm) | Dinocysts $cm^{-3}$ | Pollen $cm^{-3}$ | Spores $cm^{-3}$ | Reworked palynomorphs $cm^{-3}$ | Organic linings $cm^{-3}$ |
|---|---|---|---|---|---|
| 0.5 | 37277 | 0 | 221 | 1106 | 23339 |
| 3.5 | 44487 | 0 | 141 | 704 | 29282 |
| 8.5 | 37514 | 0 | 232 | 1510 | 19861 |
| 12.5 | 30912 | 0 | 268 | 625 | 15456 |
| 16.5 | 34286 | 0 | 279 | 1115 | 11800 |
| 20.5 | 24977 | 0 | 0 | 2997 | 11789 |
| 24.5 | 24003 | 0 | 211 | 282 | 12389 |
| 28.5 | 37520 | 0 | 0 | 472 | 8849 |
| 32.5 | 15244 | 0 | 0 | 581 | 2952 |
| 35.5 | 27255 | 0 | 0 | 826 | 6194 |
| 40.5 | 35204 | 0 | 0 | 1239 | 10634 |
| 44.5 | 39243 | 0 | 0 | 984 | 9947 |
| 48.5 | 45150 | 0 | 138 | 826 | 9498 |
| 52.5 | 30124 | 0 | 98 | 880 | 8216 |
| 57.5 | 29098 | 0 | 181 | 453 | 10878 |
| 60.5 | 22435 | 0 | 0 | 405 | 4865 |
| 64.5 | 25594 | 0 | 169 | 591 | 5659 |
| 68.5 | 22966 | 0 | 72 | 869 | 4999 |
| 72.5 | 30306 | 0 | 0 | 477 | 9816 |
| 77.5 | 26018 | 0 | 0 | 578 | 11481 |
| 80.5 | 29406 | 0 | 183 | 457 | 8402 |
| 84.5 | 40782 | 0 | 0 | 1032 | 14841 |
| 88.5 | 22873 | 0 | 71 | 1215 | 8291 |
| 92.5 | 18860 | 0 | 184 | 307 | 5099 |
| 96.5 | 31842 | 0 | 614 | 512 | 8088 |
| 100.5 | 11702 | 0 | 37 | 74 | 2355 |
| 104.5 | 45753 | 0 | 384 | 769 | 5639 |
| 108.5 | 56024 | 0 | 138 | 413 | 6332 |
| 112.5 | 46526 | 0 | 0 | 275 | 7296 |
| 116.5 | 25030 | 0 | 228 | 531 | 3565 |
| 120.5 | 14051 | 0 | 45 | 91 | 4079 |
| 124.5 | 24468 | 0 | 77 | 155 | 4723 |
| 128.5 | 30618 | 0 | 177 | 265 | 7876 |
| 132.5 | 56932 | 0 | 0 | 507 | 12332 |
| 136.5 | 30559 | 0 | 83 | 248 | 5534 |
| 140.5 | 38125 | 0 | 240 | 360 | 9112 |
| 143.5 | 26347 | 0 | 83 | 330 | 4212 |
| 148.5 | 21659 | 0 | 64 | 256 | 6792 |
| 152.5 | 17763 | 0 | 55 | 273 | 7269 |

| Depth (cm) | Dinocysts $cm^{-3}$ | Pollen $cm^{-3}$ | Spores $cm^{-3}$ | Reworked palynomorphs $cm^{-3}$ | Organic linings $cm^{-3}$ |
|---|---|---|---|---|---|
| 156.5 | 12416 | 0 | 0 | 244 | 7694 |
| 160.5 | 15783 | 0 | 0 | 305 | 10844 |
| 163.5 | 17344 | 0 | 0 | 310 | 9911 |
| 168.5 | 11081 | 0 | 0 | 241 | 4921 |
| 172.5 | 6462 | 0 | 0 | 190 | 3358 |
| 176.5 | 13049 | 0 | 0 | 124 | 6731 |
| 180.5 | 10026 | 0 | 0 | 160 | 5779 |
| 183.5 | 9682 | 0 | 0 | 250 | 6309 |
| 188.5 | 6063 | 0 | 19 | 450 | 5162 |
| 192.5 | 8997 | 0 | 0 | 560 | 6283 |
| 196.5 | 8048 | 0 | 23 | 305 | 6359 |
| 200.5 | 5969 | 0 | 0 | 282 | 5800 |
| 203.5 | 8709 | 0 | 0 | 361 | 8848 |
| 207.5 | 5193 | 0 | 17 | 183 | 5243 |

Table B.11.a. Core TWC70 dinocyst species assemblage, (Part A). Species acronyms are found in Appendix A. Note. This table has two parts (A and B) that are at the same depths but with different species.

| Depth (cm) | Ipal | Isph | Nlab | Ocen | Ocss | Oarc | Selo | Sram |
|---|---|---|---|---|---|---|---|---|
| 0.5 | 3 | 2 | 13 | 152 | 0 | 0 | 12 | 0 |
| 3.5 | 2 | 0 | 10 | 194 | 0 | 0 | 19 | 0 |
| 8.5 | 0 | 0 | 17 | 182 | 0 | 10 | 10 | 0 |
| 12.5 | 1 | 1 | 17 | 209 | 2 | 2 | 13 | 0 |
| 16.5 | 0 | 1 | 20 | 258 | 1 | 2 | 17 | 0 |
| 20.5 | 2 | 0 | 6 | 60 | 0 | 1 | 4 | 0 |
| 24.5 | 0 | 0 | 6 | 123 | 1 | 5 | 14 | 0 |
| 28.5 | 0 | 0 | 10 | 177 | 0 | 0 | 17 | 0 |
| 32.5 | 0 | 0 | 11 | 186 | 1 | 2 | 19 | 0 |
| 35.5 | 0 | 0 | 7 | 213 | 0 | 1 | 32 | 0 |
| 40.5 | 0 | 0 | 7 | 238 | 1 | 2 | 30 | 0 |
| 44.5 | 1 | 0 | 8 | 234 | 1 | 2 | 34 | 0 |
| 48.5 | 0 | 0 | 4 | 194 | 1 | 0 | 21 | 1 |
| 52.5 | 0 | 0 | 2 | 160 | 0 | 1 | 16 | 0 |
| 57.5 | 0 | 1 | 3 | 231 | 0 | 1 | 18 | 0 |
| 60.5 | 0 | 0 | 11 | 223 | 0 | 2 | 39 | 0 |
| 64.5 | 1 | 0 | 9 | 211 | 0 | 0 | 19 | 0 |
| 68.5 | 0 | 0 | 9 | 218 | 0 | 0 | 20 | 0 |
| 72.5 | 1 | 0 | 4 | 181 | 0 | 0 | 12 | 1 |
| 77.5 | 1 | 0 | 8 | 179 | 0 | 0 | 30 | 1 |
| 80.5 | 0 | 0 | 8 | 208 | 0 | 0 | 19 | 0 |
| 84.5 | 1 | 0 | 12 | 198 | 0 | 0 | 9 | 1 |
| 88.5 | 1 | 1 | 14 | 218 | 2 | 1 | 15 | 0 |
| 92.5 | 0 | 0 | 7 | 193 | 0 | 0 | 30 | 0 |
| 96.5 | 0 | 0 | 7 | 128 | 0 | 2 | 19 | 0 |
| 100.5 | 2 | 0 | 0 | 203 | 0 | 1 | 41 | 0 |
| 104.5 | 4 | 0 | 6 | 234 | 1 | 6 | 26 | 0 |
| 108.5 | 1 | 0 | 5 | 288 | 2 | 1 | 39 | 0 |
| 112.5 | 2 | 0 | 4 | 245 | 2 | 3 | 29 | 0 |
| 116.5 | 1 | 0 | 3 | 244 | 1 | 2 | 29 | 0 |
| 120.5 | 1 | 0 | 7 | 184 | 1 | 5 | 33 | 0 |
| 124.5 | 0 | 1 | 7 | 230 | 3 | 1 | 29 | 0 |
| 128.5 | 1 | 1 | 4 | 254 | 1 | 1 | 22 | 0 |
| 132.5 | 3 | 0 | 5 | 243 | 2 | 3 | 23 | 0 |
| 136.5 | 0 | 0 | 7 | 251 | 1 | 2 | 38 | 0 |
| 140.5 | 3 | 0 | 5 | 216 | 1 | 1 | 32 | 0 |
| 143.5 | 0 | 0 | 4 | 235 | 2 | 7 | 22 | 0 |

| Depth (cm) | Ipal | Isph | Nlab | Ocen | Ocss | Oarc | Selo | Sram |
|---|---|---|---|---|---|---|---|---|
| 148.5 | 2 | 0 | 4 | 203 | 1 | 2 | 23 | 0 |
| 152.5 | 0 | 1 | 2 | 191 | 0 | 2 | 26 | 0 |
| 156.5 | 2 | | 1 | 6 | | | 5 | |
| 160.5 | 2 | | 3 | 15 | | | | |
| 163.5 | 2 | 1 | | 10 | | | 6 | |
| 168.5 | | | | 10 | | 1 | 2 | |
| 172.5 | | | | 5 | | | | |
| 176.5 | 1 | | | 4 | | | 2 | |
| 180.5 | | | | 8 | | | 1 | |
| 183.5 | 2 | | | 15 | | | | |
| 188.5 | 1 | 1 | | 6 | | | 1 | |
| 192.5 | | | | | | | 1 | |
| 196.5 | 1 | | | 6 | | | 4 | |
| 200.5 | 2 | | 1 | 6 | | | 5 | |
| 203.5 | 1 | | 1 | 8 | | | 4 | |
| 207.5 | 1 | | 1 | 19 | | | 3 | |

Table B.11.b. Core TWC70 dinocyst species assemblage, (Part B). Species acronyms are found in Appendix A. Note. This table has two parts (A and B) that are at the same depths but with different species.

| Depth (cm) | Sspp | Pdal | Imin | Imic | Bspp | Bsim | Squa |
|---|---|---|---|---|---|---|---|
| 0.5 | 8 | 56 | 57 | 0 | 34 | 0 | 0 |
| 3.5 | 10 | 22 | 36 | 1 | 21 | 0 | 1 |
| 8.5 | 7 | 61 | 11 | 0 | 21 | 3 | 1 |
| 12.5 | 6 | 55 | 26 | 2 | 12 | 0 | 0 |
| 16.5 | 7 | 32 | 20 | 0 | 11 | 0 | 0 |
| 20.5 | 6 | 6 | 23 | 1 | 15 | 0 | 1 |
| 24.5 | 12 | 38 | 111 | 2 | 28 | 0 | 1 |
| 28.5 | 6 | 23 | 65 | 1 | 18 | 0 | 1 |
| 32.5 | 13 | 21 | 35 | 0 | 26 | 0 | 1 |
| 35.5 | 7 | 21 | 30 | 0 | 19 | 0 | 0 |
| 40.5 | 12 | 10 | 17 | 0 | 24 | 0 | 0 |
| 44.5 | 12 | 8 | 34 | 0 | 24 | 0 | 1 |
| 48.5 | 3 | 4 | 67 | 0 | 32 | 0 | 1 |
| 52.5 | 6 | 0 | 86 | 0 | 36 | 0 | 1 |
| 57.5 | 1 | 7 | 38 | 0 | 21 | 0 | 0 |
| 60.5 | 1 | 2 | 20 | 0 | 34 | 0 | 0 |
| 64.5 | 2 | 7 | 24 | 0 | 30 | 0 | 0 |
| 68.5 | 0 | 3 | 23 | 0 | 44 | 0 | 0 |
| 72.5 | 7 | 1 | 70 | 0 | 41 | 0 | 0 |

| Depth (cm) | Sspp | Pdal | Imin | Imic | Bspp | Bsim | Squa |
|---|---|---|---|---|---|---|---|
| 77.5 | 5 | 1 | 57 | 0 | 33 | 0 | 0 |
| 80.5 | 2 | 4 | 28 | 0 | 53 | 0 | 0 |
| 84.5 | 3 | 7 | 31 | 0 | 53 | 0 | 1 |
| 88.5 | 2 | 9 | 17 | 0 | 40 | 0 | 0 |
| 92.5 | 5 | 2 | 28 | 0 | 41 | 0 | 1 |
| 96.5 | 4 | 8 | 112 | 0 | 31 | 0 | 0 |
| 100.5 | 2 | 6 | 43 | 0 | 20 | 0 | 0 |
| 104.5 | 2 | 8 | 50 | 0 | 20 | 0 | 0 |
| 108.5 | 1 | 8 | 30 | 0 | 31 | 0 | 1 |
| 112.5 | 3 | 6 | 14 | 0 | 30 | 0 | 0 |
| 116.5 | 4 | 4 | 13 | 0 | 29 | 0 | 0 |
| 120.5 | 1 | 4 | 21 | 0 | 53 | 0 | 0 |
| 124.5 | 3 | 2 | 19 | 0 | 20 | 0 | 1 |
| 128.5 | 1 | 2 | 11 | 1 | 47 | 0 | 0 |
| 132.5 | 4 | 2 | 10 | 0 | 41 | 0 | 1 |
| 136.5 | 2 | 5 | 9 | 0 | 55 | 0 | 0 |
| 140.5 | 2 | 5 | 13 | 0 | 40 | 0 | 0 |
| 143.5 | 1 | 10 | 12 | 0 | 23 | 0 | 3 |
| 148.5 | 2 | 10 | 31 | 0 | 60 | 0 | 0 |
| 152.5 | 1 | 2 | 24 | | 75 | | 1 |
| 156.5 | | 2 | 50 | | 239 | | |
| 160.5 | | 1 | 52 | | 237 | | |
| 163.5 | | 7 | 51 | | 259 | | |
| 168.5 | | 2 | 105 | | 201 | | 1 |
| 172.5 | | | 70 | | 230 | | 1 |
| 176.5 | | | 100 | | 208 | | 1 |
| 180.5 | | 3 | 134 | | 166 | | 2 |
| 183.5 | 1 | 3 | 86 | | 203 | | |
| 188.5 | 1 | 3 | 76 | | 233 | | 1 |
| 192.5 | 1 | 2 | 168 | | 133 | | |
| 196.5 | 1 | 4 | 196 | | 130 | | 1 |
| 200.5 | 1 | 6 | 161 | | 135 | | 1 |
| 203.5 | | 3 | 176 | | 121 | | |
| 207.5 | | 2 | 120 | | 167 | | |

# REFERENCES

Aksenov, Y., Bacon, S., Coward, A.C., Holliday, N.P., 2010. Polar outflow from the Arctic Ocean: A high resolution model study. Journal of Marine Systems 83 (1), 14-37.

Aksu, A.E., Piper, D.J.W., 1979. Baffin Bay in the past 100,000 yr. Geology 7, 245-248.

Aksu, A.E., 1981. Late Quaternary stratigraphy, paleoenvironments and sedimentation history of Baffin Bay and Davis Strait. Ph.D. thesis, Dalhousie University, Halifax, N.S.

Aksu, A.E., 1983. Holocene and Pleistocene dissolution cycles in deepsea cores of Baffin Bay and Davis Strait: paleoceanographic implications. Marine Geology 53, 331-348.

Aksu, A.E., Mudie, P.J., 1985. Late Quaternary stratigraphy and paleoecology of northwest Labrador Sea. Marine Micropaleontology 9 (6), 537-557.

Aksu, A.E., Vilks, G., 1988. Stable isotopes in planktonic and benthic foraminifera from Arctic Ocean surface sediments. Canadian Journal of Earth Sciences 25 (5), 701-709.

Andersen, C., Koc, N., Moros, M., 2004. A highly unstable Holocene climate in the subpolar North Atlantic: evidence from diatoms. Quaternary Science Reviews 23, 2155-2166.

Andresen, C.S., McCarthy, D.J., Dylmer, C.V., Seidenkrantz, M.S., Kuijpers, A., Lloyd, J.M., 2011. Interaction between subsurface ocean waters and calving of the Jakobshavn Isbræ during the late Holocene. The Holocene 21 (2), 211-224.

Andrews, J.T., 1972. Recent and fossil growth rates of marine bivalves, Canadian Arctic, and Late-Quaternary Arctic marine environments. Palaeogeography, Palaeoclimatology, Palaeoecology 11 (3), 157-176.

Andrews, J.T., Ives, J.D., 1978. Cockburn'' nomenclature and the Late Quaternary history of the eastern Canadian Arctic. Arctic Alpine Research 10, 617-633.

Andrews, J.T., Tedesco, K., 1992. Detrital carbonate-rich sediments, northwestern Labrador Sea: implications for ice-sheet dynamics and iceberg rafting (Heinrich) events in the North Atlantic. Geology 20 (12), 1087-1090.

Andrews, J.T., Erlenkeuser, H., Tedesco, K., Aksu, A.E., Jull, A.J., 1994a. Late Quaternary (stage 2 and 3) meltwater and Heinrich events, northwest Labrador Sea. Quaternary Research 41 (1), 26-34.

Andrews, J.T., Tedesco, K., Briggs, W.M., Evans, L.W., 1994b. Sediments, sedimentation rates, and environments, southeast Baffin Shelf and northwest Labrador Sea, 8 - 26 ka. Canadian Journal of Earth Sciences 31 (1), 90-103.

Andrews, J.T., Jennings, A.E., Kerwin, M., Kirby, M., Manley, W., Miller, G.H., Bond, G., MacLean, B., 1995. A Heinrich-like event, H-0 (DC-0): Source(s) for detrital carbonate in the North Atlantic during the Younger Dryas chronozone. Paleoceanography 10 (5), 943-952.

Andrews, J.T., Jennings, A.E., Kerwin, M., Kirby, M., Manley, W., Miller, G.H., Bond, G., MacLean, B., 1995a. A Heinrich-like event, H-0 (DC-0): Source (s) for detrital carbonate in the North Atlantic during the Younger Dryas Chronozone. Paleoceanography 10(5), 943-952.

Andrews, J.T., MacLean, B., Kerwin, M., Manley, W., Jennings, A.E., Hall, F., 1995b. Final stages in the collapse of the Laurentide Ice Sheet, Hudson Strait, Canada, NWT: 14 C AMS dates, seismics stratigraphy, and magnetic susceptibility logs. Quaternary Science Reviews 14(10), 983-1004.

Andrews, J.T., Kirby, M.E., Aksu, A., Barber, D.C., Meese, D., 1998. Late Quaternary detrital carbonate (dc-) layers in Baffin Bay marine sediments (67°–74° n): correlation with Heinrich Events in the North Atlantic? Quaternary Science Reviews 17 (12), 1125-1137.

Andrews, J.T., Keigwin, L., Hall, F., Jennings, A.E., 1999. Abrupt deglaciation events and Holocene palaeoceanography from high-resolution cores, Cartwright Saddle, Labrador Shelf, Canada. Journal of Quaternary Science 14 (5), 383-397.

Andrews, J.T., Barber, D.C., Jennings, A.E., Eberl, D.D., Maclean, B., Kirby, M.E., Stoner, J.S., 2012. Varying sediment sources (Hudson Strait, Cumberland Sound, Baffin Bay) to the NW Labrador Sea slope between and during Heinrich events 0 to 4. Journal of Quaternary Science 27, 475-484.

Andrews, J.T., Gibb, O.T., Jennings, A.E., Simon, Q., 2014. Variations in the provenance of sediment from ice sheets surrounding Baffin Bay during MIS 2 and 3 and export to the Labrador Shelf Sea: site HU2008029-0008 Davis Strait. Journal of Quaternary Science, 29(1), 3-13.

Arthur, M.A., Srivastava, S.P., Kaminski, M., Jarrard, R., Osler, J., 1989. Seismic stratigraphy and history of deep circulation and sediment drift development in Baffin Bay and the Labrador Sea. *In*: Srivastava, S. P., Arthur, M., Clement, B., et al., (eds), Proceedings of the Ocean Drilling Program, Scientific Results, Vol. 105. Ocean Drilling Program, College Station, TX.

Azetsu-Scott, K., Clarke, A., Falkner, K., Hamilton, J., Jones, E.P., Lee, C., Petrie, B., Prinsenberg, S., Starr, M., Yeats, P., 2010. Calcium carbonate saturation states in the waters of the Canadian Arctic Archipelago and the Labrador Sea. Journal of Geophysical Research: Oceans 115 (C11).

Baldauf, J.G., et al., 1989. Magnetostratigraphic and biostratigraphic synthesis of ocean drilling program Leg 105: Labrador Sea and Baffin Bay. *In*: Srivastava, S. P., Arthur, M., Clement, B., et al., (eds), Proceedings of the Ocean Drilling Program, Scientific Results, Vol. 105. Ocean Drilling Program, College Station, TX.

Barber, D.C., Dyke, A., Hillaire-Marcel, C., Jennings, A.E., Andrews, J.T., Kerwin, M.W., Bilodeau, G., McNeely, R., Southon, J., Morehead, M.D., Gagnonk, J.-M., 1999. Forcing of the cold event of 8,200 years ago by catastrophic drainage of Laurentide lakes. Nature 400 (6742), 344-348.

Bard, E., 2001. Paleoceanographic implications of the difference in deep-sea sediment mixing between large and fine particles. Paleoceanography 16 (3), 235-239.

Barras, C., Duplessy, J.C., Geslin, E., Michel, E., Jorissen, F.J., 2010. Calibration of $\delta^{18}O$ of laboratory-cultured deep-sea benthic foraminiferal shells in function of temperature. Biogeosciences Discussions 7 (1), 335-350.

Bauch, D., Carstens, J., Wefer, G. 1997. Oxygen isotope composition of living Neogloboquadrina pachyderma (sin.) in the Arctic Ocean. Earth and Planetary Science Letters 146 (1), 47-58.

Bauch, H.A., Erlenkeuser, H., Spielhagen, R.F., Struck,U., Matthiessen, J., Thiede, J., Heinemeier, J., 2001. A multiproxy reconstruction of the evolution of deep and surface waters in the subarctic Nordic seas over the last 30,000 yr. Quaternary Science Reviews 20 (4), 659-678.

Bé, A.W.H., Tolderlund, D.S., 1971. Distribution and ecology of planktonic foraminifera. In: Funnell, B.M., Riedel, W.R., (eds), The micropaleontology of oceans. Cambridge University Press, London.

Belkin, I.M., Cornillon, P.C., Sherman, K., 2009. Fronts in large marine ecosystems. Progress in Oceanography 81(1), 223-236.

Bennike, O., 2004. Holocene sea-ice variations in Greenland: onshore evidence. The Holocene 14(4), 607-613.

Bergami, C., Capotondi, L., Langone, L., Giglio, F., Ravaioli, M., 2009. Distribution of living planktonic foraminifera in the Ross Sea and the Pacific sector of the Southern Ocean (Antarctica). Marine Micropaleontology 73 (1), 37-48.

Berger, A.L., Loutre, M.F., 1991. Insolation values for the climate of the last 10 million years. Quaternary Science Reviews 10 (4), 297-317.

Berger, W.H., Johnson, R.F., 1978. On the thickness and the $^{14}C$ age of the mixed layer in deep sea carbonates. Earth and Planetary Science Letters 41 (2), 223-227.

Bilodeau, G., de Vernal, A., Hillaire-Marcel, C., 1994. Benthic foraminiferal assemblages in Labrador Sea sediments: relations with deep-water mass changes since deglaciation. Canadian Journal of Earth Sciences 31 (1), 128-138.

Boessenkool, K.P., Van Gelder, M.J., Brinkhuis, H., Troelstra, S.R. 2001. Distribution of organic-walled dinoflagellate cysts in surface sediments from transects across the Polar Front offshore southeast Greenland. Journal of Quaternary Science 16(7), 661-666.

Bond, G., Heinrich, H., Broecker, W., Labeyrie, L., McManus, J., Andrews, J., Huon, S., Jantschik, R., Clasen, S., Simet C., 1992. Evidence for massive discharges of icebergs into the North Atlantic Ocean during the last glacial period. Nature 360, 245-249.

Bonnet, S., de Vernal, A., Hillaire-Marcel, C., Radi, T., Husum, K., 2010. Variability of sea-surface temperature and sea-ice cover in the Fram Strait over the last two millennia. Marine Micropaleontology 74, 59-74.

Bourke, R.H., Addison,V.G., Paquette, R.G., 1989. Oceanography of Nares Strait and northern Baffin Bay in 1986 with emphasis on deep and bottom water formation, Journal of Geophysical Research, 94, 8289– 8302.

Briner, J.P., Miller, G.H., Davis, P.T., Bierman, P.R., Caffee, M., 2003. Last Glacial Maximum ice sheet dynamics in Arctic Canada inferred from young erratics perched on ancient tors. Quaternary Science Reviews 22, 437-444.

Briner, J.P., Miller, G.H., Davis, P.T., Finkel, R.C., 2006. Cosmogenic radionuclides

from fiord landscapes support differential erosion by overriding ice sheets. Geological Society of America Bulletin 118, 406–420.

Briner, J.P., Michelutti, N., Francis, D.R., Miller, G.H., Axford, Y., Wooller, M.J., Wolfe, A.P., 2006. A multi-proxy lacustrine record of Holocene climate change on northeastern Baffin Island, Arctic Canada. Quaternary Research 65(3), 431-442.

Briner, J.P., Davis, P.T., Miller, G.H., 2009. Latest Pleistocene and Holocene glaciation of Baffin Island, Arctic Canada: key patterns and chronologies. Quaternary Science Reviews 28(21), 2075-2087.

Briner, J.P., Stewart, H.A.M., Young, N.E., Philipps, W., Losee, S., 2010. Using proglacial-threshold lakes to constrain fluctuations of the Jakobshavn Isbræ ice margin, western Greenland, during the Holocene. Quaternary Science Reviews 29(27), 3861-3874.

Broecker, W.S., Bond, G., Klas, M., Clark, E., McManus, J., 1992. Origin of the northern Atlantic's Heinrich events. Climate Dynamics 6, 265-273.

Bronk Ramsey, C., 2008. Deposition models for chronological records. Quaternary Science Reviews 27(1), 42-60.

Buch, E., (1990/2000). A monograph on the Physical Oceanography of the Greenland Waters. Greenland Fisheries Research Institute Report, (reissued in 2000 as Danish Meteorological Institute, Scientific report, 00-12), 405 pp.

Campbell, D.C., de Vernal, A., and shipboard party. 2009: CGS Hudson Expedition 2008029: Marine geology and paleoceanography of Baffin Bay and adjacent areas, Nain, NL to Halifax, NS, August 28-September 23. Geological Survey of Canada, Open File 5989.

Carstens, J., Hebbeln, G., Wefer, G., 1997. Distribution of planktic foraminifera at the ice margin in the Arctic (Fram Strait). Marine Micropaleontology 29, 257-269.

Castañeda, I.S., Smith, L.M., Kristjánsdóttir, G.B., Andrews, J.T., 2004. Temporal changes in Holocene $\delta^{18}O$ records from the northwest and central North Iceland Shelf. Journal of Quaternary Science 19, 321-334.

Cheng, W., Rhines, P.B., 2004. Response of the overturning circulation to high-latitude fresh-water perturbations in the North Atlantic Climate Dynamics 22, 359-372.

Clarke, G.K.C., Marshall, S.J., Hilllaire-Marcel, C., Bilodeau, G., Veiga-Pires, C., 1999. A glaciological perspective on Heinrich events. In: Clark, P.U., Webb, R.S., Keigwin, L.D. (Eds.), Mechanisms of Global Climate Change at Millennial Time Scales. Geophysical Monograph Series, vol. 112.

Clark, P.U., Hostetler, S.W., Pisias, N.G., Schmittner, A., Meissner, K.J., 2007. Mechanisms for an ~7-kyr climate and sea-level oscillation during marine isotope stage 3. Geophysical Monograph Series 173, 209-246.

Cuny, J., Rhines, P.B., Niiler, P.P., Bacon, S., 2002. Labrador Sea boundary currents and the fate of the Irminger Sea Water. Journal of Physical Oceanography 32 (2), 627-647.

Cuny, J., Rhines, P.B., Kwok, R., 2005. Davis Strait volume, freshwater and heat fluxes. Deep Sea Research Part I: Oceanographic Research Papers 52 (3), 519-542.

Curry, R., Mauritzen, C., 2005. Dilution of the northern North Atlantic Ocean in recent decades. Science 308 (5729), 1772-1774.

Curry, B., Lee, C.M., Petrie, B., 2011. Volume, Freshwater, and Heat Fluxes through Davis Strait, 2004-05*. Journal of Physical Oceanography 41 (3), 429-436.

de Vernal, A., Hillaire-Marcel, C., 2000. Sea-ice cover, sea-surface salinity and halo-/thermocline structure of the northwest North Atlantic: modern versus full glacial conditions. Quaternary Science Reviews 19 (1), 65-85.

de Vernal, A., Hillaire-Marcel, C., 2006. Provincialism in trends and high frequency changes in the northwest North Atlantic during the Holocene. Global Planetary Change 54 (3), 263- 290.

de Vernal, A., Hillaire-Marcel, C., Aksu, A.E., Mudie, P.J., 1987a. Palynostratigraphy and chronostratigraphy of Baffin Bay deep sea cores: climatostratigraphic implications. Palaeogeography, palaeoclimatology, palaeoecology, 61, 97-105.

de Vernal, A., Larouche, A., Richard, P.J.H., 1987b. Evaluation of palynomorph concentrations: do the aliquot and the marker-grain methods yield comparable results? Pollen et Spores 29 (2–3), 291–303.

de Vernal, A., Bilodeau, G., Hillaire-Marcel, C., Kassou, N., 1992. Quantitative assessment of carbonate dissolution in marine sediments from foraminifer linings vs. shell ratios: Davis Strait, northwest North Atlantic. Geology 20 (6), 527-530.

de Vernal, A., Turon, J.L., Guiot, J., 1994. Dinoflagellate cyst distribution in high-latitude marine environments and quantitative reconstruction of sea-surface salinity, temperature, and seasonality. Canadian Journal of Earth Sciences 31 (1), 48-62.

de Vernal, A., Rochon, A., Turon, J.-L., Matthiessen, J., 1997. Organic-walled dinoflagellate cysts: palynological tracers of sea-surface conditions in middle to high latitude marine environments. GEOBIOS 30 (7), 905-920.

de Vernal, A., Henry, M., Bilodeau, G., 1999. Technique de préparation et d'analyse en micropaléontologie. Les Cahiers du GEOTOP, Université du Québec à Montréal, 3, unpublished report.

de Vernal, A., Hillaire-Marcel, C., Turon, J.-L., Matthiessen, J., 2000. Reconstruction of sea-surface temperature, salinity, and sea-ice cover in the northern North Atlantic during the last glacial maximum based on dinocyst assemblages. Canadian Journal of Earth Sciences 37 (5), 725-750.

de Vernal, A., Henry, M., Matthiessen, J., Mudie, P.j., Rochon, A., Boessenkool, K., Eynaud, F., Grøsfjeld, K., Guiot, J., Hamel, D., Harland, R., Head, M.j., Kunz-pirrung, M., Levac, E., Loucheur, V., Peyron, O., Pospelova, V., Radi, T., Turon, J.-L., Voronina, E., 2001. dinoflagellate cyst assemblages as tracers of sea-surface conditions in the northern North Atlantic, Arctic and sub-arctic seas: the new "n=677" database and application for quantitative paleoceanographical reconstruction. Journal of Quaternary Science 16, 681-699.

de Vernal, A., Eynaud, F., Henry, M., Hillaire-Marcel, C., Londeix, L., Mangin, S., Matthiessen, J., Marret, F., Radi, T., Rochon, A., Solignac, S., Turon, J.L., 2005. Reconstruction of sea surface conditions at middle to high latitudes of the Northern Hemisphere during the Last Glacial Maximum (LGM) based on dinoflagellate cyst assemblages. Quaternary Science Reviews 24 (7), 897-924.

de Vernal, A., Hillaire-Marcel, C., Solignac, S., Radi, T., Rochon, A., 2008. Reconstructing sea-ice conditions in the Arctic and subarctic prior to human observations. In: Weaver, E. (ed), Arctic Sea ice Decline: Observations, Projections, Mechanisms, and Implications. AGU Monograph Series 180, 27-45.

de Vernal, A., Rochon, A., 2011. Dinocysts as tracers of sea-surface conditions and sea-ice cover in polar and subpolar environments. In IOP Conference Series: Earth and Environmental Science Vol. 14 (1), p. 012007. IOP Publishing.

de Vernal, A., Rochon, A., Fréchette, B., Henry, M., Radi, T., Solignac, S., 2013a. Reconstructing past sea ice cover of the Northern hemisphere from dinocyst assemblages: status of the approach. Quaternary Science Reviews 79, 122-134.

de Vernal, A., Hillaire-Marcel, C., Rochon, A., Fréchette, B., Henry, M., Solignac, S., Bonnet, S., 2013b. Dinocyst-based reconstructions of sea ice cover concentration during the Holocene in the Arctic Ocean the northern North Atlantic Ocean and its adjacent seas. Quaternary Science Reviews 79, 111-121.

Devillers, R., de Vernal, A., 2000. Distribution of dinoflagellate cysts in surface sediments of the northern North Atlantic in relation to nutrient content and productivity in surface waters. Marine Geology 166(1), 103-124.

Dickson, R.R., Meincke, J., Malmberg, S.A., Lee, A.J., 1988. The "great salinity anomaly" in the northern North Atlantic 1968–1982. Progress in Oceanography 20 (2), 103-151.

Dickson, R., Rudels, B., Dye, S., Karcher, M., Meincke, J., Yashayaev, I., 2007. Current estimates of freshwater flux through Arctic and subarctic seas. Progress in Oceanography 73 (3), 210-230.

Driesschaert, E., Fichefet, T., Goosse, H., Huybrechts, P., Janssens, I., Mouchet, A., Munhoven, G., Brovkin, V., Weber, S.L., 2007. Modeling the influence of Greenland ice sheet melting on the Atlantic meridional overturning circulation during the next millennia. Geophysical Research Letters 34 (10).

Dyke, A.S., 2004. An outline of the deglaciation of North America with emphasis on central and northern Canada. In: Ehlers, J., Gibbard, P.L., (eds), Quaternary Glaciations, Extent and Chronology. Part II. North America. Developments in Quaternary Science, vol. 2b. Elsevier, Amsterdam.

Dyke, A., 1999. Last glacial maximum and deglaciation of Devon Island, Arctic Canada: support for an Innuitian ice sheet. Quaternary Science Reviews 18(3), 393-420.

Dyke, A.S., Prest, V.K., 1987. Late Wisconsinan and Holocene history of the Laurentide ice sheet. Geographie physique et Quaternaire 41 (2), 237-263.

Dyke, A.S., Dale, J.E., McNeely, R.N., 1996. Marine molluscs as indicators of environmental change in glaciated North America and Greenland during the last 18 000 years. Géographie physique et Quaternaire 50(2), 125-184.

Elliot, M., Labeyrie, L., Bond, G., Cortijo, E., Turon, J. L., Tisnerat, N., Duplessy, J.C., 1998. Millennial-scale iceberg discharges in the Irminger Basin during the Last Glacial Period: Relationship with the Heinrich events and environmental settings. Paleoceanography 13 (5), 433-446.

England, J., Atkinson, N., Bednarski, J., Dyke, A.S., Hodgson, D.A., Ó Cofaigh, C., 2006. The Innuitian Ice Sheet: configuration, dynamics and chronology. Quaternary Science Reviews 25 (7), 689-703.

Erbs-Hansen, D.R., Knudsen, K.L., Olsen, J., Lykke-Andersen, H., Underbjerg, J.A., Sha, L., 2013. Paleoceanographical development off Sisimiut, West Greenland, during the mid-and late Holocene: A multiproxy study. Marine Micropaleontology 102, 79-97.

Fisheries and Oceans Canada, 2012. Ice Navigation in Canadian Waters Icebreaking Program. Maritime Services Canadian Coast Guard Fisheries and Oceans Canada, 53 p.

Forcino, F.L., 2012. Multivariate assessment of the required sample size for community paleoecological research. Palaeogeography, Palaeoclimatology, Palaeoecology 315-316, 134-141.

Fréchette, B., Wolfe, A.P., Miller, G.H., Richard, P.J., de Vernal, A., 2006. Vegetation and climate of the last interglacial on Baffin Island, Arctic Canada.Palaeogeography, Palaeoclimatology, Palaeoecology 236 (1), 91-106.

Fréchette, B., de Vernal, A., 2009. Relationship between Holocene climate variations over southern Greenland and eastern Baffin Island and synoptic circulation pattern. Climate of the Past 5, 347-359.

Funder, S., Weidick, A., 1991. Holocene boreal molluscs in Greenland—palaeoceanographic implications. Palaeogeography Palaeoclimatology Palaeoecology 85(1), 123-135.

Funder, S., (ed) 1990. Late Quaternary stratigraphy and glaciology in the Thule area Meddelelser om Gronland. Geoscience 22, 63p.

Funder, S., Kjeldsen, K.K., Kjær, K.H., Ó Cofaigh, C., 2011. The Greenland Ice Sheet during the past 300,000 years: A review. Developments in Quaternary Science 15, 699-713.

Gelderloos, R., Straneo, F., Katsman, C.A., 2012. Mechanisms behind the Temporary Shutdown of Deep Convection in the Labrador Sea: Lessons from the Great Salinity Anomaly Years 1968-71. Journal of Climate 25 (19), 6743-6755.

Gibb, O.T., Hillaire-Marcel, C., de Vernal, A., 2014. Oceanographic regimes in the northwest Labrador Sea since Marine Isotope Stage 3 based on dinocyst and stable isotope proxy records. Quaternary Science Reviews 92, 269-279.

Goosse, H., Fichefet, T., Campin, J.-M., 1997. The effects of the water flow through the Canadian Archipelago in a global ice–ocean model. Geophysical Research Letters 24 (12), 1507-1510.

Hald, M., Steinsund, P.I., 1996. Benthic foraminifera and carbonate dissolution in surface sediments of the Barents and Kara Sea. In: Stein, R., Ivanov, G.I., Levitan, M.A., Fahl, K. (Eds.), Surface-sediment composition and sedimentary processes in the central Arctic Ocean and along the Eurasian Continental Margin. Berichte Zur Polarforschung, 212, 285–307.

Hamel, D., de Vernal, A., Gosselin, M., Hillaire-Marcel, C., 2002. Organic-walled microfossils and geochemical tracers: sedimentary indicators of productivity changes in the North Water and northern Baffin Bay during the last centuries. Deep Sea Research Part II: Topical Studies in Oceanography 49 (22), 5277-5295.

Head, M.J., Harland, R., Matthiessen, J., 2001. Cold marine indicators of the late Quaternary: The new dinoflagellate cyst genus Islandinium and related morphotypes. Journal of Quaternary Science 16 (7), 621-636.

Heinrich, H., 1988. Origin and consequences of cyclic ice rafting in the northeast Atlantic Ocean during the past 130,000 years. Quaternary Research 29, 142-152.

Hélie, J.-F., 2009. Elemental and stable isotopic approaches for studying the organic and inorganic carbon components in natural samples. In Deep-Sea to Coastal Zones: Methods - Techniques for Studying Paleoenvironments. IOP Conference Series: Earth and Environmental Science 5.

Hesse, R., Khodabakhsh, S., 1998. Depositional facies of the late Pleistocene Heinrich events in the Labrador Sea. Geology 26, 103-106.

Hilbrecht, H., 1996. Extant planktic foraminifera and the physical environment in the Atlantic and Indian Oceans: an atlas based on Climap and Levitus (1982) data. Geologische Institut der Eidgen, Technischen Hochschule und der Universitat Zurich. Neue Folge: Zurich.

Hillaire-Marcel, C., de Vernal, A., Aksu, A., Macko, S., 1989. High-resolution isotopic and micropaleontological studies of upper Pleistocene sediments at ODP Site 645, Baffin Bay. *In*: Srivastava, S. P., Arthur, M., Clement, B., et al., (eds),

Proceedings of the Ocean Drilling Program, Scientific Results, Vol. 105. Ocean Drilling Program, College Station, TX.

Hillaire-Marcel, C., de Vernal, A., Bilodeau, G., Wu, G., 1994. Isotope stratigraphy, sedimentation rates, deep circulation, and carbonate events in the Labrador Sea during the last -200 ka. Canadian Journal of Earth Science 31, 63-89.

Hillaire-Marcel, C., Bilodeau, G., 2000. Instabilities in the Labrador Sea water mass structure during the last climatic cycle. Canadian Journal of Earth Sciences 37 (5), 795-809.

Hillaire-Marcel, C., de Vernal, A., Bilodeau, G., Weaver, A.J., 2001. Absence of deep water formation in the Labrador Sea during the last interglacial periods. Nature 410 (6832), 1073-1077.

Hillaire-Marcel, C., de Vernal, A., Polyak, L., Darby, D., 2004. Size-dependent isotopic composition of planktic foraminifers from Chukchi Sea vs. NW Atlantic sediments-implications for the Holocene paleoceanography of the western Arctic. Quaternary Science Reviews 23 (3), 245-260.

Hillaire-Marcel, C., de Vernal, A., Piper, D.J.W., 2007. Lake Agassiz Final drainage event in the northwest North Atlantic. Geophysical Research Letters 34 (15), L15601.

Hillaire-Marcel, C., de Vernal, A., 2008. Stable isotope clue to episodic sea ice formation in the glacial North Atlantic. Earth and Planetary Science Letters 268, 143-150.

Hiscott, R.N., Aksu, A.E., Nielsen, O.B., 1989. Provenance and dispersal patterns, Pliocene-Pleistocene section at Site 645, Baffin Bay. *In*: Srivastava, S. P., Arthur, M., Clement, B., et al., (eds), Proceedings of the Ocean Drilling Program, Scientific Results, Vol. 105. Ocean Drilling Program, College Station, TX.

Hiscott, R.N., Aksu, A.E., Mudie, P.J., Parsons, D.F., 2001. A 340,000 year record of ice rafting, palaeoclimatic fluctuations, and shelf-crossing glacial advances in the southwestern Labrador Sea. Global and Planetary Change 28 (1), 227-240.

Hodell, D.A., Curtis, J.H., 2008. Oxygen and carbon isotopes of detrital carbonate in North Atlantic Heinrich Events. Marine Geology 256 (1), 30-35.

Holland, D.M., Thomas, R.H., de Young, B., Ribergaard, M.H., Lyberth, B., 2008. Acceleration of Jakobshavn Isbrae triggered by warm subsurface ocean waters. Nature Geoscience 1 (10), 659-664.

Hulbe, C.L., 1997. An ice shelf mechanism for Heinrich layer production. Paleoceanography 12, 711-717.

Hulbe, C.L., MacAyeal, D.R., Denton, G.H., Kleman, J., Lowell, T.V., 2004. Catastrophic ice shelf breakup as the source of Heinrich event icebergs. Paleoceanography 19 (1).

Husum, K., Hald, M., 2004. A continuous marine record 8000-1600 cal. yr BP from the Malangenfjord, north Norway: foraminiferal and isotopic evidence. The Holocene 14 (6), 877-887.

Jahn, A., Holland, M.M., 2013. Implications of Arctic sea ice changes for North Atlantic deep convection and the meridional overturning circulation in CCSM4-CMIP5 simulations. Geophysical Research Letters 40 (6), 1206-1211.

Jennings, A.E., 1993. The Quaternary history of Cumberland Sound, southeastern Baffin Island: the marine evidence. Géographie physique et Quaternaire 47(1), 21-42.
Jennings, A.E., Tedesco, K.A., Andrews, J.T., Kirby, M.E., 1996. Shelf erosion and glacial ice proximity in the Labrador Sea during and after Heinrich events (H-3 or 4 to H-0) as shown by foraminifera. Geological Society, London, Special Publications 111 (1), 29-49.

Jennings, A.E., Tedesco, K.A., Andrews, J.T., Kirby, M.E., 1996. Shelf erosion and glacial ice proximity in the Labrador Sea during and after Heinrich events (H-3 or 4 to H-0) as shown by foraminifera. Geological Society, London, Special Publications, 111(1), 29-49.

Jennings, A.E., Manley, W.F., Maclean, B., Andrews, J.T., 1998. Marine evidence for the last glacial advance across eastern Hudson Strait, eastern Canadian Arctic. Journal of Quaternary Science 13 (6), 501-514.

Jennings, A., Andrews, J., Wilson, L., 2011a. Holocene environmental evolution of the SE Greenland Shelf North and South of the Denmark Strait: Irminger and East Greenland current interactions. Quaternary Science Reviews 30 (7), 980-998.

Jennings, A.E., Sheldon, C., Cronin, T.M., Francus, P., Stoner, J., Andrews, J., 2011b. The Holocene history of Nares Strait: Transition from glacial bay to Arctic-Atlantic throughflow. Oceanography 24(3) 26-41.

Jennings, A.E., Walton, M.E., Ó Cofaigh, C., Kilfeather, A., Andrews, J.T., Ortiz, J.D., de Vernal, A., Dowdeswell, J.A., 2014. Paleoenvironments during Younger

Dryas-Early Holocene retreat of the Greenland Ice Sheet from outer Disko Trough, central west Greenland. Journal of Quaternary Science 29 (1), 27-40.

Kaplan, M.R., Miller, G.H., 2003. Early Holocene delevelling and deglaciation of the Cumberland Sound region, Baffin Island, Arctic Canada. Geological Society of America Bulletin 115, 445-462.

Kaufman, D.S., Miller, G.H., Stravers, J.A., Andrews, J.T., 1993. Abrupt early Holocene (9.9-9.6 ka) ice-stream advance at the mouth of Hudson Strait, Arctic Canada. Geology 21(12), 1063-1066.

Kaufman, D.S., et al., 2004. Holocene thermal maximum in the western Arctic (0–180°W). Quaternary Science Reviews 23 (5-6), 529-560.

Kerwin, M.W., 1996. A regional stratigraphic isochron (ca. 8000 14 C yr BP) from final deglaciation of Hudson Strait. Quaternary Research 46(2), 89-98.

Knudsen, K.L., Stabell, B., Seidenkrantz, M.-S., Eiríksson, J., Blake Jr., W., 2008. Deglacial and Holocene conditions in northernmost Baffin Bay: sediments, foraminifera, diatoms and stable isotopes. Boreas 37 (3), 346-376.

Kucera, M., 2007. Planktonic foraminifera as tracers of past oceanic environments. In: Hillaire-Marcel, C., de Vernal, A. (eds), Proxies in Late Cenozoic Paleoceanography. Elsevier, The Netherlands, pp. 213-262.

Laskar, J., Robutel, P., Joutel, F., Gastineau, M., Correia, A.C.M., Levrard, B., 2004. A long-term numerical solution for the insolation quantities of the Earth. Astronomy & Astrophysics 428 (1), 261-285.

Lazier, J.R.N., 1973. The renewal of Labrador Sea Water. Deep Sea Research 20 (4), 341-353.

Ledu, D., Rochon, A., de Vernal, A., St-Onge, G., 2008. Palynological evidence of Holocene climate change in the eastern Arctic: a possible shift in the Arctic oscillation at the millennial time scale. Canadian Journal of Earth Science 45, 1363-1375.

Levac, E., de Vernal, A., 1997. Postglacial changes of terrestrial and marine environments along the Labrador coast: palynological evidence from cores 91-045-005 and 91-045-006, Cartwright Saddle. Canadian Journal of Earth Sciences 34 (10), 1358-1365.

Levac, E., de Vernal, A., Blake, W., 2001. Sea surface conditions in northernmost Baffin Bay during the Holocene: palynological evidence. Journal of Quaternary Science 16 (4), 353-363.

Lewis, C.F.M., Miller, A.A.L., Levac, E., Piper, D.J.W., Sonnichsen, G.V., 2012. Lake Agassiz outburst age and routing by Labrador Current and the 8.2 cal ka cold event. Quaternary International 260, 83-97.

Lloyd, J.M., Park, L.A., Kuijpers, A., Moros, M., 2005. Early Holocene palaeoceanography and deglacial chronology of Disko Bugt, west Greenland. Quaternary Science Reviews 24 (14), 1741-1755.

Lloyd, J.M., Kuijpers, A., Long, A., Moros, M., Park, L.A., 2007. Foraminiferal reconstruction of mid- to late-Holocene ocean circulation and climate variability in Disko Bugt, West Greenland. The Holocene 17, 1079-1091.

Long, A.J., Roberts, D.H., 2003. Late Weichselian deglacial history of Disko Bugt, West Greenland, and the dynamics of the Jakobshavns Isbrae ice stream. Boreas 32(1), 208-226.

Maccali, J., Hillaire-Marcel, C., Carignan, J., Reisberg, L.C., 2013. Geochemical signatures of sediments documenting Arctic sea-ice and water mass export through Fram Strait since the Last Glacial Maximum. Quaternary Science Reviews 64, 136-151.

Mackensen, A., Wollenburg, J., Licari, L., 2006. Low $\delta^{13}C$ in tests of live epibenthic and endobenthic foraminifera at a site of active methane seepage. Paleoceanography, 21 (2).

Manabe, S., Stouffer, R.J., 1995. Simulation of abrupt climate change induced by freshwater input to the North Atlantic Ocean. Nature 378 (6553), 165-167.
Matthews, J., 1969. The assessment of a method for the determination of absolute pollen frequencies. New Phytologist 68 (1), 161-166.

Marcott, S.A., Clark, P.U., Padman, L., Klinkhammer, G.P., Springer,A.R., Liu, Z., Otto-Bliesner, B.L., Carlsone, A.E., Ungererc, A., Padmanc, J., Hee, F., Chengh, J., Schmittnerc, A., 2011. Ice-shelf collapse from subsurface warming as a trigger for Heinrich events. Proceedings of the National Academy of Sciences 108 (33), 13415-13419.

Marret, F., Eiríksson, J., Knudsen, K.L., Turon, J.L., Scourse, J.D., 2004. Distribution of dinoflagellate cyst assemblages in surface sediments from the northern and western shelf of Iceland. Review of Palaeobotany and Palynology 128(1), 35-53.

Matthews, J., 1969. The assessment of a method for the determination of absolute pollen frequencies. New Phytologist 68, 161-166.

McAndrews, J.H., Berti, A.A., Norris, G., 1973. Key to the Quaternary pollen and spores of the great Lakes region. Life Science Miscellaneous Publications, Royal Ontario Museum, Toronto, Canada.

Miller, G.H., Wolfe, A.P., Briner, J.P., Sauer, P.E., Nesje, A., 2005. Holocene glaciation and climate evolution of Baffin Island, Arctic Canada. Quaternary Science Reviews 24 (14), 1703-1721.

Møller, H.S., Jensen, K.G., Kuijpers, A., Aagaard-Sørensen, S., Seidenkrantz, M.-S., Endler, R., Mikkelsen, N., 2006. Late Holocene environmental and climatic changes in Ameralik Fjord, Southwest Greenland - evidence from the sedimentary record. The Holocene 16, 685-695.

Moore, P.D., Webb, J.A., Collinson, M.E., 1991. Pollen Analysis, 2nd edition. Blackwell Scientific Publications, Oxford.

Moros, M., Jensen, K.G., Kuijpers, A., 2006. Mid-to late-Holocene hydrological and climatic variability in Disko Bugt, central West Greenland. The Holocene 16 (3), 357-367.

Mudie, P.J., Aksu, A.E., 1984. Palaeoclimate of Baffin Bay from 300,000-year record of foraminifera, dinoflagellates and pollen. Nature 312, 630-634.

Mudie, P.J., Rochon, A., Prins, M.A., Soenarjo, D., Troelstra, S.R., Levac, E., Scott, D.B., Roncaglia, L., Kuijpers, A., 2006. Late Pleistocene-Holocene marine geology of Nares Strait region: paleoceanography from foraminifera and dinoflagellate cysts, sedimentology and stable isotopes. Polarforschung 74, 169-183.

Muzuka, A.N., Hillaire-Marcel, C., 1999. Burial rates of organic matter along the eastern Canadian margin and stable isotope constraints on its origin and diagenetic evolution. Marine Geology 160 (3), 251-270.

Nuttin, L., Hillaire-Marcel, C., 2015. U-and Th-series isotopes in deep Baffin Bay sediments: Tracers of detrital sources and of contrasted glacial/interglacial sedimentary processes. Marine Geology 361 (1), 1-10.

Ó Cofaigh, C., Dowdeswell, J.A., Jennings, A.E., Hogan, K.A., Kilfeather, A., Hiemstra, J.F. Noormets, R., Evans, J., McCarthy, D.J., Andrews, J.T., Lloyd, J.M.,

Moros, M., 2013. An extensive and dynamic ice sheet on the West Greenland shelf during the last glacial cycle. Geology 41 (2), 219-222.

Olafsdottir, S., Jennings, A.E., Geirsdottir, A., Andrews, J.T., Miller, G.H., 2010. Holocene variability of the North Atlantic Irminger Current on the South- and Northwest shelf of Iceland. Marine Micropaleontology 77, 101-118.

Osterman, L.E. and Nelson, A.R., 1989. Latest Quaternary and Holocene paleoceanography of the eastern Baffin Island continental shelf, Canada: benthic foraminiferal evidence. Canadian Journal of Earth Science 26, 2236-2248.

Ouellet-Bernier, M.-M., de Vernal, A., Hillaire-Marcel, C., 2014. Paleoceanographic changes of Disko Bugt area West Greenland during the Holocene. The Holocene 24 (11), 1573-1583.

Pados, T., Spielhagen, R.F., 2014. Species distribution and depth habitat of recent planktic foraminifera in Fram Strait, Arctic Ocean. Polar Research, 33.

Perner, K., Moros, M., Jennings, A., Lloyd, J.M., Knudsen, K.L., 2013. Holocene palaeoceanographic evolution off West Greenland. The Holocene 23(3), 374-387.

Petersen, S.V., Schrag, D.P., Clark, P.U., 2013. A new mechanism for Dansgaard-Oeschger cycles. Paleoceanography 28, 1-7.

Peterson, B.J., McClelland, J., Curry, R., Holmes, R.M., Walsh, J.E., Aagaard, K., 2006. Trajectory shifts in the Arctic and subarctic freshwater cycle. Science 313 (5790), 1061-1066.

Polyak, L., Best, K.M., Crawford, K.A., Council, E.A., St-Onge, G., 2013. Quaternary history of sea ice in the western Arctic Ocean based on foraminifera. Quaternary Science Reviews 79, 145-156.

Punshon, S., Azetsu-Scott, K., Lee, C.M., 2014. On the distribution of dissolved methane in Davis Strait, North Atlantic Ocean. Marine Chemistry 161, 20-25.

Radi, T., de Vernal, A., 2008. Dinocysts as proxy of primary productivity in mid-high latitudes of the Northern Hemisphere. Marine Micropaleontology 68 (1), 84-114.

Ramsey, C.B., 2008. Deposition models for chronological records. Quaternary Science Reviews 27 (1), 42-60.

Rashid, H., Hesse, R., Piper, D.J.W., 2003. Origin of unusually thick Heinrich layers of ice-proximal regions of the northwest Labrador Sea. Earth and Planetary Science Letters 208, 319-336.

Rashid, H., Boyle, E.A., 2007. Mixed-layer deepening during Heinrich Events: a multi-planktonic foraminiferal $\delta^{18}O$ approach. Science 318 (5849), 439-441.

Rasmussen, T.L., Oppo, D.W., Thomsen, E., Lehman, S.J., 2003. Deep sea records from the southeast Labrador Sea: Ocean circulation changes and ice-rafting events during the last 160,000 years. Paleoceanography 18 (1), 1018.

Ravelo, A.C., Hillaire-Marcel, C., 2007. The use of oxygen and carbon isotopes of foraminifera in paleoceanography. In: Hillaire-Marcel, C., de Vernal, A. (eds), Proxies in Late Cenozoic Paleoceanography. Elsevier, The Netherlands, pp. 735-764.

Reimer, P.J., Baillie, M.G.L., Bard, E., Bayliss, A., Beck, J.W., Blackwell, P.G., Ramsey, C.B., Buck, C.E., Burr, G.S., Edwards, R.L., Friedrich, M., Grootes, P.M., Guilderson, T.P., Hajdas, I., Heaton, T.J., Hogg, A.G., Hughen, K.A., Kaiser, K.F., Kromer, B., McCormac, F.G., Manning, S.W., Reimer, R.W., Richards, D.A., Southon, J.R., Talamo, S., Turney, C.S.M., van der Plicht, J., Weyhenmeyer, C.E., 2009. INTCAL 09 and MARINE09 radiocarbon age calibration curves, 0-50,000 years Cal BP. Radiocarbon 51, 1111-1150.

Reimer, P.J., Bard, E., Bayliss, A., Beck, J.W., Blackwell, P.G., Ramsey, C.B., Buck, C.E., , Cheng, H., Edwards, R.L., Friedrich, M., Grootes, P.M., Guilderson, T.P., Haflidason, H., Hajdas, I., Hatté, C., Heaton, T.J., Hoffman, D.L., Hogg, A.G., Hughen, K.A., Kaiser, K.F., Kromer, B., Manning, S.W., Niu, M., Reimer, R.W., Richards, D.A., Scott, E.M., Southon, J.R., Staff, R.A., Turney, C.S.M., van der Plicht, J., 2013. IntCal13 and Marine13 radiocarbon age calibration curves 0–50,000 years cal BP. Radiocarbon 55 (4), 1869-1887.

Ren, J., Jiang, H., Seidenkrantz, M.-S., Kuijpers, A., 2009. A diatom-based reconstruction of Early Holocene hydrographic and climatic change in a southwest Greenland fjord. Marine Micropaleontology 70 (3), 166-176.

Rochon, A., de Vernal, A., 1994. Palynomorph distribution in recent sediments from the Labrador Sea. Canadian Journal of Earth Sciences 31 (1), 115-127.

Rochon, A., de Vernal, A., Turon, J.-L., Matthiessen, J., Head, M.J., 1999. Distribution of dinoflagellate cyst assemblages in surface sediments from the North Atlantic Ocean and adjacent basins and quantitative reconstruction of sea surface parameters. American Association of Stratigraphic Palynologists, Contribution Series No. 35.

Schröeder-Adams, C.J., Van Rooyen, D., 2011. Response of Recent Benthic Foraminiferal Assemblages to Contrasting Environments in Baffin Bay and the Northern Labrador Sea, Northwest Atlantic. Arctic, 317-341.

Scott, D.B., Mudie, P.J., de Vernal, A., Hillaire-Marcel, C., Baki, V., MacKinnon, K.D., Medioli, F.S., Mayer, L., 1989. Lithostratigraphy, biostratigraphy, and stable-isotope stratigraphy of cores from ODP Leg 105 site surveys, Labrador Sea and Baffin Bay. *In*: Srivastava, S. P., Arthur, M., Clement, B., et al., (eds), Proceedings of the Ocean Drilling Program, Scientific Results, Vol. 105. Ocean Drilling Program, College Station, TX.

Seidenkrantz, M.-S., Aagaard-Sørensen, S., Sulsbrück, H., Kuijpers, A., Jensen, K.G., Kunzendorf, H., 2007. Hydrography and climate of the last 4400 years in a SW Greenland fjord: implications for Labrador Sea palaeoceanography. Holocene 17 (3), 387–401.

Seidenkrantz, M.-S., Roncaglia, L., Fischel, A., Heilmann-Clausen, C., Kuijpers, A., Moros, M., 2008. Variable North Atlantic climate seesaw patterns documented by a late Holocene marine record from Disko Bugt, West Greenland. Marine Micropaleontology 68, 66-83.

Seidenkrantz, M.-S., Ebbesen, H., Aagaard-Sørensen, S., Moros, M., Lloyd, J. M., Olsen, J., Knudsen, M.F., Kuijpers, A., 2013. Early Holocene large-scale meltwater discharge from Greenland documented by foraminifera and sediment parameters. Palaeogeography, Palaeoclimatology, Palaeoecology 391, 71-81.

Serreze, M.C., Barrett, A.P., Slater, A.G., Woodgate, R.A., Aagaard, K., Lammers, R.B., Steele, M., Moritz, R., Meredith, M., Lee, C.M., 2006. The large-scale freshwater cycle of the Arctic. Journal of Geophysical Research 111 (C11), C11010.

Shaffer, G., Olsen, S.M., Bjerrum, C.J., 2004. Ocean subsurface warming as a mechanism for coupling Dansgaard-Oeschger climate cycles and ice-rafting events. Geophysical Research Letters 31 (24).

Simon, Q., St-Onge, G., Hillaire-Marcel, C., 2012. Late Quaternary chronostratigraphic framework of deep Baffin Bay glaciomarine sediments from high-resolution paleomagnetic data. Geochemistry, Geophysics, Geosystems 13 (11).

Simon, Q., 2013. Propriétés magnétiques, minéralogiques et sédimentologiques des sédiments profonds de la baie de Baffin: chronologie et dynamique des glaciers ouest

groenlandais, innuitiens et laurentidiens au cours de la dernière glaciations. PhD thesis, Université du Québec à Montréal, Montréal, Canada.

Simon, Q., Hillaire-Marcel, C., St-Onge, G., Andrews, J.T., 2014. North-eastern Laurentide western Greenland and southern Innuitian ice stream dynamics during the last glacial cycle. Journal of Quaternary Science 29(1), 14-26.

Simstich, J., Sarnthein, M., Erlenkeuser, H., 2003. Paired d18O signals of *Neogloboquadrina pachyderma* (s) and *Turborotalita quinqueloba* show thermal stratification structure in Nordic Seas. Marine Micropaleontology 48, 107-125.

Solignac, S., de Vernal, A., Hillaire-Marcel, C., 2004. Holocene sea surface conditions in the North Atlantic-contrasted trends and regimes between the eastern and western sectors (Labrador Sea vs. Iceland Basin). Quaternary Science Reviews 23 (3), 319-334.

Solignac, S., Giraudeau, J., de Vernal, A., 2006. Holocene sea surface conditions in the western North Atlantic: Spatial and temporal heterogeneities. Paleoceanography 21 (2), PA2004.

Spindler, M., Dieckmann, G.S., 1986. Distribution and Abundance of the Planktic Foraminifer Neogloboquadrina pachyderma in Sea Ice of the Weddell Sea (Antarctica). Polar Biology 5 (3), 185-191.

Srivastava, S.P., Arthur, M., Clement, B. et al (eds) 1989. Proceedings of the Ocean Drilling Program Scientific Results, Vol 105, Ocean Drilling Program College Station TX.

Steinhauer, S., 2012. Postglacial paleoceanography of central Baffin Bay from palynological tracers. Master's thesis, Université du Québec à Montréal, Montréal, Canada.

Stoner, J.S., Channell, J.E.T., Hillaire-Marcel, C., 1995. Late Pleistocene relative geomagnetic paleointensity from the deep Labrador Sea: Regional and global correlations. Earth and Planetary Science Letters 134 (3), 237-252.

Stoner, J.S., Channell, J.E.T., Hillaire-Marcel, C., 1996. The magnetic signature of rapidly deposited detrital layers from the deep Labrador Sea: Relationship to North Atlantic Heinrich layers. Paleoceanography 11 (3), 309-325.

Stoner, J.S., Channell, J.E.T., Hillaire-Marcel, C., Kissel, C., 2000. Geomagnetic paleointensity and environmental record from Labrador Sea core MD95-2024: global

marine sediment and ice core chronostratigraphy for the last 110 kyr. Earth and Planetary Science Letters 183 (1), 161-177.

St-Onge, M.-P., St-Onge, G., 2014. Environmental changes in Baffin Bay during the Holocene based on the physical and magnetic properties of sediment cores. Journal of Quaternary Science 29(1), 41-56.

Stravers, J.A., Miller, G.H., Kaufman, D.S., 1992. Late glacial ice margins and deglacial chronology for southeastern Baffin Island and Hudson Strait, eastern Canadian Arctic. Canadian Journal of Earth Sciences 29(5), 1000-1017

Stroeve, J.C., Serreze, M.C., Holland, M.M., Kay, J.E., Malanik, J., Barrett, A.P., 2012. The Arctic's rapidly shrinking sea ice cover: a research synthesis. Climatic Change 110 (3-4), 1005-1027.

Stuiver, M., Grootes, P.M., 2000. GISP2 oxygen isotope ratios. Quaternary Research 53 (3), 277-284.

Sutherland, D.A., Pickart, R.S., Jones, E.P., Azetsu-Scott, K., Eert, A.J., Ólafsson, J., 2009. Freshwater composition of the waters off southeast Greenland and their link to the Arctic Ocean. Journal of Geophysical Research: Oceans, 114 (C5).

Swingedouw, D., Mignot, J., Braconnot, P., Mosquet, E., Kageyama, M., Alkama, R., 2009. Impact of Freshwater Release in the North Atlantic under Different Climate Conditions in an OAGCM. Journal of Climate 22 (23).

Tan, F.C., Strain, P.M., 1980. The distribution of sea ice meltwater in the Eastern Canadian Arctic. Journal of Geophysical Research 85, 1925–1932.

Tang, C.C.L., Ross, C.K., Yao, T., Petrie, B., DeTracey, B.M., Dunlap, E., 2004. The circulation, water masses and sea-ice of Baffin Bay. Progress in Oceanography 63, 183-228.

Veum, T., Jansen, E., Arnold, M., Beyer, I., Duplessy, J.-C., 1992. Water mass exchange between the North Atlantic and the Norwegian Sea during the past 28,000 years. Nature 356 (6372), 783-785.

Volkmann, R. 2000. Planktic foraminifers in the outer Laptev Sea and the Fram Strait—modern distribution and ecology. The Journal of Foraminiferal Research 30 (3), 157-176.

Volkmann, R., Mensch, M., 2001. Stable isotope composition ($\delta^{18}O$, $\delta^{13}C$) of living planktic foraminifers in the outer Laptev Sea and the Fram Strait.Marine Micropaleontology 42 (3), 163-188.

Wadley, M.R., Bigg, G.R., 2002. Impact of flow through the Canadian Archipelago and Bering Strait on the North Atlantic and Arctic circulation: An ocean modelling study. Quarterly Journal of the Royal Meteorological Society 128 (585), 2187-2203

Wang, J., Mysak, L.A., Ingram, R.G., 1994. Interannual variability of sea-ice cover in Hudson Bay, Baffin Bay and the Labrador Sea. Atmosphere-ocean 32 (2), 421-447.

Weaver, A., Hillaire-Marcel, C., 2004. Global warming and the next ice-age. Science 304, 400-402.

Wekerle, C., Wang, Q., Danilov, S., Jung, T., Schröter, J., 2013. The Canadian Arctic Archipelago throughflow in a multiresolution global model: Model assessment and the driving mechanism of interannual variability. Journal of Geophysical Research: Oceans 118 (9), 4525-4541.

Wendeberg, M., Richter, J.M., Rothe, M., Brand, W.A., 2011. δ18O anchoring to VPDB: calcite digestion with 18O-adjusted ortho-phosphoric acid. Rapid Communications in Mass Spectrometry 25 (7), 851-860.

Williams, K.M., 1990. Late Quaternary paleoceanography of the western Baffin Bay region: evidence from fossil diatoms. Canadian Journal of Earth Sciences 27, 1487-1494.

Wu, Y.S., Tang, C.L., 2011. Atlas of ocean currents in eastern Canadian waters. Canadian Technical Report of Hydrography and Ocean Sciences no. 271.

Xiao, W., Wang, R., Polyak, L., Astakhov, A., Cheng, X., 2014. Stable oxygen and carbon isotopes in planktonic foraminifera Neogloboquadrina pachyderma in the Arctic Ocean: An overview of published and new surface-sediment data. Marine Geology 352, 397-408.

Yashayaev, I., 2007. Hydrographic changes in the Labrador Sea, 1960–2005. Progress in Oceanography 73, 242–276.

Yashayaev, I., Loder, J.W., 2009. Enhanced production of Labrador Sea Water in 2008. Geophysical Research Letters 36 (1), L01606.

Young, N.E., Briner, J.P., Stewart, H.A., Axford, Y., Csatho, B., Rood, D.H., Finkel, R.C., 2011. Response of Jakobshavn Isbræ, Greenland, to Holocene climate change. Geology 39(2), 131-134.

Young, N.E., Briner, J.P., Rood, D.H., Finkel, R.C., 2012. Glacier extent during the Younger Dryas and 8.2-ka event on Baffin Island, Arctic Canada. Science 337 (6100), 1330-1333.

Zonneveld, K.A.F., Versteegh, G.J.M., de Lange, G.J., 1997. Preservation of organic walled dinoflagellate cysts in different oxygen regimes: a 10,000 years natural experiment. Marine Micropaleontology 29,
393-405.

Zonneveld, K.A.F., Versteegh, G.J.M., de Lange, G.J., 2001. Palaeoproductivity and post-depositional aerobic organic matter decay reflected by dinoflagellate cyst assemblages of the Eastern Mediterranean S1 sapropel. Marine Geology 172, 181-195.

Zonneveld, K.A., Bockelmann, F., Holzwarth, U., 2007. Selective preservation of organic-walled dinoflagellate cysts as a tool to quantify past net primary production and bottom water oxygen concentrations. Marine Geology 237 (3), 109-126.